DEVELOPMENT OF A ZINC OXIDE NANOWIRE INTERPHASE FOR ENHANCED STRUCTURAL COMPOSITES

By

GREGORY JOHN EHLERT

A DISSERTATION PRESENTED TO THE GRADUATE SCHOOL
OF THE UNIVERSITY OF FLORIDA IN PARTIAL FULFILLMENT
OF THE REQUIREMENTS FOR THE DEGREE OF
DOCTOR OF PHILOSOPHY

UNIVERSITY OF FLORIDA

2012

To all of those big and small who helped me along the way

ACKNOWLEDGMENTS

I first acknowledge Professor Henry Sodano for giving me a start in graduate school and working with me over these years as a graduate student. His willingness to guide while letting me solve many of my own problems has built my skill set and confidence to be an independent researcher. Dr. Sodano's willingness to explore beyond our combined expertise has been the singular shaping function of my research. Without his influence, I would undoubtedly be less successful in my pursuits. I also acknowledge Dr. Yirong Lin for starting the project and teaching me how to be a productive researcher who gets results without getting too distracted from the main goals of life. Mr. Ulises Galan has been a tireless partner in the project, developing many facets of the broader project harmoniously with my efforts. Both Dr. Lin and Mr. Galan have been outstanding colleagues and friends, helping all of us to enjoy life as the people that make each day rewarding. Drs. Josh and Adam Loukus must be acknowledged for catalyzing my initial thoughts that a Ph.D is not relegated to solving problems on a blackboard all day, but rather can combine technical expertise with an engineer's intuition to solve real problems. I thank all of the students, past and present, in the MASS Lab for their help – there are too many to mention specifically. I would also like to graciously thank Dr. Jeff Baur for seeing potential in me as a future researcher and creating opportunities at the Air Force Research Lab through the co-op program. Dr. Baur's positive outlook and incessant smiles excite and energize even the most cynical students and in the end, attitude is the dominant factor in enjoying life's journey. Dr. Matt Maschmann contributed immensely to my ability to succeed at AFRL and always provided doses of long range realism, tempered with brotherly humor.

Steven and Kathy Ehlert deserve thanks beyond description, no one can really quantify the positive influence of siblings and specifics will never do their intelligence and maturity justice. My beloved fiancée Nancie Thompson has been a source of reason, discipline, persistence, laughter, fun and most of all love throughout all the days, although it was most appreciated on the particularly onerous ones. Finally, the support and encouragement of my parents has and will continue to mold my life in a positive way. I can only hope to raise children with a fraction of the love and dedication that my parents have had for me.

TABLE OF CONTENTS

Page

LIST OF TABLES

LIST OF FIGURES

Abstract of Dissertation Presented to the Graduate School
of the University of Florida in Partial Fulfillment of the
Requirements for the Degree of Doctor of Philosophy

DEVELOPMENT OF A ZINC OXIDE NANOWIRE INTERPHASE FOR ENHANCED STRUCTURAL COMPOSITES

By

Gregory John Ehlert

May 2012

Chair: Henry A. Sodano
Major: Mechanical Engineering

Continuous fiber reinforced polymers (CFRPs) form the backbone of the high strength, low density material systems that will be central to the next generation of transportation vehicles. CFRPs, with a compliant matrix between relatively stiff fibers, localize stress at the interface between the two different phases to cause the interface to dominate many bulk material properties. As such, the two phase composite design problem generally has three selections; fiber, matrix and the interface between the two.

This work has developed a unique ZnO nanowire interphase to improve the properties of the interface. Whiskerization, the deposition of an array of whiskers on the surface of a fiber, enables enhancement of the interfacial properties by causing fibers to interlock thus allowing the formation of a graded interface to reduce the stress concentration between the two phases. Whiskerization techniques have existed for some time; however ZnO nanowires offer a radical departure from existing technologies because ZnO nanowires can be deposited at low temperatures (90 °C) aqueous solutions. The high performance afforded by ZnO nanowires is documented for the first time in this work.

This work will demonstrate the ability of a ZnO nanowire interphase to reinforce the interface of both aramid and carbon fiber composites. The interfacial shear strength of single fiber aramid composites is enhanced by 41% and single carbon fiber composite are improved by 110% with this process. Lamina scale testing on unidirectional carbon fiber composites demonstrates a 37% increase in shear strength and a 38% increase in shear modulus for the affected fibers. Given that ZnO nanowires are grown directly onto the underlying fiber, the interface between the nanowires and fiber will have low surface area and minimal interlocking, which implies that the chemical adhesion of the nanowires is strong. This work develops new functionalization procedures that directly control the interface chemistry to enhance the adhesion of the ZnO nanowires to the fiber. A critical contribution of this work, beyond the development of this new interfacial reinforcement material, is the identification of the mechanism controlling the strong adhesion which can be used to engineer other materials or achieve further advances.

CHAPTER 1
INTRODUCTION

Humans have engineered composite materials to solve challenges since nearly the outset of modern civilization. Wood, concrete and bricks exemplify the ability of composites to solve problems more effectively and efficiently than strict monolithic materials. Most natural systems do not use monolithic materials, they employ complex hierarchical composite materials that range from interacting proteins up to complete bones and muscles. Consistent with preceding generations, modern structural composite materials have been developed to offer some of the highest performance across a broad range of properties, in particular shedding high atomic number metals for lower density carbon and silicon based materials. Composite materials have been and will continue to be a topic of intense study for engineers as the demand for lower density structural materials continues to grow.

This work focuses on composites for structural applications, in particular continuous fiber reinforced polymer composites (CFRP). CFRP composites offer very high structural performance with low weight because the structural reinforcing fibers (carbon, aramid) are high strength while employing low density constituents. Structural fibers trend toward higher strength by the small physical dimension which limits the number and size of flaws that initiate failure [1]. Consequently, composite materials offer unprecedented specific strength, stiffness and toughness, when properly integrated into structures, and stand as one of the chief ways that future products can meet our society's efficiency goals.

In spite of the advantages offered by composite materials, composites are inherently different to process and model, thus adoption has been slowed. The market

for aluminum is still 80 times larger by mass and metals are the default lightweight structural material in many transportation applications [2,3]. Existing metal production facilities are not easily retooled to produce composites and the investment required to increase production is slow to return income. Researchers in academia, government laboratories and corporate laboratories still have many crucial developments to make regarding composite materials design, implementation, production, maintenance and repair. This effort will not be in vain as composites remain one of the best options for improving the efficiency and reducing the impact of future material systems.

1.1 Motivation

Composite materials offer significant promise for future structures, particularly in weight sensitive systems such as transportation and wind turbines. The extremely high specific stiffness and specific strength of composite materials is predicted to lead to a new phase of development across the industry [1]. Manufacturers have begun massive projects to scale up production facilities to start commoditizing the production of carbon fibers for structural applications with the expectation of increased demand. With suppliers beginning to reach critical mass, carbon fibers and composites receive greater position towards becoming a sector of large growth. Figure 1-1 shows the predicted growth of the carbon fiber market and the expected 9 million pound annual growth rate. A modest estimated price of $7 per pound during the next 4 years predicts that carbon fiber sales alone will exceed $1B by 2015 [2], not including resin systems or value added engineering design time. The composites industry needs to be in a position to stand ready to answer society's demand for low-density structural materials to meet the great commercial interest that is predicted in the coming decades.

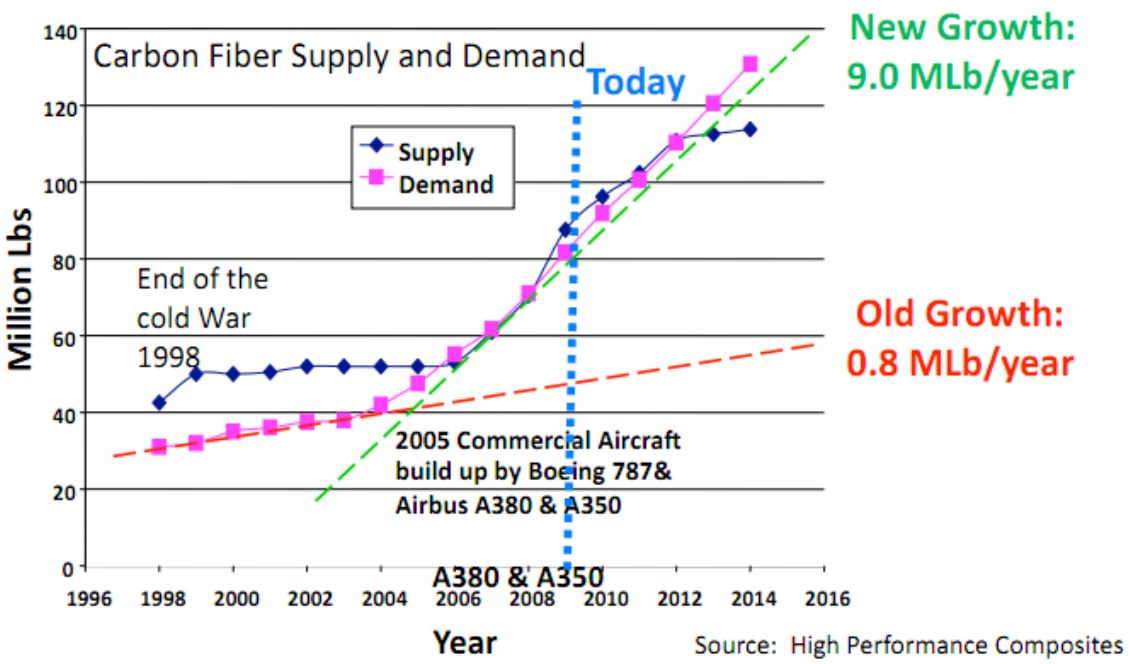

Figure 1-1.Volume of structural carbon fiber market. Milestone aircraft utilizing large volumes of carbon fiber are indicated on the timeline with fitted growth rates. [Reprinted with permission from Warren, CD. Carbon Fiber Composites Technology Development. Workshop on Low Cost Carbon Fiber Composites for Energy Applications: Oak Ridge National Laboratories, 2009.]

The design of a two phase composite is in essence a three part optimization problem where the fiber, matrix and interface must be integrated to form a strong composite [4]. The interface between fiber and matrix in CFRPs plays a dominant role in governing several of the bulk composite properties, such as shear strength, transverse strength and mode I fracture toughness. Improvements to the interface of a composite can reduce the thickness of composites in structural applications, improve the damage tolerance, and increase the number of applications where composites are desirable. Elastic properties of composite materials are routinely and reliably predicted through comprehensive analysis of the constituent properties. The same principles do not always extend to plastic properties or fracture properties [5].

Prediction of composite strength is a complex undertaking, usually requiring some estimation of the interface strength or toughness because the failure mechanism often involves fracture at or near the interface [5]. In many instances, the drastic changes in local compliance lead to crack deflection along the interface between the stiff fiber and compliant matrix. Furthermore, the crack deflection and crack bridging across fibers means that many of the fracture mechanics problems occur at discontinuous interfaces [5,6]. Mechanics based models will likely lead designers to focus on the singularity at the discrete interface and most models will probably indicate that grading the interface will reduce the peak stress observed in the material system. Unfortunately, designers are not left with many choices to eliminate this discrete interface between the fibers and matrix as creating graded interfaces on fibers approximately one tenth the diameter of a human hair remains a significant challenge and area of research.

A second approach to improving the interface between the fiber and matrix is to examine the chemistry between the two surfaces and attempt modification by creating fiber to matrix cross linking to improve interface strength. Creating crosslinks between fiber and matrix requires that the matrix have a specific chemistry that can react with the often immobile surface functional groups on a structural fiber. A modern structural polymer must have strong neat properties (strength, toughness, stiffness, damping) and desirable processing characteristics (viscosity, cure temperature, vapor pressure, product shelf life), while balancing cost, toxicity and safety hazards. Adding specific chemical groups to the long list of requirements will make a complex task next to impossible; there may simply be too many constraints for a desirable solution to meet them all. This work will review attempts to change fiber surface chemistry, termed fiber

functionalization, highlighting the advantages and disadvantages of existing functionalization technologies and ultimately motivating the use of the nanowire interphase developed here.

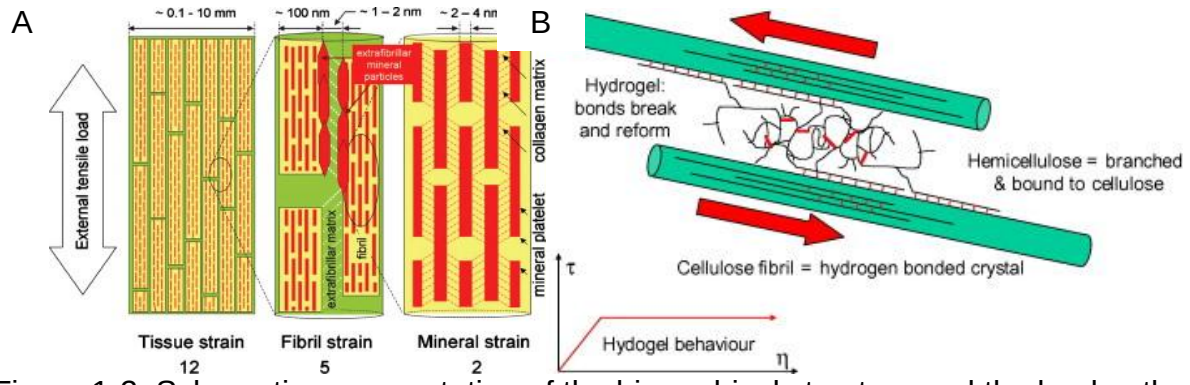

Figure 1-2. Schematic representation of the hierarchical structure and the load paths enabled by functionally graded interfaces in natural systems. A) The hierarchical structure of bone showing a functional gradient on the mineral level provided by collagen fibrils. B) Hemicellulose bound to structural cellulose fibrils as the source of interaction between two fibrils. The load is transferred across a radially graded interface. [Reprinted with permission from Fratzl P, Weinkamer R. Nature's hierarchical materials. Progress in Materials Science 2007;52(8):1263-1334.]

One of the fastest ways to optimize or enhance structural materials is to examine natural systems, which have already undergone thousands of years of refinements. Natural systems are among the most damage tolerant and structurally efficient in existence; evolution has truly crafted a model of material system performance that engineers to this day cannot replicate. This work is inspired from one structural feature in the human body, specifically the use of hierarchical structures and graded interfaces, instead of discrete interfaces to reduce peak stresses in natural material systems. Figure 1-2 shows a schematic of how functional gradients between structural features reduce stress concentrations at the interfaces in natural systems like bones and cell walls. In the natural cases, collagen fibrils or hemicellulose protrude radially from the structural fibers, decreasing in concentration radially as a function of 1/r. The graded

properties reduce the stress concentration by eliminating a discrete interface. The addition of fibrils or hemicellulose provides an additional design variable, enabling coupling between structural element and matrix by creating an additional dimension in the polymer design space. This work will employ a bio- inspired hierarchical design in composite materials to reduce the stress concentration at the interface and improve bulk performance of the material using graded interfaces.

A plethora of creative interfacial treatments for composites have been invented to date, many of which have inspired aspects of this work. Interfaces are unavoidable in composites and there are two broad classifications of methods to improve interface strength; enhanced chemical interactions and enhanced physical interactions. Methods that improve chemical interactions, physical interactions or some combination of the two will be reviewed in detail below.

1.2 Review of Interfacial Treatments

1.2.1 Chemical Functionalization

Chemical functionalization treatments work to increase the interaction between fiber and matrix through improved surface wetting and increased chemical bonding or interaction between fiber and matrix. Chemical functionalization is inherently married to the chemical structure of the matrix because surface wetting depends on compatibility of the two surfaces and cross linking depends on favorable chemical reactions. The following sections will review relevant work to carbon and aramid fiber functionalization, much of which is specific to epoxy based thermoset matrices. These specific matrices have played a key role in many structural composites in the aerospace industry causing them to be well characterized and of great interest. Future composites may employ higher temperature polyimide matrices as faster commercial and military aircraft

demand higher operating temperatures; however these matrices are not particularly well studied in structural applications yet. The difference in chemistry of high temperature polyimide and bismaleimide matrices leaves a substantial portion of the chemical functionalization techniques ineffective, highlighting one of the flaws of the chemical functionalization approach to solving the interface problem [7].

1.2.1.1 Chemical oxidation

Chemical oxidation is the process of oxidizing organic fibers to both increase surface roughness for physical interlocking and create polar oxygen groups that improve wetting to enable chemical interactions between fiber and matrix. Generally, oxidation of aramid fibers is harmful to the tensile strength and has not been performed on aramid fibers [8]; thus this section will focus mainly on carbon fibers. A variety of oxidizing chemicals can be used for this process with most reactions occurring in liquids. Reaction progress is, like most other chemical reactions, accelerated through increased temperatures and reactant concentrations. This work mainly focuses on aramid and carbon fiber composites and thus the literature review will center on these two crucial structural fibers. Most other organic and polymeric fibers will behave like aramids or carbon fibers thus are well represented by the subsequent review. Inorganic fibers such as glass and alumina are fully oxidized and thus show no structural changes due to oxidative treatment. Alternative grafting procedures must be implemented for inorganic oxide fibers to achieve similar results, but these types of fibers are not the subject of this work.

Oxidative treatments have been applied to carbon fibers from nearly the time when graphitized rayon fibers were first commercialized in the 1960s [9]. Nitric acid oxidation of polyacrylonitrile (PAN) based carbon fiber was detailed very early by Rand et al. [10].

The authors demonstrated the acid treatment increased the active surface area from 3 to 30 times and that degassing the fibers post treatment created significant microporosity in the material. The surface of the fibers after oxidative treatment is decorated with various oxygen containing groups and the specific functional groups were not fully characterized in the work.

Waltersson published a series of three articles [11-13] that begin by chemically oxidizing PAN based carbon fibers in nitric acid to create hydroxyl and carboxylic acid groups. The latter papers demonstrate the reaction of these groups with diamines, hoping to form direct crosslinks with epoxy based polymer matrices. The work showed interesting results when the electron spectroscopy for chemical analysis (ESCA) data is analyzed based upon relative peak intensities, estimating the surface coverage of the oxidation, and grafting procedure based upon molecular size. Although the work did not delve into the impacts of these treatments on the mechanical properties of the resulting composite, it did demonstrate the effectiveness of an H_2SO_4/HNO_3 solution for oxidizing carbon fibers.

Nitric acid oxidation continued to be a subject of research in the subsequent decades. Pittman and his colleagues reported that the oxidation of carbon fibers in HNO_3 when followed by a wash in aqueous NaOH helped to remove the heavily oxidized surface layers of the carbon fiber and create a surface suitable for cross linking with a polymer matrix [14]. Furthermore, through angle resolved x-ray photoelectron spectroscopy (ARXPS), Pittman and his team were able to identify the mechanism for the etching and opening of pores during oxidation. ARXPS also indicated that the NaOH wash after HNO_3 oxidation removed a few layers of surface material and

revealed an oxygen-rich subsurface, effectively increasing the oxygen content on the surface of the fibers. The article provides an in-depth study of the mechanism of oxidation from a series of spectroscopic experiments and proves the etching and subsurface oxidation that occurs during the processes, shown schematically in Figure 1-3.

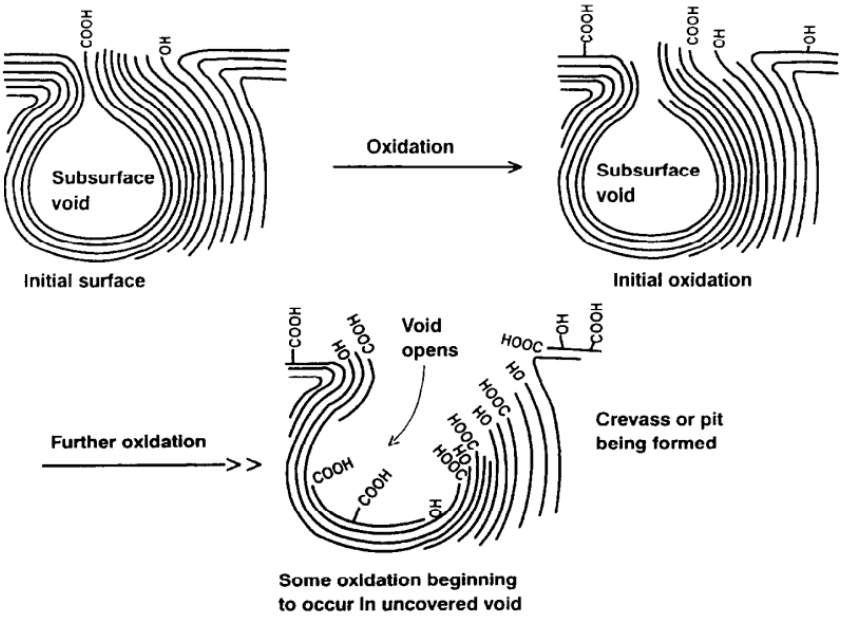

Figure 1-3. Mechanism of defect formation and oxidation of carbon fiber surfaces. Oxidative treatments can cause structural defects to become more pronounced, leading to interlocking with the polymer matrix but also reduced in plane composite properties. [Reprinted with permission from Pittman CU, He G-, Wu B, Gardner SD. Chemical modification of carbon fiber surfaces by nitric acid oxidation followed by reaction with tetraethylenepentamine. Carbon 1997;35(3):317-331.]

The focus of the article by Gardner et al. [15] was on the chemistry and the interfacial strength impacts were primarily neglected. The impacts are alluded to and the article indicates that an understanding of the mechanisms of surface oxidation can lead to an improved interface. A follow-up study confirmed many of these measurements through methylene blue adsorption [16]. The authors identified that the number of acidic oxygen groups per unit surface area did not significantly change

following further oxidation; the number of acidic groups simply increased with the surface area from subsurface oxidation. The combined results of these two studies clearly indicate that carbon fibers oxidized in HNO_3 show a complex and layered set of oxygen containing functional groups. The creation of these groups leads to the opening and etching of subsurface pores, which can be revealed through swelling in a basic solution or through the entire removal of the layers with a strong base. After a period, the etching is even visible at the modest magnification afforded by analysis with a SEM, as shown in Figure 1-4. These functional groups and pores are postulated to improve the interfacial shear strength; however conclusive data is lacking from these studies.

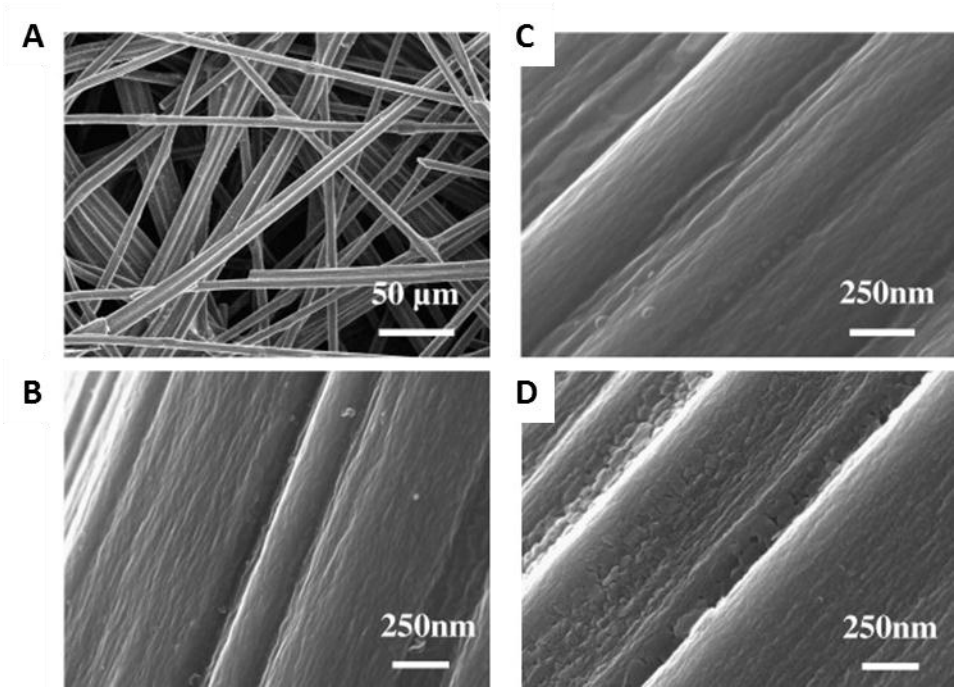

Figure 1-4. Surface morphology of carbon fiber after chemical oxidation for a,b) 0 minutes, c) 15 minutes and d) 4 hours.[Reprinted with permission from Zhang G, Sun S, Yang D, Dodelet J, Sacher E. The surface analytical characterization of carbon fibers functionalized by H2SO4/HNO3 treatment. Carbon 2008;46(2):196-205.]

One interesting theory is that the highly aromatic carbon structure of the carbon fibers is susceptible to nitration through the use of the mixture of H_2SO_4/HNO_3, the

typical starting point for the synthesis of many substituted aromatic compounds [17]. While this is the standard reaction employed to create nitro groups on smaller aromatic molecules, Zhang et al. has shown that the reaction does not produce these groups on carbon fibers [18]. Perhaps more insightful is the distinct spectroscopic evidence provided by Zhang to show that the source of the desirable COOH groups is transitory –O, –S and –N species and the chemistry of a large conjugated graphene sheet is fundamentally different than a large aromatic molecule. This result, while not intended to apply to carbon fibers for structural composites, provides an explanation for some of the inconsistency of carbon fiber oxidation with traditional molecular organic chemistry. The principles established by the preceding works on oxidation have defined the chemistry of graphitic fibers fairly well and enabled the implementation of this technology. Ultimately, interfacial shear strength can be improved through the oxidation of structural carbon fibers [19] and the selection of the specific wet chemicals comes down to an argument of the economics of production.

1.2.1.2 Electrochemical oxidation

Electrochemical oxidation of structural fibers applies primarily to carbon fibers since polymeric fibers are not conductive and thus do not maintain a uniform electrochemical potential along the length of the fiber. Carbon fibers are particularly well studied in this regard, for example Sherwood and colleagues have published a series of 25 articles over the course of 19 years on the subject. Various electrolytes have been proven to be effective for removing the weakly bonded outer layer as well as opening up pores and increasing the surface roughness of the material to improve interlocking.

It is difficult to specifically identify the seminal inventor of electrochemically oxidized carbon fibers; however Paul was one of the first when he filed for a British Patent on the process in 1976 [20]. Many studies on the electrochemical reaction of graphite have been performed for its use as a counter electrode or in industrial processes; thus the chemistry is fairly well understood [21]. While the chemistry is similar, the difference in surface area and crystal structure of carbon fibers makes the analysis and experiments interesting and applicable to the industry at large. The first electrochemical study published by Sherwood and Proctor [22] analyzed the formation of oxygen containing complexes in sulfuric and ammonium bicarbonate electrolytes. Oxygen containing functional groups on the surface amplified with increasing electrochemical potential and the results were different dependent on the electrolytes used.

In follow up articles, the authors identify that the electrolyte affects the reaction mechanism, which in turn impacts surface products resulting in increased surface area [23,24]. Figure 1-5 shows both Atomic Force Microscope and XPS data that demonstrates the change in surface roughness and the change in surface chemistry after oxidation. Although the surface chemistry can affect interface strength through enhanced wetting, the authors found the main advantage of electrochemical oxidation to be the roughening or mechanical keying of the fiber to the matrix, which is responsible for the increases in interfacial strength.[25]. Further research on the subject continued to focus in chemistry, culminating with articles presenting spectroscopic identification of interactions between electrochemically oxidized fibers and some representative polymer matrices [26-28]. The spectroscopic evidence of the interactions does indicate that

surface chemistry plays a significant role in interface strength however, the role of keying or the roughening of the surface cannot be understated and was specifically studied by another article [29], which will be reviewed in more detail later.

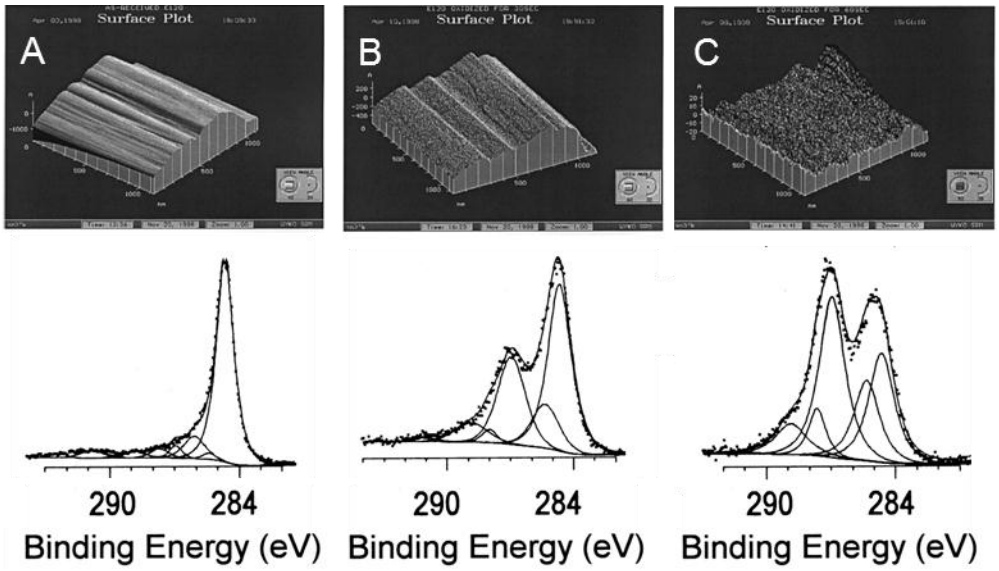

Figure 1-5. Atomic force microscope images and X-ray photoelectron spectroscopy analysis of the surface of electrochemically oxidized carbon fibers. A) Carbon fibers as received, B) carbon fibers oxidized at 0.5A for 10 seconds and C) carbon fibers oxidized at 0.5A for 60 seconds. The oxidized fibers show increased oxygen functional groups after oxidation. The functional groups are primarily low oxidations, C-OH, C-O-C, C=O; rather than COOH. [Reprinted with permission from Wang Y, Zhang F, Sherwood PMA. X-ray Photoelectron Spectroscopic Study of Carbon Fiber Surfaces. 23. Interfacial Interactions between Polyvinyl Alcohol and Carbon Fibers Electrochemically Oxidized in Nitric Acid Solution. Chemistry of Materials 1999;11(9):2573-2583.]

A particularly important aspect of the electrochemical oxidation procedure is the propensity for damage to the intrinsic mechanical properties of the fibers. Some of the articles written by Sherwood et al. describe that fibers treated for longer periods of time became so weak that they were unable to be handled in the laboratory environment. Specifically, they found that, “the strength of treated carbon fibers was degraded by the oxidation process, the fibers being so weakened that they broke under normal handling [30].” This was confirmed by testing performed during the development of this work

where the tensile strength in nearly every configuration was diminished by at least 15% and in some cases 35%. This severe reduction eliminates many of the advantages to employing carbon fiber in structures and has in large part motivated the development of this work. In particular, the electrochemical oxidation experiments motivated the development of new non-oxidative carboxylic acid treatments described in detail throughout the remainder of this work.

1.2.1.3 Thermal oxidation

The thermal oxidation reaction oxidizes carbon fibers in similar fashion to electrochemical or chemical oxidation reactions except that the thermal oxidation reaction is completed at high temperature in an oxidizing atmosphere. One advantage of thermal oxidation for a production environment will be reduced capital expenditures since the manufacturing of carbon fiber requires high temperature furnaces with a controlled atmosphere. The resulting chemical reactions will differ in mechanism and effect to produce a surface with a broad distribution of hydroxyl, ether and carbonyl groups [31]. This type of oxidation does not intercalate the graphitic layers like chemical oxidation, limiting the formation of pits or pores, and as a result the process is quite reversible by performing a high temperature thermal reduction in an inert atmosphere [32].

Thermal oxidation produces a variety of oxygen containing functional groups on the surface of the fiber, ranging from hydroxyl and ether groups to carboxyl and ester groups. Unfortunately, the atmospheric oxidation does not have the specificity required by many chemical derivation procedures. Thermal oxidation was studied in detail by Zielke et al., specifically focusing on the surface chemistry and decomposition products [33,34]. Zielke et al. specifically noted that many of the functional groups after oxidation

were not stable in subsequent washing procedures. The washing procedure actually increased the content of carboxylic acid on the surface of the fiber because the washing was able to hydrolyze surface anhydrides created during the oxidation. Zielke et al. also confirms the wide variety of functional groups present on the surface and validates the efficacy of the surface treatment for improved interlaminar strength in high temperature thermoplastic composites. While thermal oxidation has been proven quite effective for interfacial enhancement, many studies do not emphasize the impact of the functionalization on the tensile strength of the fibers [35]. The creation of surface defects, roughness and a wide variety of functional groups would limit the applicability of thermal oxidation in many interface applications.

1.2.1.4 Radical trapping grafting

Radical trapping grafting offers an entirely different approach to functionalization from typical oxidative procedures. Instead of consuming the material to create surface roughness and desirable functional groups, radical trapping grafting employs radical molecules that react with the free electrons in the graphitic structure of the carbon fiber to create a new covalent bond, leaving a surface terminated with the molecule of choice [36]. As a surface reaction, radical trapping grafting is most effective with high surface area particles. Benzene and other small aromatic molecules do not have the capacity to hold a charge and the particles must be macromolecules or particles that are large enough to stabilize a charge. Tsubokawa has led the field in radical trapping grafting, publishing extensively and demonstrating the use of the radical trapping grafting technique in a plethora of applications [37-41]. Figure 1-6 shows a typical reaction where the graphitic carbon traps the radical to form an additional covalent bond and graft a polymer to the fiber. Radical trapping grafting is effective for creating a desired

surface functionality however the yield is typically low and molecules or polymers that form radicals are often unstable and require precautions to prevent undesired polymerization reactions [36]. Radical trapping grafting is not effective with aramids or most polymeric fibers because they lack the necessary graphitic structure to stabilize the radical and create a new covalent bond.

Delamar et al. has proven that radical trapping grafting can create enough surface functional groups to improve the adhesion of carbon fiber to a thermoset epoxy matrix [42]. The procedure is one of a series of papers from the same authors and includes additional works on developing a process to make the electrochemical reduction of aryl diazonium salts feasible [43-48]. The reduction process creates radicals that react with free electrons stabilized in the graphitic structure of carbon fiber or other resonant aromatic materials. The reaction is performed in an aprotic solvent such as acetonitrile and in this particular procedure, 4-nitrophenyl groups grafted to the surface are electrochemically reduced in an acid after grafting to form primary amine groups which crosslink with the epoxide groups in the polymer matrix. One of the important advantages to this procedure is that the graphite fiber is not weakened through the process of radical grafting because the fiber is not consumed or oxidized during processing. This method creates covalent crosslinks to the polymer matrix without inducing defects in the fiber however; the method is extremely complex and may not meet the typical production requirements. The procedure requires skillful operation of sophisticated and sensitive reagents, and the multistep process requires electrochemical equipment in addition to a highly educated process engineer to set up maintain the system.

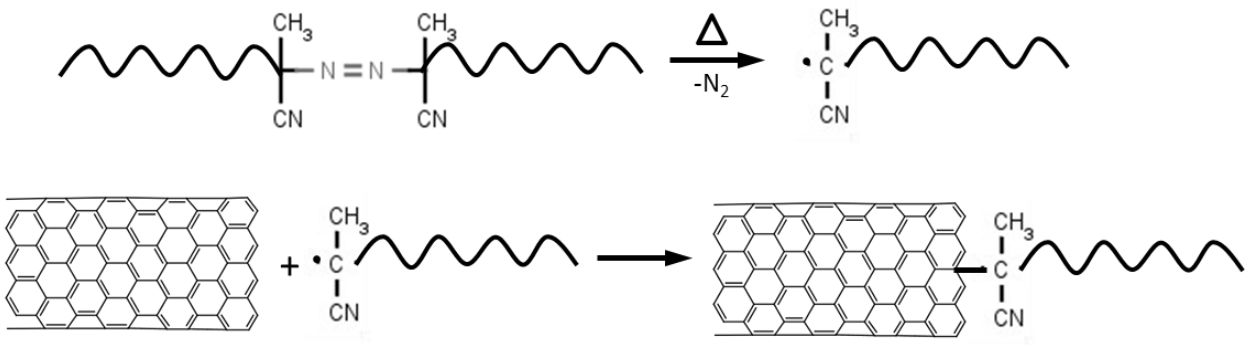

Figure 1-6. Radical trapping reaction scheme. Termination of a living azo-polymer onto a graphitic carbon nanostructure resulting in grafting of the polymer to the surface of particle.

1.2.1.5 Functional group grafting

The grafting of functional groups pursues the use of existing surface functional groups as reactive sites to graft polymers or other materials to the surface of the fiber. In principle, oxidative processes create oxygen groups toward this end however; it has been shown that earlier roughening of the surface is the root cause of the success of the oxidative processes [29]. Functional group grafting mainly pursues the use of existing functional groups on the fiber surface, rather than the creation of new ones. Carbon fibers have a broad array of functional groups and as such are not suitable candidate for chemically specific reactions to graft to the surface. Aramid fibers are chemically pure and thus make a much more reliable and effective fiber for functional group grafting. Aramid fiber composites have shown improved interfacial strength with functional group grafting through at least two reaction mechanisms [49-52].

Several authors have published chemical procedures employing a metalation - bromination reaction scheme similar to Figure 1-7 below [49,50,52,53]. The scheme employs the secondary nitrogen inherent to the aramid fiber structure to exchange the relatively inert proton for a highly reactive metal ion, like Na^+. This metal ion is then reacted with a halide (Cl^-, Br^-) to graft the molecule of interest to the surface of the fiber

with a newly formed covalent bond. The reaction is beneficial as it produces high yield and is accompanied by obvious color changes to indicate the progress of the reaction. This type of reaction does suffer from a few noteworthy disadvantages. First, reactions involving NaH or any alkali metal hydride tend to be unstable and require special inert atmosphere handling. Perhaps more significantly, the efficacy of the treatment is compromised by the severe damage the process inflicts upon the fiber tensile strength, as shown in Figure 1-8. Aramid fibers are typically selected for the high strength to weight ratio, and processes that effectively trade off tensile performance for interfacial strength offer only a modest improvement over existing technology. To date, there is little work demonstrating that the reaction in Figure 1-7 can be adjusted to mitigate the negative effects on the inherent fiber tensile strength.

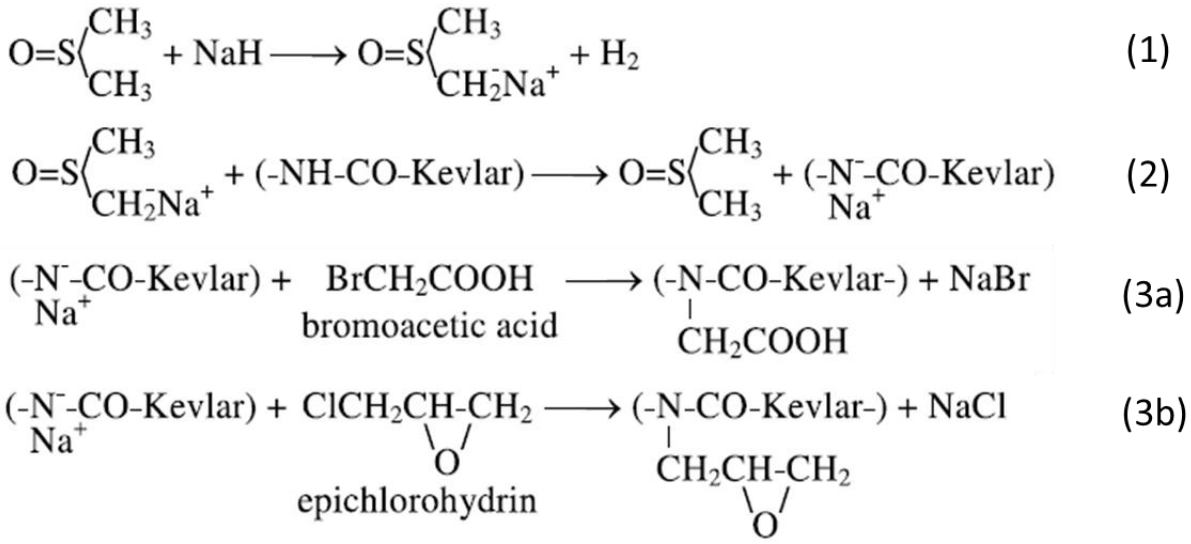

Figure 1-7. Metalation – bromination reaction scheme for grafting to aramid fibers. The metal complex is prepared in (1), the proton is exchanged for the metal ion in (2) and the desired molecule is grafted to the fiber surface in (3). The scheme presents two possible terminal groups; a carboxylic acid in (3a) and an epoxide in (3b). [Reprinted with permission from Park S, Seo M, Ma T, Lee D. Effect of Chemical Treatment of Kevlar Fibers on Mechanical Interfacial Properties of Composites. Journal of Colloid Interface Science 2002;252(1):249-255.]

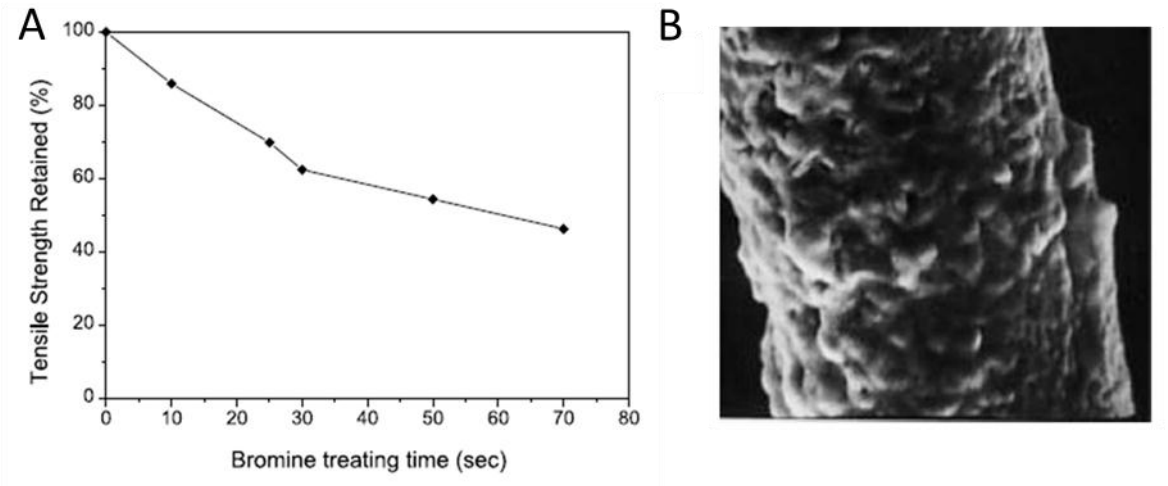

Figure 1-8. (A) Effect of bromine treating time on tensile strength of aramid fibers. (B) The surface of the fibers indicates swelling, pitting and damaging of the fiber during the functionalization reaction, explaining the observed reductions in tensile strength. [Reprinted with permission from Park S, Seo M, Ma T, Lee D. Effect of Chemical Treatment of Kevlar Fibers on Mechanical Interfacial Properties of Composites. Journal of Colloid Interface Science 2002;252(1):249-255.]

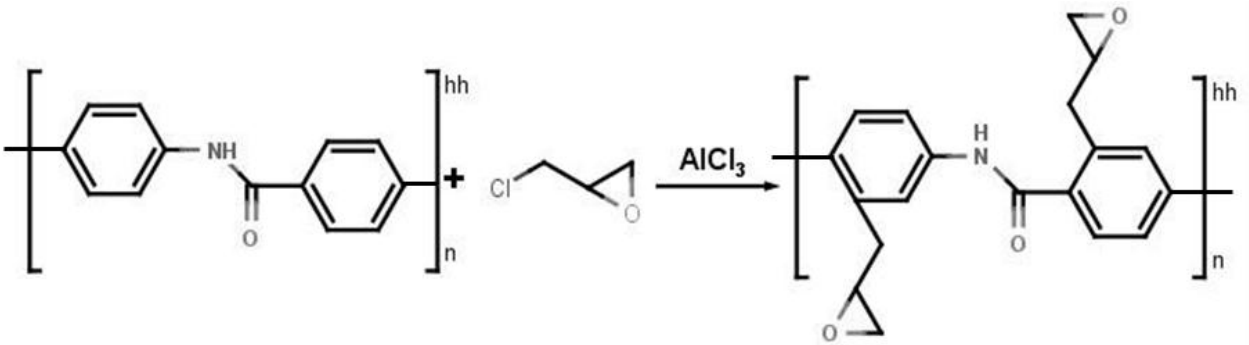

Figure 1-9. Friedel – Crafts functionalization reaction of aramid fibers for use with epoxy based thermoset polymer matrices.

A second technique to functionalize aramid fibers for enhanced interface strength grafts to the aromatic ring present in the fiber chains. The technique has only been recently demonstrated [54] and the number of researchers documenting success is very limited. The Friedel –Crafts reaction has been employed for aromatic functionalization on an industrial and research scale for over a century and the technique appears very promising. The functionalization procedure reacts the aramid fibers with a chlorine

terminated target molecule in the presence of aluminum chloride. Liu et al. elected to react with epichlorohydrin, as shown in Figure 1-9, in order to functionalize the fibers with the chemical groups that constitute an epoxy thermoset matrix [51]. Liu et al. also demonstrates that the reaction has no impact on the tensile strength, probably due in part to the fact that the crystallinity and polymer chains remain largely undisturbed with the required reaction conditions. This reaction is challenged by requirements of very strict anhydrous conditions and procedure redevelopment if a different molecule or functional group was desired in grafting for a different polymer matrix.

1.2.2 Plasma Functionalization

Plasma functionalization capitalizes on the high reactivity of plasma to rapidly functionalize the underlying fibers. The reactions are typically performed in a high vacuum environment and can react with the entire surface area, including pits, cracks and crevasses. This process requires special chambers, high voltage high frequency electrical power supplies and mandates batch processing. Plasma functionalization is applicable to fibers of all types, carbon, aramid, nylon, and glass. Plasma functionalization limits the selection of available reactants, with most researchers focusing on simple gases. The excess charge and energy inherent to plasma applies to the molecules fed into to functionalize the fibers. Large molecules often destabilize and split into smaller components yielding various functional groups on the surface. This reaction requires very little time to effectively coat the surface of the fibers, which is a distinct advantage for the production environment.

1.2.2.1 Oxygen plasma functionalization

One of the natural functionalization procedures that researchers have investigated is an oxygen plasma functionalization [55-70]. Oxygen plasmas create a mixture of

oxygen functional groups on the surface of the fiber, in pursuit of the same end as the chemical, electrochemical and thermal oxidation procedures discussed earlier. Ozone plasmas have been investigated by several authors and found to produce fairly high oxygen content to ostensibly enhance interface strength [71-73].

Park et al. has demonstrated that room temperature ozone treatment does increase the critical stress intensity factor and that the critical energy release rate of ozone modified carbon fibers [75]. Park et al. cite the improved fiber – matrix interactions, which is attributed to the higher surface energy of the ozone modified fibers measured through contact angle studies. The increased adhesion as a result of the ozone treatment is clearly observed in the fracture surfaces of the test samples in Figure 1-10. Figure 1-10A shows clear debonding at the interface between the fiber and matrix; while Figure 1-10B shows a strong adhesion and tortuous cohesive failure of the polymer matrix. Although the authors do not report tensile data for the treated fibers, it is likely diminished due to the creation of additional surface defects. Two similar articles have been published by Li and coauthors, performing similar analysis of ozone treated carbon fibers [35,72].

Much of the oxygen plasma functionalization work published overlaps with a variety of ammonia, argon and nitrogen plasma techniques, as evidenced by one review paper in plasma treatments for interfacial enhancements [29]. As will be reviewed later, the literature related to plasma functionalization is broad and the conclusions drawn from it remain nearly as varied. Multiple critical reviews on this subject alone exist, contributing to an even more complete analysis of the literature in this area [29,74-76]. Ultimately, differences in technique, experimental design and conclusions drawn from

the data can lead one to discern that with proper development and control, oxygen plasma functionalization can be effective for enhancing the interface strength, although it has not entirely solved the interface problem in composites.

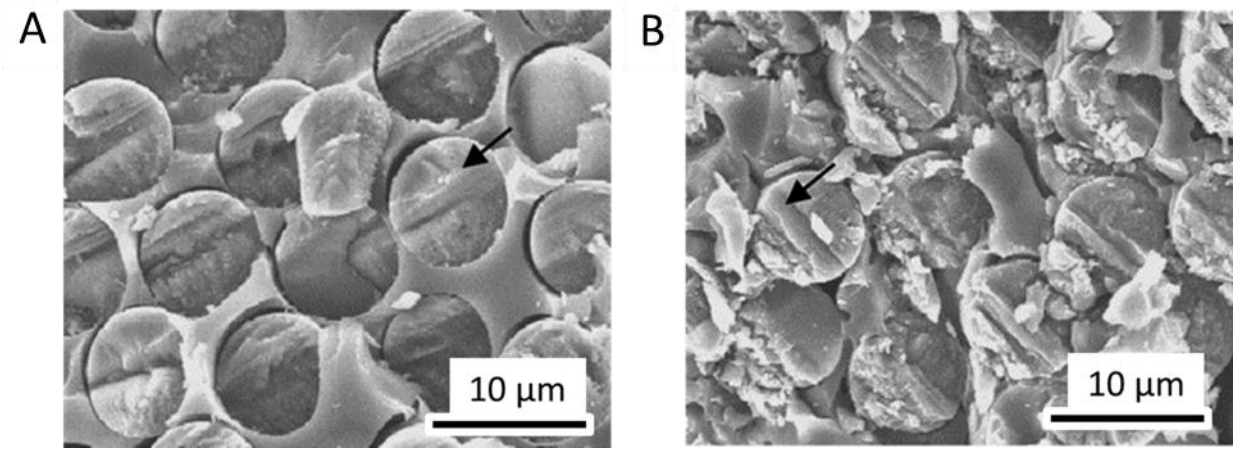

Figure 1-10. Fracture surface of carbon fiber epoxy composites with A) fibers as received and B) fibers oxidized in an ozone plasma. [Reprinted with permission from Park S, Kim B. Roles of acidic functional groups of carbon fiber surfaces in enhancing interfacial adhesion behavior. Materials Science and Engineering: A 2005;408(1-2):269-273.]

1.2.2.2 Amine and ammonia plasma functionalization

Both aramid and carbon fiber composites have shown interfacial shear strength improvements from ammonia plasma treatments. Carbon fibers in ammonia plasma treatments have shown promising improvements in interfacial shear strength directly attributed to the creation of chemically grafted amine groups. Many scientists have advocated for this approach and many industrial producers employ the technology, Jones is perhaps the most visible researcher with some of the most highly cited articles on the subject [29,77-79]. Some of the most important contributions made by Samman, Farrow and Jones were to conclude three specific features of ammonia plasma treatments. First, ammonia plasma treatments improve the interfacial shear strength of carbon fiber epoxy composites. Second, the plasma treatment does not have an impact

on surface roughness or tensile strength of the fibers. Finally, Samman, Farrow and Jones demonstrated that the surface functionality was highly dependent upon exposure to air and furthermore, exposure to air had an impact the interfacial shear strength by enabling the buildup of a physisorbed blocking layer on the surface [29,78,79].

Other researchers have demonstrated similar results to Jones and his colleagues, the interest specifically related to plasma treatments can be attributed to its establishment as an integral component of advanced fiber manufacture [57,69,75,76,80,81]. The review of a variety of papers from a broad time span supports continued interest in plasma functionalization, in particular ammonia plasma functionalization as an effective interface treatment. Unfortunately, the great variety of papers written has led to almost as various a set of conclusions. Some papers demonstrate vastly increased surface roughness and etching of the fibers after treatment, while others are able to attribute the observed improvements in interface strength explicitly to the surface chemistry. There is additional variance in the equipment, procedures and analysis used to determine the effects of plasma treatments. The main conclusion to be drawn from the extensive literature is that plasma treatments can be precisely tuned to produce improved interface strength without reduced tensile strength. Given this benefit however, it must be noted that significant treatment development is required and the method is not universal for all fibers and conditions.

Aramid plasma functionalization treatments show notable improvements with minimal reductions in tensile strength [82-85]. Sheu and Shyu have reported typical results for ammonia plasma surface treatment of aramid fibers and clearly demonstrate

the efficacy of the treatment to enhance interfaces in composites. Sheu and Shyu do report a modest reduction in tensile strength while the process is tuned to minimize the surface etching and pitting common to oxidative functionalization. Interfacial shear strength improvements of nearly 100% are reported, shown below in Figure 1-11 [84,86-88]. Brown et al. confirmed the improvement in their study, although they observed a decrease in ballistic strength, which was attributed to higher fiber matrix bonding [89]. It is safe draw the same conclusions as carbon fiber plasma functionalization, the technique is effective but not universally applicable and requires significant development to implement without reducing the fiber tensile strength.

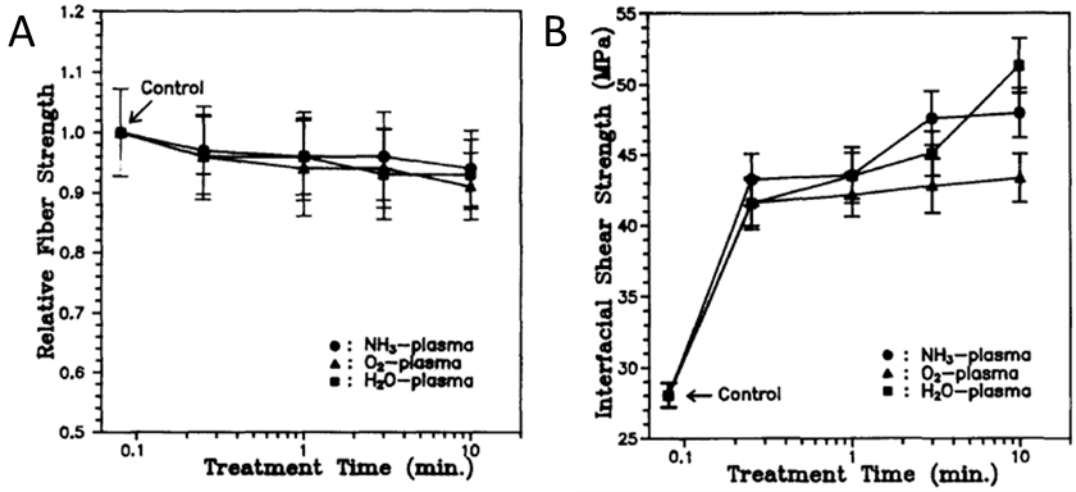

Figure 1-11. Effect of various plasma treatments on A) aramid fiber tensile strength and B) interfacial shear strength of an epoxy composite. [Reprinted with permission from Sheu GS, Shyu SS. Surface properties and interfacial adhesion studies of aramid fibres modified by gas plasmas. Composites Science and Technology 1994;52(4):489-497.]

1.2.3 Physical Interface Treatments

Physical interface treatments are methods that do not rely upon chemical interactions to improve interface strength which include roughening, whiskerization and polymer interphase deposition. With the exception of whiskerization, roughening and

polymer interphase deposition are inherently married to chemical treatments, albeit for separate reasons.

Roughening on the scale of a single structural fiber is impractical through most physical manufacturing methods such as sanding or modifying the production process to add roughness. Roughening is most easily accomplished through thermal or chemical oxidative methods, both of which were reviewed as chemical treatments earlier. It should be noted that oxidative treatments are effective in part due to the physical treatment that coincides with the chemical treatment. For the purposes of this work, oxidative treatments are classified as chemical treatments. Roughening has never been especially popular as a treatment because surface defects and pits typically limit the properties of an individual fiber [90]. As such, experiments that specifically attempt to roughen the fiber for improved interfacial strength are not viewed as viable long term solutions.

There has been much debate historically surrounding the relative contribution of surface roughness and surface chemistry on the interfacial strength in a composite [29,32,91-97]. The debate between the relative contribution of chemistry versus roughness and interlocking has been noted as ongoing as recently as 2004 [98]. Experiments to isolate these effects depend heavily on the specific fiber, matrix and chemical treatments performed. Almost all chemical treatments lead to some significant changes in the surface roughness, convoluting the results from inseparable treatments. Significant differences between investigators over time has led to a variety of opinions reported over a span of nearly 30 years. This work will attempt to introduce another treatment that involves both chemical adhesion and mechanical interlocking.

Whiskerization is one of the primary physical means of increasing interfacial strength and was first patented by Milewski in 1967 [9]. Historical figures from the patent filed by Milewski as well as some of the earliest publications of whiskerized composites are shown in Figure 1-12 and Figure 1-13. Originally Milewski, an early advocate of whiskers and other defect free nanomaterials, pursued the direct growth of whiskers on fibers for 'bifiber' composites. He reported increased interfacial improvements from the results published by the Naval Ordnance Laboratory among others preceding the patent application [99]. Whiskerization increases interfacial shear strength by interlocking the fiber with the matrix and increasing the surface area for interaction between the two. The whiskers themselves must be strongly adhered to the surface of the fiber in order to be effective in promoting an enhanced interface. Whiskerization creates two interfaces where only one existed previously, both new interfaces must be stronger in order to result in globally improved interface strength. Each whiskerization technique will be discussed in detail, focusing not only on the resulting composite performance, but also the mechanism for adhesion of the whiskers to the surface of the fibers.

Carbon and aramid fibers are the focus of this research; a few properties of the fibers related to the growth of whiskers must be noted. Graphitic carbon is thermally stable (in an inert atmosphere) and can maintain mechanical properties after heat treatments in excess of 2000°C [19]. Carbon is soluble in several transition metals such as Fe and Ni, which are used as catalysts in some carbon nanostructure growth processes [100]. Aramid fibers are polymeric and thus cannot be heat treated to temperatures in excess of 160°C without damaging the underlying fiber structure and

strength [101]. Heating aramid fibers above 500°C not only leads to degrading structural changes, but the fiber loses mass due the oxygen present in the structure of the fiber. Many whiskerization processes require high temperatures or metal catalysts that can damage the fiber tensile strength [102], the underlying property that makes the fibers so desirable. There are some processes for aramid fibers that limit the exposure of the fiber to high temperature degradation; however these processes still weaken the fiber and create the very same tradeoff that traditional roughening procedures try to eliminate [103]. While certain applications and designs sacrifice tensile strength, the goal of this research is to preserve the intrinsic properties of the fiber while improving the interfacial shear strength.

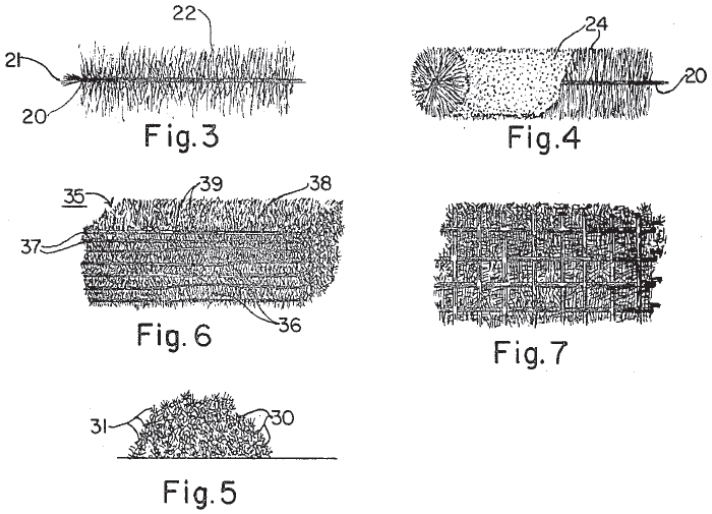

Figure 1-12. Schematics of whiskerization on the surface of structural fibers from the patent filed by Milewski. [Reprinted with permission from Milewski JV, Shyne JJ. Method of Treating the Surface of a Filament. 1967(US003580731).]

1.2.3.1 Ceramic whiskerization

Ceramic whiskers were the first to be applied to structural fibers, notably published by the Naval Ordnance Laboratory in 1966 and shown in Figure 1-13 [99]. It is difficult to determine precisely who first invented the technique because much of the work at the time was proprietary or classified. One can be certain that the idea had been conceived

and executed in the early 1960s, prior to publication by the Naval Ordnance Labratory [104]. Initially the goal was to improve bulk polymers by mixing in high strength, micron sized whiskers or nanofibers. It was later noted by Milewski that interfacial performance improved if the whiskers were located directly at the surface of traditional reinforcing fibers. This whisker location improved the surface geometry of the fibers and reinforced the polymer at the most highly loaded location, the interface of polymer and fiber [9]. Milewski and colleagues mainly worked with ceramic whiskers grown through chemical vapor deposition processes; thus the focus of much of the early work is SiC, Si_3N_4, Al_2O_3 and AlN.

SiC was the favorite choice for whiskerization in its early development because of its proclivity to bond very well to the carbon fiber. This was favorable as the SiC whiskers use the fiber as the carbon source during the reaction. SiC whiskers are typically grown at high temperatures using chemical vapor deposition at 900 °C to 1600 °C [105]. SiC whiskers grown on carbon fibers by Milewski and others were demonstrated to be effective for interfacial enhancement both of polymer (low modulus) and carbon (high modulus) matrix composites [105]. SiC whiskers grown on carbon fibers are typically 10 -1000 nm in diameter and 100 nm to 10 µm long, with exceptional crystallinity. Most methods employ a deposition growth approach instead of a catalyst based approach where the precursors are evaporated and then deposit on the surface of the fibers [106], which eliminates having to remove the catalyst after growth. The technique failed to achieve wide scale adoption in industrial production because the growth process was too complicated and the whisker growth process led to diminished reinforcing fiber properties.

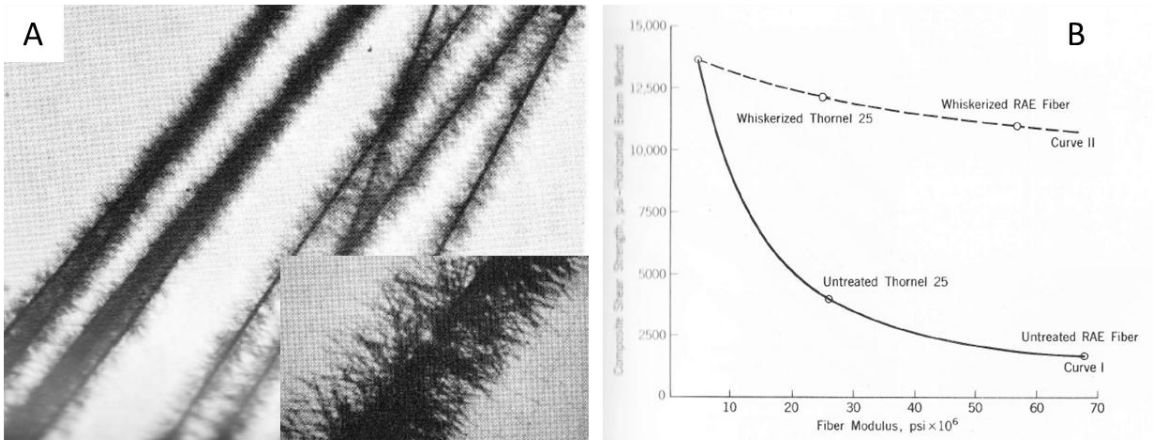

Figure 1-13. Some of the earliest published whiskerization data showing A) carbon fibers with SiC whiskers grown on the surface and B) a substantial improvement in the composite shear strength. (Adapted from Milewski [99] in Lubin's Handbook [104]) [Reprinted with permission from Lubin, G. Handbook of fiberglass and advanced plastics composites. Huntington, N.Y: R. E. Krieger Pub. Co, 1975.

TiO_2 whiskers have also been grown on carbon fibers through an aerosol process for use in phenolic matrix composites. TiO_2 whiskers were employed toward a similar end by researchers in the former Soviet Union and it is possible, that this was the first demonstration of a whiskerization treatment for interfacial enhancement. The whiskers were shown to be effective in improving the shear and compressive properties of the material [107,108]; although the authors focused more on the mechanics of why interface strength matters, rather than the materials science of how the TiO_2 is an effective reinforcement. Whisker size was not reported; however Gunyaev does compare TiO_2whiskers to SiC and Si_3N_4 whiskers and observes that all are effective as an interfacial treatment and all have significant deleterious effects on the tensile strength of the underlying fibers.

Other ceramic nanowires do not appear to be as effective as SiC, Si_3N_4 or TiO_2; although it is unclear specifically why. It should be noted that only one very recent whiskerization process has previously been presented to work for aramid fibers

because they simply cannot withstand the high temperatures required for processing of most whiskers [103]. The processing required to produce whiskers on various fibers is limiting the adoption of whiskers to enhance the interfacial shear strength of composites.

1.2.3.2 Carbon nanotubes and carbon nanofibers

The ceramic whisker community laid much of the groundwork for future nanomaterials by establishing that smaller materials often exhibit higher strengths because of the lower probability of defects. The development of carbon nanotubes and carbon nanofibers as reinforcing filler for polymers was encouraged by the extraordinary mechanical properties of the individual nanotubes [109]. Carbon nanotubes and nanofibers were developed by Downs et al. for hierarchical fibers even before carbon nanotubes had become as ubiquitous as they are today. Later, the carbon nanotubes and nanofibers were proven effective for interfacial reinforcement, consistent with their prediction that the technique would be effective for achieving that end [100,108,110].

One of the first demonstrations of carbon nanomaterials for interfacial enhancement was in 2002, when single walled carbon nanotubes were shown to improve single fiber interface strength by 15% [111]. The authors briefly mentioned that the fiber tensile strength was degraded during the process. Seven years later, researchers at the US Air Force Research Laboratory were able to tune the process to sufficiently maintain fiber tensile strength and improve interface strength by using specific carbon fibers in addition to adjusting growth and catalyst conditions [102,112]. An image of the hierarchical fibers developed at the US Air Force Research Laboratory is shown in Figure 1-14. Researchers at Imperial College have also investigated and developed carbon nanotube hierarchical fibers for implementation, publishing numerous

articles evaluating the efficacy of the treatment [113-116]. Researchers at Massachusetts Institute of Technology pursued a similar goal; however they elected to demonstrate the technology on alumina fibers instead of carbon – thus avoiding any detrimental impacts on the tensile strength. They were able to effectively scale growth to perform Mode I fracture toughness testing on hierarchical fibers and demonstrate that the macroscale composite properties dominated by interfacial shear strength can be improved through the hierarchical architecture [117,118]. The net result of the articles demonstrates that carbon nanotube hierarchical architectures can effectively improve composite interfaces when processing of the nanotubes is suitably adjusted and developed.

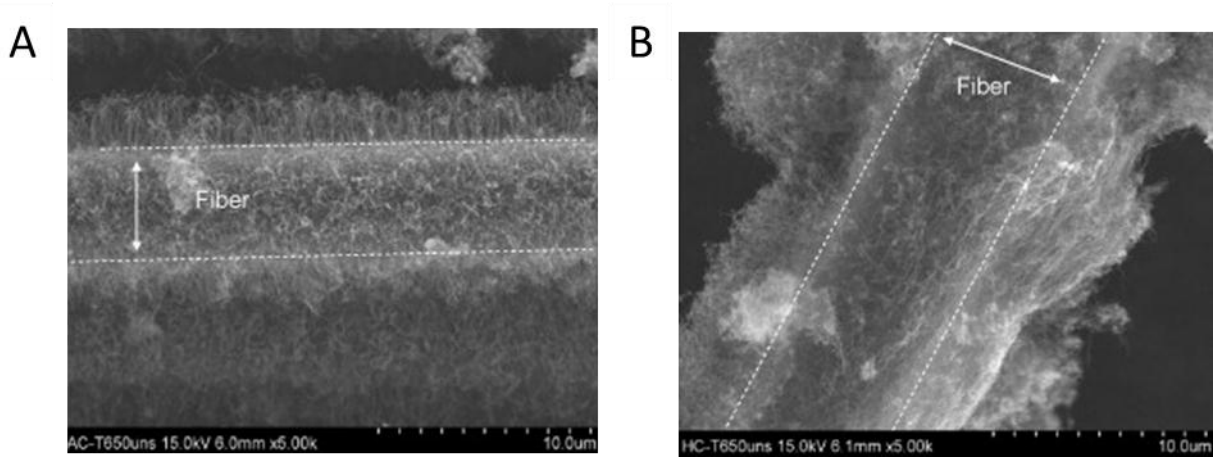

Figure 1-14. Carbon fiber with carbon nanotubes grown on the surface. a) Shows radially aligned carbon nanotubes, while b) shows randomly oriented carbon nanotubes. [Reprinted with permission from Sager RJ, Klein PJ, Lagoudas DC, Zhang Q, Liu J, Dai L, Baur JW. Effect of carbon nanotubes on the interfacial shear strength of T650 carbon fiber in an epoxy matrix. Composites Science and Technology 2009;69(7-8):898-904.]

1.2.3.3 Natural nanomaterials for hierarchical fibers

Hierarchical fibers can also be created with naturally derived nanomaterials. While the field is still in its infancy, natural fibrils from bacterial cellulose can be grown from the surface of structural fibers to improve the interface strength [119,120]. Biologists have

long studied the growth of cellulosic fibrils and found cellulose or other proteins to exhibit a hierarchical, crystalline structure that leads to relatively high mechanical performance from a natural, biodegradable material. The growth of a natural material is typically performed on natural fibers (sisal, jute) to create a biodegradable, environmentally friendly alternative composite to the traditional petroleum-based carbon fiber – epoxy matrix composites. The mechanical performance of these composites has limited their widespread adoption, stronger interfaces could increase the use of biodegradable composites in industrial applications.

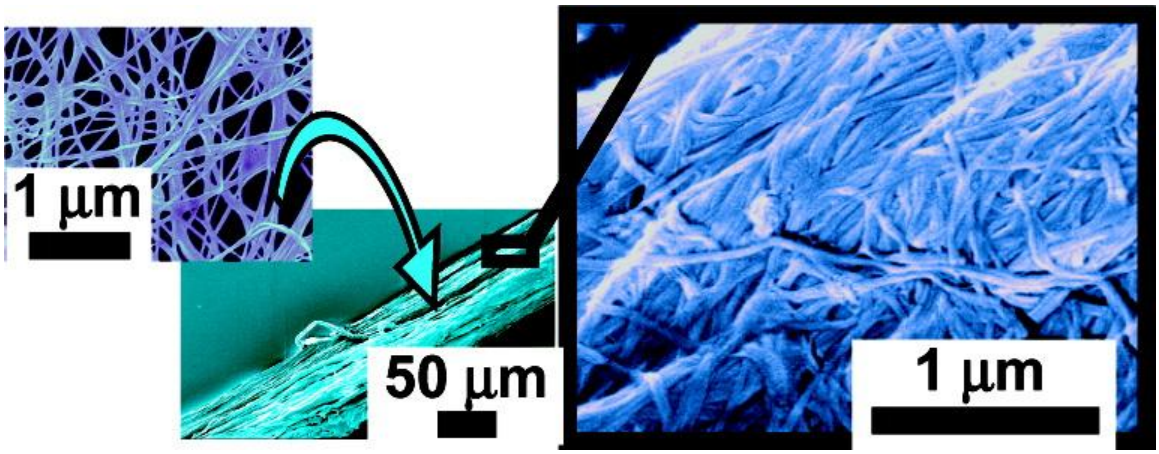

Figure 1-15. Bacterial cellulose on the surface of sisal fibers creating an enhanced hierarchical interface. The natural whiskers improved interface strength with a cellulose acetate butyrate matrix by 50%. [Reprinted with permission from Pommet M, Juntaro J, Heng JYY, Mantalaris A, Lee AF, Wilson K, Kalinka G, Shaffer MSP, Bismarck A. Surface Modification of Natural Fibers Using Bacteria: Depositing Bacterial Cellulose onto Natural Fibers To Create Hierarchical Fiber Reinforced Nanocomposites. Biomacromolecules 2008;9(6):1643-1651.]

One example of the natural surface whiskerization of a sisal fiber is shown in Figure 1-15. The surface of the sisal fibers is typically smooth and the addition of randomly oriented fibrils on the surface of the sisal fibers reinforces the interphase to provide more of a gradient in mechanical properties. The deposition of the bacterial cellulose improved the interface strength of the composite by 50% but caused cohesive

failure of the surrounding polymer matrix instead of adhesive failure for the bare fiber composites. Natural surface whiskerization is still a very new emerging field, but it stands as a novel approach to producing natural, renewable composites with sufficient mechanical properties.

1.3 Overview of Contributions

The research performed here serves as a template for the development of enhanced composite interfaces in high strength structural fibers. The work here takes an approach combining chemical treatments with physical interface enhancements to provide a methodology for future interface design. By using an inorganic interphase, ZnO nanowires, the design space is opened to enable fiber functionalization that does not damage the underlying fiber properties and creates a functional gradient in the polymer matrix not requiring further demands on the design of structural polymers. This research also presents some broadly applicable surface treatment techniques and demonstrates the low temperature growth of nanowire arrays on structural fibers.

1.3.1 Functionalization of Aramid Fibers without Reduction in Tensile Strength

One significant contribution of this research is the publication of a technique to functionalize aramid surfaces with carboxylic acid groups without reducing the tensile strength of the fibers. The reaction hydrolyzes the polymer chains in the amorphous shell of the aramid fibers to create a primary amine and a carboxylate salt. The second step of the reaction is to perform an ion exchange wash with a mineral acid to remove the metal ion and create a carboxylic acid group. This process has not been demonstrated in the literature prior to this work, in particular the ion exchange has not been seen as previous research has unsuccessfully attempted to graft to the primary

amine group. Spectroscopic evidence and change in material properties is presented to demonstrate the effectiveness of this technique.

1.3.2 Functionalization of Carbon Fibers without Reduction in Tensile Strength

A novel carboxyl functionalization technique for carbon fibers is developed for this research. The technique utilizes existing hydroxyl defects to graft short chain carboxylic acid terminated molecules to coat the surface in carboxylic acid groups without requiring oxidation of the fiber or introducing further defects to the fiber surface. The one step grafting procedure represents a significant departure from preexisting techniques that either attempt to oxidize the fiber surface or employ radical capture reactions to functionalize the fiber surface. The reaction conditions are optimized and the effect of the functionalization on the fiber tensile strength is detailed.

1.3.3 Growth of Whiskers on Aramid Fibers

The growth of aligned arrays of inorganic nanowires on aramid fibers has remained a challenge; in particular achieving adhesion of the nanowires to the inert surface of aramid fibers. With the development of the surface functionalization technique to improve adhesion, the first growth of nanowires for structural enhancement of aramid fibers is presented. Prior to this work, nanowire growth on structural fibers required prohibitively high temperatures or vacuum environments that the fibers simply could not resist. The low temperature solution processing of ZnO nanowire arrays enables the growth of nanowire arrays on aramid fibers and the functionalization enables strong adhesion. The following research details the growth procedures and mechanical testing, which shows up to 40% improvement in the interfacial shear strength of the resulting composite.

1.3.4 Growth of Whiskers on Carbon Fibers

This research contributed here also provides an in depth study of interface enhancement in carbon fiber composites through the growth of ZnO nanowire arrays on the fiber surface. Fiber functionalization enables strong adhesion of the nanowires to the fiber and mechanical testing shows that single fiber composite interface strength can increase 100% and large scale composite shear strength can increase 38%, with no tradeoff in tensile performance. This work is one of the first describing a solution based growth method of nanowires on the surface of carbon fibers, a major development in interface engineering for composites.

1.3.5 Demonstration of Mechanism of Adhesion of ZnO Nanowires to Aramid and Carbon Structural Fibers

The central contribution of this work is the demonstration of the mechanism of adhesion between ZnO nanowires and the two structural fibers studied. The addition of the ZnO nanowire interphase creates two interfaces in place of the single fiber – matrix interface. Both of the new interfaces must be superior to the previous interface if a bulk increase in interfacial shear strength is observed. The increased surface area and mechanical interlocking afforded by the aligned nanowire array interface nearly guarantees that that nanowire – matrix interface is stronger than the previous fiber – matrix interface. The contribution of this work identifies the chemical mechanism of adhesion of ZnO nanowires to structural fiber surfaces. The demonstration of surface chemistry control and identification of the effect of chemistry on interface strength is the key, original scientific contribution of this work and has applications across a wide array of materials engineering applications.

CHAPTER 2
SURFACE TREATMENT OF STRUCTURAL FIBERS

The addition of an interphase to a structural composite creates two new interfaces to replace the existing fiber to matrix interface. This work focuses on the development of a ZnO nanowire interphase, which creates a high surface area interface with the polymer matrix. The second interface created, between the ZnO nanowires and the fiber, has the same surface area and surface roughness as the previous interface between fiber and polymer matrix, illustrated in Figure 2-1. Surface area and interlocking are dominant factors in determining interface strength [121,122]; however changing these parameters often damages the fiber and creates a design tradeoff that is not acceptable in all applications. Behind these two factors, chemical interactions at the surface are the most significant in determining interface strength, thus much of this work focuses on controlling the surface composition of the fiber. Chapter 2 addresses the modification of aramid and carbon fibers to create the desired surface functional groups to control and enhance the strength of the fiber – ZnO interface.

The hypothesis of this research is that ZnO nanowires interact with carboxylic acid groups on the surface of the fibers and as such, functionalization procedures will focus on this desired functional group. Chapter 2 will develop new functionalization procedures for use in creating or removing carboxylic acid groups on the surface of the fibers. Original functionalization schemes for both aramid and carbon fibers will be presented.

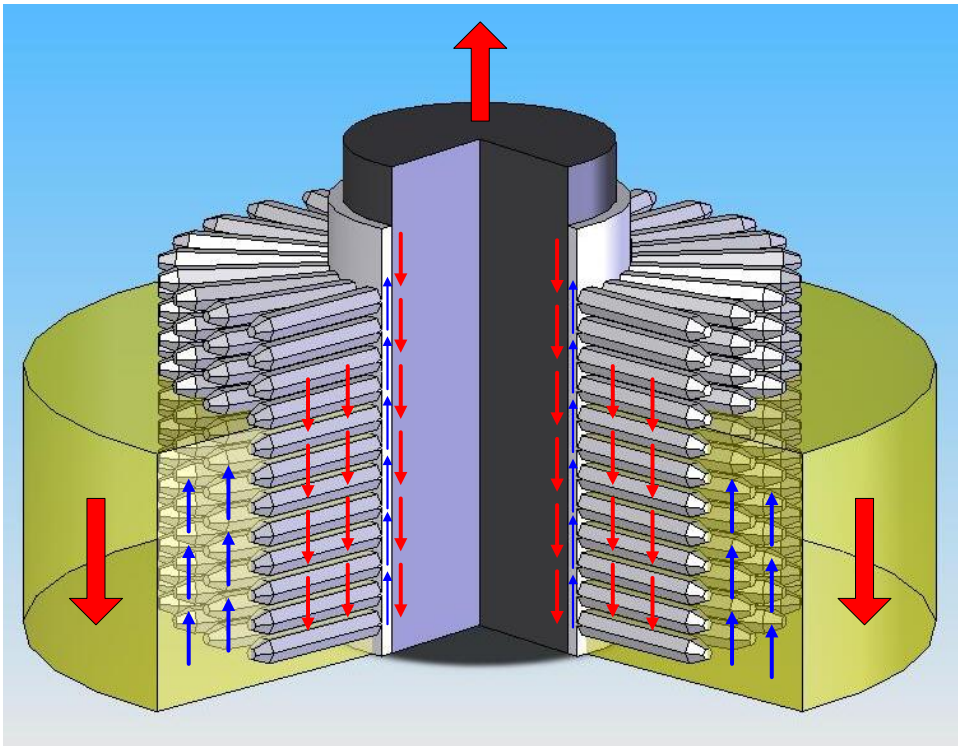

Figure 2-1. Schematic of load transfer across interfaces during pullout of a ZnO nanowire coated fiber. The addition of ZnO nanowires creates two interfaces in place of the previous fiber – matrix interface.

2.1 Surface Functionalization of Aramid Fibers

Several techniques for the functionalization of aramid fibers were previously reviewed in Chapter 1 as they were employed to directly enhance bonding with epoxy based polymer matrices. Many of these techniques relate to forming primary amines, the active functional group in epoxy resin curing agents [104]. This work focuses on using carboxylic acid functionalization to coordinate and interact with the ZnO nanowires and thus only functionalization procedures that produce carboxylic acid are sought. While functionalization procedures exist to produce carboxylate salts [123], no procedure has been published to date that produces carboxylic acid on aramid fibers [124].

2.1.1 Reaction Mechanism of Aramid Functionalization

The existing functionalization technique that most closely produces carboxylic acid groups was first reported by Keller [125] and later developed and validated by Chatzi and colleagues [123]. The reaction is relatively simple and illustrated in step 1 of Figure 2-3, adapted from the seminal paper by Keller et al. [125], it is well known that strong bases can hydrolyze amide bonds (which is often used to break down proteins in biochemical analysis) to create a carboxylate salt and a primary amine [17]. The functionalization was originally designed by Keller et al. to utilize the surface coverage of primary amines for cross linking with epoxy matrices and the creation of a carboxylate salt was incidental [126,127]. Keller et al. ended at this point of the functionalization and attempted to improve the interfacial shear strength directly through functionalization.

The hydrolysis of the amide bond in the aramid fiber chain is shown in the first reaction of Figure 2-3. Strong bases are highly effective for catalyzing the hydrolysis of the amide bond and the process proceeds from the surface inward, breaking a few surface chains and then working inwards. The microstructure of aramid fibers is generally recognized to contain radial pleats of crystallites coated with a highly aligned aramid polymer shell, although there is some debate as illustrated in Figure 2-2. The crystalline fibrils in the center of the fiber, shown in Figure 2-2, contribute to the strength and enable the extreme toughness for which aramid fibers are famous [128,129]. It should be noted that this hierarchical fibrilar structure is the same structure that creates the unmatched toughness and damage tolerance of natural systems [130]. This microstructure is also particularly advantageous for surface functionalization procedures as the thin surface layer is susceptible to chemical functionalization procedures without

damaging the load bearing, hierarchical fibrils in the center of the fiber. The process must be tuned to minimize internal structural damage [131]. The reader is referred to a detailed study of the deformation and failure mechanisms caused by the skin – core structure of aramid fibers for a more in depth study of the skin – core deformation mechanisms [132]. It should be noted that neither Keller et al. nor Chatzi discuss the impact of this functionalization scheme on the tensile strength of the fibers, thus it remains unknown if this procedure can be tuned to produce the desired functional groups without deleterious effects on the mechanical properties of the fibers.

Hydrolysis of an amide bond in a strong base produces a primary amine and a carboxylic acid; however the basic environment with free Na^+ ions inevitably leads to the formation of carboxylate salts instead of carboxylic acid [17]. Figure 2-3 describes the reaction creating carboxylate salts in the first step due to the high pH and high concentration of Na^+ ions. Sodium, as well as aluminum, ions were found to contaminate the ZnO growth solution, resulting in poor nanowire growth. Recent work has identified that certain ions like magnesium and aluminum can act as growth inhibiting layers on the individual ZnO nanowires by preferentially bonding to specific facets of the crystals [133]. This can be used for rational shape control in some instances however, the sodium left on the surface of the aramid fibers after functionalization was found to disrupt growth in subsequent experiments. This is detailed further in the ZnO growth section of Chapter 3. The problems caused by Na^+ contamination motivate the development of this functionalization procedure.

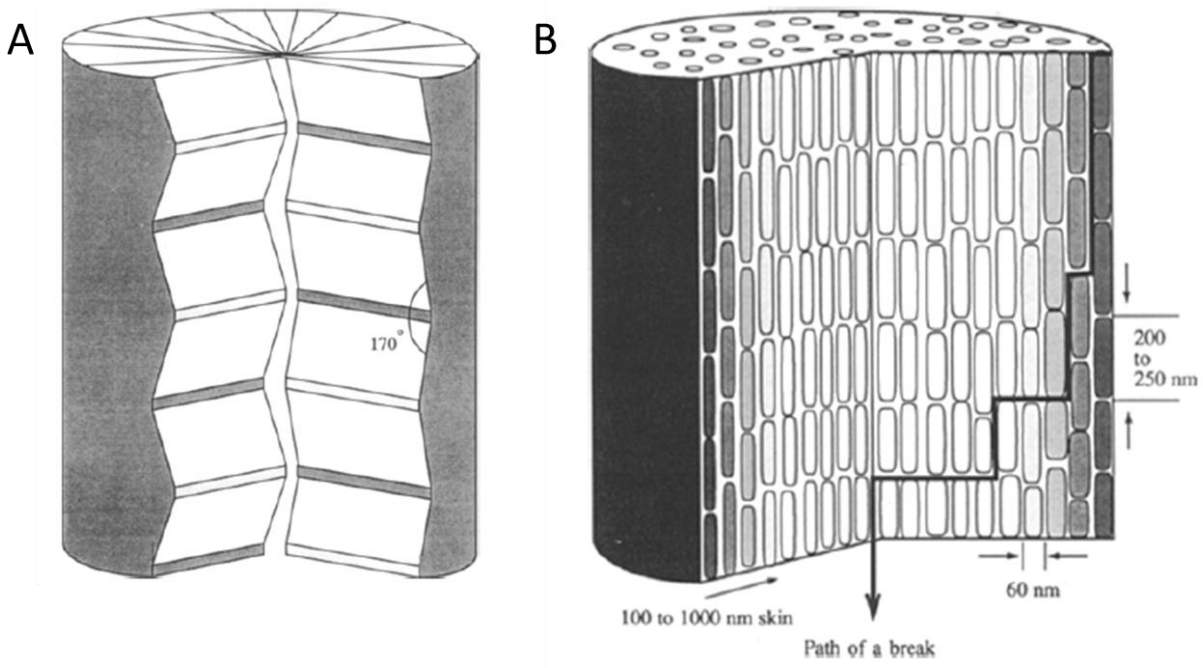

Figure 2-2. Proposed hierarchical microstructures of aramid fibers. The microstructure is generally accepted to be a combination of the two with an internal fibrilar structure aligned into radial pleats. The hierarchical structure leads to tortuous crack paths and spalling which dissipates energy and yields the incredibly toughness characteristic of aramid fibers. [Reprinted with permission from Kalantar J, Drzal LT. The bonding mechanism of aramid fibres to epoxy matrices. Journal of Materials Science 1990;25(10):4186-4193.]

The ion exchange wash developed here will remove the detrimental sodium ions and replace them with protons. Carboxylate salts can be reversibly converted to carboxylic acid by increasing the concentration of H^+ ions to replace the Na^+ ions bound to the carboxylate group, which is most easily accomplished with a strong acid. The second reaction of Figure 2-3 shows the ion exchange wash utilizing hydrochloric acid to remove the Na^+ ions and replace them with H^+ ions to create carboxylic acid groups. Hydrochloric acid is selected because it is a readily available strong acid and is not known to dissolve aramid fibers like concentrated sulfuric acid. The ion exchange wash must also preserve the previous functionalization and should not cause additional reactions to alter the surface chemistry. Strong acids are also capable of catalyzing the

hydrolysis of amides [17], although not as efficiently as strong bases. The hydrochloric acid ion exchange wash will provide the fibers with the chemistry required without disrupting the growth of the ZnO nanowires.

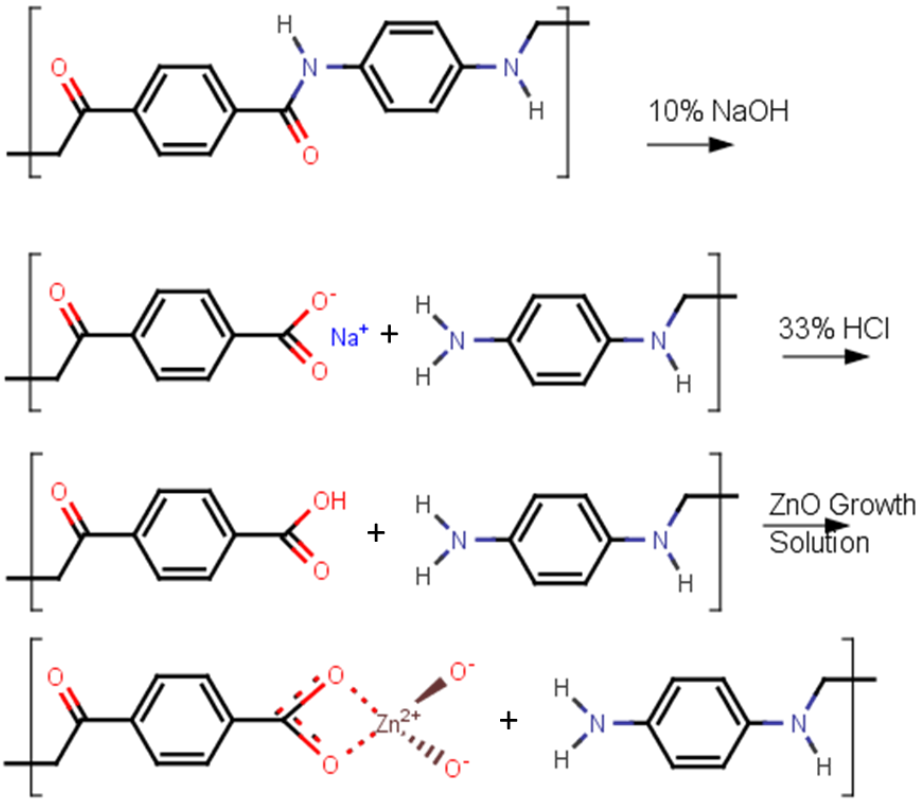

Figure 2-3. Functionalization reaction of aramid fibers through cleavage of amide bond. First the amide linkage is cleaved to create a carboxylate group and a primary amine group. The carboxylate group is then stripped of the Na^+ ion through an ion exchange wash. Finally, the ZnO nanowire growth solution enables the carboxylic acid to act as an anchor site for a Zn^{2+} ion in the ZnO crystal.

The thermodynamics of ZnO nanowire growth are well documented and described in more detail in Chapter 3, relying mainly upon the temperature and pH dependence of various $Zn(OH)_x$ and $Zn(NH_3)_x$ species to gradually precipitate high quality, single crystal nanowires [134]. The nanowires begin growing from a polycrystalline seed layer which is formed through the deposition and crystallization of 1-5 nm quantum dots onto

the surface of the fiber. These quantum dots form a cohesive layer and interact with the functional groups on the surface of the fibers [124].

2.1.2 Experimental Methods for Aramid Fiber Functionalization

Unidirectional aramid fibers were purchased from CST Sales (Tehachapi, CA). The aramid fibers were then washed in two successive chloroform baths followed by absolute ethanol to remove a manufacturer applied surface adhesive. The fibers were dried for 30 minutes under vacuum at 80°C and then rinsed in acetone and ethanol to remove any further organic surface contaminants. Fibers were functionalized by soaking in a 10% aqueous NaOH solution that was cooled to 23°C. Fibers were soaked for 20 minutes in an open beaker and then washed several times in large quantities of deionized water. Fibers were then dried for 60 minutes at 100°C under vacuum. An ion exchange process was then performed on the functionalized fibers through an acid wash in a beaker of 33% HCl for 10 seconds and then rinsed several times in deionized water. The fibers were again dried at 100°C for 60 minutes under vacuum and mounted for XPS and FTIR analysis.

A Bruker IFS 66 v5 vacuum spectrometer was used. Functionalized fibers were strung across a plate and IR radiation transmitted through a hole in the plate. The sample chamber was under vacuum to reduce the effects of water and CO_2 on the data. The x-ray photoelectron spectrometer experiments were run at ultra high vacuum, <10-8 Torr, with excitation from an Al kα single anode source. The samples were mechanically mounted with a non-magnetic mask and charge compensation was performed with a 4eV flood gun above the sample near the condenser lens. Machine control and data collection was performed with Avantage software and data analysis, including peak decomposition, was performed in CASA XPS.

2.1.3 Spectroscopic Verification of Functionalization

Several methods exist to identify the chemical structure of organic fibers, although not all specifically probe the surface of the fibers. Organic chemists generally probe molecular structure through mass spectroscopy, Fourier transform infrared spectroscopy and nuclear magnetic resonance spectroscopy. When combined with various chromatography and thermal characterization methods (thermogravimetric analysis and differential scanning calorimetry), a clear picture of the molecular structure emerges. While chromatography is often used to separate molecules based upon surface adsorption, the other techniques listed above are bulk techniques and not surface sensitive. Materials science contributes surface sensitive techniques such as x-ray photoelectron spectroscopy, auger electron spectroscopy and secondary ion mass spectroscopy which are surface sensitive but not structurally sensitive. From these techniques, FTIR and XPS are selected to characterize the surface of the aramid fibers. FTIR has fairly high chemical specificity and is very sensitive to the molecular structure of the material. FTIR is not constrained to the surface and the surface signal can be dominated by the signal from the bulk. For graphitic fibers, this is particularly impactful as graphite is an excellent black body absorber and it is very difficult to obtain a reliable signal, thus FTIR will only be used for aramid fibers. XPS is selected because it has some chemical sensitivity and is highly surface sensitive. While the structural resolution is limited, XPS can discern the number of polar bonds that a carbon atom has which can identify some of the functionalization that will be completed here. These two techniques will be used to identify the aramid functionalization and the results will be discussed below.

2.1.2.1 Fourier transform infrared spectroscopy

Transmitted IR studies were performed to validate the chemical structure of the fibers. The characteristic absorbance was collected in the IR range from 4000 cm^{-1} to 400 cm^{-1} and will be sensitive to organic carbon bonds [135]. In order to account for slight sample to sample variations in signal intensity, absorbance spectra were normalized by the absorbance at 864 cm^{-1}, which is characteristic of amide substituted aromatic rings and consistent with the literature [123]. It is observed in Figure 2-4 that the peak corresponding to C-N absorption,[135] ~1110 cm^{-1}, was reduced in relative intensity following the sodium hydroxide treatment. Sodium hydroxide is a well-known catalyst for hydrolysis of the amide bond and this is expected to be the bond severed during the reaction. The alternative explanation would be severance of the aromatic C – N bond however, the reaction conditions are not suitable for an aromatic substitution reaction of this form [136]. The reduced absorption is attributed to the reaction and creation of surface functional groups through hydrolysis of the amide bond. Since the reaction conditions are quite mild for only a brief time, the reaction is presumed to occur mainly on the surface and not progress to the inner fibrils of the fiber. Unfortunately, FTIR spectroscopy is a transmission technique; signals are averaged over the entire volume of the sample and thus the small portion of polymer chains on the fiber surface that are broken result in a relatively weak modification of the IR signal as can be seen in Figure 2-4. The variation in the IR signal measured was found to be repeatable.

After the initial hydrolysis of the amide bond, a carboxylate salt remains instead of the desired carboxylic acid group. It was observed that carboxylate groups did not encourage or even permit the attachment of ZnO nanowire arrays. This was attributed to the presence of the Na^{+} ion at the bonding site of the carboxylic acid group or the

contamination of the growth solution by Na^+ ions, as reviewed earlier. The ion exchange wash was developed to remove the Na^+ ions without catalyzing the condensation reaction which would reverse the functionalization. A strong acid is chosen in order to increase the concentration of free protons to replace the missing Na^+ ions. Since acids also catalyze the hydrolysis of amide bonds, reversal of the functionalization is not expected to occur. A 33% HCl solution ion exchange wash is shown to remove the carboxylate salt absorbance [137] created during functionalization. Figure 2-5 shows an increase of carboxylate absorbance after functionalization followed by a return to as received levels after the acid wash, validating that the acid wash is effective in removing Na^+ contamination.

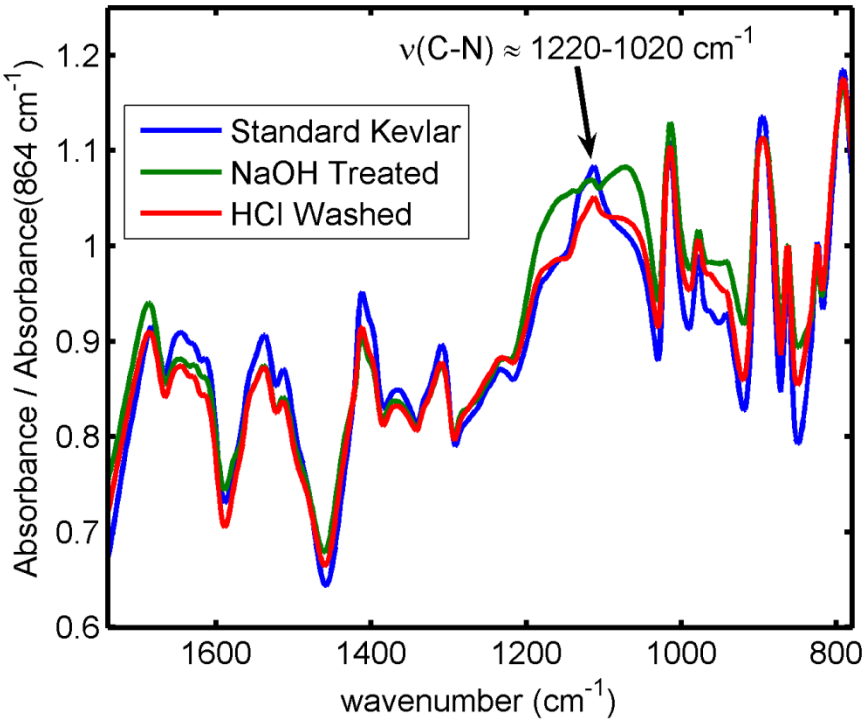

Figure 2-4. Reduced absorbance of C-N stretching due to cleavage of the amide linkage during functionalization.

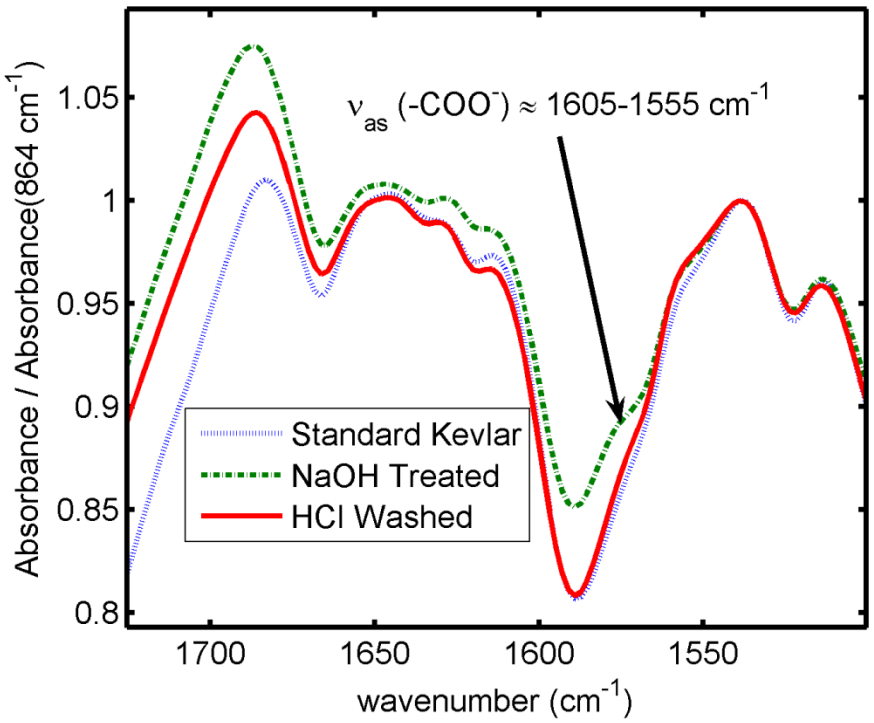

Figure 2-5. Absorbance of carboxylate salt group on functionalized aramid fibers. Indicated shoulder corresponds to anti-symmetric stretching of the -COO$^-$ bond.

2.1.2.2 X-ray photoelectron spectroscopy

X-ray Photoelectron Spectroscopy (XPS) provides analysis of the surface functional groups by analyzing the bonding states of the atoms present on the surface of the sample. The survey scan analysis of the fibers will indicate the surface composition of the fibers. Aramid fibers, as received, have three bonding states of carbon, one bonding state of nitrogen and one bonding state of oxygen. The chemical functionalization treatment should create one new state each of carbon, oxygen and nitrogen; thus four carbon peaks, two oxygen and two nitrogen peaks are fit to each high resolution scan of each element. In order to validate the chemical treatment and surface functionality, the hypothesized C1s peaks must be listed and compared to collected spectra. It is expected that carbon, oxygen and nitrogen will all be present

and most other elements will not be present; specifically sodium which should be removed by the ion exchange wash. The aromatic carbon state, C1, theoretically appears 10 times per monomer in Figure 2-6, which should yield an area fraction of 10/14 or 71.4%. C2 occurs two times per monomer and should show 2/14 or 14.3%; C3 should also appear one fifth as often as C1, occurring twice. Furthermore, the creation of a new bonding state corresponding to a carboxylic acid could occur as many as 2 times per monomer unit for full progression of the reaction. Since the carboxylic acid groups are all from hydrolyzed amide links, the concentration of carboxylic acid groups and the amide links (2 carbons per monomer) should sum to the concentration of the aromatic substituted carbons (2 carbons per monomer), which are not expected to be affected by the functionalization procedure.

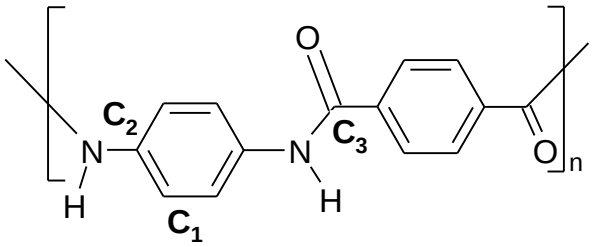

Figure 2-6. Carbon states in aramid fibers, as received.

Samples analyzed by XPS consisted of bundles of aramid fibers mechanically mounted to an aluminum holder with screws and masks. The x-ray source is difficult to focus with sufficient intensity and thus a large area of fibers is illuminated; a circle approximately 1 mm in diameter. This contains several thousand fiber surfaces and thus the measurement averages over the entire spectrum of fibers. The photoelectron escape depth for the samples is expected to be 1-3 nm, effectively making this a surface technique that is capable of penetrating a few atomic layers and not much more than that. The area of the peaks measured is somewhat uncertain as the fitting can

lead to variation in the peak intensity; however peak areas of 1% can certainly be measured above the noise floor. Furthermore, the fitting procedure used for much of the data is done through a regression algorithm and thus does introduce bias from the operator. Peak location sensitivity is within 0.1 eV; although this is again much more sensitive to the fitting procedure used than the physical instrument capabilities. XPS is certainly a technique that is capable of measuring the phenomenon explored here, provided certain factors are accounted for.

One particularly important aspect of performing an XPS study on insulating polymeric samples is the accumulation of surface charge. Since the sample accepts an x-ray (zero charge) and emits an electron (-1 charge), the sample will accumulate a positive charge. This charge will help to restrain the electron, and electrons of a higher energy will be emitted and detected. The peaks of the sample collected will be shifted, sometimes by a few eV or by as many as 50-100 eV in extreme cases. The techniques developed to compensate for this include the use of conductive masks or low energy electron flood guns [138]. The first technique employed on this sample was to place a mask consisting of a metallic sheet with a small hole in it over the fibers to maximize contact with the ground path. Second, a low energy (4 eV) electron emitter was used to drop electrons on the surface from above the collection lenses to compensate for the accumulated charge. The spectra were also minimally corrected based on the well-established value for the binding energy [138] of an aromatic carbon, the largest peak center was shifted to 284.7 eV. The peaks were analyzed for spread (full width at half maximum) and center location.

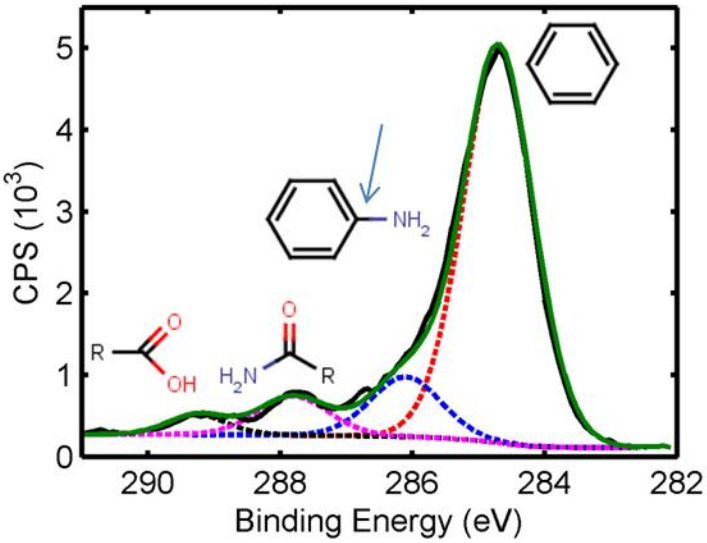

Figure 2-7. Decomposed bonding states of C1s energy region with labeled chemical structures, showing the presence of functional groups on the aramid fiber surface. Table 2-1 shows the relative fraction of each state.

The collected spectra of intensity at various binding energies are decomposed into a sum of Gaussian-Lorentzian distributions centered at various locations. A Shirley background was subtracted and the peaks decomposed as shown in Figure 2-7. Peak labels were introduced to show the chemical bonding state associated with the particular carbon. Four individual peaks best matched the collected data in the carbon region on the functionalized fiber, which is also consistent with the theorized number of peaks. The peak locations align with values presented by Beamson and Briggs [138] in their analysis of the bonding states of various polymers. The broad elemental composition scan indicated that the fiber had only carbon, oxygen and nitrogen present, which was consistent with the theorized hydrolysis reaction and ion exchange wash.

As can be seen in Table 2-1, the peak fit locations align remarkably well with the predicted locations. The largest peak, aromatic carbon, was aligned to match the literature value [138] and compensate for the charging, thus showing no error. The charging difference is expected to be nominally the same on all electrons and so all

peaks are shifted by the same amount. In order to validate the reaction and ensure that the carboxylic acid groups are not from contamination, the state concentrations must be compared. It is theorized in Figure 2-3 that the functionalization reaction splits the amide linkage while preserving the aromatic amine group. The concentration of aromatic amines is expected to remain constant and the sum of carboxylic acid groups and amide linkages should remain equal to the aromatic amine concentration. A higher concentration of aromatic carbon is observed, the sum of the carboxylic acid state of carbon and the amide link state of carbon (10.9%) is very close to that of the aromatic amine (11.7%). Furthermore, the concentrations are correct which further validates the conclusions of the functionalization. Table 2-1 shows that amide links are still present, showing that only a limited fraction of the surface polymer chains are broken and the mechanical properties are not expected to be degraded because the internal fibrilar structure is maintained.

Table 2-1. Theoretical and experimental bonding state peak locations and concentrations showing excellent agreement between peak locations and published values. The stated concentrations of carboxylic acid and amide bond sum to the concentration of aromatic substituted carbon which is consistent with the proposed reaction.

Chemical Structure	Peak Location (eV)	Peak Fit (eV)	Error (eV)	Theoretical State Concentration	Measured State Concentration
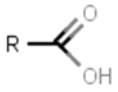	289.18 289.33	289.25	0.07 -0.08	00.0%	3.24%
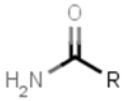	287.97 288.59	287.80	-0.17 -0.79	14.3%	7.61%
	284.70	284.70	0.00	71.4%	77.5%
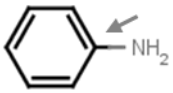	285.94	286.10	0.16	14.3%	11.7%

The novel functionalization of aramid fibers presented here clearly demonstrates the efficacy of the treatment for creating the desired surface chemistry. The combination of FTIR spectroscopy and XPS strengthens the claim because the signal generation mechanism differs, reducing the likelihood that contamination is influencing the measurements since both techniques confirm the same result. The mechanical properties of the fiber after functionalization will be discussed in Chapter 4 to provide a complete review of the impacts of the functionalization.

2.2 Surface Functionalization of Carbon Fibers

2.2.1 Motivation for Alternative Functionalization Procedures

The lifetime of high performance carbon fiber reinforced composite materials is often limited by a weak interface between the fiber and surrounding polymer matrix [94,139]. This is of particular concern because the interface between the fibers and matrix plays an important role in determining the macroscopic shear, transverse and out of plane properties of a composite [4]. Carbon fibers contain a high fraction of graphitic carbon, which gives the fibers high strength, but also makes them less reactive. The non-polar nature of the graphitic bonds as well as their high stability prevents the fibers from covalently crosslinking or interacting with the surrounding polymer matrix [94]. The functionalization of carbon fiber surfaces to enhance the interaction between the fibers and matrix has been an academic and commercial pursuit for over 30 years. As a result, plasma treatments [59,66,140-145], chemical oxidation [146-148], electrochemical treatments [149-154], high temperature atmospheric oxidation [74,155,156], radical trapping grafting [157-160] and surface functional group grafting procedures [161-163] have all emerged as viable techniques for surface functionalization of graphitic carbon. Plasma, chemical, electrochemical and

atmospheric processes typically employ strong oxidizing chemicals or oxidizing atmospheres to create polar oxygen groups from the existing carbon in the fiber. While the addition of functional groups has been shown to effectively increase the interfacial interaction between the fibers and matrix [141,144,147,153], the techniques tend to consume the base fiber and the reactions aggressively create pits in the surface of the fiber. Oxidative functionalization does not create a specific surface chemistry; nor does it achieve the end goals of this work because of the often negative effects on the base fiber strength.

While quantitative tensile data is rather sparse, it is quite clear that plasma [140,142,143], chemical [147,148], electrochemical [149] and atmospheric [156] oxidation procedures hastily roughen the surface of the fiber, drastically alter the crystal structure and significantly change the chemical state of the surface of the fiber. It is well known that surface defects can have drastic effects on the tensile strength of a fiber so must be avoided. Experimental testing will show that even a mild electrochemical oxidation procedure can reduce the tensile strength of the fiber by 35%. One previous report states that heavy electrochemical oxidation can make the fibers so fragile that they are impossible to handle, even in a laboratory environment [164]. In addition to severely damaging the core fiber strength, oxidation creates a mixture of C-OH, C=O, COC and COOH functional groups; which makes further chemical derivation difficult with a low yield. An ideal functionalization process will create uniform functional groups on the surface of the fiber without any impact on the tensile strength or surface roughness. This objective necessitates the development of non-oxidative, carboxylic

acid specific functionalization techniques to create a suitable surface for the attachment of a ZnO interphase.

2.2.1.1 Carboxyl functionalization through defect grafting

Grafting offers an alternative to oxidative functionalization that does not create additional defects on the surface and preserves fiber tensile strength. Polymer grafting methods to graphitic carbon have primarily focused on smaller reinforcements like carbon black powder, carbon nanofibers and carbon nanotubes; a similar chemistry applies to carbon fiber [36]. Grafting methods can be broadly divided into two categories, radical trapping reactions and reactions with surface functional groups. Radical trapping reactions employed in the functionalization of carbon fiber [157], carbon nanotubes [159], carbon black powder [165] and vapor grown carbon nanofibers [158] can effectively create the desired functionality; however the reactions tend to require complicated, unstable reagents and long reaction times [166]. Electrografting of aryl diazonium salts is also an effective radical trapping mechanism for functionalizing carbon fiber surfaces; but it employs similarly unstable reagents and requires electrochemical equipment for the reaction [157].

Grafting to existing surface functional groups has been well studied for carbon nanotubes [161,163,167] and vapor grown carbon nanofibers [36] yet many methods begin with an oxidative step to generate defects for higher grafting yield [36,163,167]. While the reduction in mechanical properties of nanoscale reinforcements is typically outweighed by the improved dispersion of the fillers, oxidation of carbon fiber does not offer the same advantages and pre-oxidation steps should be avoided if possible. After creation of surface oxygen groups, many nanoscale grafting methods treat carboxylic acid groups with thionyl chloride to create highly reactive and useful acyl chloride

groups [36,161-163]. Acyl chlorides are among the most reactive carbonyl groups and can bond with a number of functional groups to create a variety of chemical structures [17]. A functionalization process that creates additional grafting sites, specifically carboxylic acid groups, without the damaging effects of oxidation would have a number of applications and uses as a starting point for further chemical derivations.

The following sections present a new approach to surface functionalization that grafts desirable surface functionality (carboxylic acid) without oxidation, plasmas or other treatments that harm the mechanical properties of carbon fiber. The developed reaction bonds a short carbon chain to surface hydroxyl groups to form a pendent carboxylic acid with a relative surface coverage of up to 9.2%, thus constructively employing the large mixture of surface groups to create more carboxylic acid groups that are well suited for further chemical conversion or direct bonding to a polymer matrix. Since there is no oxidation or breaking of carbon-carbon bonds, the fiber should maintain full tensile strength after functionalization. Furthermore, the chemical purification of the surface and generation of a larger number of useful functional groups can assist in further grafting reactions to create high yield grafts without requiring a pre-oxidation step that frequently harms the fiber. One report indicates that the grafting yield of terminal amino groups on chemically oxidized carbon fiber was 6 – 13% [16], thus the grafting procedure demonstrated here is similar in yield to existing alternatives.

2,2-dimethyl-1,3-dioxane-4,6-dione (isopropylidene malonate, also known as Meldrum's acid) is employed frequently in the synthesis of macromolecules. Meldrum's acid is often reacted with phenol to form a carboxylic acid terminated ester [168-175]. Carboxylic acid functional groups can easily be converted to other functional groups

through many common reactions in organic chemistry, which is one reason why they are so often used as a building block for macromolecular synthesis. This work focuses on reacting pendent hydroxyl groups on the surface of carbon fibers with Meldrum's acid to create carboxylic acid terminated esters on the surface. These functional groups will be covalently linked to the fiber itself for strong attachment and the terminal carboxylic acid will provide chemical flexibility for a wide variety of applications. Additionally, Meldrum's acid reactions are known to have very high yield, over 80% [168]; thus a high density, complete coverage of functional groups is expected. The high reaction yield, non-oxidative nature, and ability to generate the versatile carboxylic acid group make this functionalization treatment ideal for carbon fibers. This section presents a new grafting reaction for carbon fiber functionalization, where the existing hydroxyl groups are simply and efficiently converted into terminal carboxylic acid groups for a variety of further grafting or chemical procedures.

2.2.1.2 Carboxyl functionalization through selective oxidation of existing defects

The surface functionalization with Meldrum's acid grafts a carboxyl terminated molecule onto existing hydroxyl defects to create a surface effectively functionalized with carboxylic acid. A second approach is to convert the existing defects into carboxylic acid with a selective oxidation. This type of oxidation is derived from previous graphitic carbon nanotube chemistry research and has been termed up-conversion in some instances. A mixture of perchloric acid and potassium permanganate selectively oxidizes the existing oxygen functional groups to carboxylic acid, without being so aggressive as to consume C – C bonds and create additional

defects. The following section will describe how selective oxidation is able to create carboxylic acid groups on carbon fiber without reducing the tensile strength.

One of the earlier documentations of a perchloric acid selective oxidation for graphitic carbon was in 1999 by Burghard et al. [176] in purifying and functionalizing carbon nanotubes after a nitric acid cleaning process. The selective oxidation enabled a Langmuir – Blodgett film deposition of the carbon nanotubes. Future works slowly began to adopt the up-conversion process as a subsequent step to the standard oxidative functionalization of carbon nanotubes [163], beginning with Sainsbury et al. [177] and followed later by others [178,179]. Carbon fiber has a similar graphitic structure to carbon nanotubes and similar oxidative selectivity is expected for both materials. This selectivity will preferentially oxidize existing surface defects without cutting tubes or breaking the graphitic sheets of a carbon fiber, enabling the intrinsic material properties to be maintained. This process stands to offer the same advantages as Meldrum's acid through a different chemical reaction by avoiding plasma, electrochemical or thermal oxidation procedures. This section will document both novel functionalization techniques and present the spectroscopic evidence for the reactions. The mechanical testing of the fibers will be presented in Chapter 3.

2.2.2 Experimental Methods of Carbon Fiber Functionalization

2.2.2.1 Materials

Hercules IM8 carbon fibers from Hexcel were cleaned by gentle rinsing in chloroform and ethanol in a beaker. The fibers then were vacuum dried at 80 °C prior to use. Great care was taken to minimize handling of the fibers during cleaning and mounting stages. In particular, the gauge section of the fibers used for tensile tests was never handled; only the free ends of the fibers were manipulated. In addition, the fibers

were received explicitly with no manufacturer applied surface treatment. Isopropylidene malonate (Meldrum's Acid), toluene, benzene, mixed xylenes and potassium permanganate were all purchased from Alfa Aesar and used as received. N,N-dimethylformamide (DMF) was purchased from Mallinckrodt Chemicals and used as received. Citric acid and perchloric acid (60%) were purchased from Fisher Scientific and used as received.

2.2.2.2 Fiber functionalization

Carbon fibers with 6 cm lengths were cleaned as listed above and refluxed in either 0.01M or 0.05M isopropylidene malonate in the given solvent. After the given treatment time, the fibers were rinsed three times in ethanol and then dried in air. Selected samples were also washed in boiling water and observed to show the same X-ray photoelectron spectroscopy (XPS) trace as ethanol washed samples.

Separate experiments for upconversion began with 6cm tows of the same carbon fibers in a 100 mL flask. A mixture of 21 mL of perchloric acid, 20 mL of water and 90 mg of potassium permanganate was sonicated for 4 minutes at room temperature. The mixture was then poured over the carbon fibers for 10 minutes, at which point 42 mL of a 0.0148M citric acid solution was added and mixed in. The brownish purple solution turned clear in a matter of seconds as the citric acid was preferentially oxidized to quench the reaction. The fibers were then washed thrice in ultrapure water and dried in air.

The hydrazine reduction technique was performed with the same starting materials, which were then refluxed in 10% hydrazine hydrate (98%, Alfa Aesar) in water for 10 hours. The fibers were washed in ultrapure water three times and dried. The nitric acid oxidation was performed in 100 ml of nitric acid (70%, Fisher) by

refluxing for 8 hours. Fibers were cleaned with Soxhlet extraction in 18.2 MΩ·cm water for 6 hours and dried at 70 °C.

2.2.2.3 Spectroscopic analysis of functionalized fibers

Fibers to be analyzed by XPS were vacuum dried at 100 °C for 4 hours and then loaded into a high vacuum exchange chamber (<2 x 10^{-8} mbar) overnight prior to sample analysis. All experiments were performed with a pressure of less than 1.5 x 10^{-9} mbar. Carbon fibers with 3 cm lengths were mounted underneath copper masks with stainless steel screws to avoid contamination from hydrocarbon sources like double sided tape. All data was collected on a VG ESCALAB 220i-XL and processed using CASA-XPS. All samples were excited by an Al k-α (1486 eV) monochromated x-ray source and a through-the-lens electron flood gun was used to compensate any charge losses. Electrons were collected at a 90 ° take-off angle and x-rays excited the fibers from an angle of 45° from the axis of the fiber. Corrections of less than 2 eV were applied to some of the samples in order to align the main C1s peak at 284.7 eV. Each high resolution spectrum was first fit with a Shirley background and then decomposed into four components, one for each oxidation state, to fit the data. Fitting was performed with the aid of CASAXPS using the built in Marquette regression function, with the initial fit starting from the authors' best attempt. Each dataset was fit with curves (a Gaussian 70% - Lorentzian 30% mixture, GL30) that were constrained in location and FWHM to realistically model the chemistry of the fiber and capability of the instrumentation, respectively. The instrumentation was calibrated for peak width on a sample of commercially available highly oriented pyrolytic graphite (NT-MDT, Zelenograd, Moscow, Russia), which resulted in a peak width of 0.6 eV. All peaks had a constrained FWHM of 1.1-1.7 eV and peaks were constrained at 284.5-285.5 eV, 285.5-287.0 eV,

286.5-288.0 eV and 288.0-290.0 eV. It was observed through a series of preliminary samples that occasionally the low binding energy side of the peak would not match the GL30 curve shape because the fiber to mask contact was not always sufficient. The residuals of all data at binding energies higher than the main C-C peak were tested for normality with a χ^2 test, assuming estimated mean and variance, and a 5% confidence level. Thermogravimetric analysis (TGA) was performed in air with 15 mg samples of fibers, at a heating rate of 10 °C/min.

2.2.3 Defect Grafting with Meldrum's Acid

Carbon fibers are known to be decorated with pendent hydroxyl groups and typically these occur in the highest concentration compared to other oxygen functional groups [180,181]. Hydroxyl groups can often act as nucleophiles in organic reactions due to the lone pairs present on the oxygen atom. Meldrum's acid is susceptible to nucleophilic attack of the carbonyl carbon atom (positions 4 and 6) [171], which induces a ring opening reaction to form the malonic acid ester. The reaction typically follows the mechanism presented in Figure 2-8 where the nucleophilic oxygen atom opens the ring in one concerted step and then balances the molecule with a proton transfer. This reaction is often employed with a terminal hydroxyl group as the nucleophile, primary amines are also very effective nucleophiles for this reaction because they have a lone pair that is highly accessible [170,171]. Previous reactions have presented high yields, over 80% [168], which suggests that the functionalization should proceed close to completion to convert nearly all of the hydroxyl groups on the surface of the fiber into terminal malonic acid esters.

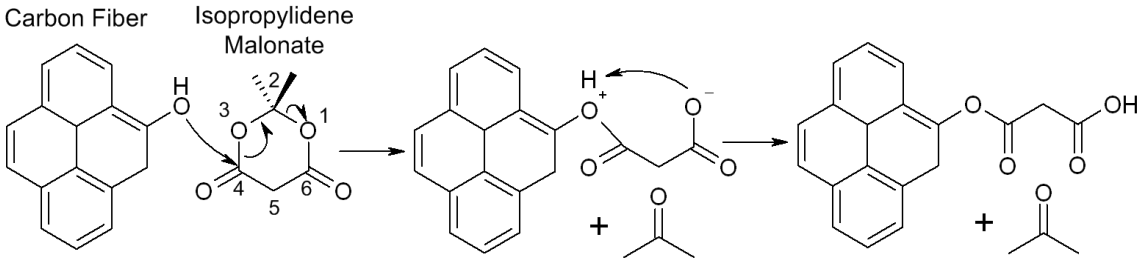

Figure 2-8. Ring opening reaction of isopropylidene malonate (Meldrum's Acid) with pendent hydroxyl group [171][158][158][158][158]. Numbers near the ring indicate the ring position. Carbon atoms 4 and 6 are subject to nucleophilic attack, which causes the ring to open leaving a terminal malonic ester.

X-ray photoelectron spectroscopy (XPS) is used to determine if the reaction creates the desired functional groups on the surface of the fibers. XPS is selected because it has the ability to resolve carboxylic acid functional groups and the sampling depth is only ~3-5 atomic layers [182]. First, survey spectra are collected to determine the elemental composition of the fiber surface. The only elements observed are carbon and oxygen, which is as expected since carbon fiber is generally thought not to contain significant quantities of other elements detectable by XPS on the external surface. The C1s and O1s regions are also analyzed with a high resolution spectrum to determine the specific content of each functional group. Four functional groups are observed in carbon fiber, corresponding to each oxidation level. Each high resolution spectrum is decomposed into a sum of the four components observed in carbon fiber; specifically C-C (284.7 eV), C-OH (286.5 eV), C=O (287.5 eV) and COOH (289.0 eV). Figure 2-9A shows a schematic of each type of functional group and the binding energy of the peak associated with it. There is ambiguity in some groups, specifically between an epoxide group and a hydroxyl group which have a peak separation (0.1 eV) [138] that is less than the instrumentation FWHM peak width (0.6 eV for Au 4f7/2), making these two groups indistinguishable by XPS.

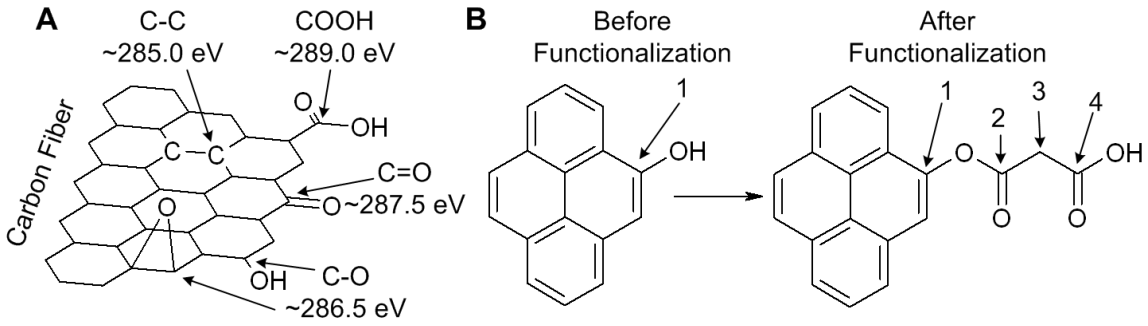

Figure 2-9. A) Typical oxygen functional groups on the surface of carbon fibers. Each group is labeled with the corresponding core electron binding energy measured by XPS. The carbon atoms in epoxide and hydroxyl groups have very similar binding energies and are indistinguishable through XPS analysis. B) Carbon states of each carbon atom before and after grafting onto the surface of a carbon fiber. Carbon 1 is measured at ~286.5 eV, carbons 2 and 4 are measured at ~289.0 eV and carbon 3 is measured at 286.9 eV.

Samples treated with Meldrum's acid showed higher carboxylic acid surface content than as-received samples; however the individual functional group content must be analyzed in order to determine the true surface coverage of the functional group. By creating a short chain functionalization, each hydroxyl group is converted into a malonic acid ester; which has more than one state of carbon. The four carbon atoms involved in the functionalization are shown in Figure 2-9B. Carbon 1 is the carbon from the base carbon fiber which is bound to the pendent hydroxyl group prior to functionalization. After functionalization, it is linked by an ester, having a binding energy of 286.6 eV and is indistinguishable from a hydroxyl group; thus the observed hydroxyl content should not decrease following functionalization of the fibers. Carbon 2 is added as a part of the malonic acid ester and has a binding energy of 289.0 eV; which is a part of the carboxylic acid peak. Carbon 3 has a binding energy of 286.9 eV [183] which is in the carbonyl peak of 287.2 eV. Finally, Carbon 4 is a typical carboxylic acid with a binding energy 289.0 eV. It is thus expected that for each terminal carboxylic acid group added, two carboxylic acid signals, and a additional signal near carbonyl will be detected. A

5% increase in carboxylic acid groups from this functionalization procedure should appear as a 5% increase in carbonyl signal and a 10% increased carboxyl signal.

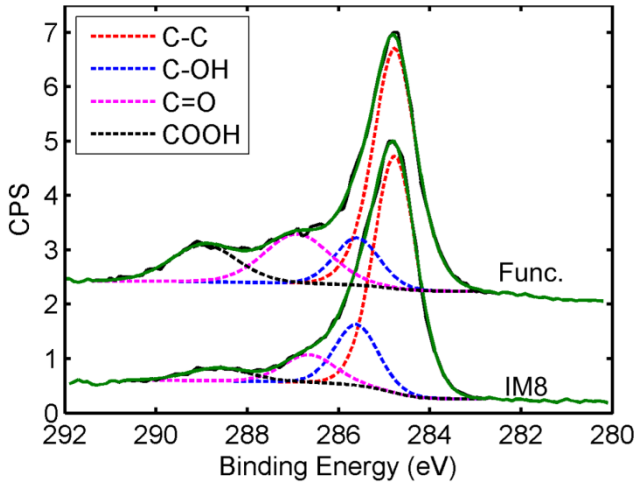

Peak (eV)	IM8	MA6-3
C-C (~284.7 eV) Carbon	68.0%	66.1%
C-OH (~286.5 eV) Hydroxyl	17.3%	7.3%
C=O (~287.5 eV) Carbonyl	9.5%	13.5%
COOH (~289.0 eV) Carboxylic Acid	5.2%	13.1%

Figure 2-10. Typical high resolution C1s XPS spectrum of fibers before and after functionalization. Each curve is decomposed into 4 components, as labeled in both the figure and the table. The functionalization procedure increases the surface coverage of carboxylic acid and also shows a signal increase in carbonyl content due to the other carbon atoms in the chain. Curves are offset for clarity. Functionalized sample was refluxed in toluene at 110 °C, 0.05M for 120 minutes.

Figure 2-10 shows a typical C1s region of carbon fibers before and after functionalization, the fibers were reacted in toluene at 110 °C, 0.05M for 120 minutes. The raw data is fit with a Shirley background and decomposed into Gaussian-Lorentzian 30 peaks. The as-received fibers are very similar to previously studied fibers [149,150,181] indicating that the samples are free of hydrocarbon contamination and surface sizing. The concentration of each group for both samples is shown in the table in Figure 2-10. The carboxylic acid proportion increases from 5.2% to 13.1%. Since each molecule provides 2 signals, the increase is only half of the 7.9% difference, or 4.0% additional coverage. The additional 4.0% of surface coverage of carboxylic acid is added to the initial 5.2% for a total useable surface coverage of 9.2%. This is accompanied by an increase in the carbonyl content of 4.0%, or equal to the number of

added molecules (4.0%); which supports the reaction mechanism in Figure 2-8 and the structure of the molecules on the surface of the carbon fiber as shown in Figure 2-9. If higher surface coverage of functional groups is required, then this reaction could be employed after an oxidative treatment to convert the hydroxyl groups into carboxylic acid groups.

2.2.3.1 Effect of experimental conditions on functionalization

A variety of solvents (benzene, toluene, xylene and DMF) were employed in this study to determine the most effective solvent for functionalizing the fiber. Typically, the reactions were performed by refluxing the solvent [168,169,173-175]; however a lower temperature was also attempted with DMF and toluene. Toluene was found to give the best functionalization results because it has a boiling point of 110 °C and avoids reactions with the reagents. Benzene was found to be slightly less effective as a solvent and xylene was found to inhibit the reaction as to yield no significant functionalization. Refluxed DMF and DMF at 100 °C were also found to inhibit the reaction. Meldrum's acid does begin to decompose in air at ~100 °C , reaction temperatures from 110 °C [168,169,174,175] to 120 °C [173] are widely accepted to follow the reaction mechanism in Figure 2-8. Solvents must be selected carefully to avoid alcohols, ketones and nitrogen nucleophiles as Meldrum's acid can react with certain common solvents [171].

Once toluene was selected as the most effective solvent, a full set of samples were produced and analyzed to examine the effects of reaction temperature (50 °C, 80 °C, 110 °C), concentration (0.01M, 0.05M) and time (30, 60, 120, 240 minutes). The observed C1s regions for each sample are shown in Figure 2-11. The reaction time was observed to have little effect on the reaction under all reaction conditions. The

reaction temperature and concentration did affect the final functionalization. At lower temperatures (50 °C and 80 °C), the reaction does not create as many functional groups which explains why benzene was found to be less effective than toluene. While the previous reactions with Meldrum's acid in synthesis refluxed samples for more than 8 hours [168,175], this work focuses on surface reactions and thus the reaction is expected to proceed much more rapidly.

Concentration was also observed to affect the number of functional groups on the surface of the fiber. An initial concentration of 0.01M for a 50 mL solution was chosen for the 0.033g of carbon fiber. This amount was chosen because it was enough to functionalize 1000 times the surface area of the fibers reacted, based upon expected surface coverage of surface groups and typical reaction yields. The higher carboxylic surface content was achieved with 0.05M after experimenting. Table 2-2 and Figure 2-11 show that, at both 80 °C and 110 °C, the fibers yield more carboxyl functionalization when treated with 0.05M than with 0.01M. A concentration of 0.1M was also attempted, but the functionalization had saturated and yielded the same amount of surface functionalization as 0.05M.

The third parameter studied was temperature, which was found to be the most important. The three temperatures were selected to give a broad range of reaction conditions, from full reflux to gentle heating. A temperature of 50 °C was found to be too low to functionalize the surface, while 80 °C was found to give some additional coverage but not the full coverage that the reaction is capable of delivering. Finally, as shown in Figure 2-11 and Table 2-2, full reflux in toluene yielded the highest coverage of functional groups. This was expected because the reaction mechanism utilizes less

stable intermediates and breaking of bonds, which requires input energy. Finally, the experiments performed here are consistent with previously published results, which also required high temperatures for the reaction [168,169,173-175].

Table 2-2. Peak locations and relative concentrations for each sample analyzed. Four peaks were fit to each sample which correspond to the chemical states shown at the top. All reactions were performed in toluene.

Conc.	Temp.	Time (min)	C-C		C-O		C=O		COOH	
			285.0 eV		286.5 eV		287.5 eV		289.0 eV	
0.01M	50 °C	30	59.0%	284.7	28.7%	286.1	5.2%	287.4	7.1%	288.9
		60	57.4%	284.8	25.3%	286.2	8.7%	287.5	8.7%	289.0
		120	79.3%	284.8	13.4%	286.2	2.9%	287.5	4.4%	288.8
		240	75.1%	284.8	15.5%	286.1	4.3%	287.6	5.2%	289.0
	80 °C	30	74.8%	284.8	14.8%	286.2	3.9%	287.4	6.5%	288.9
		60	72.6%	284.8	17.0%	286.1	4.7%	287.4	5.8%	289.0
		120	73.8%	284.8	15.7%	286.1	5.0%	287.5	5.4%	289.1
		240	67.6%	284.8	18.4%	286.0	7.1%	287.3	6.9%	289.0
	110 °C	30	63.9%	284.8	16.0%	286.1	10.7%	287.4	9.5%	289.1
		60	73.2%	284.8	12.4%	286.3	6.1%	287.5	8.3%	289.1
		120	64.1%	284.8	14.8%	286.1	11.6%	287.4	9.5%	289.1
		240	68.9%	284.9	17.5%	286.2	5.4%	287.6	8.2%	289.2
0.05M	50 °C	30	69.4%	284.8	17.7%	285.9	5.8%	287.2	7.2%	288.8
		60	74.5%	284.7	13.5%	286.0	6.4%	287.1	5.5%	288.9
		120	74.0%	284.9	15.8%	286.4	3.9%	287.7	6.3%	289.1
		240	71.9%	284.7	16.6%	286.1	4.6%	287.3	6.9%	288.7
	80 °C	30	77.1%	284.7	12.4%	286.0	4.7%	287.1	5.8%	288.7
		60	75.7%	284.7	15.7%	286.1	2.7%	287.4	5.9%	288.8
		120	72.7%	284.7	17.6%	286.0	4.3%	287.6	5.5%	289.1
		240	70.4%	284.7	17.7%	286.0	5.0%	287.3	7.0%	289.0
	110 °C	30	70.7%	284.8	12.7%	286.4	7.4%	287.5	9.2%	289.0
		60	63.6%	284.6	15.6%	286.1	8.7%	287.3	12.2%	288.7
		120	58.9%	284.7	17.0%	285.9	11.6%	287.2	12.5%	288.9
		240	73.4%	285.1	11.5%	286.9	5.0%	287.8	10.1%	289.1

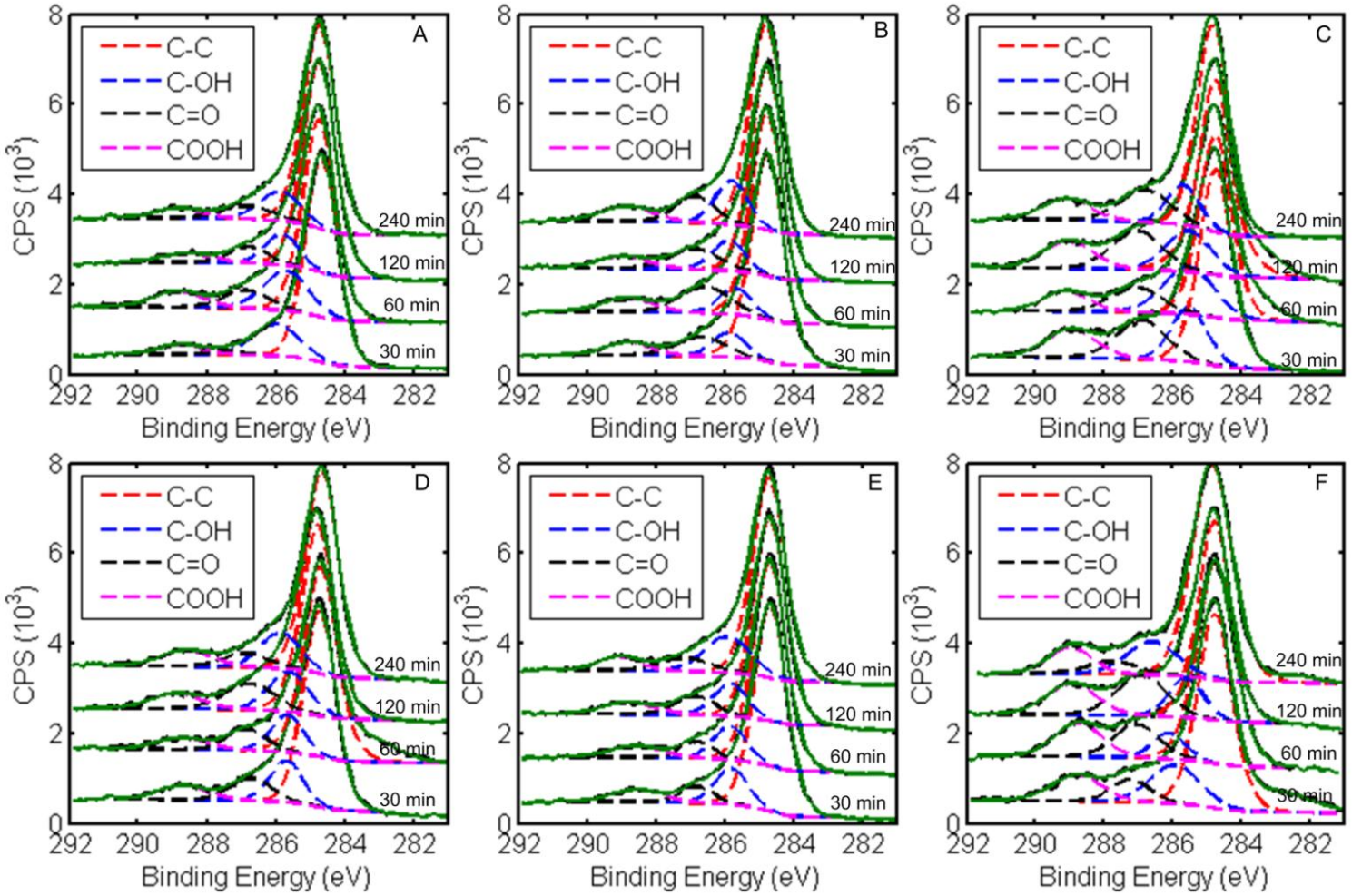

Figure 2-11. High resolution C1s surface spectra of functionalized fibers. Each sample was treated in a Meldrum's Acid / toluene solution and then analyzed. The reaction progresses to completion in less than 30 minutes and increases yield with increased time and increased temperature. Three different temperatures and two different concentrations were evaluated, A) 0.01M 50 °C, B) 0.01M 80 °C, C) 0.01M 110 °C, D) 0.05M 50 °C, E) 0.05M 80 °C, F) 0.05M 110 °C.

2.2.3.2 Verification of molecular grafting

The carbon fiber surfaces were analyzed after functionalization with scanning electron microscopy (SEM). Fibers were analyzed to determine surface morphology and indicate the presence of a deposited polymer or organic layer. The reaction presented here grafts short terminal malonic esters onto the surface but is not expected to etch the fiber to create additional pitting or deposit a significant organic coating. In order to prepare the samples for surface analysis, fibers after functionalization and cleaning were extracted in toluene for 16 hours, water for 8 hours or toluene (16 hrs) and water (8 hours), sequentially. Surface topography of five fibers is presented in Figure 2-12 and shows that the fiber maintains similar morphology before functionalization, after functionalization and after all extraction procedures. Figure 2-12 demonstrates that Soxhlet extraction with a non-polar (toluene) or polar (water) solvent does not significantly change the surface morphology, which implies that the esters are not weakly adsorbed to the surface of the fiber.

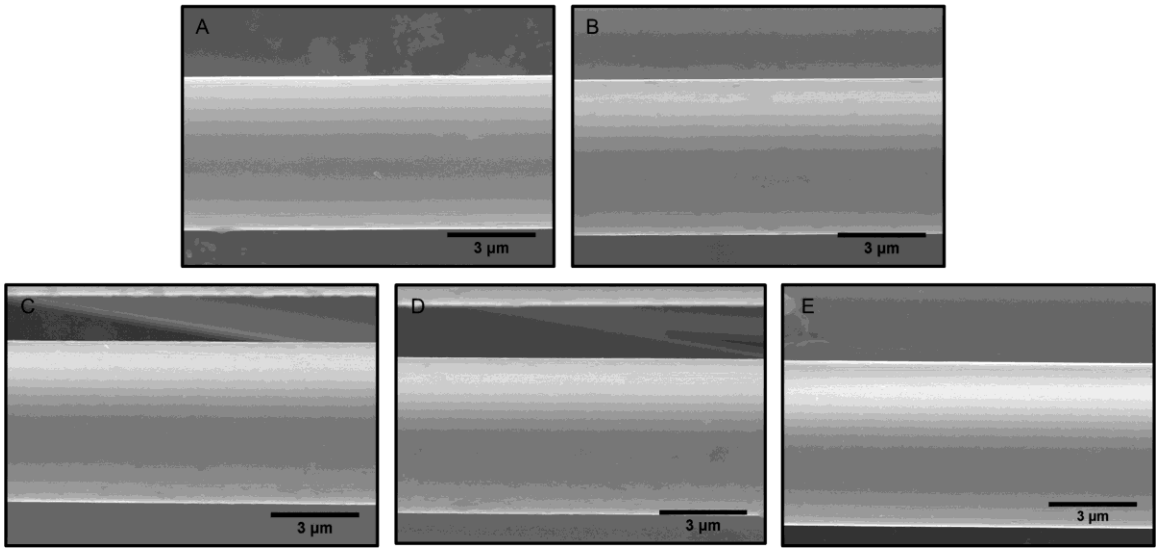

Figure 2-12. Surface of A) an as received carbon fiber and B) a fiber after functionalization. Fibers extracted in water (C,E) and toluene (D,E) show little change in the surface, indicating that the grafted layer is strongly bound, not adsorbed.

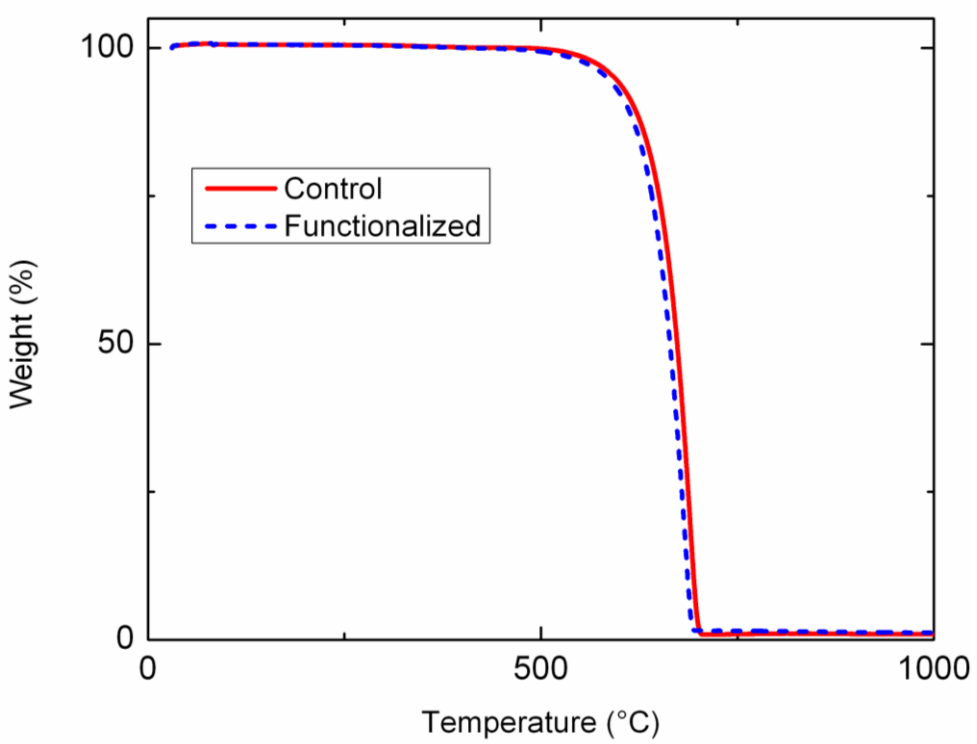

Figure 2-13. Thermogravimetric analysis (TGA) of IM8 fibers before and after functionalization. Neither set of fibers loses mass below 500 °C, indicating that the functional groups are not adsorbed but strongly chemically bound. Furthermore, a negligibly small weight fraction of functional groups is responsible for the increased carboxylic acid signal because the derivatives are smooth with only one peak; which indicates this is a small molecule grafting procedure.

Thermogravimetric analysis (TGA) measures the thermal decomposition and stability of a material. Carbon fibers are stable in air at much higher temperatures than common polymers or many organic contaminants because the graphitic carbon is quite stable. TGA of fibers with and without functionalization should reveal the presence of polymeric sizing, organic contaminants or self-polymerization of the Meldrum's acid. TGA, in Figure 2-13, revealed that there was no significant reduction in the decomposition temperature, which implies that the fibers maintain thermal stability before and after functionalization. This is consistent with expectations since a small coverage of surface groups will not significantly oxidize the material. The data also

reinforces the claim that the process does not increase the surface area of the fibers because increased surface area would assist the oxidation of the fibers during the TGA experiment. The TGA also shows that both sets of fibers exhibit no sizing or significant drop off in mass until over 500 °C; well above the thermal stability of most polymers and organic sizing materials. The relative mass of functional groups on the surface of carbon fiber is much less than the mass of the fibers themselves; thus the TGA shows that the signals observed in the XPS are from an insignificant mass of functional groups and not a surface coating layer.

2.2.3.3 Summary of defect grafting with Meldrum's acid

A novel carboxylic acid functionalization procedure employing a ring opening reaction of Meldrum's acid has been investigated in a variety of experimental conditions. It was observed that solvent, temperature and concentration all had effects on the amount of surface functionalization, while reaction time (in the range tested) showed no trends in the final surface coverage of carboxylic acid groups. Surface functionalization was confirmed with XPS and is consistent with the proposed reaction mechanism. Surface morphology was analyzed by SEM, which revealed no significant roughening, pitting or change in the surface topology, even after extraction in polar and non-polar solvents. TGA confirmed that the signals observed in the XPS data were due to short molecule grafting to the core fiber and not adsorbed layers or reactions with sizing materials. Single fiber tensile testing will later show no reduction in the tensile strength and Weibull shape factor, indicating that the functionalization procedure does not induce additional defects to the surface of the fiber. This new application of a well-established reaction grafts useful carboxylic acid groups onto existing hydroxyl groups to yield a relative surface coverage of 9.2%, without the need for a pre-oxidation step. This

functionalization procedure will be used to provide a suitable surface for the interaction of ZnO nanowires with structural fibers later in this work.

2.2.4 Selective Oxidation of Carbon Fiber

The surface functionalization with Meldrum's acid grafts a carboxyl terminated molecule onto existing hydroxyl defects to create a surface effectively functionalized with carboxylic acid. Another approach is to convert the existing defects into carboxylic acid with a selective oxidation. This type of oxidation is derived from previous graphitic carbon nanotube chemistry research. Specifically the reaction, termed up-conversion, uses a mixture of perchloric acid and potassium permanganate to selectively increase the number of carbon oxygen bonds of the existing oxygen functional groups, without being so strong to create additional defects. The results of chemical and topographical studies of selectively oxidized or up-converted fibers are discussed below.

The reaction to selectively oxidize carbon fibers entails entirely inorganic reactants and does not have the same sensitivity as typical organic reactions. In spite of the adoption of the selective oxidation by a number of groups, only a limited number of papers have discussed the actual mechanism of oxidation. A number of studies from the organic chemistry community have been performed regarding the general mechanism of oxidation of permanganate ions in acidic solutions [184]. Specifically, Lee and Brownridge provided detailed measurements of reaction constants, identification of the transient species of the reactions and provided an example of the reaction mechanism, shown in Figure 2-14 [185]. Their work demonstrated the effectiveness of the reaction and showed the preference of the permanganate ion to oxidize existing defects up to carboxylic acid, rather than form new defect sites by oxidizing carbon – carbon bonds. With the extensive background built up in the

chemistry literature, it comes as no surprise that the additional steps were added to standard oxidation steps for carbon nanotubes.[176-179]

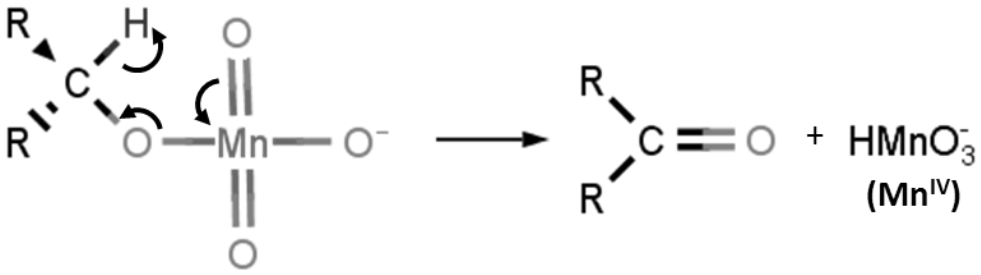

Figure 2-14. Mechanism of oxidation of organic compounds by permanganate compounds in acidic solutions.

Following a similar characterization as the defect grafted fibers, fibers with selective oxidation were analyzed in XPS, AFM, SEM and through various mechanical tests. The measurement of the impact on mechanical properties will be detailed in Chapter 3. It should be noted that the experimental conditions in many papers are not varied, specifically, temperatures, times and concentrations remain very consistent between reports that employ this technique. Lee and Brownridge showed that many of the products are transient and are more than sufficiently complete after ten minutes [185]; thus there is no need to pursue longer reaction times. In this work, the temperature is not increased as a reaction variable because high temperature perchloric acid reactions can cause perchlorates to evaporate and form explosive crystals in the fume hood or on glassware. Most authors do not report need for extensive heating to improve reaction yields and in this work temperature is held constant to preserve safety. It will be shown later that the technique does deliver carboxylic acid comparable to that produced with defect grafting and thus the reaction is kept consistent with prior procedures.

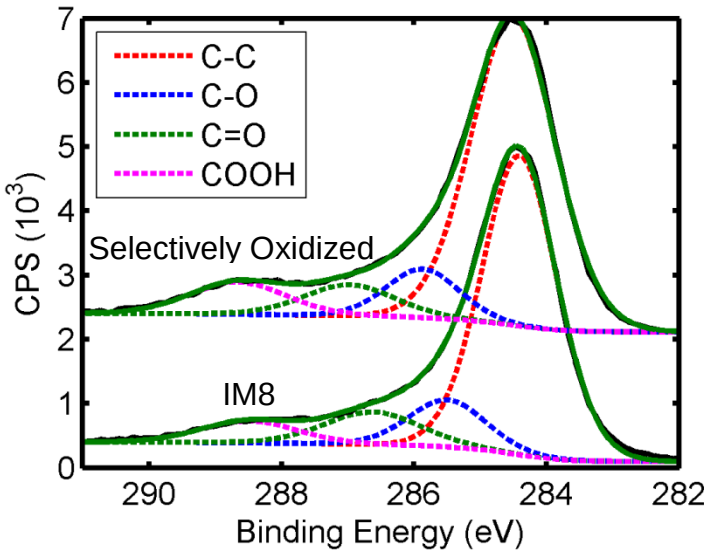

Figure 2-15. High resolution XPS scan of carbon fibers after selective oxidation with permangnates in perchloric acid.

The most important facet in establishing the efficacy of selective oxidation is measuring changes in the surface chemistry. As detailed earlier, this is most effectively accomplished on a carbon fiber substrate using XPS. Figure 2-15 shows the XPS data from selectively oxidized fibers and fibers as received. It is clear that the fibers show a significant increase in the carboxylic acid content because the signal at 289.0 eV is almost 4% higher. The total oxygen content remains largely unchanged because the reaction only converts the number of existing functional groups without creating new ones. The mathematical fitting procedure indicates that the oxygen content decreases, this is because of the ambiguity of the peaks at 285.5 eV and 284.7 eV. The area concentrations in Table 2-3 were fitted using the same procedure detailed earlier. The selectively oxidized fiber shows a reduction in the hydroxyl/ether peak that is due to the selective oxidation of those groups into carboxylic acid, through the mechanism proposed by Lee in Figure 2-14.

Topographical surface scans of typical fibers are shown below in Figure 2-16D. The surfaces were probed by atomic force microscopy in contact mode and great care was taken to use mounting procedures that avoid possible adhesive contamination on the fibers. To accomplish this, a two part epoxy adhesive was wicked into a piece of paper while ensuring that the roughness of the paper was still visible. This indicated that the paper held the epoxy entirely and no droplets had formed on the surface that could wick over or along the fiber. The paper was then flipped and a single fiber was placed onto the back side of the paper where the epoxy had wicked through. The fiber stuck to the partially wetted paper and after curing the epoxy, the fiber is rigidly held in place without surface wetting from the epoxy below. Double sided tape was avoided because it tends to damage the tip of the AFM and it becomes difficult to assure that the tip will not accumulate and deposit the adhesive on the surface of the fiber.

Table 2-3. Relative surface coverage of various functional groups on selectively oxidized carbon fibers.

Peak (eV)	IM8		Selectively Oxidized	
C-C (~284.7 eV) Carbon	68.0%	284.8 eV	73.3%	284.5 eV
C-OH (~286.5 eV) Hydroxyl	17.3%	286.0 eV	10.0%	285.9 eV
C=O (~287.5 eV) Carbonyl	9.5%	287.3 eV	8.0%	287.0 eV
COOH (~289.0 eV) Carboxylic Acid	5.2%	288.8 eV	8.7%	288.7 eV

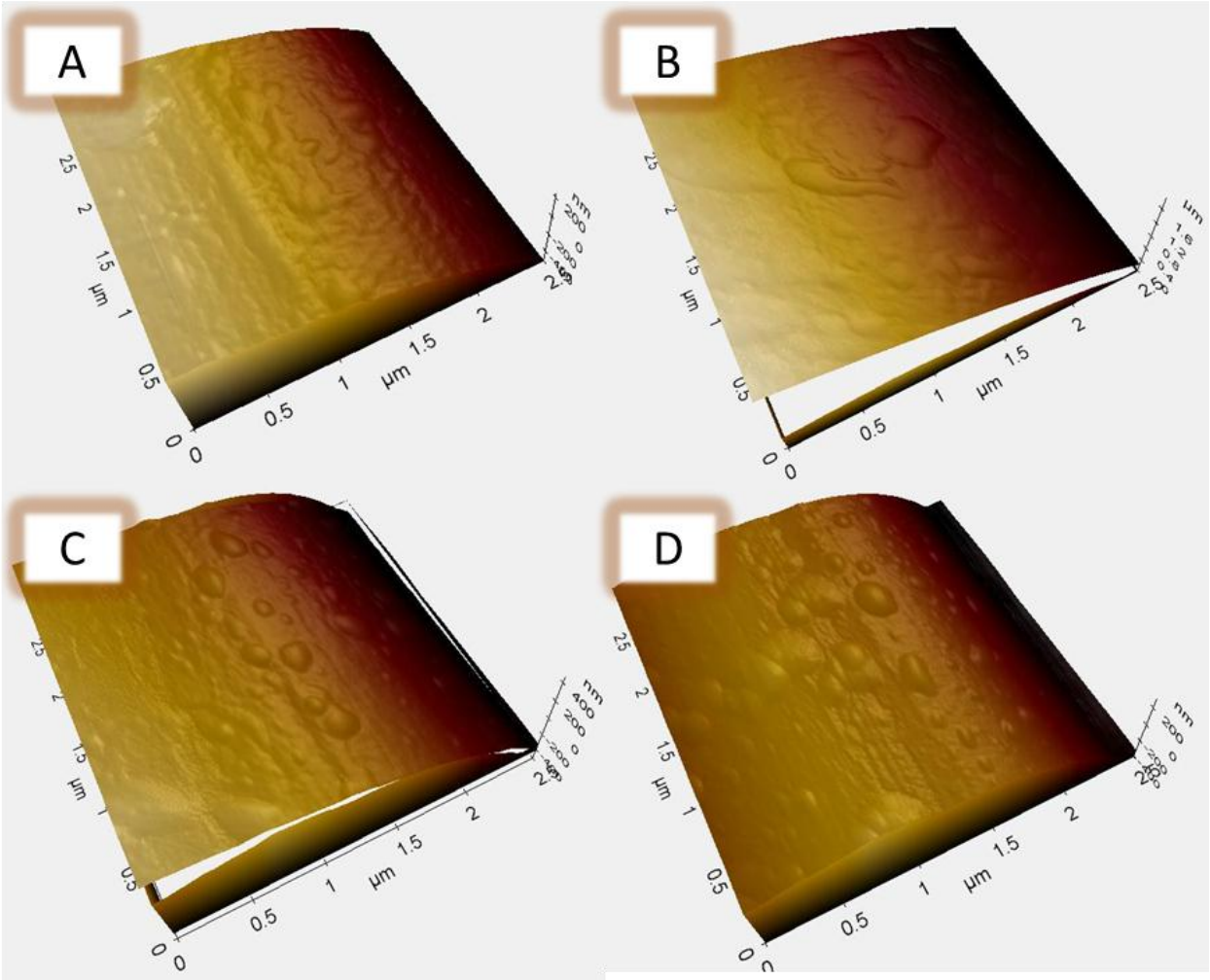

Figure 2-16. Surfaces of various fibers after surface functionalization. A) Hydrazine reduced fibers, B) IM8 fibers as received, C) defect grafted fibers and D) selectively oxidized fibers all show similar topography indicating that none of the techniques etch or roughen the fiber.

Figure 2-16D shows that after oxidation, the surface has no additional defects, etching or pitting that would be expected from a strong oxidation procedure. The topographical data indicates that the fibers have the same surface roughness and are expected to decompose the same as IM8 fibers. The defect grafting results in Figure 2-13 show that molecular surface changes without an increase in roughness or surface area preserves the thermal stability of carbon fibers and similar results are expected for the modified fibers. Chapter 3 will show that this procedure also preserves the

mechanical properties of the fiber because there is no increase in the roughness or surface defects. The topographical information combined with the surface chemistry data indicates that the functionalization provides the desired outcomes of increased carboxylic acid content without increased roughness.

Selective oxidation with potassium permanganate is a well-known and commonly employed method for converting alcohols into carboxylic acid in organic molecules. The advantage, when applied to carbon fiber, is that while potassium permanganate oxidations directly target existing hydroxyl groups, they do not oxidize C – C bonds and thus do not affect the tensile strength of the fibers. Etching of the surface or consumption of the underlying carbon is not expected with this reaction. The selective oxidation process is efficient, inexpensive and easily scaled to continuous, high speed fiber production. This section has demonstrated that carboxylic acid groups can be created on the surface, as measured by XPS. This process will provide an additional option to increase carboxylic acid for stronger interactions with ZnO nanowires interphases.

2.2.5 Reduction of Carbon Fibers to Remove Oxygen Groups

Two techniques that produce carboxylic acid have been presented above and this work focuses on identifying if carboxylic acid creates adhesion between ZnO nanowires and the surface of carbon fibers. As such, a control is also developed whereby carboxylic acid groups are removed from the fiber through a reduction process. This section will describe the reduction as well as elucidate its effects on the fibers. This reduction technique is not intended to be implemented in the production of carbon fibers; rather it will serve as a control to validate the mechanism of adhesion proposed in this work, enabling future systems of nanowire interphases in composite materials.

Graphitic carbon does not cross link with many common structural polymers and thus reduced carbon fibers have not been the subject of intense study [186]. Carbon fibers, in graphitic form, are by definition very reduced by the thermal treatments used to produce them. Typically, oxygen and nitrogen functional groups do remain after thermal graphitization and a strong reducing agent will be used to remove these groups. A strong chemical reducing agent is selected because most graphitization temperatures exceed 2000 °C, thus thermal reduction is unlikely to succeed in removing the remaining functional groups. Most should already have been reduced during production [19].

Graphene, the building block of graphitic structures, is often produced through the intercalation of oxidizing acids to create graphene oxide, single layers of oxidized graphene [187]. Frequently, authors have desired to restore the conjugated electron structure to these materials by chemically reducing them. The most effective method to date for restoring the carbon – carbon bonding in graphene oxide is a combination of hydrazine and thermal reduction in vacuum [188]. Borrowing from the large body of graphene oxide research, this work will employ a hydrazine reflux to reduce the surface of the fibers and remove oxygen functional groups. High temperature vacuum heat treatments require specialized equipment that was prohibitively expensive for these experiments and hydrazine refluxes are found to be sufficient for the purposes of this work. Specifically, a hydrazine reflux reduces the concentration of carboxylic acid on the surface of the carbon fiber down to a desired level for comparison.

Fibers were received and prepared similarly to previous functionalization treatments. Instead of refluxing with isopropylidene malonate or immersing in the

selective oxidation mixture, fibers for the reduction process were added to a 10% V/V solution of hydrazine hydrate (98%, Alfa Aesar, Ward Hill, MA) in deionized water. The fibers were refluxed for up to 8 hours and then washed multiple times in deionized water. XPS and tensile experiments followed the same preparation and procedures listed earlier.

The effectiveness of the hydrazine reflux was determined with XPS, to identify the quantity of oxygen containing functional groups on the surface of the fibers. The curve fitting procedure was consistent with the sections in Chapter 2. Figure 2-17 shows the traces from the XPS and Table 2-4 shows the associated decomposition of each peak area. It is clear that in comparison to the fibers as received, the fibers refluxed in hydrazine show reduced oxygen functional group intensity with 3.55% carboxylic acid compared to 5.2% on the fibers as received. Additionally, the carbonyl group content also significantly dropped as a result of the treatment, going from 9.5% to 3.6%. Although the hydroxyl/ether content did not drop much, from 17.3% to 15.0%, the carbon – carbon content increased from 68.0% up to 78.6%. This implies that potentially, carbonyl and carboxylic defect sites were reduced to hydroxyl or ether while hydroxyl or ether groups are eliminated and carbon – carbon bonding was partially reformed.

Alternative explanations for the data are possible and thus the potential for other mechanisms to create similar data must be investigated. One such plausible explanation for this data could be that the hydrazine reflux caused the fiber to swell and etch away the surface oxidized layers. Surface topography can show evidence of etching or swelling by a noticeable change in surface topography. Figure 2-16A and

Figure 4-16B show that the surface of the hydrazine reduced fiber is largely unmodified compared to IM8 fibers as received or fibers reduced after nitric acid oxidation. The drawing and stretching striations are still visible and there does not appear to be additional roughening along the fiber axis. The alternative mechanism of functionalization is not responsible for the surface changes observed by XPS; rather direct chemical reduction of surface groups causes the observed changes. Since the roughness is unchanged, this fiber will serve as an experimental control demonstrating that fewer oxygen functional groups reduces the adhesion of ZnO nanowire coatings on the fiber surfaces.

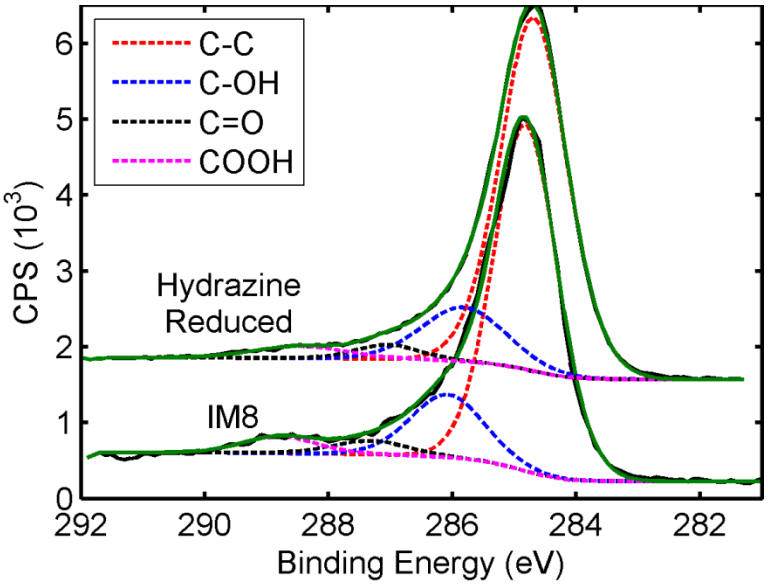

Figure 2-17. High resolution C1s binding energy scan of hydrazine reduced and IM-8 as received fibers. The carboxylic acid and other oxygen functional groups are reduced by the hydrazine reflux to create a control fiber for future testing.

This section has quantitatively demonstrated a reduction procedure for further removal of functional groups from the surface of carbon fibers. While the intent is not to apply reduction procedures as a functionalization, the technique will serve as a control for further testing of the specific impact of chemistry on interface strength. The process efficiently and effectively removes functional groups from the surface of the fibers to

create a more C – C bonding than fibers as received. The chemicals involved are additionally not expected to etch or intercalate the graphitic layers of the carbon fibers and damage the underlying fiber properties. The changes in surface chemistry, combined with the preservation of the surface roughness and tensile strength of the fibers ensures that these fibers will enable comparisons to be drawn between the various fibers.

Table 2-4. Relative surface coverage of various functional groups on hydrazine reduced carbon fibers as measured by XPS.

Peak (eV)	IM8		Hydrazine Reduced	
C-C (~284.7 eV) Carbon	68.0%	284.8 eV	78.6%	284.4 eV
C-OH (~286.5 eV) Hydroxyl	17.3%	286.0 eV	15.0%	285.5 eV
C=O (~287.5 eV) Carbonyl	9.5%	287.3 eV	3.6%	286.7 eV
COOH (~289.0 eV) Carboxylic Acid	5.2%	288.8 eV	2.9%	288.1 eV

2.2.6 Summary of Carbon Fiber Functionalization Techniques

The modification of the surface of carbon fibers is achievable through both organic and inorganic reactions. These reactions can create functional groups, remove functional groups or graft to existing groups to effectively change the fiber surface. While some procedures do react with the underlying structural backbone of the fiber, the procedures listed above are specifically selected to eliminate the need to react with the structural backbone of the fiber and instead focus on reactions with the surface of the fiber to create the desired outcome. Two novel procedures have been developed here and two additional procedures have been characterized for this work. First, a defect grafting strategy has been developed that grafts malonic acid esters to naturally occurring hydroxyl groups on the surface of the fibers. Second, an inorganic selective

oxidation procedure has applied to carbon fibers to create carboxylic acid groups directly from existing oxygen defect sites. These two procedures increase the concentration of carboxylic acid groups without destroying the structural backbone of the fiber or increasing the surface roughness of fiber. These techniques will be used to create a surface that can adhere ZnO nanowires to carbon fibers for structural composites. Two additional techniques are also developed to analyze the chemical bonding mechanism between the ZnO interphase and the fiber. A reduction technique is created to remove carboxylic acid with hydrazine, based upon the methods for reducing graphene oxide [188]. An oxidative technique with nitric acid is developed to create a mixture of oxygen functional groups with higher oxygen content than the previous methods. These techniques were characterized with XPS, among other techniques, to determine the chemical state of the surface. A summary of all of the XPS data for carbon fibers is shown in Figure 2-18, which clearly shows a variety of carbon states at the surface of the fibers. In addition, the data in Figure 2-18 has been tabulated in Table 2-5. The functionalization techniques developed for this work do create a variety of chemical states to assess the interaction with the ZnO nanowire interphase.

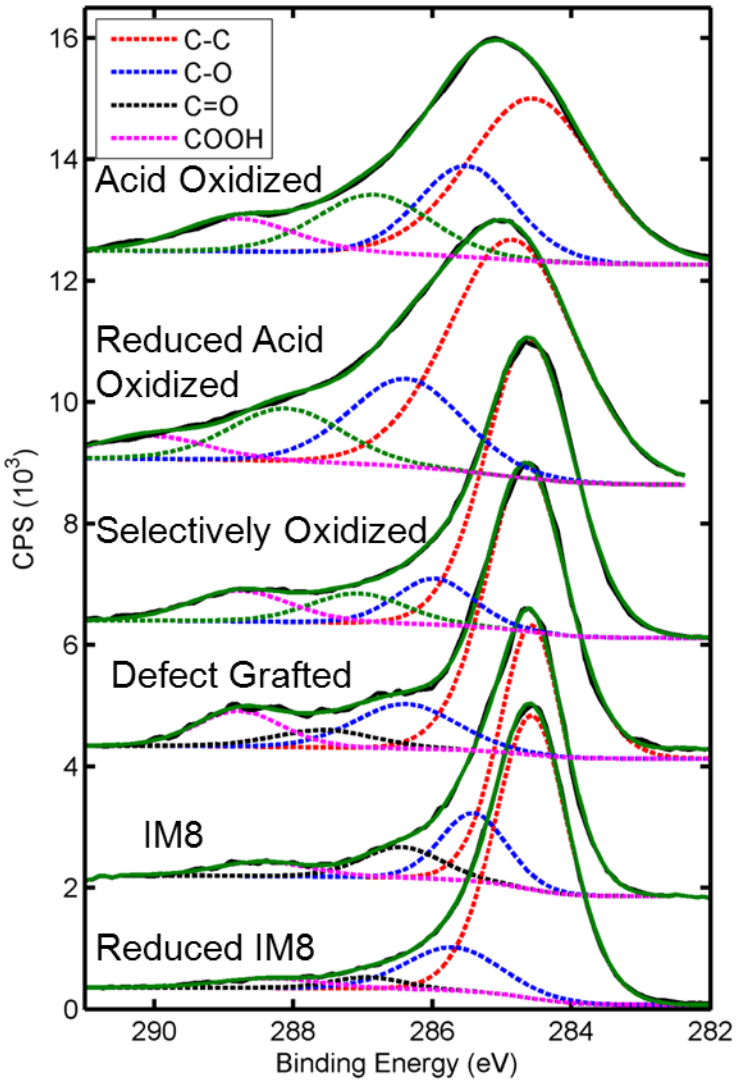

Figure 2-18. Comparison of the carbon state at the surface of carbon fibers with each functionalization treatment developed.

Table 2-5. Carbon state concentrations of carbon fibers in each functionalization procedure employed in this work, as fit by the regression algorithm.

Peak Location (eV)	Reduced IM8	IM8	Selectively Oxidize	Defect Grafted	Reduced Acid Oxidized	Acid Oxidized
C – C (~284.7) Carbon	78.6%	68.0%	73.3%	66.1%	62.1%	52.0%
C – O (~286.5) Hydroxyl	15.0%	17.3%	10.0%	07.3%	20.3%	22.0%
C = O (~287.5) Ketone	03.6%	09.5%	08.0%	13.5%	12.2%	16.6%
COOH (~289.0) Carboxylic Acid	03.0%	05.2%	08.7%	13.1%	05.3%	09.3%

2.3 Chapter 2 Summary

Chapter 2 has presented the fundamental research developed in this work related to fiber surface treatment. Specifically, the fiber surface functionalization schemes that have been developed to create favorable surfaces for ZnO nanowire growth and adhesion. This included the application of chemical reactions to achieve new, positive results in the functionalization of structural fibers. The reactions were validated with multiple material characterization techniques, in particular XPS to measure the quantity of surface functional groups.

The functionalization of aramid fibers is performed with an adapted hydrolysis reaction. A strong base hydrolyzes the amide linkage to form a carboxylate salt and a primary amine. This is followed by an ion exchange wash with a strong acid to create an increased surface coverage of carboxylic acid groups to which ZnO will be attached. The functionalization of carbon fibers entails four techniques. Two new techniques are developed for this work, a defect grafting and a selective oxidation technique. The defect grafting is an organic reaction in which hydroxyl defects are grafted to form malonic esters and create a surface effectively terminated in carboxylic acid. The second new technique is a selective oxidation where existing oxygen functional groups are preferentially oxidized to carboxylic acid while the structural backbone remains undisturbed by the reactants. The other functionalization techniques are developed as experiments to help determine what chemical interactions are causing a strong adhesion of the ZnO to the surface of carbon fibers. A reduction technique is verified to remove oxygen functional groups, specifically a hydrazine reflux adapted from graphene oxide reduction literature. Lastly, nitric acid oxidation is also evaluated, which creates a mixture of various oxygen functional groups and roughens the surface.

Chapter 2 details the synthetic methods and characterization to produce fibers with a ZnO nanowire interphase. Chapter 3 demonstrates the growth of ZnO nanowires on structural fibers and the fabrication of hierarchical composites. Chapter 4 will detail the effects of this interphase on the structural properties of the composite.

CHAPTER 3
FABRICATION OF HIERARCHICAL COMPOSITES WITH A ZNO NANOWIRE INTERPHASE

One of the goals of this work is to grow arrays of ZnO nanowires on the surface of structural fibers for composites. This section will detail the growth of ZnO nanowires on the surface of structural reinforcing fibers for composite materials. This represents a major advance in the composite materials field as this work is the first to present the growth of ceramic nanowires on aramid fibers for structural enhancement. This work is one of the first descriptions of a low temperature solution based growth of ZnO nanowires on structural fibers, the others also originating within the multiscale adaptive structures and systems laboratory [189]. The low temperature processing of ceramic nanowires is one of the chief advantages of employing ZnO nanowires in the whiskerization and thus great detail will be provided to disseminate the research findings.

The second part of the chapter will detail the selection of the composite, both processing methods and the polymer matrix. The materials and methods selected are justified and the reasoning may assist future work in extending this technology to other polymeric matrices or processing methods. The second half Chapter 3 will also assess composite quality, detailing the volume fraction of the composites, wetting of the nanowires and interface quality between the ZnO interphase and the structural fibers.

3.1 Review of ZnO Nanowire Growth Methods

ZnO has intrinsic properties of interest across a range of disciplines, causing it to become one of the most studied topics in materials science [190]. As a wide band gap semiconductor, ZnO nanowire can effectively function as a field emitter, laser, gas sensor, solar cell and transparent electrode. ZnO is easily processed into arrays of ZnO

nanowires where the geometry of a high aspect ratio nanowire can improve various properties on a large scale. Two major processes exist for creating ZnO nanowire arrays, broadly classified into chemical vapor deposition and low temperature solution growth methods.

Chemical vapor deposition of ZnO is effective for creating higher aspect ratio nanowires (>100), typically employing solid precursors to deposit ZnO nanowires at high temperature (~900°C) and low pressure (~3 mbar). One of the more popular techniques is the carbothermal growth method where bulk ZnO powder is mixed with graphite or another carbon source to reduce the evaporation temperature of the ZnO, which then deposits as nanowires downstream on the substrate [119,190-195].[190][190][190] This particular method presents problems for the proposed growth of ZnO nanowires on polymer and graphite fibers. The high temperatures involved would likely damage or graphitize most polymeric fibers, while carbon or graphite fibers would likely evaporate into the same CO species responsible for reducing the evaporation temperature of the ZnO. Carbon fibers have been employed as a substrate in chemical vapor deposition for ZnO nanowire field emitters [194,195]; however tensile testing did not accompany the results and it is likely that the growth caused, for this work, an unacceptable tradeoff in fiber tensile properties. The vapor – liquid – solid deposition process will probably not achieve the goals set out in this research because the capital equipment is too costly and the possibility of fiber damage is too high.

Fortunately, ZnO is a versatile ceramic and nanowires can also be deposited through solution based growth methods. Solution based growth methods typically require little more than hotplates and beakers to complete so the technology is much

more accessible than methods like magnetron sputtering, molecular beam epitaxy, chemical vapor deposition and pulsed laser deposition. Most nanowire array processes begin with a polycrystalline seed layer on the substrate followed by aqueous chemical precipitation of the nanowires through the reaction demonstrated in Figure 3-1. The ZnO precipitates onto the substrate seed layer by depositing onto the existing facets of the seed layer, slowly growing a single crystal.

$$(CH_2)_6N_4 + 6H_2O \leftrightarrow 6HCHO + 4NH_3$$

$$NH_3 + H_2O \leftrightarrow NH_4^+ + OH^-$$

$$2OH^- + Zn_2^+ \rightarrow ZnO(s) + H_2O$$

Figure 3-1. Reaction governing precipitation of ZnO during the most common aqueous solution based growth method [134].

Solution deposited ZnO often grows in a nanowire or nanorod shape because certain crystal facets of the wurtzite crystal structure have higher energy and polarity, leading to a preferential deposition of ZnO on those surfaces. This phenomenon leads to growth occurring in the <0001> direction of the crystal, typically with an aspect ratio (length / diameter) of approximately 10, which is the difference of growth rate of the $\{0001\}$ face and the $\{10\bar{1}0\}$ or $\{1120\}$ faces [196]. This process can be enhanced or restricted through the addition of specific chemicals that preferentially adsorb to the faces of growth. Specifically, branched polyethyleneimine (PEI) can be added to adsorb to the non-polar $\{10\bar{1}0\}$ or $\{1120\}$ faces, resulting in nanowires with aspect ratios approaching 100 [196]. It has been recently shown that metal ions can also be added to the growth solution to achieve a similar end, resulting in aspect ratio control over a range of 1000 [197]. Citric acid and polyvinyl alcohol have the opposite effect, preferentially adsorbing onto the $\{0001\}$ face and creating hexagonal plates instead of

aligned nanowires [198,199]. The volume of research related to controlled growth of ZnO nanowires makes it a choice ceramic for whiskerization because the growth can tailored to optimize material performance.

The solution based growth of ZnO nanowires has been fairly well studied [200-206], resulting in thermodynamic modeling to yield continuous processes as well as assessment of the mechanism for growth [207-210]. This has resulted in a fairly comprehensive understanding of how to scale the ZnO nanowire growth from a laboratory scale batch process to a continuous flow compatible with large scale manufacturing [211,212].

This work will make use of portions of this existing literature, specifically in two places. The first and most important aspect is the ability to control nanowire diameter through the grain size of the seed layer [205,213]. The nanowires grow competitively from the seed layer deposited before growth, thus the smaller grains create more individual sites for crystal nucleation and the nanowires grow with a smaller diameter. The diameter of the nanowires was shown to be a significant factor in the interfacial shear strength [213]. The morphology effects are a subject of interest and relevance to this work; however they are not the focus and primarily this work will use the control established previously to optimize the effects of surface chemistry.

The second aspect is the use of precipitation control techniques to reduce the deposition of larger scale microrods or ‘flowers’. The flowers are observed to be detrimental to interfacial shear performance, causing large scale debonds and unusual stress fields that convolute the mechanical testing results. The microscale rods are spontaneously precipitated out of the growth solution and gradually accumulate on the

bottom of the growth containers. As such, several researchers have employed physical techniques to remove the majority of the rods, namely physical rinsing [214,215] or by growing on an upside down substrate suspended by surface tension [216] so that any microrods are not deposited onto the substrate. While these are certainly effective for large planar substrates, a vertically suspended single fiber tends to accumulate microrods on the surface upon removal of the fibers from the solution as some of the microrods accumulate on the surface and deposit in a fashion similar to Langmuir-Blodgett film deposition. One notable research group has demonstrated a method to control the spontaneous precipitation of the microrods [217]. The group maintained a higher concentration and thus a faster growth rate of the nanowires while avoiding the deposition of larger scale microrods that reduced device quality by reducing the propensity of the Zn ions to precipitate out. This work will make use of their experience to produce fibers with little or no 'flowers' for maximum composite quality.

3.2 Growth of ZnO Nanowires on Structural Fibers

The best approach to growing ZnO nanowires is the solution based growth method widely reported in the literature, which employs a zinc salt and an ammonia base, most frequently hexamethylenetetramine. Alternative strategies for the growth of ZnO nanowires, such as chemical vapor deposition, do not offer the low temperature processing advantages afforded by solution based growth methods. The solution based growth method is widely tunable; however the tuning methods all rely upon the mechanism of preferential growth in the <0001> direction, as established in the literature [214]. Section 3.1 provided a broad look at how ZnO nanowires were grown and provided an understanding of the chemical mechanism. This section will detail the growth of ZnO in the context of growing on small structural fibers.

ZnO nanowires are grown in the solution method through a slow ammonia induced precipitation method, as described earlier in Figure 3-1. A typical image of ZnO nanowires on aramid fibers and carbon fibers is shown in Figure 3-2. The nanowires begin precipitating from small ZnO seed crystals and then grow quickly along the <0001> direction, competing for additional growth ions to form a radially aligned array. They deposit as nanowires and not particles because the growth rate in the <0001> direction of the crystal is approximately ten times higher than the <1120> or <$10\bar{1}0$> directions [196]. Control of the aspect ratio of the nanowires is attained by manipulation of the surface energies and relative growth rates of the different growth faces. This can be accomplished by a variety of polymers or ions that preferentially adsorb onto crystal faces, interfering with the deposition of additional Zn^{2+} and O^{-2} ions. While rational control can be provided with the appropriate polymer or ion, contaminants of the growth solution can create unintended consequences during the growth on structural fibers through the same mechanism. The cleanliness of the glassware, cleanliness of any supports for the fibers and the handling of the growth substrates prior to growth is of the utmost importance to the successful growth of high quality ZnO nanowire arrays on structural fibers. Common contaminants include aluminum ions, sodium ions, polymeric residue from acetone and organic components in common adhesives. The cleaning procedure used during the growth of ZnO nanowires in this work is to wash polymeric holders in boiling ultrapure water, wash in acetone and finally rinse in absolute ethanol. Subsequent handling is performed with nitrile gloves and the frames are only placed in contact with clean, oil free surfaces.

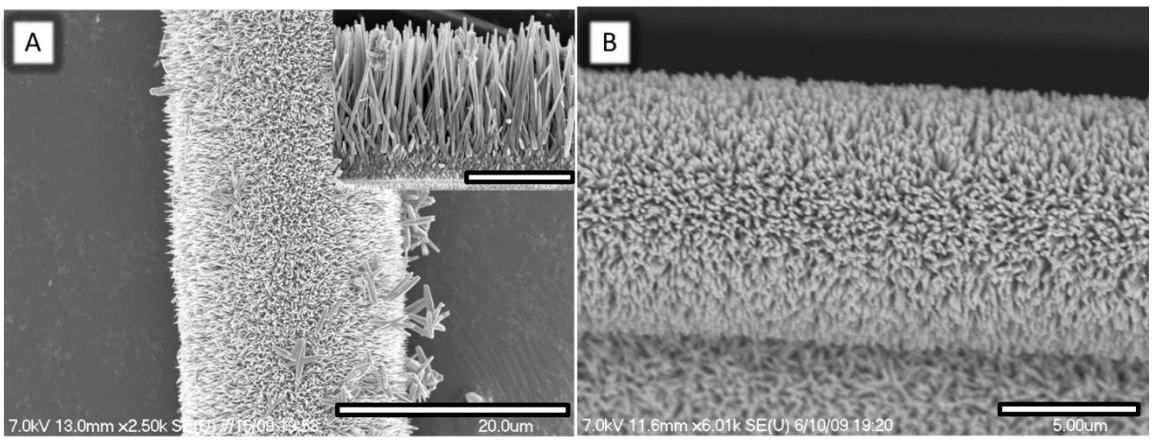

Figure 3-2. Typical ZnO nanowires grown on A) aramid fibers and B) carbon fibers. Scale bars are A) 20 µm, 3 µm inset and B) 5 µm, respectively.

The second critical factor in the growth of ZnO nanowire arrays is the deposition of the polycrystalline seed layer from which the nanowires nucleate. Typically, the seed layer is formed by first creating a dilute suspension of ZnO nanoparticles, depositing the solution on the fibers and then annealing the seeds to create a thin, conformal, polycrystalline layer on the fibers. This, the first step of the two step growth process, is as critical as the actual growth of the nanowires. Poor seeding technique will produce bad nanowires and there are several components where the seeding process can be compromised. As with the rest of the glassware above, all glassware for synthesis of the ZnO nanoparticle seeds is cleaned in water, acetone and ethanol prior to use. Additionally, part of this work included attempting to grow on a wide array of fibers from different times during fiber production. With sufficient cleaning, nearly any fiber of suitable composition can be grown on, including carbon, aramid, glass and silicon carbide. Cleaning must be aggressive enough to remove water soluble molecules that could adsorb to the polar or non-polar faces of the ZnO nanowires or seeds. The most difficult fiber to grow ZnO nanowires on was a carbon fiber withdrawn from the production line immediately after exiting the highest temperature graphitization furnace.

This fiber required a hot wash in dimethylsulfoxide, a strong polar solvent that was able to dissolve residual polymer or small organic molecules. Often a sufficiently strong organic solvent can remove the organic contaminants. A variety of non-oxidative techniques can be used to clean the fibers if sufficient care is taken to avoid contaminating the growth solution. Lack of cleanliness of all the components used in the synthesis of the seeds is one common failure mechanism for the growth of the seeds, but it is not the only mechanism.

The conformal seed layer must be deposited on the fiber in order to enable the growth of nanowires. During the seeding process, the fibers are dipped in the colloidal suspension of ZnO nanoparticles and annealed at 150 °C for ten minutes, three times. If fibers and growth frames were not allowed to cool in air for five to ten minutes between annealing steps, large sections of the nanoparticle seed layer would break off, ostensibly due to thermal shock upon quenching in the seed suspension primarily consisting of ethanol. These missing sections would not grow nanowires as there is nothing to nucleate from, leading to poor nanowire growth like the one shown below in Figure 3-3. The seed layer is still a brittle, thin ceramic and rapid strains or high strains can easily damage it. The small fiber diameter means that the radius of curvature of a bent fiber must be very small in order to crack the coating; much smaller than routine handling imparts on the fiber.

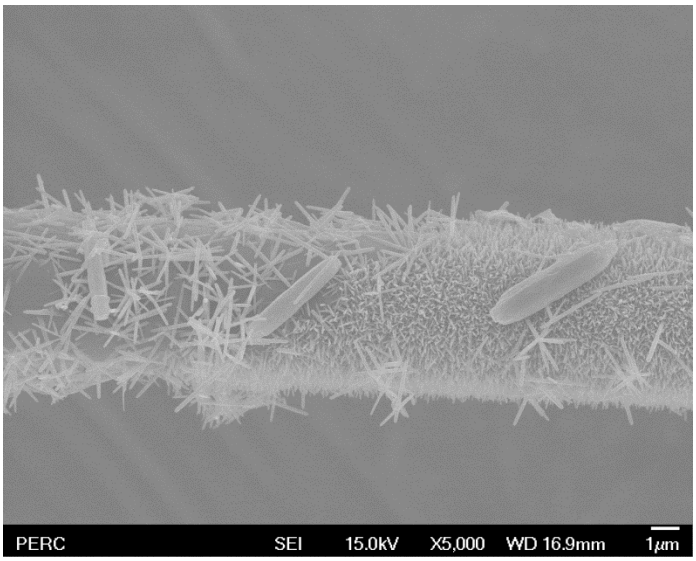

Figure 3-3. Scanning electron microscope image of fiber with partial growth of ZnO nanowires. The ZnO seed layer was fractured and debonded due to thermal shock. Aligned nanowires do not grow in locations where there is no seed layer. Spontaneously precipitated ZnO microrods floating in the solution can physically deposit on the surface of the fiber; however they do not increase the interfacial shear strength.

Beyond the seed layer, the grain size must be appropriate in order to nucleate dense arrays of nanowires. This can be controlled by increasing the growth time of the nanoparticles to enhance their size prior to annealing. The nanoparticles grow through well described Ostwald ripening models that show particle volume growth rate as a constant with time; although the model doesn't include the initial non-linear nucleation phase. While an intense study of the nucleation and growth of ZnO nanoparticles is outside the scope of this work, it is important to note that the detailed work by Hu et al. provides specific information on the mechanism and modeling of the growth of the nanoparticles.[218] Specifically, Hu et al. showed that various alcohols can be used to synthesize ZnO quantum dots and developed models showing that the growth was diffusion limited. While Hu provided a detailed analysis of various combinations of solvents and reaction temperatures, this work will employ only the reaction with ethanol and only at 65 °C. This combination is selected because ethanol is more widely

available than the other alcohols investigated and provides the highest growth rates. Temperatures significantly in excess of 65 °C can approach the boiling point of the solvent and increase the probability of solvothermal reactions or glass bottle failure due to accumulated pressure.

While the article by Hu et al. provides great detail about how to synthesize the materials and how to model the growth specific techniques that were absent from their paper will be included in this work. These techniques both improve consistency and impact resulting nanowire growth. First, it was stated that the growth of ZnO is highly dependent upon polarity of the surfaces, any agent that may preferentially adsorb and reduce growth rate of a specific direction must be avoided. This means that only absolute, undenatured ethyl alcohol should be used, additional purification is generally not required. In addition to organic contaminants, metallic contaminants should also be avoided, especially resisting the temptation to use aluminum foil covered beakers. Finally, the article by Hu specifically notes growth rates at 25 °C and 35 °C, which means that the particles will continue to grow during the cooling period as well as any time spent on the shelf. The experiments performed in this work use seeds that are deposited on the fibers immediately after cooling, avoiding any more than a short waiting period on the shelf. This contrasts with the work by Hu and many others in the reviewed literature who report shelf lives of 2-3 weeks Consistent cooling procedures, whether it be ambient cooling through convection or liquid quench cooling in cold water, are additionally required for repeatable seed growth times and thus, repeatable nanowire dimensions. Maintaining stock solutions of the precursor 0.0125M $Zn(COO)_2 \cdot 2H_2O$ and 0.02M NaOH in ethanol was found not to affect the growth of

seeds. Seed growth time, growth temperature and time in storage must be consistently controlled to create repeatable nanowire arrays.

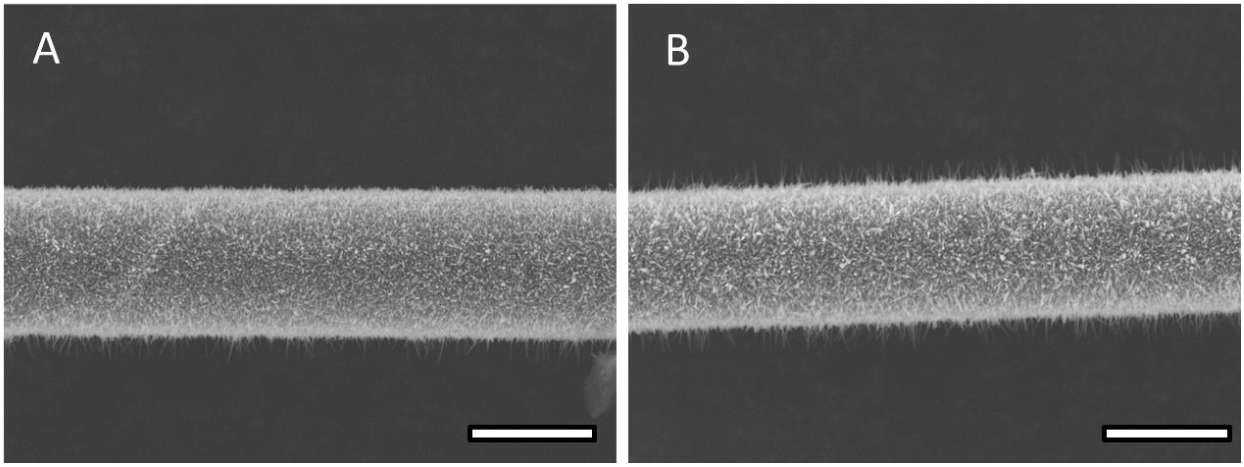

Figure 3-4. Nanowires of varying diameter controlled through varying seed growth time from 20 minutes to 45 minutes. Note that all images are taken at the same magnification. Scale bar is 5 µm.

As stated by Hu et al., the volumetric growth rate of the seeds is approximately constant with time. This work employed longer seed growth times to modulate the diameter of the final nanowires. Galan et al., in conjunction with this research effort, demonstrated that the various seed growth times yielded nanowires with controllable nanowire diameter [219]. Figure 3-4 shows SEM images of two cases of nanowires, differing only in seed growth time, at 20 minutes and 45 minutes. The discrete ZnO quantum dots grow into a solid ZnO film during the 150 °C annealing step after deposition. Adjusting either the annealing temperature or annealing time will inevitably change the grain size of the film placed into the ZnO growth solution. The effects of annealing temperature on final nanowire diameter were beyond the scope of this research because the support frames that the structural fibers were mounted on are nylon and thus could not handle significantly higher temperatures. Lower temperatures were not investigated as it would reduce the cohesion of the film and potentially limit

adhesion of the seed layer to the fibers. Future work may include adjustment of the annealing parameters to control nanowire size; however seed growth enables control sufficient for most demands of this work.

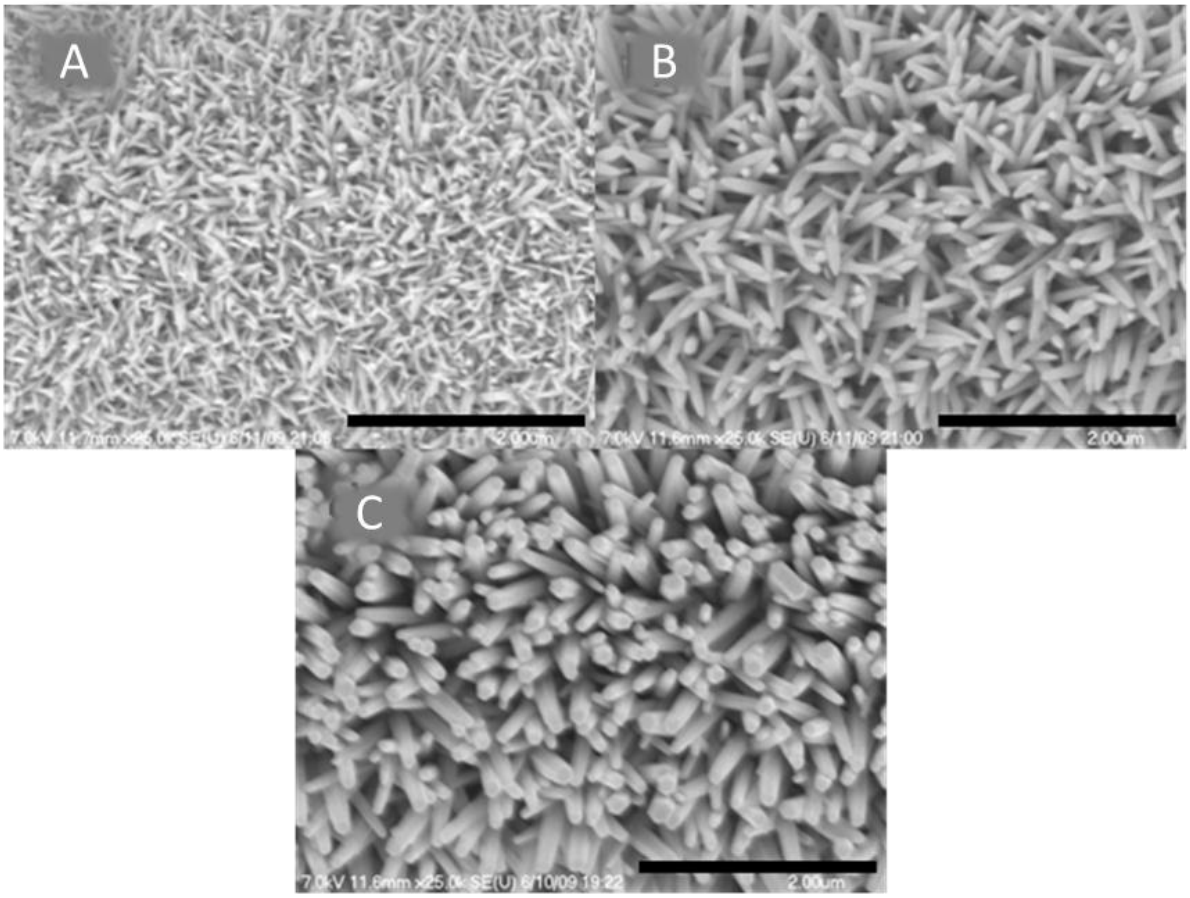

Figure 3-5. ZnO nanowires of varying diameter grown on carbon fibers, (a) 5 mM PEI concentration, (b) 1 mM PEI concentration and (c) No PEI added. Growth time is 2.5 h for all conditions. All SEM pictures were taken at 25k magnification and have a 2 μm scale bar. [Reprinted with permission from Galan U, Lin Y, Ehlert GJ, Sodano HA. Effect of ZnO nanowire morphology on the interfacial strength of nanowire coated carbon fibers. Composites Science and Technology 2011;71(7):946-954.]

Another mechanism to control nanowire diameter is the implementation of a selective polymer adsorbent such as polyethyleneimine (PEI). PEI, in low concentrations can be used to preferentially adsorb on the non-polar faces and enhance the relative growth rate in the <0001> direction. The adsorbent on the sides of the

nanowire leads to restricted growth, even in light of varying nucleation. PEI adsorption represents a proven and useful mechanism that can help to tailor the nanowires to the specific application of interest. The process has been detailed extensively in previous work as a part of this lab [189,219]. The nanowires employed in this work were consistently sized and typically grown simultaneously to avoid any effects of morphology. It has been shown that the length and diameter of the nanowires can impact the interfacial shear strength measurements [189,219]; however this work focuses on the effect of interface chemistry and thus this factor was controlled to be constant. The nanowires for this work were measured to be approximately 70 nm in diameter and 750 nm in length.

The second step, the solution growth of the nanowires, also shows some behavior that can delay future researchers in the development of this technology. One problem that has been continually reported throughout the development of solution grown ZnO nanowires is the spontaneous precipitation of larger scale ZnO microrods in the growth solution. The chemical reactions listed in Figure 3-1 do not have any specific dependence to grow on the nanoscale. Nanowires are nucleated and maintained in this reaction by diffusion limited growth conditions, where local reactant concentrations limit the growth rate and multiple nucleation sites compete for reactants. Global reactant concentrations in the solution far away from the nanoscale ZnO seeds are often much higher and can grow much larger particles, rather than nanowires. These micron sized particles are nucleated spontaneously in the solution and often consume the majority of the reactants by mass, typically harmlessly floating around in the growth solution until slowly settling at the bottom of the reaction vessel. It should be advised that this is not

always the case and the microrods can deposit and adhere to the surface of the nanowires. In some applications this does not pose as a problem. With this application a single microrod can easily eclipse the diameter of the fiber in at least one direction, which leads to the unintended effect of creating a large stress concentration rather than a gradient to reduce stress. The presence of microrods or flowers on the surface of structural fibers was found to reduce the interface strength. This was particularly evident during the single fiber fragmentation testing, discussed in detail in Chapter 3, where it was observed that the areas with flowers showed few cracks and smooth uniform areas showed a higher density, indicating a stronger interface.

After the microrods deposit they become difficult to remove, thus an important consideration in developing the growth solutions is mitigating the deposition of the microrods. As stated earlier, the ZnO growth reaction creates non-uniform reactant concentrations at the location of nanowire growth, yet the nanowires grown into uniform arrays. One successful attempt to control the nucleation and deposition of the spontaneous microrod formation was to reduce the reactant concentration from 25mM to 1mM. It was observed that the growth of ZnO nanowires was not significantly deterred by lower reactant concentrations, in spite of the logical notion that growth rate should be inhibited due to a different pH from reduced hexamethylenetetramine decomposition and lower Zn^{2+} ion concentration. The ZnO microrod concentration was reduced for that exact reason, which leads to the conclusion that the bulk solution concentrations are not always the same as the local growth environment. Reduced precipitation and growth of ZnO microrods significantly reduced the probability of attachment to the surface. Other factors, such as not stirring the solution, also helped.

Previous researchers, while not as explicitly, have also stated that measures have been taken to reduce the deposition of microrods. Articles from Professor Z.L. Wang's research group generally describe the growth as occurring in an oven with the substrate suspended face down at the top of the solution, which would preclude stirring and force the microrods to settle harmlessly at the bottom of the solution away from the growth substrate [216]. Some research has also indicated that the addition of ammonia can inhibit the precipitation of ZnO while still permitting it at the nucleation sites on the seed layer [217]. Perhaps the most common technique to remove the undesirable precipitates is significant washing after growth to agitate the nanowires. While even mild sonication will remove the nanowires, washing in flowing water can remove many of the microrods. During this work washing in water was found to be insufficient, possibly due to the high curvature and enormous surface area of the fibers. Inverted substrate support isn't easily achieved with a fiber substrate and the complex method to chemically prevent precipitation requires ammonia in a closed reaction vessel, significantly complicating the growth procedures. For this work, the reduced concentration mitigates microrod deposition sufficiently to enable high quality single fiber testing. The second key step is flooding the growth container with clean water to wash away as many microrods as possible prior to removal of the fibers from the growth solution, preventing a Langmuir – Blodgett deposition and providing fluid motion to minimize the deposition of microrods.

The novelty of growing ZnO nanowire arrays on small structural fibers necessitates new supports for fibers, different from that of traditional Si wafers. This work focuses extensively on single fiber testing but also explores scale up and issues

associated with it. Carbon and aramid fibers, at a density of ca 2.1 g/cc and 1.4 g/cc respectively, sink in water and thus if not constrained will accumulate microrods on the bottom of the reaction vessel. Two approaches are used to hold the fibers in the desired configuration. Single fibers are mounted to nylon frames whereby individual fibers are held to the frames by epoxy. This eliminates the need to separate the fibers after growth and holds the fibers vertical during growth so that they do not accumulate excess ZnO microrods. This approach reliably produces high quality nanowires suitable for single fiber analysis, specifically single fiber fragmentation testing.

Large scale growth of ZnO nanowires on carbon fibers for full scale composite samples requires slightly different mounting geometry. Complete tows are grown on by creating a loose fitting lid on top of the growth container that has slots where u-shaped loops are hung and held in place. The individual tows must be exfoliated and allowed free fiber motion in order to fully allow the precursor chemicals to diffuse in between the fibers and coat each fiber in the tow. Furthermore, the increase in surface area to be coated with nanowires necessitated returning to the frequently published concentration of 25 mM for each reactant and maintaining large solution volumes to prevent depletion of the growth solution. The full scale composite specimens to be discussed later were grown using several hanging tows hung from a notched lid in two liters of growth solution.

The largest scale sample attempted during this research was ten meters long, wrapped on a wide frame to keep the tow spread as much as possible. The frame was placed into a nineteen liter polyethylene bucket which was heated in a water bath to 90 °C. This growth was attempted as a simulation of what a reel to reel process might be

able to produce. The nanowires did not entirely coat the fiber tow but. this does not mean that the process was a failure. Most of the surface fibers were coated and the correct system of combs and spreaders would probably enable a reel to reel process to be successful in growing nanowires for a large scale industrial use. The solution based growth method employed here is highly robust and with sufficient development could be scaled up to coat industrially relevant quantities of fibers.

Several attempts were made to grow on woven fabrics, with limited success. ZnO nanowires can easily be grown on the surface of the fabric, coating the fibers on the surface of the fabric, extending several fibers deep into the weave. The tortuous path filtering into the center of the weave typically limited diffusion of the reactants and prevented any growth of nanowires inside the tow. The woven geometry maintains dense tows even upon wetting with water. This slows down transport and any reactants that begin to move toward the internal fibers to precipitate out and deposit as nanowires on a fiber closer toward the outside surface of the weave. The nanowires grow very well on woven fabrics. This however amounts to only a surface coverage that can reinforce the interlaminar region of a composite and not improve the interfacial or intralaminar shear strength.

Several throughout the community have expressed interest in determining if reel to reel processing of nanowires such as these would be possible. My personal contention is that ZnO nanowire arrays are the most realistic whiskerization material for reel to reel processing investigated to date. Although carbon fiber production necessitates high temperature inert gas furnaces this type of equipment is expensive, difficult to maintain and requires an enormous amount of inert gas, which makes the addition of SiC

whiskers or CNTs an expensive and difficult proposition. At the time of this writing, a continuous reel to reel processing method would contain a seed bath followed by an in line annealing furnace. Rollers and tanks would be made out of stainless steel or epoxy coated steel as these materials would prevent contamination of the growth solution. Growth would be accelerated through electrochemical growth methods [220] employing conductive rollers and the conductivity of at least the graphite fibers to increase the growth rate. The ZnO solution would be maintained through a continuous process similar to the one detailed by Richardson et al. [207,212]. Recirculation would ensure that the fibers are able to sufficiently grow nanowires in a continuous fashion, eliminating fluctuations due to repeated refreshing of the growth solution. Schematically, the process would look similar to Figure 3-6 and is planned as a future extension of this research.

Structural fibers can be coated in ZnO nanowire arrays with relative ease given certain protocols are followed. There is nothing fundamentally challenging to applying the process in a reel to reel production environment and the solution based growth method is both environmentally friendly and economically viable. Uniform arrays of nanowires require cleanliness of both the growth and handling equipment as ions or organic molecules can interfere with the deposition. Proper care in designing the handling frames and supports can help reduce the likelihood of mircorod deposition onto the fiber substrate, allowing high quality nanowires that will produce significant interface improvements in subsequent composites.

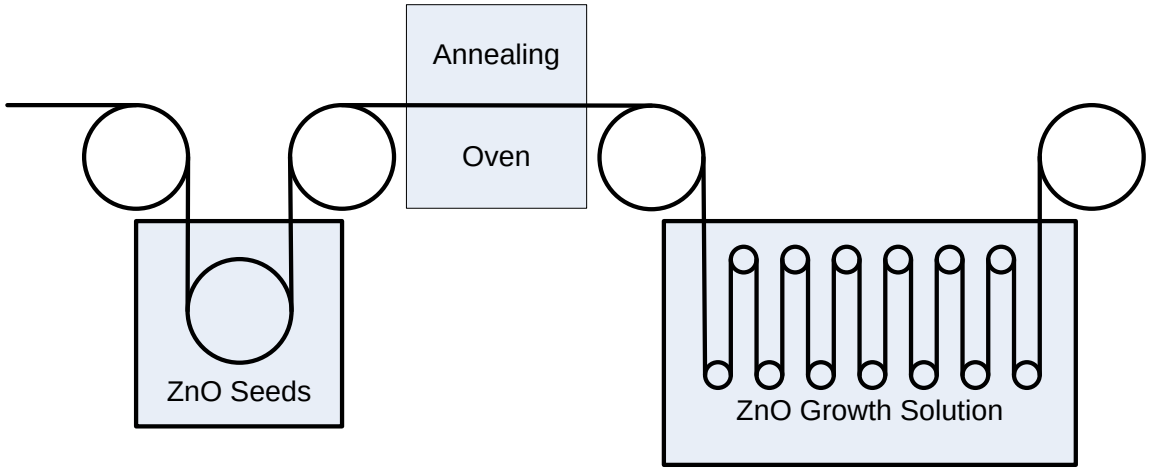

Figure 3-6. Proposed schematic of continuous reel to reel growth of ZnO nanowire interphase.

The specific experimental parameters used to grow nanowires for this experiment have been detailed above; however for clarity they are listed here. Zinc acetate dihydrate, zinc nitrate hexahydrate, sodium hydroxide, hexamethylene tetramine and ethyl alcohol were used as received. The seeds were synthesized by creating stock solutions of 0.0125 M zinc acetate dihydrate and 0.02 M sodium hydroxide in ethanol. The solutions required brief heating to 65 °C with vigorous stirring to dissolve. The solutions were then cooled to room temperature. 24 mL of the NaOH solution and 24 mL of the zinc acetate solution were added to 60 and 192 mL of ethanol, respectively. The two solutions were heated to 65 °C with vigorous stirring in a pyrex jar with a lid for 15 minutes. Once the temperature equalized, the solutions were mixed with vigorous stirring and heated at 65 °C for 45 minutes, maintaining vigorous stirring during growth. After 45 minutes, the seed solution was left to cool in ambient conditions and used within 8 hours.

Carbon fibers were mounted on nylon frames for growth with double sided masking tape and then Devcon 5 minute cure epoxy. After the epoxy cured, the tape was removed to leave the fibers attached to the frames. The entire frame was then

place in boiling acetone, boiling ethanol and finally left to soak in boiling 18.2 MΩ·cm water, which leached out any contaminants. After drying, the frames were dipped in 300 ml of the seed solution prepared before and annealed for 10 minutes at 150 °C. The frames were then removed from the annealing oven and allowed to cool for 5 minutes, before repeating the process of dip – anneal – cool two more times.

The single fiber growth processes employed in this work used a consistent set of growth times and reactant concentrations to attain relatively similar ZnO nanowires. A solution of $Zn(NO_3)_2 \cdot 6\ H_2O$ (0.001 M) and hexamethylene tetramine (0.001 M) was preheated to 90 °C. The growth frames were added into the beaker and a flat bottom flask or watchglass was placed on top to maintain as much of the water as possible. After 2.5 hours, the solution was flooded with 18.2 MΩ·cm water until the solution was clear and near ambient temperature. The fibers were then dried and used in the next characterization or analysis step.

3.3 Fabrication of Structural Composites with a ZnO Nanowire Interphase

Structural composites can be fabricated with many techniques to achieve any of dozens of particular characteristics, such as minimal cost, surface finish, cycle time, product quality, etc. With awareness of the extreme diversity of processing methods for composites, the work in this work is restricted to the technique known as wet layup. In the wet layup techique dry fibers are mixed with a liquid polymer resin and then heated to cure the polymer. A variety of polymers can be used, ranging from melted thermoplastics like polyetheretherketone to liquid thermosets such as vinyl ester resins. Polymer matrices for composites are incredibly diverse and the selection of the polymer matrix for this work did not consider every possible matrix or processing method. This section is not intended to serve as a review of processing of composites but rather it is

meant to justify the processing methods selected and provide an assessment of the impact of a ZnO nanowire interphase on this common model system. A ZnO nanowire interphase will influence other processing techniques not described here, but these remain outside the scope of this work.

3.3.1 Selection of Polymer Matrix

The selection of a polymer matrix will have drastic effects on both the performance of the composite and the requirements of the processing design. The goal of this work is to develop a ZnO nanowire interphase, and the underlying science, so that it can be implemented in structural aerospace components. These components are largely produced with thermoset polymer matrices, either from preimpregnated laminae (prepreg) or from wet lay up of dry fiber preforms. The polymer selected for this work will be a thermoset polymer similar to one used in prepregs or utilized in wet lay-up procedures. The dominant class of thermoset polymer matrices in aerospace components is epoxy based polymers because they provide a highly preferable combination of processing characteristics, thermal stability and mechanical properties. Epoxy based resins are commonly used in both prepreg and wet lay-up processes, standard practices well refined and known throughout the industry. This work will employ a thermoset epoxy resin over alternatives such as vinyl ester, polyester or phenolic resins because epoxy is more common in high performance composites. Vinyl ester, polyester or other resins are often selected for processing of large components or to reduce the high temperature curing requirements. Most of this work is performed on a small scale with high quality laboratory equipment so there is little added cost of high performance processing equipment. The testing of flat laminae imposes few constraints on processing because of component geometry.

Narrowing the choice of the polymer to a thermoset epoxy resin, there still exist several thousand different polymers that meet the criteria. While one can rule out adhesive epoxy meant to attach two rigid components, a large class of epoxy based polymers includes a mixture of epoxy polymers and thermoplastics which must be evaluated for use in this work. These toughened matrices are excluded on the grounds of simplicity and availability. Many toughened resins are only available as prepregs and their exact composition is a closely guarded trade secret. Commonly available epoxy resins include the Epon™ series from Momentive (formerly Hexion, Shell), as well as competitive offerings from BASF, Dow Chemical, Cytec Engineered Materials and Du Pont among others. Amine based curing agents include the Jeffamine™ line from Hunstman, Epikure line from Momentive and a series of alternatives from competing chemical companies. Combinations of resins and curing agents are as diverse as their applications, leading to a vast array of options that do not need to be weighed.

For this work a low viscosity resin is desired, that is well understood, and widely documented throughout the scientific literature in addition to being readily available in quantities smaller than 55 gallons. This Epon™ series of resins most closely matches these criteria as they are the most commonly published and widely available with the continental United States. Within this group, Epon™ 828 and 862 are the most common as simple diglycidyl ethers of bisphenol A and F, respectively. Epon™ 862 is specifically chosen for this work as it has the greatest compatibility with low viscosity curing agents to improve processing of composites. To complete the polymer system selection, Epikure™ 9553 is prefered over the Jeffamine™ series and other polyalkylamine and polyetheramines. Epikure™ 9553 is commonly published in

conjunction with Epon™ 862, it comes from the same supplier (Momentive), and offers a low processing viscosity. The resin system selected for this work will realistically represent a high performance epoxy matrix that is applicable to structural composites; both prepreg and wet lay-up components. The resin will be suitable for processing in a laboratory and provide mechanical properties, listed in Table 3-1, on the order of those expected in state of the art composites. This resin system, because it is well known throughout the community, will give researchers an immediately recognizable baseline to compare their specific polymer matrix system to and a starting point for process development.

Table 3-1. Mechanical Properties of the polymer matrix system used in this work. The epoxy was mixed 100:16.9 pbw and cured at 100 °C for one hour and 160 °C for one hour.

Material Property	Heat Deflection Temperature	Glass Transition Temperature	Tensile Strength	Tensile Modulus	Tensile Elongation
862/9553	90 °C	107 °C	71.7 MPa	2.55 GPa	15.1 %

3.3.2 Selection of Processing Method

Several methods exist for processing composites, including pultrusion, wet lay-up, prepreg layup, chopped fiber spraying, resin transfer molding, and more. Although a review of all possible methods is beyond the scope of this work, the methods above will be briefly addressed to provide context for the selection of the wet lay-up method. The discussion will detail the impact the addition of ZnO nanowires already developed for production will have on the processes, rather than on the development of the methods.

Pultrusion consists of pulling continuous fibers through a resin bath and then curing the fiber – liquid resin composite in a heated die as the composite is continually extracted. This remains a popular technique for mass production; however it is often

beyond the scope of a laboratory environment because batch sizes are measures in kg or tonnes, rather than grams. It is a concern that consolidation and flow of the resin during the pultrusion process, which squeezes the fibers together and creates flow in the matrix, could damage the alignment of the nanowires. While the nanowires can be damaged locally when contacted with tweezers, this far exceeds the stresses generated in pultrusion and it will be shown later that typical composite processing pressure is not high enough to damage the nanowires. The major difficulty in creating composites with pultrusion is creating effectively continuous fibers with ZnO nanowires.

Prepreg lay-up is one of the most popular industrial techniques for producing highly stressed structural components because it provides a high degree of process control. A prepreg is purchased preimpregnated with mixed, cooled resin that begins to cure when it reaches elevated temperatures. The materials in as purchased condition have controlled amounts of resin to yield repeatable volume fractions and require minimal motion of the resin, limiting voids in the composite. The production of prepregs is highly specialized and requires large quantities of fibers to operate with any efficiency. Implementing a ZnO nanowire interphase would require the same large scale quantities required for pultrusion. Once those are produced, there is no other fundamental reason why ZnO nanowire coated fibers would have any difficulty being processed on existing prepreg production lines.

Wet lay-up of composites is favored among composites laboratories as it requires very little capital intensive equipment and is widely adaptable to various experiments. The wet lay-up technique consists of a dry fiber preform placed in a mold and then is infiltrated with a liquid polymer resin. Resin transfer molding uses a closed mold in a

similar fashion by pumping resin through a pressure, while vacuum assisted resin transfer molding uses a vacuum to pull resin through in the same manner. Wet lay-up only requires, at a minimum, a one sided mold. The mold can easily be integrated into an oven for elevated temperature curing as required by the Epon™ 862/ Epikure™ 9553 resin system. The single fiber composites used in fragmentation are also produced through a wet lay-up technique so consistency, as much as possible, can be maintained when scaling up from single fiber to lamina scale.

The processing method selected for this work is primarily the wet lay-up, both with and without vacuum. The low viscosity of the Epon™ 862/ Epikure™ 9553 resin system mitigates the potential for the formation of bubbles, eliminating the need for vacuum degassing in small single fiber fragmentation samples. Larger samples, such as the v-notch shear samples, require vacuum degassing to eliminate voids and maximize fiber volume fraction. The resin system does require an elevated temperature cure to achieve the maximum properties. Curing is completed in an oven or on a hotplate, ensuring that the high temperatures required for maximum mechanical properties are maintained.

The wet lay-up technique employed in these experiments generally applies to two types of samples, single fiber composites for single fiber fragmentation and unidirectional laminae for v-notch shear testing. The single fiber composites are cast into silicone rubber molds that have the shape of the desired specimen cast into them, demonstrated by the geometry shown in Figure 3-7. The molds are coated with mold release (Buehler, Lake Bluff, IL, USA) and then a single fiber is placed inside. Where possible, small metallic clips (ca. 1g) are used to pretension the fibers and reduce the

strain that must be applied in order to cause the fiber to begin to fragment. In many cases, a hotplate is used to assist in curing the specimens. As many hotplates have magnetic stirrers, one must be cognizant and only use the metallic clips when the effect of the magnetic stirrer can be minimized. The polymer matrix is mixed in a small container and then the mold is filled with polymer by using a pipette. The samples are solidified for 60 minutes at about 30 – 40 °C and then placed in a convection oven to cure for one hour at 100 °C followed by one hour a 160 °C. Fabrication of aramid fiber composites follows a similar procedure however the composites are fabricated with much more significant preload, ca. 10g.

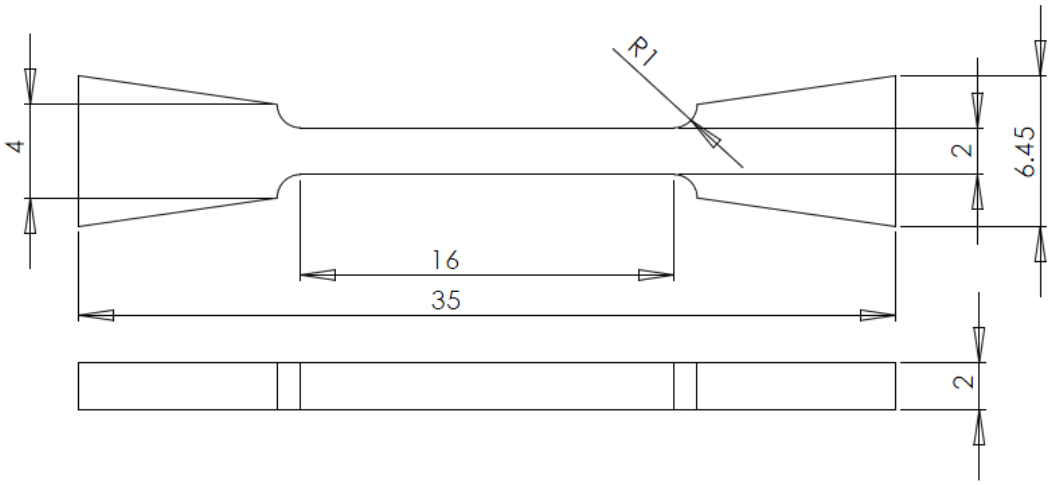

Figure 3-7. Drawing of dogbone shaped specimen for single fiber fragmentation testing, following the dimensions of Feih et al. [221].

Larger scale composites are made through a wet lay-up technique that includes vacuum bagging to reduce the presence of voids in the sample. To make larger laminae for the v-notch shear samples, a mold is machined out of two thick aluminum plates. Aluminum is selected because it is relatively inexpensive, easy to machine, sturdy, and thermally conductive. The mold is created with a channel of the appropriate width to ensure that all fibers contribute to the sample and none are wasted. Several

tows of fibers are placed into the channel followed by wetting with the polymer resin. Once the appropriate amount of fibers and resin are placed in the channel, the mold is closed and pressed to create the composite. The compression is accomplished in two ways; first, through the application of a vacuum bag to use atmospheric pressure to clamp the mold and second by using a load frame to compress the sample. Even a small compressive stress applied to such a large area corresponds to a very high force requirement; thus pressing must be performed with a load frame. Once fully compressed and held, while the excess resin flows out, the molds effectively maintain location and spring back very little. At this point, the mold is transferred to hotplate and heated to finish curing the composite. It should be noted that 4 channels are provided in each mold, two wide channels for 0° specimens and two narrow channels for 90° specimens. One channel is filled with control fibers and one with nanowire coated carbon fibers. In this manner any inconsistencies in curing, compression, volume fraction or voids is identical and processing variations, in as much is possible, are removed. The large scale lamina are then cut to size and instrumented for material testing.

One of the dominant factors in a composite is the relative volume fraction of fibers and matrix. The fiber volume fraction is present in nearly every equation for prediction of the bulk material properties from constituent properties. The fiber volume fraction of the composites was measured for these composites by following ASTM D3171 [222], the test for fiber volume fraction. The test procedure requires that pieces of the composite be cut out, weighed and then placed in heated nitric acid. The hot oxidizer attacks the polymer resin, oxidizing the linear polymer chains. The fibers, while etched

slightly, remain largely in-tact and are weighed to determine the mass of fibers. Assuming no voids in the composite and the manufacturer's specified densities for the polymer and fiber, one can compute the fiber volume fraction to be

$$v_f = \frac{m_f \rho_m}{m_t(\rho_f + \rho_m)} \tag{3-1}$$

where m_f is mass of the fibers, m_t is the total mass, ρ_f is the fiber density, and ρ_m is the matrix density. The average of two samples of the bare fibers and nanowire coated fibers yielded volume fractions of 49% and 50%, respectively. The composites have effectively the same volume fraction, which is slightly lower than that of a typical prepreg composite. Higher volume fraction composites are preferred because they contain more of the strong fiber phase, rather than the comparatively weaker polymer phase. The maximum packing factor of circles in infinite space is 91%; however prepreg composites can only achieve volume fractions approximately 60% to 70%. A volume fraction of 50% does compare favorably with other similar unidirectional wet lay-up composites, which typically have volume fractions ranging from 50% to 60%. The volume fraction is a good indicator that the composite processing is on par with industry standard and these experiments indicate that the addition of ZnO nanowires will not affect the achievable volume fraction. Finally, the volume fraction of these composites is comparable to other samples tested in the literature thus the data is representative of what the technology can bring to future materials.

One natural question is the relative volume fraction of ZnO, in particular as it relates to the volume fraction calculations of composite properties. ZnO is entirely soluble in strong acids, dissolving into Zn^{2+} ions by the reaction

$$ZnO\ (s) + 2H^+\ (aq) \rightarrow Zn^{2+}\ (aq) + H_2O\ (l) \tag{3-2}$$

Given that the digestion occurs in nitric acid (70%), any ZnO present will be completely consumed in the acid and the fiber mass will be the true fiber mass. Thermogravimetric analysis can offer some insight as to the relative mass of ZnO in order to determine the volume fraction of ZnO present. Analyzing a ZnO coated carbon fiber at high temperatures in an oxidizing atmosphere will oxidize the carbon while preserving the ZnO, the ZnO will not change the chemical state in oxidizing atmospheres. Figure 3-8 shows that a hierarchical fiber contains approximately 5.9 wt% ZnO. Given that the density of ZnO is 5.606 g/cc and the density of carbon fiber is 1.79 g/cc, the volume fraction of ZnO is computed to be 2.1% of a hierarchical fiber. Combining this with the fact that the fibers are only 50% of the composite volume, a reasonable approximation for the volume fraction of ZnO in the composite is 1% or less, which is generally not enough to be included as a third phase in continuum based models of composites.

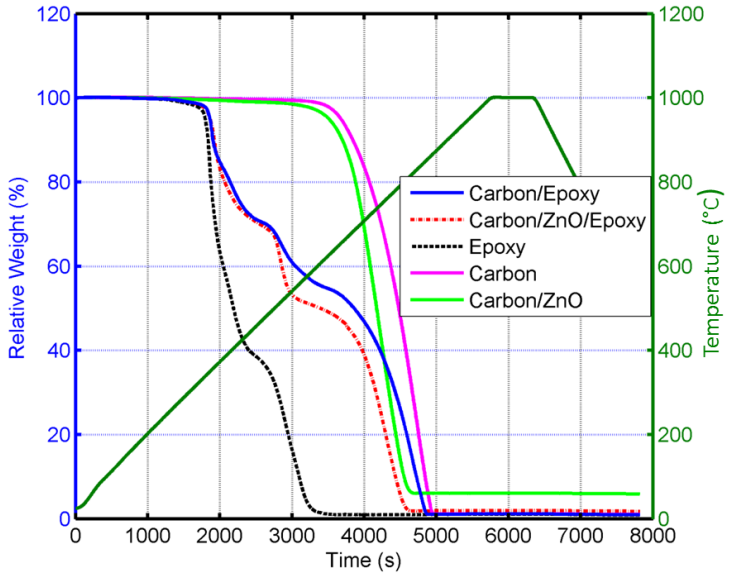

Figure 3-8. Relative mass loss of hierarchical fibers and their composites. Traces show that ZnO accelerates the final stages of oxidation of the epoxy composite (above 500 °C). In addition, the hierarchical fiber without a polymer matrix shows that the ZnO is approximately 5% of the total hierarchical fiber mass.

Carbon fibers often come with a polymeric sizing layer which is intended to reduce the susceptibility of the fiber to damage during weaving. This layer would obviously have enormous effects on the surface chemistry and properties of the fiber. XPS is one method to identify polymer sizing layers as the polymer often has additional elements besides oxygen and carbon or the carbon atoms will be in different configurations which will slightly change the binding energy. XPS can occasionally mislead researchers, so the absence of sizing layers is often confirmed with TGA. Figure 3-8 and Figure 2-13 both show oxidation profiles for bare carbon fiber. The oxidation shows the decomposition of a single compound that begins around 600 °C. Most polymers do not handle temperatures nearly this high. The only compound consisting solely of carbon that can withstand temperatures of this magnitude are the graphitic allotropes (buckminsterfullerene, graphene, carbon nanotubes, graphite) and diamond. The TGA proves that there is no sizing applied to the fibers and the data analyzed here is that of graphitic carbon fibers, not a polymeric sizing layer.

3.3.3 Interface Quality at the Fiber and Nanowire Surfaces

A great concern within the nanocomposites community is the exfoliation of the filler. Particle interaction forces do not follow the same scaling laws as fluids or polymers. Very frequently nanomaterials, when mixed into polymers for composites, do not disperse as one might desire [223]. When attempted this leads to aggregations of particles with voids in between the particles as resin cannot wet such a small volume. This is of concern for the development of this composite because if the polymer is not able to wet the individual nanowires on the surface of the fibers, then the voids created at the interface between nanowires and the polymer matrix will eliminate the advantages claimed about increased surface area and mechanical interlocking.

Following similar logic, it is also of the utmost importance that the ZnO nanoparticle seed layer completely conform to the surface of the carbon fiber to prevent voids from initiating interface cracks. This section will analyze the quality of both the polymer nanowire interface and the ZnO fiber interface, specifically focusing on the wetting of the nanowires and the presence of voids.

The wetting of nanowires was determined through cross sectional analysis of individual wetted fibers. The first sample is one that is sectioned and polished through standard metallographic techniques, using a wafering saw and lapping films to polish the surface. The composite was then analyzed with a scanning electron microscope to identify the fibers, matrix, and ZnO nanowire interphase. Prior to analysis, a thin layer of amorphous carbon is evaporated onto the specimen to enable charge dissipation that accumulates on the surface during the analysis. Energy dispersion x-ray (EDX) spectroscopy is used to identify the presence of the individual elements, carbon, zinc, and oxygen. The results of the EDX spectroscopy are then used to create a two dimensional map of the elemental distribution in the composite to identify if there are excessive voids or if the polymer matrix wets the nanowire interphase. Figure 3-9 shows the elemental map of the cross sectioned composite sample. Although this image is not entirely conclusive in verifying that the nanowires have been wetted by the polymer matrix, the elemental map does demonstrate several important features. The elemental map also verifies the identification of the phases as epoxy, fiber, and interphase and confirms what is already intuitive. The polymer matrix, epoxy resin, has a combination of carbon and oxygen. The interphase is ZnO, zinc and oxygen. The carbon fibers are a highly reduced graphitic carbon that, while a small fraction of oxygen

or nitrogen might be present, is effectively pure carbon. The maps and cross section confirms that the location of the ZnO nanowires is preserved after wetting, fabrication and handling of the composite. Specifically, all of the Zn is present at the interface between the fibers and matrix, with the exception of some residual flowers or microrods next to one of the fibers.

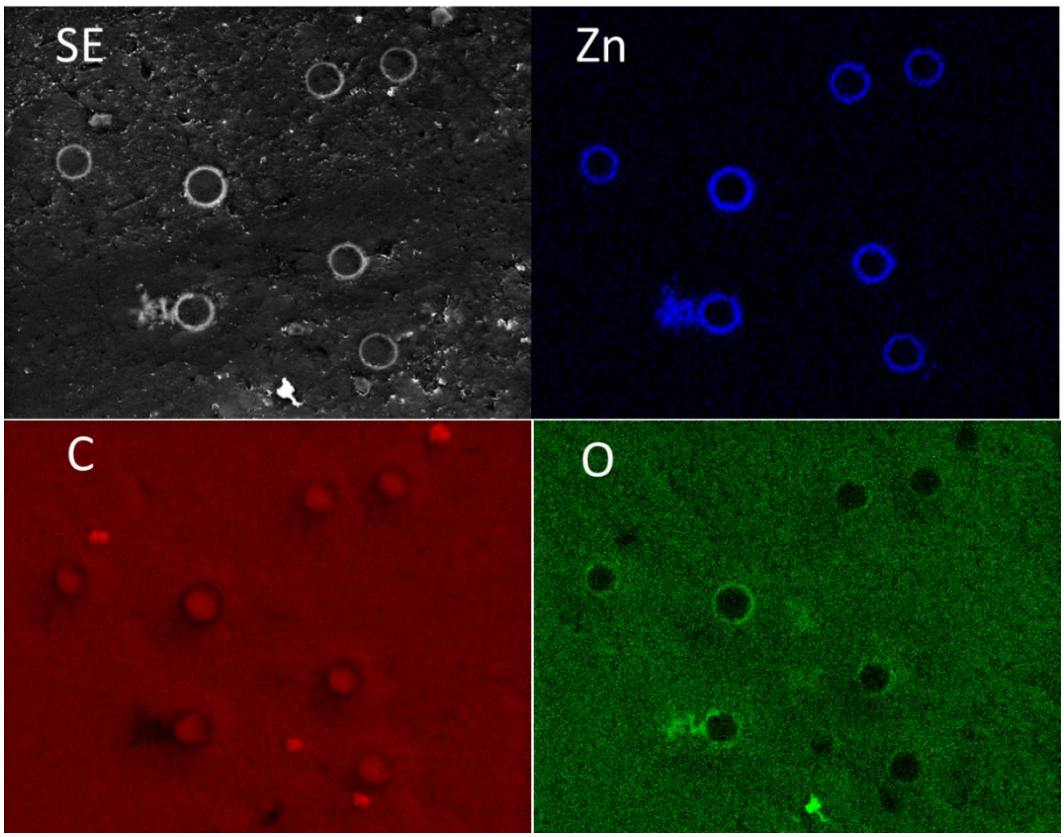

Figure 3-9. Cross section of carbon fiber composite with ZnO interphase on the fibers, imaged with secondary electrons and labeled SE. Energy dispersive x-ray spectroscopy is used to create an elemental map of carbon, oxygen and zinc, labeled C, O and Zn, respectively.

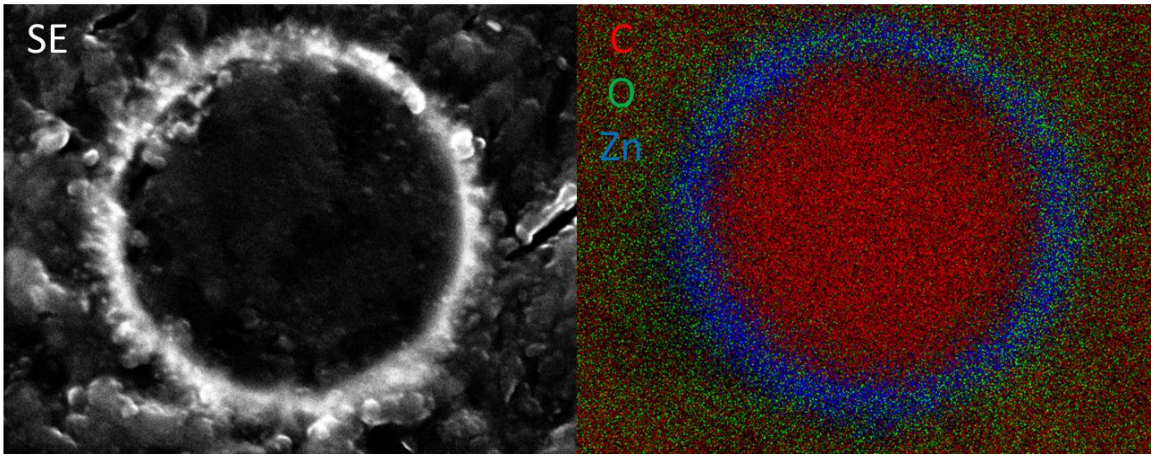

Figure 3-10. High magnification elemental map of a single fiber cross section. The legend shows carbon is red, oxygen is green and zinc is blue. The cross section clearly shows that the nanowires are still located at the interface between fiber and matrix.

In order to avoid the problems caused by polishing the sample, a focused ion beam mill is used to section a fiber that was wetted with epoxy. The focused ion beam does not remove material directly through abrasion but rather through collision of the surface with high energy gallium ions. In this way, it does not generate stresses in the fiber or cause any smearing of the fiber. Figure 3-11 clearly demonstrates that the polymer penetrates deep in between the nanowires, even without the help of vacuum. The surface wetting is fairly consistent, as previous work has shown that the addition of nanomaterials to the surface of fibers actually improves wetting by drawing in polymer via capillary action [117]. The second important aspect to note in the image is the orientation of the nanowires. Although higher aspect ratio nanomaterials increase the surface area, very often the additional length makes the nanowires extremely compliant and the allows the nanowires to coalesce at one end to form fibers with what are termed, ‘mohawks’. There fibers do not maintain a strict radial alignment of the nanomaterials around the fiber, but rather the hierarchical fiber has a tee shaped cross section. The use of ZnO nanowires with an aspect ratio of about 10 does not suffer

from this fate rather the nanowires maintain the alignment as grown during handling and wetting of the polymer. This provides direct evidence that the interface between the ZnO nanowires and the polymer matrix is strong and free of voids.

The second interface of study is the ZnO – fiber interface. Given that the seeds are small ZnO quantum dots deposited to form a polycrystalline film, it is a concern that the film might be porous or the interface might contain voids. While an SEM can resolve individual nanowires and the pores in between them, imaging the seeds used to grow the ZnO nanowires is not possible in an SEM. A transmission electron microscope (TEM) is employed to view the ZnO – fiber interface quality. The TEM will be used to identify the presence of voids in the ZnO seed layer as well as identify if the seed layer is conformal to the underlying fiber surface. The sample for the TEM was prepared with the FIB by milling a ZnO nanowire coated carbon fiber into a wedge shaped specimen. The specimen was then removed and rotated to orient the thin, wedge shaped cross section perpendicular to the electron beam. This is a tedious process requiring the assistance of an expert operator of both the FIB and TEM.

The TEM image in Figure 3-12 shows two regions of the sample. The ZnO region is identified by the polycrystalline structure, with each nanoparticle seed oriented randomly. The random orientation of the seeds is due to their physical deposition and demonstrates that even after annealing, the particles do not sinter into a single crystal film but rather coalesce into a polycrystalline layer. The random orientation causes the subsequent nanowire growth to also be random. The constraint of the underlying fiber and surrounding nanowires forces the nanowires to grow from the fiber radially outward, the only direction that permits continued growth. The region labeled as carbon is the

carbon fiber, which appears as an amorphous layer. It is well known that the crystalline graphitic regions of carbon fibers exist internally and most carbon fibers have an amorphous carbon shell around a graphitic core. This microstructure is created by the surface PAN chains that do not align during the drawing process and thus do not achieve the same degree of graphitization that the internal chains do [19]. This distinction provides a useful contrast for the image because it positively identifies the two phases. The inset of Figure 3-12 shows a higher magnification image of the interface between one nanoparticle and the underlying carbon fiber. It is difficult to draw a line defining the interface as the particle and fiber are in immediate, conformal contact and show no voids at the interface. The lack of voids bodes well for the potential adhesive forces pulling the two phases together and demonstrates positively that the seed layer is completely conformal to the surface of the fiber. The growth mechanism of the nanowires can also be rationalized as the TEM image demonstrates the ZnO seed layer formed through a coalescence of particles to create a continuous, polycrystalline film. Larger seeds would impact the coalescence and crystal grain size, as would annealing temperature and annealing time. Future works may include this technique to quantify the relationship between seed diameter and the resulting nanowire diameter.

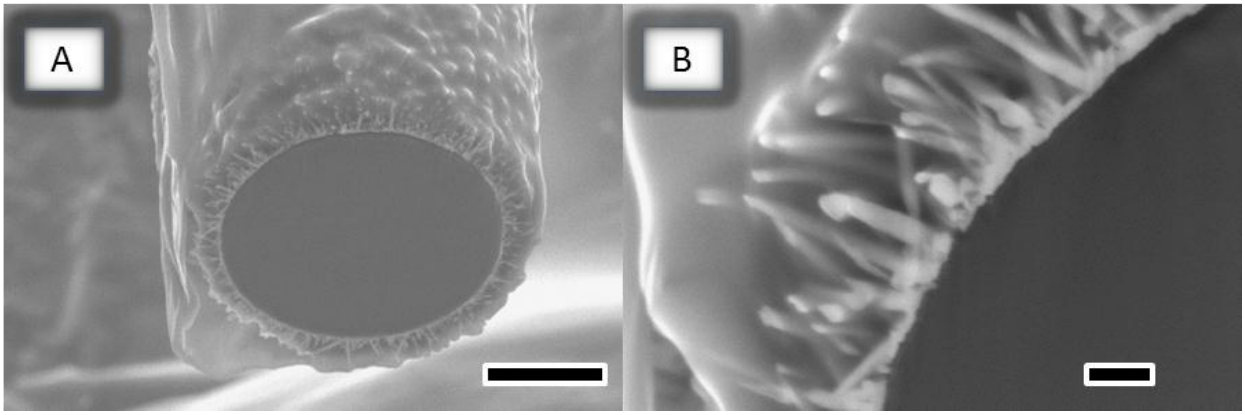

Figure 3-11. Carbon fiber with ZnO interphase wetted with epoxy and sectioned with a focused ion beam mill. Ion milling does not require abrasion and enables the image to show full wetting of the polymer matrix without smearing the polymer to distort the view of the nanowires. Scale bars are 2 μm and 200 nm in A and B, respectively.

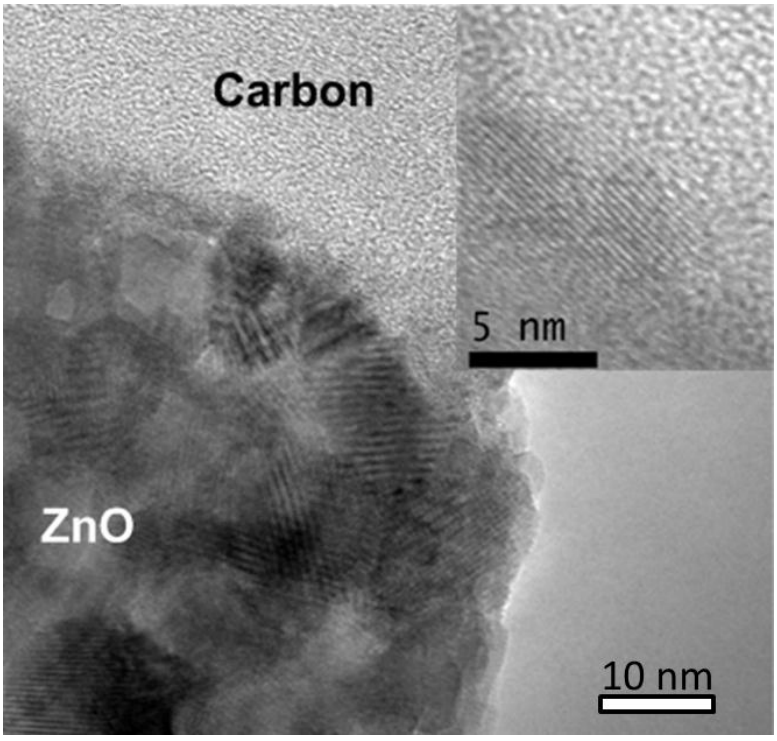

Figure 3-12. Bright field transmission electron microscope image of the interface between the polycrystalline ZnO seed layer and the underlying structural carbon fiber. The polycrystalline seed layer, deposited through evaporation of a suspension of nanoparticles, conforms directly to the surface of the underlying fiber with no voids or defects. The inset shows a nearly indistinguishable transition from the crystalline ZnO seed to the amorphous surface layer of the carbon fiber.

3.3.4 Experimental Methods for Compsite Fabrication

Single fiber fragmentation samples were prepared by first placing a single fiber into a silicone rubber mold. A 100:16.9 mixture of Epon 862 and Epikure 9553 was placed into the mold on an aluminum block resting on a hot plate. The carbon fiber samples were not pretensioned for this experiment as it was not found to be necessary (epoxy matrix had high strain to failure) and greatly increased the probability of fiber failure before the polymer matrix cured. The hotplate was heated to 90 °C, which heated the molds to approximately 45 °C. After 1 hour, the samples were rigid and demolded. The samples were then placed into a convection oven where they were heated for 1 hour at 100 °C and 1 hour at 160 °C. After curing, the samples were sanded flat with 600 grit sandpaper and then polished to a mirror finished with 800 grit paper. Samples were tested under the microscope with a combination of polarized and transmitted light to reveal the cracks. Strain was applied until the number of cracks saturated, but prior to the sample failing.

3.3.5 Summary of Composite Fabrication Results

This section has described the selection of both the polymer matrix and the processing methods to be used in the composite. A thermoset epoxy polymer is chosen because it most realistic, representing a structural polymer for aerospace components. Wet lay-up processing is selected as the primary technique for its reasonable similarity to industrial processes without requiring extensive development or excessive batch sizes. This section also discussed the impact of the processing on the resulting composites, specifically examining the composites after the required handling and infiltration with the polymer matrix. It is clear that infiltration of the nanowire interphase with the polymer matrix can create the desired graded interface of two materials to

reduce the stress concentration at the interface. Various sectioning techniques demonstrate that the nanowires do not exhibit a strong propensity to fall off of the fibers during processing and maintain their adhesion to the fibers during handling. Finally, it is demonstrated that neither the polymer – nanowire interface nor the nanowire – fiber interface contain voids or defects that might threaten the properties of the composite.

3.4 Chapter 3 Summary

Chapter 3 has detailed how to grow ZnO nanowire arrays on small structural fibers. The nanowire arrays are synthesized with a two-step solution based growth process. First, a suspension of ZnO nanoparticles is created and the nanoparticles are deposited on the surface to act as seeds. The fibers are then placed into the growth solution and ZnO nanowires precipitate competitively from the polycrystalline seed layer. The fibers are typically mounted on nylon support frames to minimize the deposition of the larger microrods on the surface that spontaneously precipitate in the growth solution. Furthermore, a flood washing procedure is implemented to carry away excess microrods. Once the microrods deposit on the nanowire arrays, they become extremely difficult to remove. Finally, the sensitivity of the process to organic or metallic contaminants has also been detailed and rationalized based on the polarity of the ZnO growth facets and the tendency to adsorb ions or organic molecules.

Chapter 3 also describes the fabrication and analysis of hierarchical composites. The fabrication methods are detailed, as are the reasons for selection. A two part liquid thermoset epoxy is selected because it represents a reasonable approximation of a high performance structural polymer, while being universally known and easy to draw comparisons within the wider research community. A wet lay up method is selected as it enables fiber wetting and high quality part fabrication without requiring full production

scale processing equipment. Hierarchical composites are first analyzed for fiber volume fraction through standard acid digestion techniques. The fibers are sectioned to assess wetting of the nanowire arrays and nanowire alignment after infiltration with the polymer. Finally, a cross section of the interface between the ZnO nanoparticle seeds and the structural fiber is analyzed to determine if voids or gaps are present. No voids are are present at the interface between the ZnO seed particles and the structural fiber which gives preliminary evidence that a strong chemical interaction draws the seeds close to the fibers.

CHAPTER 4
MECHANICAL TESTING OF STRUCTURAL FIBERS AND COMPOSITES

This work examines the structural properties of fiber reinforced composites with a novel ZnO nanowire interphase. Chapter 4 will detail the testing of composites with ZnO nanowires. Furthermore, analysis of failure surfaces in a variety of composites will be combined with the previously established knowledge of the surface chemistry to identify the role of surface chemistry in the adhesion of the ZnO interphase. Chapter 4 will begin with a review of interface test methods and detail the mechanical evaluation of the composite. The results of several mechanical tests performed on composites with a ZnO nanowire interphase are presented. The mechanical test results in conjunction with the various functionalization treatments will be the foundation for identification of the failure interface. Failure surface analysis and sample cross sectioning will help to identify both the interface of failure and the proposed surface interaction. Finally, the results will be summarized to provide a guide for improving the adhesion of ZnO nanowires to the surface of structural fibers for structural enhancement. The key contribution of this work is the presentation of a mechanism of adhesion to scientific literature as well as demonstrating a methodology to the application of whiskerization in structural composites.

4.1 Mechanical Characterization Methods of Structural Composites

The complex mechanical behavior of a typical two phase fiber reinforced composite is drastically affected by load transfer from fiber to matrix. For example, the failure of a composite generates debonding between fiber and matrix because the properties of the two phases, such as ultimate strain, are different. Even a simple case such as the uniaxial loading of a unidirectional composite incurs interface debonding

upon failure of the material. Interface strength is pervasive throughout modeling efforts in composites [5] but the direct measurement of interface strength is complex and can be influenced by the method of measurement [224]. As such, many methods exist to characterize interface strength indirectly from the mechanical test results. Some of these methods exist for single fiber composites and some for larger scale laminae. This section will review both the single fiber and lamina scale interface characterization methods, highlighting advantages and disadvantages of each technique.

4.1.1 Single Fiber Composite Interface Testing

The most intuitive interface measurement technique is the direct pull-out or push-out test. A segment of a single structural fiber is embedded in a polymer matrix and then removed by loading it along the fiber axis. Generally, assuming a simple shear lag model that will be detailed later, the interface strength is expressed as

$$\tau_{max} = {}^{F_{ult}}/_{\pi dl} \tag{4-1}$$

where F_{ult} is the peak load during the test, d is the diameter of the fiber, and l is the embedded length of the fiber. This type of test provides the most direct path to measuring interface strength.,There are several facets that can limit the utility of the test and make implementation of a pull-out or push-out procedure difficult to perform and replicate. Several research groups have published extensive studies related to both push-out and pull-out [224,225]; thus the two techniques will be separated and reviewed independently.

The model above in Equation 4-1 is typically referred to as the shear lag model, owing to derivation of it by Cox from the force balance of thin segments [226]. The thin segments described by Cox, when integrated along the embedded depth of the fiber,

will yield Equation 4-1; however there also exists other single fiber tests that infer interface strength by employing the same model, namely single fiber fragmentation. The shear lag model forms a simple and reliable approximation of the state of stress at the interface. There are circumstances where the model is limited, especially when considering plasticity and failure. Refined models can improve the accuracy of the predictions of stress distribution throughout the composite [227]. More elaborate models of the interface stress distribution are not always beneficial, in particular when analyzing experimental data, as the number of parameters to fit often increases. Correctly and accurately employing models beyond the typical shear lag model could improve the quantification of interface parameters. The increased complexity must be rigorously justified and very often even simple interface parameters have proven difficult to measure from site to site [225]. The analysis of the single fiber techniques in this work is founded on the rudimentary shear lag model which assumes a uniformly loaded interface. The assumption of this work is that any bias introduced in the measurement of interface strength due to inaccuracies of the shear lag model will be equal. All fibers examined in this work will be compared to a reference case and improvements relative to the reference will be reported. No other models will be discussed as the justification for the increased complexity, as far as this work is concerned, cannot be rigorously proven.

4.1.1.1 Pull-out and microdroplet interface testing

Pull-out testing, for the purposes of this review, will be considered as techniques that place the single fiber in tension during a single fiber interface characterization technique. The first measurement technique is to embed a fiber into a droplet of liquid resin and then either cure or cool the droplet to solid [228]. The fiber is gripped and

then pulled out from the sample while the load displacement trace is recorded to determine the ultimate load and thus the interfacial shear strength of the composite. There are several facets to this technique that must be addressed in order to draw appropriate conclusions out of the data. First, by substituting the axial stress for ultimate load in Equation 4-1, the equation can be rewritten to demonstrate that axial stress in the fiber required initiating fiber pull-out increases linearly with embedded depth and decreases with increasing diameter.

$$\sigma_{fiber} = {}^{4\ell}/_{d}\,\tau_{int} \tag{4-2}$$

Most structural fibers, including kevlar and carbon fiber, are very small in diameter, on the order of 5 μm to 15 μm. In spite of the high tensile strength of the fibers, which causes a high tolerance for axial fiber stress, the small diameter necessitates an extremely small embedded depth in order to satisfy the conditions for pull-out. Typically, this is achieved with custom built experimental configurations that include a precise screw mechanism to move the fiber into the droplet and a microscope objective to optically measure the depth that the fiber is inserted into the droplet [116]. If a sufficiently small embedded depth can be repeatedly maintained, then the technique offers perhaps the most direct measure of interface strength of a composite.

Pull-out tests also have some other flaws that must be overcome in order to verify the accuracy of the results. Perhaps the most difficult problem is one of wetting the polymer matrix around the fiber. Naturally, strong composite materials consist of a fiber and matrix that are mutually compatible to ensure wetting of the matrix on the fibers and preventing voids in large scale composites. When inserting the fiber into the polymer matrix, the liquid polymer can often wick up the fiber in a thin coating or film, causing a

drastic change in the embedded depth as shown schematically in Figure 4-1A. Furthermore, the thin coating does not satisfy the dilute composite assumption underpinning the test and this can manifest itself as a cohesive failure of the thin shell rather than an interface debond and pull out from the matrix, as shown in Figure 4-1B. This situation would be exacerbated with a nanowire coated fiber as capillary action will cause the matrix to climb a significant distance up the fiber. Quantitatively determining the embedded depth when some of the matrix debonds and some cohesively breaks away from the droplet is a challenge. Finally, while the shear lag model is sufficient for most pull-out analysis, the stress state in a wicked polymer droplet will differ substantially from that predicted by the shear lag model.

In addition, the pull-out test also suffers from a difficulty of alignment. Conceivably, a fiber can be inserted down into a liquid resin droplet and held in position while the droplet solidifies. For a thermoset resin, common for structural composites of interest, this can often take more than one hour. If one tests many samples to average out the significant variation present on the small scale, this procedure can be prohibitively slow. If one were to embed several fibers simultaneously and pull each one individually after solidification, alignment would be difficult and could have a significant role in the failure mode by superimposing bending stresses, impacting the results of the experiment. Overcoming these difficulties enables this technique to be applied to measure interfacial shear strength; however this has not been accomplished yet and to date pull-out remains largely a specialized technique employed by only a handful of researchers worldwide [116,225,229,230].

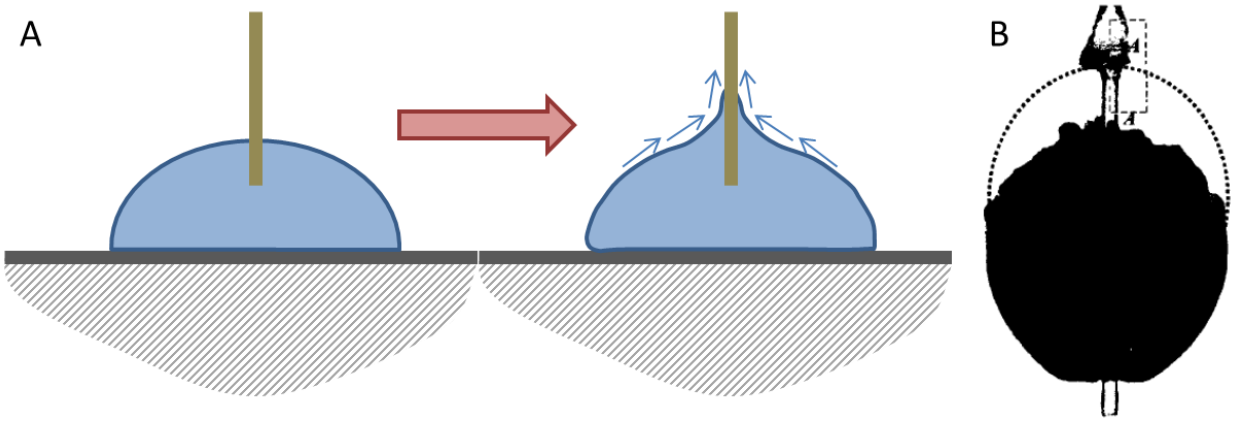

Figure 4-1. A) Schematic of matrix wicking during curing or insertion of fiber for fiber pull-out test. B) Cohesive failure of the polymer matrix illustrating the uncertainty of the location of the failure and importance of the dilute composite assumption. [Reprinted with permission from Drzal LT, Herrera-Franco PJ, Ho H. 5.05 - Fiber–Matrix Interface Tests. In: Editors-in-Chief: Anthony Kelly, Carl Zweben, editors. Comprehensive Composite Materials. Oxford: Pergamon, 2000.]

An alternative to flat droplet pull-out testing is the microdroplet test. To perform this test, a small droplet of polymer is deposited on a structural fiber. The fiber is then threaded through a small hole or between two jaws of a micro-vise. As the fiber is pulled through, the droplet eventually is caught by the jaws and held until the fiber pulls through the droplet. An analysis identical to the previous pull-out test is employed to measure the interfacial shear strength. A liquid thermosetting resin is applied in this fashion by using a small fiber to take up some of the polymer and then deposit it onto the fiber to form a small droplet. This droplet is cured in place, although great care must be taken when applying to droplet to avoid dragging the brush along the fiber creating a thin film on the surface of the fiber. While the microdroplet test has been shown to provide a reasonable estimate of interfacial shear strength, microdroplet testing also suffers from some limitations [224]. First, the small volume of the microdroplet can impact the curing kinetics of thermoset polymer droplets because the two components of the polymer matrix can have different volatilities, leading to incorrect stoichiometry

when scaling down to small volumes [231]. A second problem has received more attention, the problem related to the boundary conditions at the front of the droplet. There has been debate among researchers [224] as to the possibility of the microdroplet being squeezed on the leading edge, superimposing a compressive stress at the interface and reducing the propagation of a shear crack at the interface during the test. This could lead to an overestimation of the pull-out load when compared to other techniques. Further, the use of a knife edge, square edge, or beveled edge on the micro-vise/hole to restrain the droplet can influence the degree of compressive stress applied to the droplet and influence the results. This problem has been modeled to assess the effects of this phenomenon; however site to site consistency remains a fundamental issue for microdroplet testing [225].

Single fiber interface testing techniques based upon tensile loading of the fiber clearly suffer from limitations in both the uniformity of the stress state and the practicality of the experiments. While a few instances of pull-out testing are present in the literature, it remains a limited technique for laboratory assessment and has not been adopted by industry as a whole during composite development. These techniques, while they might enhance the quality of this work, serve more as a supplement and do not enable a rapid commercial transition of this technology or the most reliable assessment of the impacts of the interphase on the structural properties of the composite.

4.1.1.2 Push-out testing

Push-out testing is governed by mechanics similar to pull-out testing inasmuch as the shear lag model remains valid. Thus, push-out provides a direct measurement of interfacial shear strength by loading the fiber until a crack develops at the interface and

permits motion. A few distinct differences affect the fabrication and testing of the samples. It should be noted that a vast quantity of literature exists regarding the push-out test but is not primarily focused on glass or carbon fiber polymer matrix composites. Push-out was extensively developed for the characterization and analysis of ceramic matrix fiber composites. Ceramic fibers such as Al_2O_3, SiC, and B are often larger in diameter than a typical glass, graphite or aramid fiber, often times 100 μm to 200 μm in diameter. As Equation 4-2 indicates, a larger diameter fiber greatly reduces the axial stress required to cause a push-out, so the larger diameter ceramic fibers are easier to push out than a typical graphite, glass, or polymeric structural fiber. Decreasing the embedded depth or sectioned depth of the fibers can reduce the axial stress to an acceptable level to permit a small structural fiber to be pushed out.

Major issues arise when scaling the push-out test down to small structural fibers. Most push-out testing is performed with a metal or ceramic wire indenter that offers high stiffness and hardness, which minimizes tip deformation and wear. High aspect ratio indenter tips with small diameters are difficult to manufacture and not widely available. In particular, cylindrical tips are unusual and challenging to produce with conventional indenter tip manufacturing equipment. Most tips are sold as cones or spheres, shapes that have some form of draft angle which must be accounted for when determining the depth that the fiber is pushed in. Consequently, the draft angle limits the depth that can be achieved during push-out. Assuming a rigid fiber and rigid matrix, the fiber would be pushed through the sample with the tip eventually hitting the perimeter of the hole left behind by the fiber. The interference of the tip with the hole will increase the load required to advance the tip further; leading to erroneous push-out results. Generally,

small angle tips are difficult to prepare and a conical tip is limited to a double angle of about 40°, similar to Figure 4-3. Researchers might try to make the tip as small as possible but the rigid fiber assumption breaks down due to the singularity caused by such a small contact area. The fiber will deform where the tip may advance without advancing the fiber or the tip could indent and split the fiber to generate compressive stress at the interface. These scenarios can be circumvented by improved tip manufacturing techniques that at the time of publication are not achievable.

In spite of these two flaws, push-out was attempted as a part of this work with the hope of providing high fidelity interface characterization, instead of the inherently statistical single fiber fragmentation test. Similar work had been achieved with a custom built indenter inside of a scanning electron microscope and it was surmized that a standard nanoindenter could achieve similar results [232]. First, a multi-fiber (fewer than 10) composite is cast and cross sectioned to create a film with fibers oriented perpendicular to the polymer. The section is polished to a transparent finish and the fibers are located. Rather than attempt to align the fiber above a support hole, a portion of the fiber is removed with through focused ion beam milling. The sample is flipped and the fiber pushed from the backside with a small nanoindenter tip. The small relief provides a location for the fiber to be pushed into and enables the fiber matrix sliding sought in the test. A schematic of the setup is shown in Figure 4-2. Preliminary calculations showed that even a reasonably small hole of 15 μm does not provide sufficient support for push-out to measure the interfacial shear strength. With a hole larger than the fiber, the cross section deflects and develops a significant component of tensile stress at the interface, shown schematically in previous work by Qian et al. [116]

in Figure 4-4A. This design combines with the expected mode II loading to create a mixed mode facture scenario. This differs from the intended measurement as well as the single fiber fragmentation tests that also measure interfacial shear strength. For carbon fibers, a maximum hole diameter of 8 µm was found to be sufficient for minimizing the contribution of the tensile stresses to the push-out measurement and creating the desired shear stress distribution, as shown in Figure 4-4B. Creating a hole of 8 microns in a support is achievable with existing microfabrication technology, with either lithographic techniques or laser micromachining. Aligning the fiber with that support substrate underneath a nanoindenter is a prohibitively complex undertaking. As a result, the relief option was selected, with full knowledge that potential beam damage or deposition of the ablated material could occur.

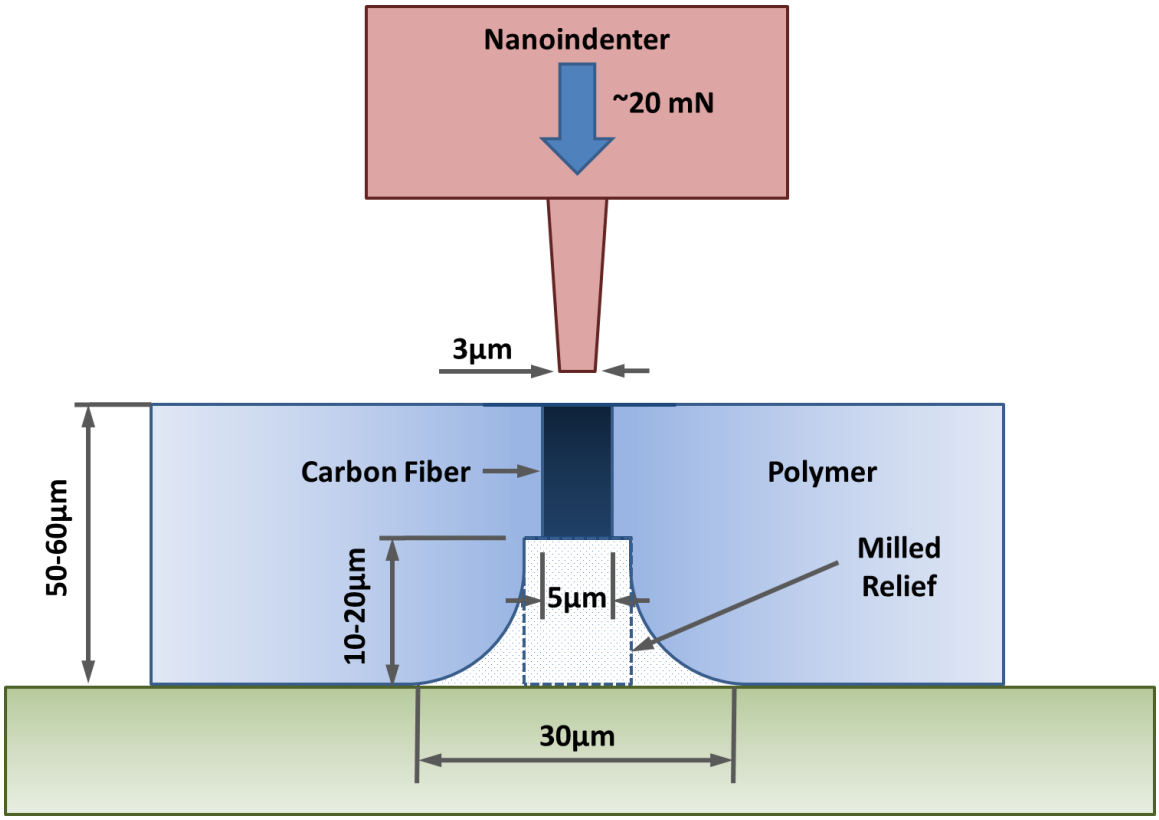

Figure 4-2. Schematic of push-out test attempted with nanoindentation.

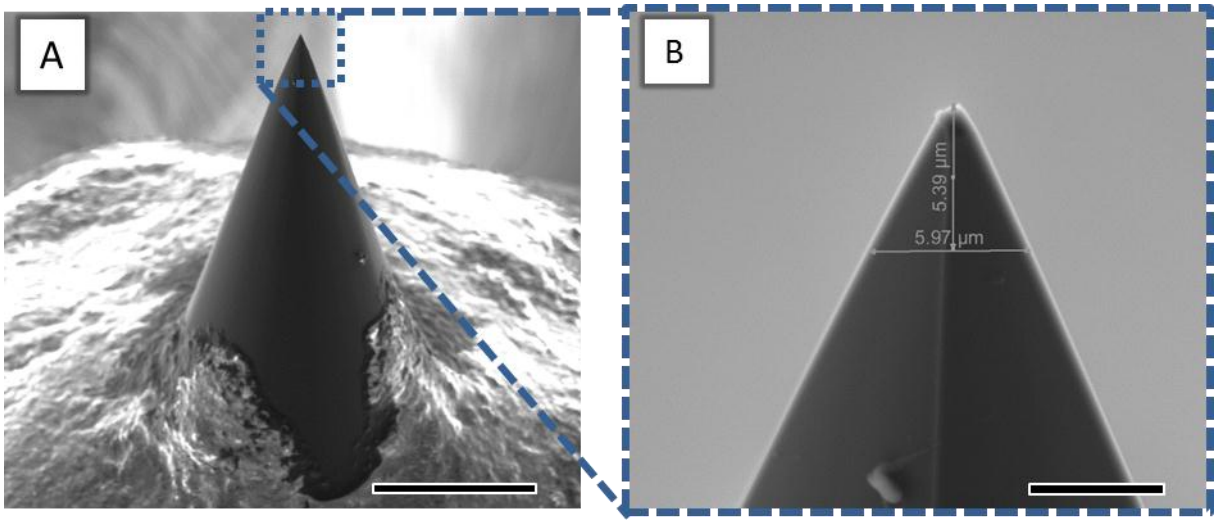

Figure 4-3. Scanning electron microscope images of the tip used for push-out of the carbon fibers at A) low and B) high magnification. Scale bars are 200 µm and 5 µm, respectively.

Push-out was found to be ineffective for interface testing because of the inherent properties of the polymer matrix. The structural epoxy matrix employed in this work is tough, even below the glass transition temperature of the material, because the material is designed to be inherently resistant to cracks in the pure polymer region. The comparatively low modulus leads to large deformations of the film and prevents the debonding that is intended during the push-out test. In general, push-out is determined by identifying a drop in the load as the crack moves the length of the fiber and removes the constraint between fiber and matrix. The sliding fiber still has significant resistance to push-out; however it remains less than the peak load. As shown in Figure 4-5, the load displacement graph of the carbon fiber micropush-out tests does not at any point drop off; however there are slope changes where the slope increases. Increasing slope, as far as push-out is concerned is likely due to interference of the tip with the relief hole. It is expected that during the process of the push-out the indenter may eventually force the fiber down to the rigid support or the indenter might push the fiber deep enough to cause interference.

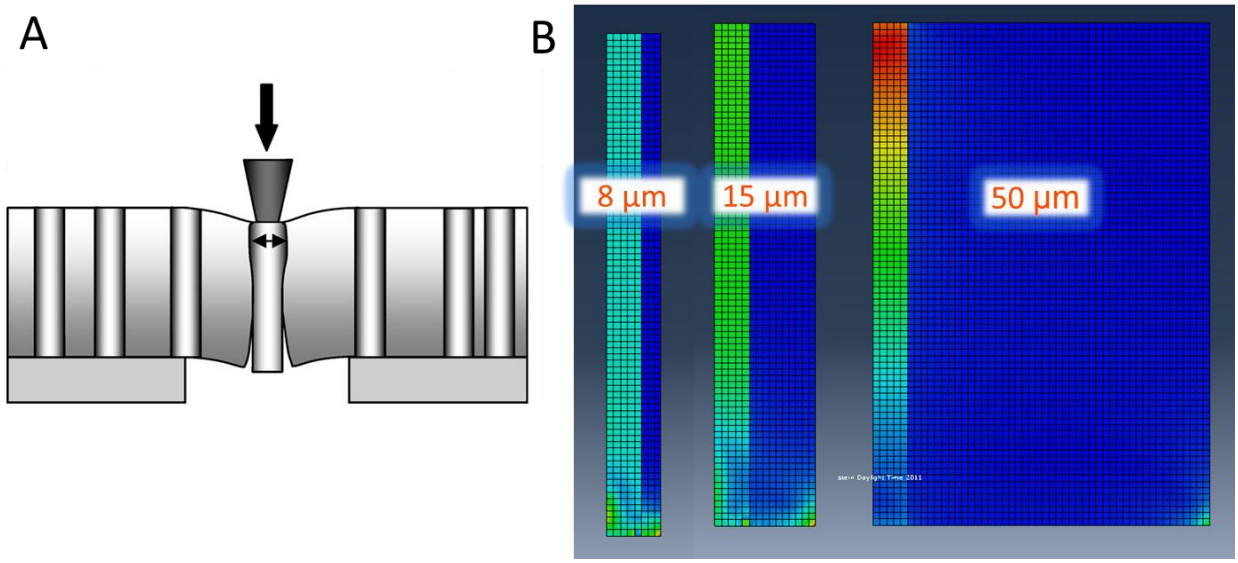

Figure 4-4. A) Schematic of tensile stress developed at fiber matrix interface, published by Qian et al. B) Shear stress distribution simulated through a finite element method demonstrating that a small support hole is required to develop the desired interface failure mechanism. [Reprinted with permission from Qian H, Bismarck A, Greenhalgh ES, Shaffer MSP. Carbon nanotube grafted carbon fibres: A study of wetting and fibre fragmentation. Composites Part A: Applied Science and Manufacturing 2010;41(9):1107-1114.]

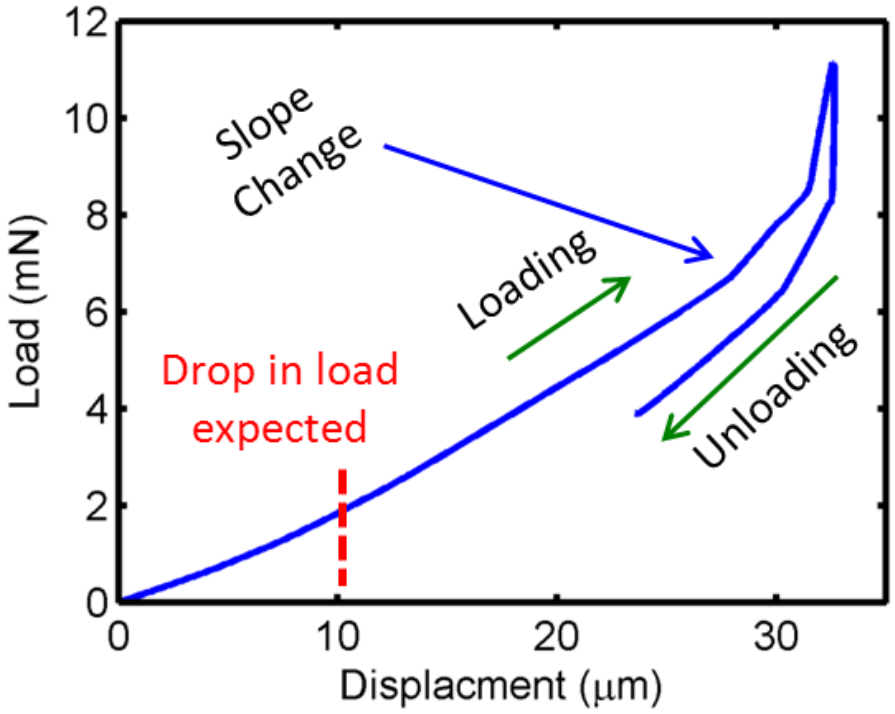

Figure 4-5. Example of load displacement push-out test. No drop in load indicating adhesive failure or slipping was observed.

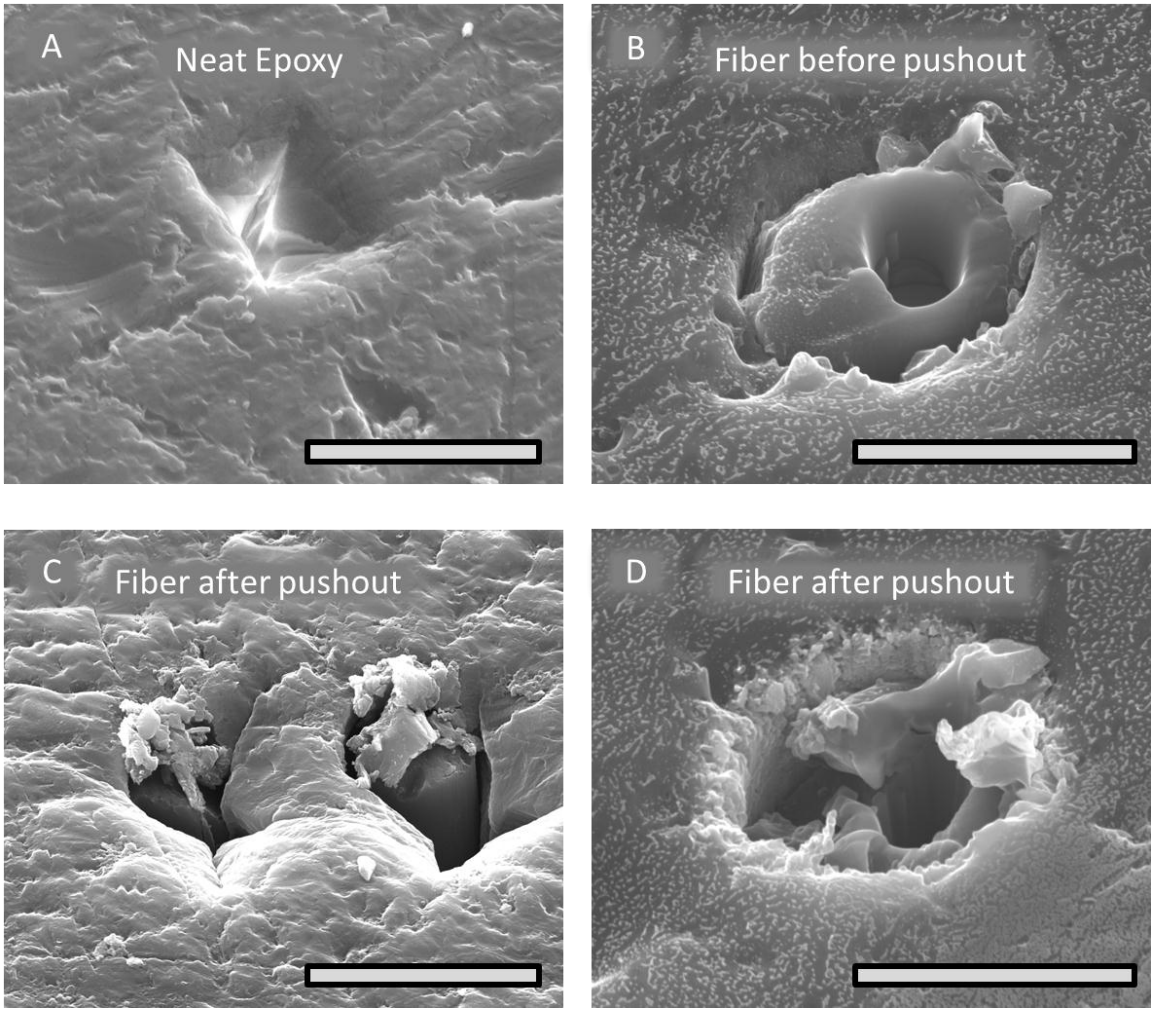

Figure 4-6. Analysis of failure of push-out samples. Images are of the top surface that has been pushed in by the indenter. A) Indentation of neat epoxy showing tearing and deformation of the polymer. B) Top surface of a single fiber with detent machined to keep the indenter tip centered on the center of the fiber. C) Fibers after push-out showing extensive deformation of the polymer and the indenter tip off location. D) Fiber with detent after push-out showing large plastic deformation and chipping of polymer and fiber. Scale bars are 10 μm, 5 μm, 10 μm and 5 μm, respectively.

Beyond analyzing the load displacement data, samples were analyzed with an SEM after push-out testing to assess the failure of the interface. Instead of a effectively rigid body motion between the fiber and matrix, significant deformation was observed in the polymer matrix. This discovery violated the one of the assumptions of the test, namely that the dilute composite is relatively rigid. Elastic and plastic deformation of the

matrix likely accounts for the difference between the expected indenter head displacement and the actual displacement required to generate forces high enough for interface debonding. Figure 4-6 shows the surfaces of fibers before and after push-out. Figure 4-6C shows that the tip moves off the center of the fiber to the interface when not constrained, leading to fiber failure through crushing and fracture. Figure 4-6D shows a push-out sample with a detent to restrain the indenter tip yet there is still significant damage to the fiber and the motion is far from rigid to the fiber. Although the figure also shows debonding between the fiber and ZnO nanowires remaining in the polymer, it remains impossible to discern from the load displacement data what the interface strength should be measured as. Push-out is a popular technique and could serve as a measure of interface strength, there remain several issues with the technique that have to be overcome for the results to serve as a strict guide of the research.

4.1.1.3 Single fiber fragmentation testing

Given the difficulties of pull-out and push-out testing, alternative procedures were sought to measure the interface strength of a single fiber composite. One such procedure that is widely employed in the composites community is the single fiber fragmentation test [221]. A single fiber is embedded into a larger polymer matrix, for this work a 2 mm x 2 mm x 16 mm gauge section of a larger polymer dogbone is used. As the dogbone is pulled, the fiber will begin to fracture. The application of more strain causes the fiber to break in more locations, with each segment transferring load across the interface via shear. The fragments get so small that the surface area is not sufficient to cause the fiber to break again. By measuring the average fragment length, one can estimate the critical length to be

$$\ell_c = {}^4/_3\,\bar{\ell} \tag{4-3}$$

where $\bar{\ell}$ is the total number of fragments divided by the gauge length of 16 mm. The critical length is the same as originally explored Kelly and Tyson in their famous shear lag model. The critical length is the length at which the fiber cannot support the load that can be applied through shear across the interface. Using a force balance and the simple shear lag model, one can obtain

$$\tau = \frac{\sigma_f(\ell_c)d}{2\ell_c} \tag{4-4}$$

where σ_f is the fiber tensile strength and d is the fiber diameter. The tensile strength of small structural fibers is known to be controlled by defects, which was discussed earlier. When measuring the fiber tensile strength, a shorter gauge length reduces the probability of a defect being present in the gauge section of the fiber. The measured strength of fibers increases as shorter and shorter gauge lengths are considered. In the single fiber fragmentation test, fragment length can be on the order of 200 μm; substantially shorter than the typical 25.4 mm gauge length. The tensile strength must be corrected as a function of gauge length, or in this case the critical fragment length, of the fiber [221]. Considering a maximum fiber strain of 3%, the displacement of the crosshead during the test would be 6 microns. Measuring tensile specimens at such short gauge lengths is quite difficult as strain gauges or extensometers are not practical. The displacements of the crosshead of the load frame are so small that error can enter the measurements. Rigorously designed and validated experimental test frames have been built to make these types of measurements and small structural fibers are found to behave as expected. The defect controlled failure of the fibers can be consistently and

accurately fitted to a Weibull distribution. The tensile strength of various gauge length specimens are measured and fitted to the following equation

$$\sigma_f(\ell_1) = \sigma_f(\ell_0)\left(\frac{\ell_0}{\ell_1}\right)^{1/m} \tag{4-5}$$

where *m* is the Weibull modulus fitted to the data of $\sigma_f(\ell)$. This relationship, detailed elsewhere, will be employed to analyze the fragmentation strength of the data.

One facet often missing from reviews of single fiber fragmentation testing reports is the lighting used during the test. Single fiber fragmentation testing is performed on smooth, monolithic structural fibers embedded in a transparent polymer matrix. This leads to a fairly predictable view of the cracks and relatively few locations where light can be internally reflected to confuse the operator. Most tests are performed under a microscope and viewed with transmitted, polarized light. The polarization enables the operator to view local strain concentrations and distributions during the test. The typical test creates these brightly colored distributions exclusively at cracks in the monolithic fiber and makes it easy for an operator to identify the correct number of cracks. Hierarchical fibers can create unusual failure patterns that can confuse an operator when viewed strictly with polarized light. The nanowires are capable of debonding from the surface of the fiber and reflecting light back in a manner that appears to be a crack. The crack can be correctly identified in this work by adding a second light source in the plane of observation that shines into the cracks. The cracks then appear bright white as the fiber is broken while debonding regions remain dark because the fiber blocks the light. Through this technique, the possibility of false crack identification can be reduced as shown in Figure 4-7. Carbon fiber single fiber fragmentation data in this experiment was collected using this technique.

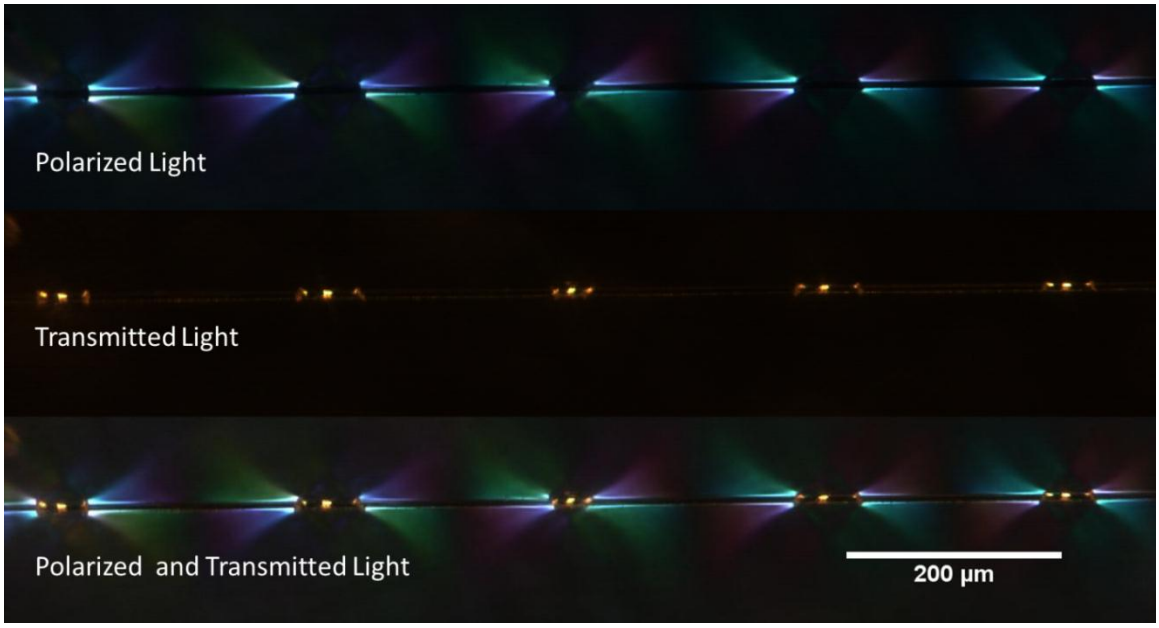

Figure 4-7. Micrographs from single fiber fragmentation testing. Two light sources were used during testing, both polarized light and transmitted light. There are 5 cracks of the fiber; however failure to employ both light sources could mislead the researcher.

Single fiber fragmentation offers reliable interfacial shear strength measurements without the drawbacks that exist for pull-out or push-out techniques. The samples are comparatively easy to prepare and test. With the exception of the lighting issue listed above, the test is robust and repeatable between different operators. The pull-out and push-out tests rely upon the load – displacement curves which, in particular with push-out tests, can include erroneously high or low stresses. Single fiber fragmentation uses the fiber strength to infer the stress state and then averages over 20 – 100 segments in the length of a single sample. This helps average variations without requiring dozens of pull-out tests and is a key factor in the reliability of the test. Single fiber fragmentation testing is selected as the single fiber interface test method for this work because it offers a robust measurement of the property desired while enabling rapid sample fabrication and testing.

4.1.2 Lamina Scale Interface Testing

Interfaces play a crucial role in the behavior of a composite lamina in a variety of loading scenarios. Failure of a lamina is strongly influenced by the interfacial shear strength of the composite. The prediction of composite properties from the properties of the constituents has been a pursuit of both industry and academia for many years. A substantial amount of modeling directly addresses how the interface affects composite properties [5]. Most loading scenarios and failure modes depend on the interface strength; certain cases enable a more direct interpretation of the properties. For example, the axial loading of a unidirectional composite shows that failure strength is dependent on the interfacial shear strength. The failure of this type of composite generates both Mode I and Mode II crack propagation along the interface during failure. It is difficult to assess the specific dependence of composite strength on interfacial shear strength. This section will evaluate the common composite testing techniques to provide both a background on the subject in the context of the measurements sought and a justification for the selection of the appropriate experimental technique.

4.1.2.1 V-notch shear testing

Although modeling the failure of uniaxially loaded laminae can be complicated, there are other loading scenarios that are much easier to interpret. Perhaps most relevant to interfacial shear strength is the v-notch shear or Isopescu shear test, shown in Figure 4-8. In this test, a double v-notch sample is subjected to direct shear loads. The particular geometry of the test generates a very nearly pure shear in the gauge section [233,234], while deformation in the supporting tab region is extremely small. The appropriate application of strain gauges (45° to the loading axis, in the plane of the lamina) enables measurement of the shear strain without including machine or fixture

compliance that could influence the results. The v-notch shear test directly yields both shear modulus and shear strength of the material because it measures the shear deformation of a unidirectional lamina. The shear of a unidirectional lamina provides an excellent measure of interfacial effects. Rather than a multimode fracture problem with tensile and shear stresses at the interface, loading occurs mostly in shear across the interface. The stress is transferred across the interface, from fibers to matrix, thousands of times across the sample. It is expected that reinforcing this region with a ceramic interphase will increase both the elastic stiffness as well as the fracture toughness. V-notch shear testing is the preferred lamina scale method for measuring interfacial shear strength and will be employed in the analysis of the ZnO nanowire interphase developed in this work.

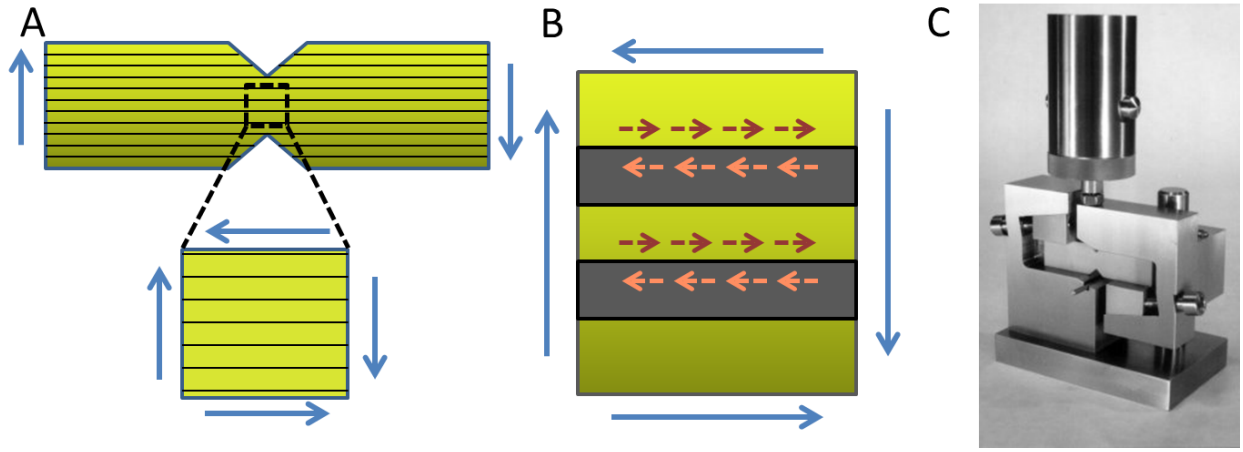

Figure 4-8. Schematic of ASTM D5379 V-notched beam method. A) Loading of a unidirectional lamina generating shear stress in the gauge section. B) Magnified schematic view of single fibers, transferring stress to the matrix across the interface. C) Photograph of a typical test fixture where the v-notched beam is restrained in a stainless steel test fixture.

4.1.2.2 Compression testing

Compressive failure of a unidirectional lamina also depends heavily upon interface strength, albeit through a different mechanism. Compressive loading of a unidirectional

lamina leads one to conclude that the long slender fibers behave much like columns, subjected to Euler – Bernoulli buckling rules. A typical fiber reinforced composite material has a soft, low modulus polymer matrix surrounding the fibers, typically 100 times lower, which allows the analysis of fiber buckling load to be assumed to follow the Euler – Bernoulli relations to a degree. Pure buckling of the individual filaments of a composite is the typical compressive failure mechanism of a composite material. The constraints imposed by the polymer matrix change the behavior significantly. As the fiber deflects, assuming the lowest energy buckling mode with a wavelength of 2ℓ, tensile and compressive stresses perpendicular to the fiber are applied. The tensile stress is increased until the ultimate, interfacial strength is exceeded and the fiber buckles. The buckle propagates to neighboring fibers like a wave and the global material is determined to have failed [235]. It can easily be observed that higher interfacial strength directly improves the compressive strength by enabling higher compressive loads before initiating failure in the material [235]. The relationship of the applied load or compressive stress to the interfacial strength remains complex and a more direct measurement less subject to errors is desirable. Compression testing remains only a comparative assessment of the interfacial strength; however important the measured strength is for implementation in structural design.

4.1.2.3 Short beam shear testing

Short beam shear testing is very popular for interlaminar shear strength testing. It is often highly related to interfacial shear strength, but not the same. A short beam, a beam with a thickness on the order of the length and depth, violates the assumptions of the standard Euler – Bernoulli beam model and generates significant shear stresses through a lamina. Industrially, short beam shear testing is widely employed to

characterize the interlaminar shear strength although caution must be employed when directly inserting the measurement into design calculations. Short beam shear testing can be applied to both unidirectional and woven composites with two different failure criteria. Woven composites generally exhibit a polymer rich interlaminar region because the multiple plies of the composite do not perfectly pack together. This polymer region is weaker than the areas reinforced with fibers and in a short beam test, cracks to cause a delamination of the composite. The thickness of region depends greatly upon the processing techniques employed during fabrication of the composite. Typical procedures with autoclave cured composites will generally yield an interlaminar region on the order of 15 – 30 μm thick [236,237]. Considering that the growth of ZnO nanowires is generally limited to about 2 microns on a carbon fiber and 5 microns for an aramid, the length of the nanowires is not sufficient to bridge the entire interlaminar region. Thus the region will fail cohesively and failure is controlled by the polymer strength and fracture toughness. The ZnO nanowires developed for this work are unlikely to impact the interlaminar strength of a woven composite because they are not long enough to fully reinforce the interlaminar region.

Short beam shear strength testing of unidirectional laminae explores a different failure mode because the weave of the fibers no longer prevents the fibers from coalescing into one uniform composite. Reinforcement of the polymer region would thus occur on the order of fiber spacing; assuming a high volume fraction and proper consolidation of the composite would be no greater than fiber diameter. Even if an area of large fiber to fiber spacing exists, it is unlikely that it will span the entire lateral dimension of the composite and lead to failure of the material. The reinforcement local

to the fiber will enhance both elastic and fracture properties of the interface to improve the overall properties of the composite. The test is expected to enhance the material; however caution must be exercised with relation to short beam shear testing. The short beam shear test generates, in the best case, a parabolic distribution of shear stress through the thickness of the composite. The parabolic stress distribution forces the test to be more sensitive to failure at the center of the composite than elsewhere. The linear region of the force displacement response does not correlate directly to shear modulus or tensile modulus; it is a complex combination of the two. Short beam shear strength testing is very capable of qualitatively assessing interfacial improvements and providing quantitative short beam strength measurements for design. Short bean shear strength testing does not measure the more fundamental properties of shear modulus, G_{12}, and shear strength, τ_{12}. Given the extreme difficulties in scale up constraining the number of samples, this work will employ V-notched shear lamina testing in lieu of short beam shear testing.

4.1.2.4 Mode I fracture toughness testing

The measurement of mode I crack propagation is associated with interfacial shear strength for the same reasons that woven short beam shear testing is. Stronger adhesion between the fibers and matrix can often improve mode I delamination resistance, but it remains ultimately dominated by the strength of the pure polymer layer. The association does not imply that there is a strict, universal causation whereby a stronger interface can vastly improve interlaminar toughness. Mode I crack propagation tests are typically performed on woven composites where a relatively thick, purely polymeric interlaminar region exists between the fibrous preforms. Performing a crack opening test perpendicular to the laminate propagates a crack through the pure

polymer region because most often this region has the lowest fracture toughness. While the interface between the fiber and matrix offers the least resistance to crack propagation, constraining crack growth to the interface creates a complex, difficult path that requires more energy than fracturing the neat polymer resin. Mode I crack propagation tests generally analyze the crack as propagating in a relatively straight line through the polymeric interlaminar region.

The pure polymer region often causes composite failures in both static and fatigue scenarios. This property has caused it to be a subject of study and engineering to improve the bulk composite properties by increasing the toughness and damage resistance of the polymeric phase. In many instances, toughened polymer matrices provide a polymer matrix with intrinsic fracture properties that significantly exceed the toughness of the interface, even when considering the increased crack propagation length. Often interface debonding is common and interfacial shear strength dominates the measured fracture toughness. Improving the interfacial shear strength for a composite in these conditions does significantly improve the bulk mode I fracture toughness and thus mode I testing can be used to qualitatively compare interfacial shear strength. The tortuous and unpredictable crack propagation path is difficult to model and the measurement of interfacial shear strength relies on inducing debonding along its crack path. Mode I fracture toughness testing, while extremely important for the design and implementation of composites in structures, is simply too unpredictable to directly measure interfacial strength.

4.1.2.5 Transverse tensile testing

Most composite laminae are assumed to be transversely isotropic materials, a researcher can consider two directions of interest. The first direction of interest, the

axial direction, is generally aligned in the fiber direction and exhibits a specific set of properties. The second direction, perpendicular to the fiber direction, is considered the transverse direction and isotropic in any direction in the plane perpendicular to the fiber direction. The transverse properties of a unidirectional lamina are highly dependent upon the interfacial properties because the stronger, stiffer fiber phase does not individually support the applied transverse loads. The stiff fiber phase supports load by transferring it back and forth from fiber to matrix across the interface at the boundaries of each fiber. The abrupt change in material properties creates an immense stress concentration at the interface and generally initiates and propagates cracks very effectively. The measured properties are highly sensitive to interfacial strength and the interface strength can be easily measured and interpreted, much like the v-notch shear test.

This work does not include transverse tensile testing primarily because it quantifies the interfacial tensile strength more than the interfacial shear strength. Single fiber fragmentation measures interfacial shear strength and consistency, in conjunction with parsimony during the scale up of the measurements from the single fiber to the lamina scale is preferred. Future works related to this dissertation could include transverse tensile testing as well as the plethora of other qualitative interfacial tests discussed earlier to contribute a rigorous evaluation and measurement of the interfacial strength. This work focuses on the scientific understanding of how surface chemistry affects adhesion, thus instead of additional lamina testing to quantify the interface strength attention is directed toward the modulation of measured interface strength through surface chemistry control. V-notch shear testing is clearly the single, preferred

lamina scale test for identifying the effect of the ZnO nanowire interphase. V-notch shear testing demonstrates that it is possible to scale this interphase to larger composites and provide direct measurement of properties that can be interpreted in conjunction with single fiber testing.

4.2 Tensile Strength of Modified Fibers

One of the chief advantages of ZnO nanowires as an interphase, instead of other nanomaterials like carbon nanofibers or SiC whiskers, is that the low temperature benign processing does not damage the tensile strength of the fibers. In addition, the carboxyl functionalization treatments applied to carbon fibers are also specifically created to minimize the risk of creating fiber damage. It is of particular importance that the impact of the functionalization techniques applied here is measured. Reductions in the tensile properties of the fibers, as a result of both functionalization and growth of the ZnO nanowires, causes tradeoffs in the in plane composite properties for interfacial and shear properties, which is counter to the goals of this research.

In addition to the overarching goal of the research, to improve interface strength without reducing tensile strength, the research techniques applied here specifically require that the tensile properties be measured. Single fiber fragmentation infers the interface strength based on estimates of the tensile strength of the segments. It is well known that handling and processing of structural fibers can cause significant changes in the tensile properties. Ergo, the only way to ascertain correct measurement of the interfacial strength through fragmentation is to measure directly the fiber tensile strength. Fragment lengths observed in testing are often extremely short. Shorter structural fiber segments are less likely to have a defect in the gauge length and generally have a higher tensile strength than longer gauge length sections. Most

published data is taken with a single gauge length which precludes quantifying the effect of gauge length on the measured tensile strength. This phenomenon will be addressed and accounted for in the following section. The results of the tensile tests will then be used to quantify the interface strength and the effects of the treatments on the in-plane composite properties.

4.2.1 Methods for Tensile Testing of Functionalized Fibers

4.2.1.1 Introduction

The importance of the tensile testing to the overall scope of this work warrants a review of the techniques for and analysis of working with small structural fibers. Much of the study of interface treatments in the literature has been focused on surface chemistry and surface roughness while neglecting to measure or report the effect on tensile strength of the fibers. The contention of this work is that the two are inextricably dependent. Any interfacial treatment must be accompanied with a realistic assessment of the impact on the in-plane properties of the composite which necessitates fiber tensile testing.

Single fiber tensile testing is both widely known and widely published in the scientific literature. This work will not forge new methods for the testing or analysis of small filaments but it will review the relevant characterization and serve as a template for future interphase development. The goal is to provide in – plane characterization in the context of interfacial treatment, beginning with the single fiber tensile properties. The tensile properties of structural filaments are generally evaluated following ASTMC-1557 [238]. The filaments are mounted onto a paper tab with epoxy or directly in soft rubber lined grips. The fibers are then strained until failure, with care taken to prevent both grip slippage and failure at the grip location. After failure, the standard requests

that the fibers be measured to determine the diameter of the tested fibers. This is often impractical when testing many fibers and has been omitted in this work. Any single fiber tensile sample set presented in this work includes an average of twenty tests which reduces the contribution of any single small or large fiber. Performing the test is largely similar to any other tensile test and will not be described beyond the standard in this work.

The analysis of single structural fiber data is slightly more than the simple averaging of tensile tests. While mean values for strength and failure strain are reported, the failure of small structural fibers is primarily controlled by the presence of defects and does not follow a standard normal distribution. Failure more closely follows a Weibull distribution and thus the Weibull distribution has become widely accepted for fitting failure data of structural fibers. The Weibull distribution is defined by the cumulative density function

$$p(x) = 1 - e^{-(x/\lambda)^k} \tag{4-6}$$

where x is the failure point (stress, strain, time, etc.), λ is the Weibull scale factor, and k is Weibull shape factor or Weibull modulus. Most structural fibers are linear elastic up to the point of failure and exhibit very little plasticity or flow. Under this assumption, the ultimate stress and ultimate strain are directly related by the elastic modulus which is consistent with experiments. If the failure stress fits a Weibull distribution, then the failure strain should fit a Weibull distribution as well. For the analysis in this work, both failure stress and failure strain are fit to Weibull distributions and confidence intervals are estimated to the scale factors.

The scale factor is fairly intuitive, scaling the distribution of the quantity of interest to the appropriate value and yielding something similar to a mean value. Evaluating the Weibull distribution for the mean value, one finds that the mean can be evaluated as

$$\bar{x} = \lambda \cdot \Gamma\left(1 + {}^{1}/_{k}\right) \tag{4-7}$$

If the shape factor, k, is one, the equation reduces to $\bar{x} = \lambda$ and the scale factor is equivalent to the arithmetic mean. When the shape factor is not equal to one and instead is closer to five (typical of carbon fibers), then the equation reduces to $\bar{x} \cong 0.91\,\lambda$. Independent of the exact value, visualizing the scale factor as an arithmetic mean will provide a reasonable understanding of the term.

The shape factor affects the fit of the data in other ways. Generally, one can think of the shape factor as describing the degree of spread or variation in the data. High scale factors correlate to samples that fall in a narrow range. Taking the limit of the probability density function with increasing shape factor leads to the well know Dirac Delta Function, or impulse function. The cumulative density function, simply the integral of the probability density function, becomes a step function and thus all samples fail at the same value. Low shape factors describe a distribution that has wide variation. This distribution accompanies fibers with extensive defects, which follow a probabilistic distribution that leads to some low failures and some high failures. Oxidative procedures form defects on the surface of the fibers and lead to extreme variation between fibers as some defects are large enough to cause premature failure. Oxidation tends to reduce the shape factor by inducing defects in the fiber and thus reporting the shape factor adds valuable information when characterizing fiber tensile properties.

The second place where defect driven failure substantially affects the measured tensile strength is in the size effect [90]. The size effect, ultimate stress is not independent of the size of sample measured, is the dominant reason that fibers such as glass and graphite are so much stronger than their bulk counterparts. This is trait is capitalized to create materials with unprecedented properties by shrinking the diameters yet the same phenomenon applies to the length of fiber tested. It takes higher stress to break a shorter fiber than a longer one. In a test such the single fiber fragmentation where very short fragments are generated, the ultimate tensile strength of the short fragments can be dramatically higher than the strength of fibers that are typically measured. It is extremely difficult to measure the tensile properties of short fibers simply because they are nearly impossible to manipulate without onerous techniques and machinery. Fibers to 200 μm can be tested with some micromechanical test setups, the time and cost is not justified for continuous structural fibers. To account for the gauge length a relationship is experimentally determined for measurable gauge lengths, which, are then extrapolated to shorter lengths to determine the strength.

Given the distribution of flaw sizes and Weibull distribution that the fiber failure fits, a logarithmic transform is used to linearize the behavior. Natural logarithms transform both the failure stress and gauge length and then a linear relationship is fit between the data to predict the ultimate strength at short gauge lengths. The resulting strength values correspond well with fibers that have been tested at extremely short gauge lengths. The predicted strength values can then be inserted into the equations for single fiber fragmentation, Equation 4-4, to enable the test to infer the interface strength.

4.2.1.2 Experimental methods

Scanning electron microscope images to examine the surface of the fibers were obtained by placing a small tow on double sided carbon tape and imaging the samples at 15 kV. Single fibers of each treatment condition were tested similar to ASTMC-1557 [41] to determine the fiber tensile strength. Single fibers were mounted to paper templates with a 25 mm gage length by epoxy. The fibers were aligned and strained at 8.0 μm/s until failure. Each specimen was examined for linear elastic behavior and a sample of at least 20 fibers of each condition was tested. To comply with established standards, each fiber should be measured after failure. The fiber diameter (5.45 μm) is very small and in order to get an accurate measurement, they must be measured in a scanning electron microscope. The measured values differs slightly from the nominal diameter of 5.2 μm provided by the manufacturer. The sheer number of samples tested throughout this work (>1000) makes measuring each fiber impractical. A sample of 38 randomly selected fibers from the batch as received was analyzed to generate a mean diameter of 5.45 ± 0.1 μm, which was then used to compute tensile strength. Aramid fibers, not requiring the same graphitization and stretching steps have a more uniform diameter so the manufacturer listed value of 12.5 μm is assumed for kevlar fiber strength measurements.

4.2.2 Tensile Properties of Aramid Fibers

The ZnO nanowires interphase is designed to significantly improve the interfacial strength in aramid fibers. To be effective the interphase must also preserve the fiber properties such that the composite's in plane properties are maintained. To demonstrate this single fiber tensile testing has been performed to characterize the in-plane strength, which is dominated by the fiber's axial properties. The results of the

single fiber tensile strength are shown in Figure 4-9. It can be seen in this figure that the strength of the fiber is not negatively influenced by either the functionalization or nanowire growth processes. This result is a major advantage of this work because past efforts for the chemical modification of the fiber surface to achieve increased adhesion with the matrix have all seen improved interfacial properties at the cost of the fiber strength. No other current whiskerization technique is compatible with polymer fibers because of the high temperature processing required. Since the growth process is performed at 90 °C, well below the degradation temperature of aramid fibers, the nanowire growth does not affect the fiber integrity. The strength of the fiber slightly increases following functionalization which is attributed to removal of the weak outer layer of the fiber during functionalization. The ZnO seeded fibers show slightly higher strength than the bare fibers. This result is attributed to the hard ceramic coating on the surface that effectively acts as a sizing layer, mitigating damage and defects on the surface. This demonstrates that neither the functionalization nor growth processes will negatively impact the in – plane properties of the composite.

The reaction does not progress in the strictly intuitive manner, where strength drop is linear or exponential with functionalization time and higher temperatures merely accelerate the same reaction progress. Tensile strength data was collected with reaction temperatures up to 90 °C and large tensile strength reductions were observed. The reductions are attributed to the increased reactivity aggressively hydrolyzing deeper into the fiber. This is fairly consistent with most expectations, increased temperature typically speeds reactions. Increased time did not show the same effects. The functionalization does not follow a typical first order system in that after 20 minutes, the

functionalization reaction appears to change and either reverts back or begins creating a secondary reaction product. Twenty minutes is the maximum functionalization time, regardless of temperature. As the functionalization was not developed significantly beyond what was required for effectively adhering the ZnO nanowires, these products remain unknown. The functionalization reaction is more aggressive, in terms of impact on tensile strength, at higher temperatures yet it shows the same sensitivity to the precise twenty minute timeline. Previous work related to the hydrolysis functionalization has not specifically commented about this facet of the time sensitivity, a detailed examination of the article by Koenig demonstrates this consistent pattern [123]. Future researchers employing this technique should be cautious to avoid prolonged functionalization times and the degree of functionalization should instead be modulated with temperature.

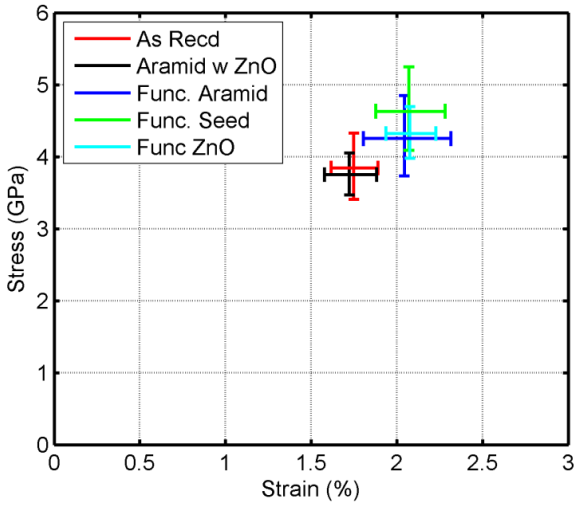

Figure 4-9. Tensile strength of modified aramid fibers showing no degradation in fiber tensile strength. The fibers tested were as received, as received with ZnO nanowires, functionalized fibers, functionalized with ZnO seeds and functionalized with ZnO nanowires. The error bars represent 95% confidence intervals on the estimated Weibull scale factor for both the failure stress and failure strain.

4.2.3 Tensile Properties of Carbon Fibers

The first measurement of fibers coated with ZnO nanowires was performed very early on in the project and was slightly less rigorous than the rest of this work. It paved the way for future testing and remains no less valid in the context of the other analyses performed. Figure 4-10 shows that ZnO nanowire coated carbon fibers have no change in ultimate tensile properties, specifically ultimate strength. The test results show that the addition of ZnO nanowires on the surface of the fibers does not influence the measure of tensile properties. The confirmation is not as certain as possible yet the results are valid for confirming the hypothesis that the low temperature processing of the nanowires does not damage the fiber. Examining the approximate slope of the failure points indicates that the modulus remains unchanged. The ZnO coating, while high in modulus, is discontinuous except at the thin seed layer and will not support a significant amount of load. The low fraction of ZnO will not significantly change the longitudinal properties of the material.

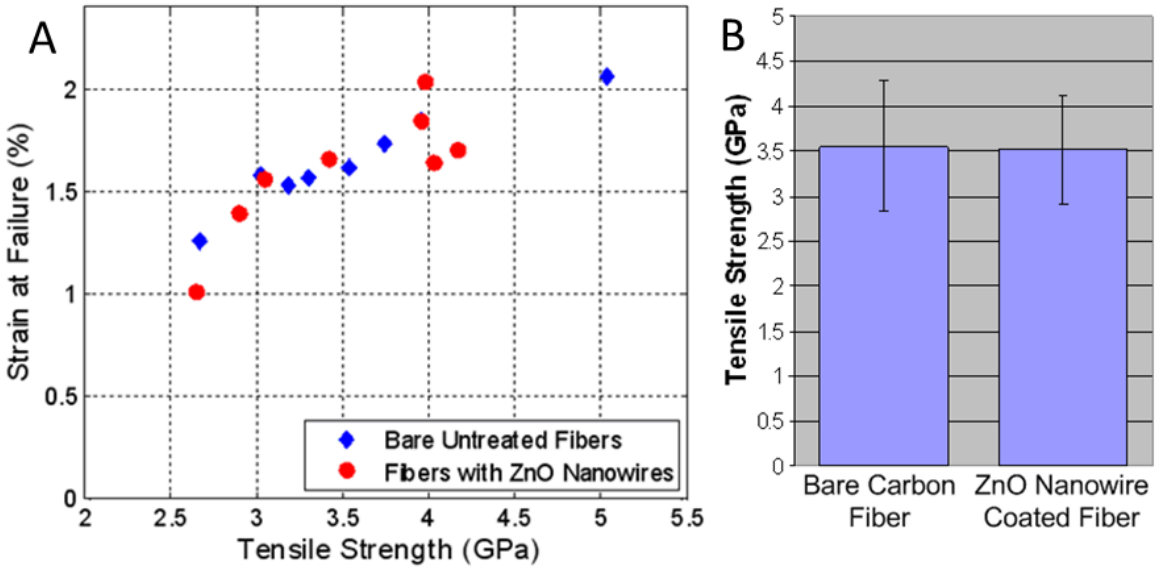

Figure 4-10. Tensile properties of carbon fibers coated with ZnO nanowires. A) Failure stress and failure strain of each fiber tested. B) Average tensile strength with 95% confidence intervals.

The tensile strength of the defect grafted carbon fibers after treatment is of utmost importance to establish the efficacy of a functionalization procedure. Single fiber tensile testing is used to evaluate the strength of fibers after the functionalization treatment. The results of tensile testing are presented in Figure 4-11. Carbon fiber failure strength is known to follow a Weibull distribution rather than a normal distribution. Failure is dominated by the presence of random flaws causing a 'weakest link' at failure [239,240]. Each set of fibers was fit to a Weibull distribution, for both failure stress and failure strain. The confidence intervals indicated in Figure 4-11 are the 95% confidence limits of the scale parameter of the distribution for both the stress and strain. The fibers do not experience any appreciable reduction in scale parameter due to the functionalization treatment because there was no roughening of the surface or breaking of the C-C bonds in the core of the fiber. Each individual fiber tested showed linear elastic behavior until failure, which is expected from carbon fiber. The elastic modulus remained relatively constant, which is another indication that the internal and surface structure of the fiber is not harmed by the functionalization procedure. The Weibull shape parameter significantly differs from the control for some sets of fibers. All shape parameters are either equal to or higher than the shape parameter of the control fibers, 5.14. Table 4-1 shows the Weibull shape parameters for each sample tested, along with 95% confidence intervals for each value. Defects are known to generate the "weakest link" failure mode of carbon fiber [240] which is modeled by the Weibull distribution, specifically the shape parameter of the fitted model. A higher shape parameter corresponds to less variability in the strength data and lower flaw distribution [239] which implies that additional defects are not generated through the

functionalization process. The shape parameter of 5.14 agrees with a previously reported value of 5.21 for intermediate modulus carbon fiber [59,112]. The Weibull scale parameter and Weibull shape parameter are not decreased after functionalization. The grafting reaction mechanism and conditions ensure that the core fiber structure, tensile strength and quantity of surface defects are maintained after the functionalization.

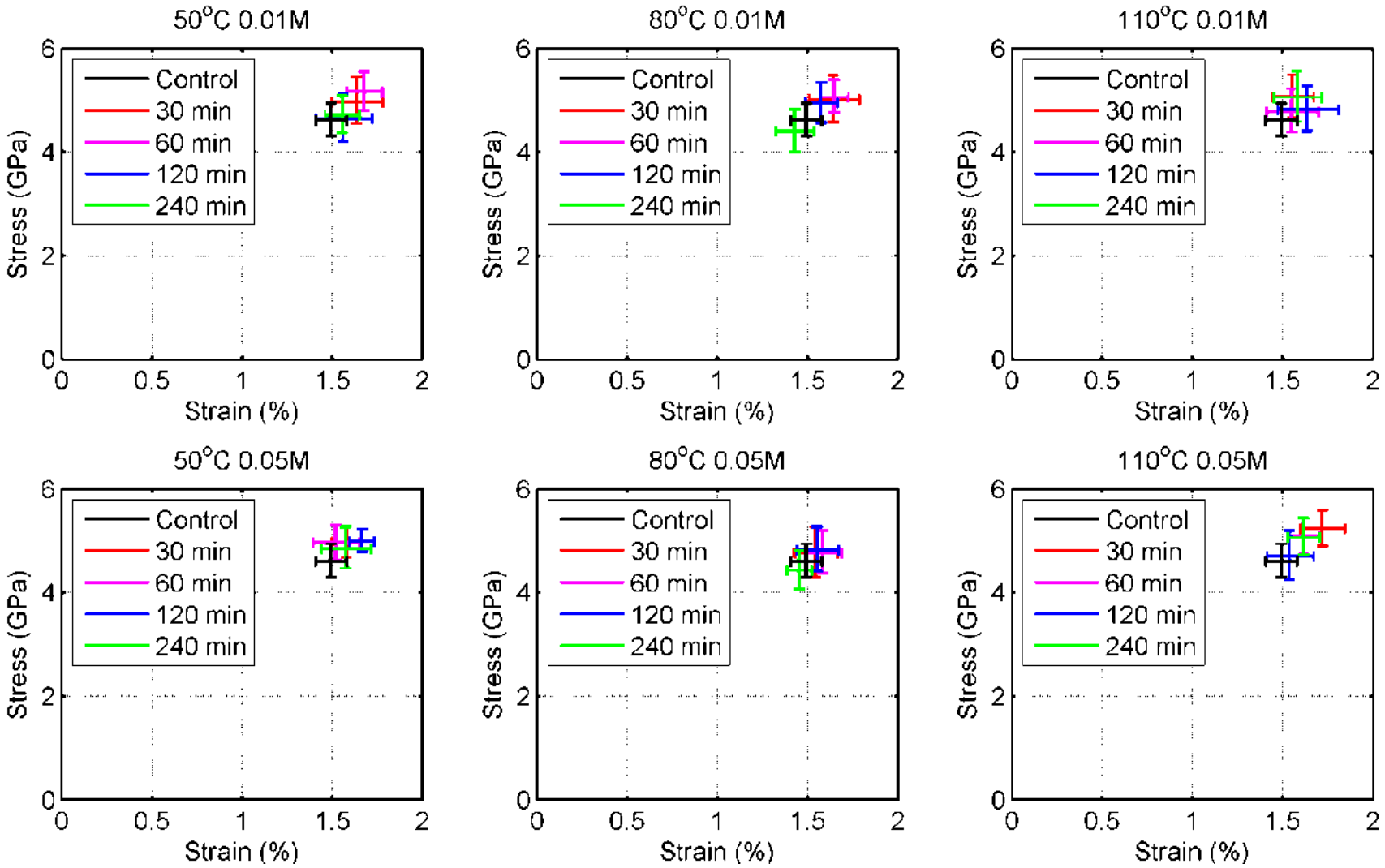

Figure 4-11. Single fiber tensile strength of each functionalization treatment condition. The non-oxidative functionalization procedure does not reduce the tensile strength of the fibers while enhancing the surface chemistry. Note that the same set of control fibers is presented on all 6 data sets. Error bars represent the 95% confidence intervals on the fitted Weibull scale factor for both failure stress and failure strain.

Selective oxidation is predicted to have a minimal effect on the tensile strength of the fibers because it shows a preference to oxidize carbon oxygen bonds rather than carbon – carbon bonds. This feature limits the damage that could occur to the surface and limits the defects that might be created on the fiber which are the dominant cause of the fiber failure. This work does not emphasize the optimization of the reaction conditions but rather demonstrates the reaction to be effective for the creation of carboxylic acid groups on the surface of the fiber. There are only two conditions to be tested, selectively oxidized fibers and IM8 fibers as received. Figure 4-12 shows the tensile strength of the fibers before and after selective oxidation. The failure strain appears higher, which would indicate a lower modulus, this result is within the reasonable expectations of the fibers. Comparing this result to some of the fibers that had defect grafted carboxylic acid functionalization shows that the scale parameter of 1.72% is not out of line with some of the fibers tested. The most important parameter in this testing is the failure stress, rather than strain, because it is the most sensitive to defects and provides the best context for the design of large scale composites.

Table 4-1. Fitted Weibull shape parameter for strength of each fiber functionalization case. While some fibers do show significantly higher shape parameters, this indicates a more predictable fiber with fewer flaws. The left numbers indicate the fitted value, while the right numbers are the 95% confidence interval maximum and minimum estimates.

		Weibull Shape Parameter											
		0.01M						0.05M					
		50 °C		80°C		110 °C		50 °C		80 °C		110 °C	
Time (min)	30	5.18	7.45 3.60	5.15	7.31 3.63	5.63	7.83 4.05	7.48	10.46 5.35	4.65	6.44 3.36	8.22	12.41 5.44
	60	6.28	8.97 4.40	7.44	10.64 5.20	5.27	7.52 3.69	6.82	9.62 4.83	5.41	7.60 3.85	6.74	9.56 4.75
	120	4.70	6.49 3.40	5.90	8.21 4.24	5.08	7.21 3.58	10.91	15.43 7.71	5.22	7.40 3.68	4.64	6.55 3.28
	240	6.17	8.56 4.45	4.97	7.06 3.50	4.81	6.81 3.41	5.61	7.77 4.05	5.90	8.54 4.07	6.52	9.31 4.57

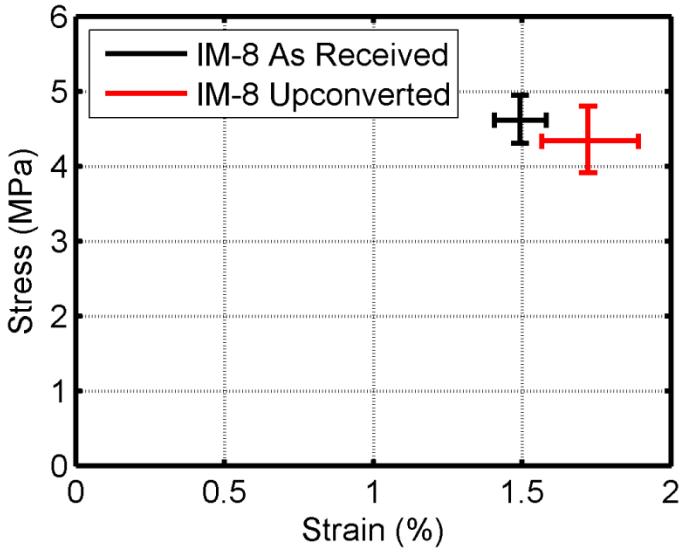

Figure 4-12. Failure stress and failure strain of selectively oxidized carbon fibers. Error bars represent 95% confidence interval estimates of Weibull scale factor for failure stress and failure strain.

One of the important contributions of this work is modulation of interface strength with surface chemistry, demonstrating the effect of surface chemistry in the adhesion of ZnO nanowires to the surface of structural fibers. Techniques are developed to add oxygen to the surface and techniques are developed to remove oxygen, namely hydrazine reduction. The goal of developing the reduction is not to enhance composites, instead the reduction will focus on measuring the interface strength of a composite with lower oxygen surface content. Single fiber fragmentation testing infers the interface strength from the tensile strength of the fibers, tensile testing must be performed to ensure that the correct interface strength is measured.

The reduction of carbon fibers is not expected to affect the tensile strength of the fibers. Oxygen functional groups do not form the backbone of the carbon fiber, the oxygen containing groups are typically grafted as pendants. Removal of the functional groups will not disrupt the crystallinity or sever some macromolecule affecting the fiber strength. Hydrazine is not known to attack carbon – carbon bonds, in particular it is not

known to etch or intercalate graphite and acts as a stable support during reactions where other compounds are reduced. Figure 4-13 shows similar behavior to that of the selectively oxidized fibers where the failure stress remains unchanged and failure strain is slightly higher. The fiber tensile strength is maintained and the fiber tensile strength values of 4.5 GPa can be used to compute the interfacial shear strength.

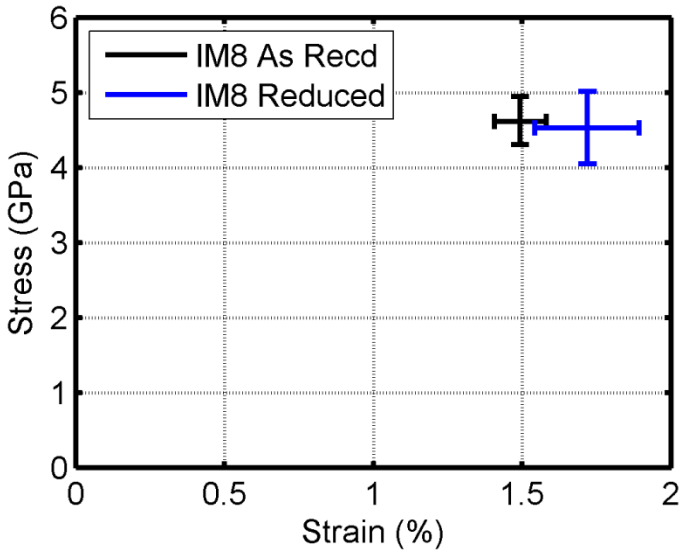

Figure 4-13. Failure stress and failure strain of reduced carbon fibers. Error bars represent 95% confidence interval estimates of Weibull scale factor for failure stress and failure strain.

AFM surfaces scans are also performed on the surface chemistry of each case to detect changes in topography. Topographical changes in fibers indicate etching that could negatively impact the fiber tensile properties or positively influence the interfacial measurements. Zhdan et al. [91] demonstrated that by oxidizing and then thermally reducing the fibers, interface enhancement could be preserved in spite of chemical changes. The importance of functional groups versus roughness and surface area, addressed in Chapter 1, underscores the importance of measuring roughness prior to analysis and drawing conclusions based on interface strength data. Figure 2-16 shows that each of the four treatments of fibers (as received, selectively oxidized, defect

grafted, reduced) yield similar surface roughness. Etching or pitting is not discernible in the images and, taken in conjunction with the tensile data, indicates that the fibers have different surface chemistry and identical surface area and roughness.

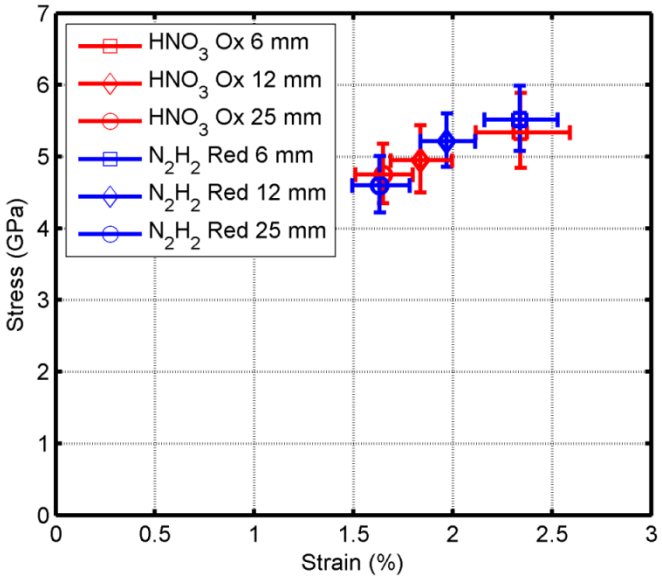

Figure 4-14. Tensile strength of fibers oxidized in nitric acid and fibers oxidized and then reduced in hydrazine. The tensile strength increases with smaller gauge lengths. There is little difference between the oxidized and oxidized – reduced fibers.

A final portion of this work required the use of oxidized fibers, fibers oxidized in nitric acid, as a test of interface chemistry. The tensile strength of these fibers is also quantified to assess interface strength. The results of this test were employed extensively in single fiber fragmentation testing; the tensile strength was also estimated at short gauge lengths. Figure 4-14 shows that both the oxidized and oxidized – reduced fibers have similar tensile strengths. Both sets of fibers show the expected gauge length sensitivity, short fibers have higher failure strength. Figure 4-15 shows the same strength data presented on a Weibull plot that can be used to extrapolate the tensile strength at extremely short gauge lengths. The fitted curve is then employed in

the processing of the single fiber fragmentation data to yield the interfacial shear strength.

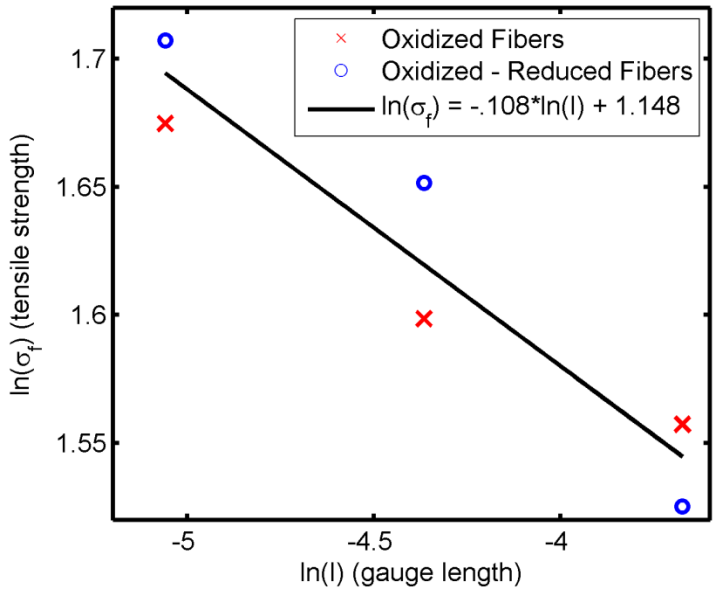

Figure 4-15. Weibull plot of strength for various gauge length samples. The strength at extremely short gauge lengths can be extrapolated from the gauge lengths presented here. A line is fit to the data to determine tensile strength (Pa) as a function of gauge length (m).

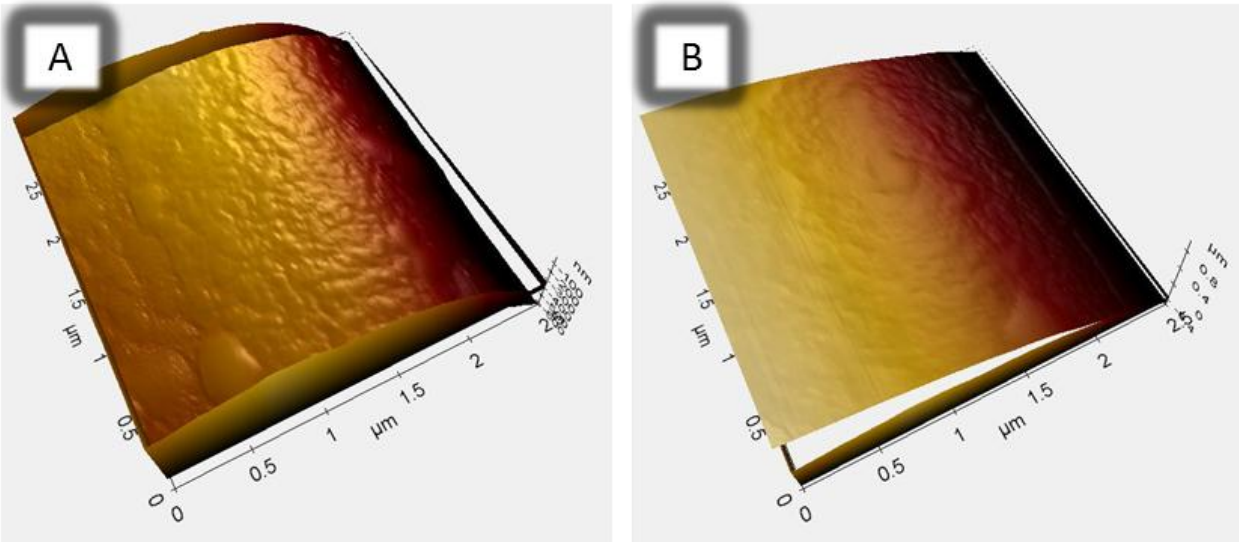

Figure 4-16. Atomic force microscope images of A) fibers after nitric acid oxidation and B) oxidation followed by hydrazine reduction. The roughness of each fiber is very comparable, the only real difference remains the surface functional groups.

The fibers for this experiment were prepared in this manner to test the interface strength. Nitric acid oxidation, as shown in Chapter 2, creates large amounts of a variety of oxygen functional groups. It can roughen the fiber, which is a dominant factor in interface strength. This work employs nitric acid oxidation as a method to create surface chemistry changes, with roughness changes being a necessary byproduct. Comparison of the interface strength of an oxidized fiber to a fiber as received could be complicated by changes in the surface roughness, which has a profound, yet unquantifiable effect. To overcome this limitation, the oxygen groups on the surface of those fibers are removed through the hydrazine reduction developed earlier. The elimination of the oxygen groups does not induce changes in the surface roughness and thus the difference between an oxidized fiber and an oxidized – reduced fiber would only be surface chemistry. AFM surface scans in Figure 4-16 illustrate the changes in surface topography necessitating the comparison of the fibers and the sequential processing used to create the reduced fibers.

The tensile strength of fibers oxidized in nitric acid, shown in Figure 4-14, is very comparable to that measured for fibers as received. The reason that the fibers do not appear to show significant damage due to the oxidation remains elusive, which is confirmed by the lack of roughening shown in Figure 4-16. The 4 hour nitric acid reflux remains an undesirable approach to functionalizing carbon fibers for other reasons, including processing concerns. During the course of this work, existing functionalization techniques, in particular electrochemical oxidation, were attempted to create the desired functional groups without reducing the tensile strength and may serve as a point of reference for future researchers. The tensile strength is severely compromised with

even a mild electrochemical oxidation in nitric acid. Oxidation times ranged from only 20 seconds to 60 seconds with different galvanostatic currents. Figure 4-17 shows the raw tensile strength data and the dramatic reduction in properties even with short oxidation times. These reductions in the tensile strength were accompanied by miniscule changes in the surface chemistry, as measured by XPS and shown in Figure 4-18. Electrochemical oxidation, widely documented in the scientific literature and widely used in industrial production, does not generate the desired surface chemistry or suitably maintain structural properties of the fiber.

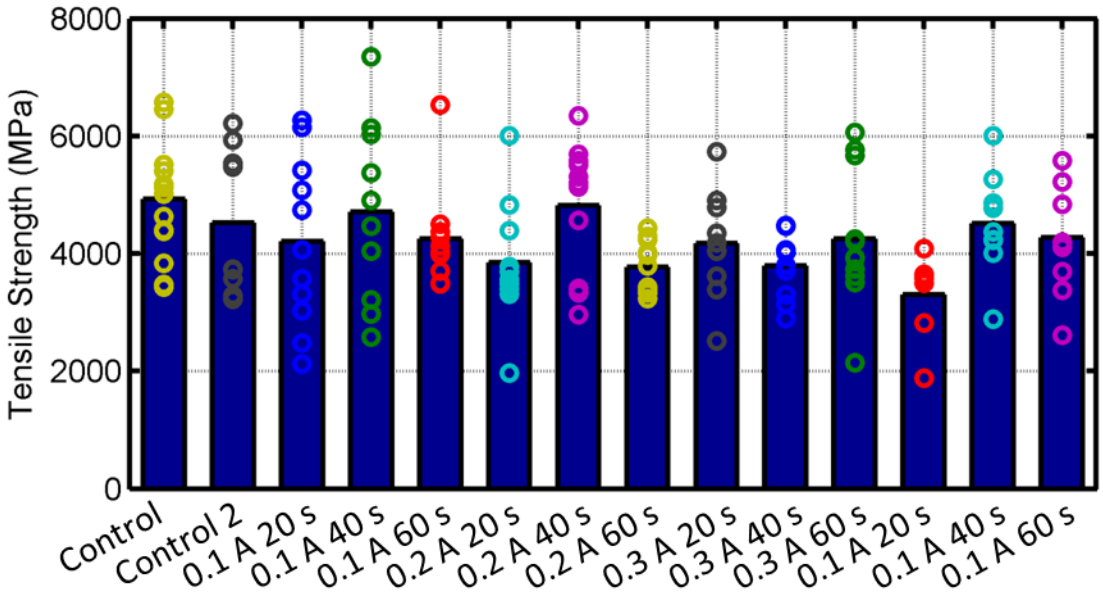

Figure 4-17. Tensile test results of electrochemically oxidized carbon fibers. Bars labeled 'Cont' are control specimens, IM7 as received. EC1-EC3 are fibers oxidized with 0.1 amperes of current for 20, 40 and 60 seconds, respectively. EC4-EC6 were oxidized with 0.2 amperes and EC7-EC9 were oxidized with 0.3 amperes of current.

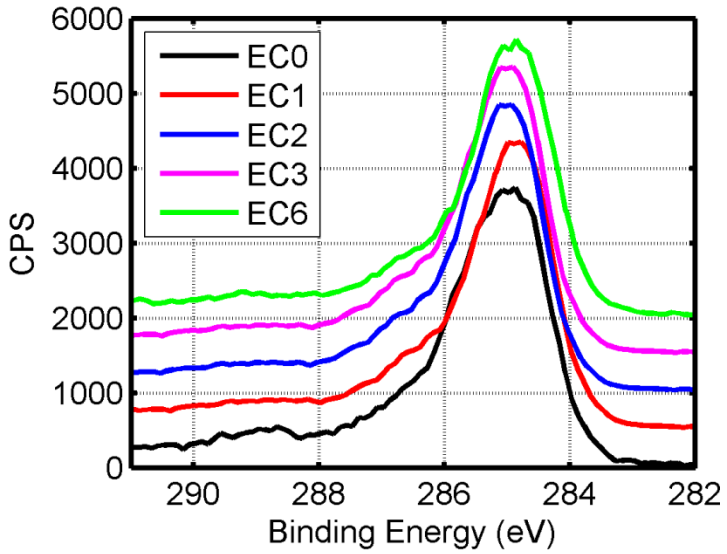

Figure 4-18. High resolution XPS scan of the carbon binding energy region. Various electrochemical treatments do not appear to substantially change the surface chemistry while dramatically affecting the tensile strength. Nomenclature is consistent with Figure 4-14.

4.3 Interface Test Results

Interface testing is the keystone to the scientific contribution of this work. It will be shown that ZnO nanowires improve the interfacial shear strength of single fiber aramid and carbon composites. Large scale v-notch shear specimens show enhanced shear modulus and shear strength, which is ascribed to the improved interface. This section will probe the viability of ZnO nanowires to enhance structural composite interfaces. Beyond demonstrating an improved interface, this work will also investigate the chemical adhesion mechanism between the fiber and ZnO nanowires. Specific functionalization techniques were developed in this work to create a variety of different fibers with varying surface chemistry. These treatments include a carboxyl functionalization of aramid fibers, two carboxyl functionalization procedures of carbon fiber, general oxygen functionalization of carbon fiber and reduction of carbon fiber to remove oxygen functionality. The aramid fiber interface strength will be shown to be

entirely dependent upon the carboxyl functionalization procedure developed earlier. This inspired the carboxyl functionalization of carbon fiber toward the same end, improving interfacial shear strength by anchoring the ZnO nanowire interphase to carboxylic acid groups. Owing to the natural presence of oxygen containing groups on the surface, carbon fibers do not show the same selectivity towards carboxylic acid as aramid fibers do. It will be shown that carbon fiber – ZnO interfaces are generally enhanced by the presence of any oxygen functional groups, not exclusively carboxylic acid. The demonstration of physical property modulation through control over interface chemistry is a significant scientific contribution. This work can serve as a template for other ceramic interphases or structural fibers by providing a guide for the development and testing of fiber functionalization procedures. The understanding of the role of interface chemistry with physical properties extends beyond structural fibers and may create impacts in laminated materials or other hierarchical materials.

4.3.1 Interface of Failure

The interface of failure was discussed theoretically earlier, to assess the effect of surface chemistry it must be verified that the ZnO to fiber interface is the weakest and dominates failure. This is expected to be the case because the ZnO to fiber interface has the least mechanical interlocking and the lowest surface area. To assess this, failure surfaces of both large scale composites and single fiber composites were analyzed. The location of the nanowires after failure of the material was used to determine the interface of failure, whether they are embedded in the polymer, remain on the fiber or are absent entirely from the image.

A single fiber composite was prepared by placing a single carbon fiber with a ZnO nanowire interphase into a droplet of polymer (Epon™ 862/ Epikure™ 9553). Upon

curing, the droplet was sputter coated with a thin layer of gold and then machined with a focused ion beam mill. The ion beam milled through the fiber approximately 30 µm away from the edge of the droplet to ensure that the embedded depth was shallow enough to cause pull-out and not tensile fiber failure. The sample was removed from the mill and the fiber was manually pulled out of the milled droplet. The sample was reexamined for the location of the nanowires to determine if the nanowire – polymer or nanowire – fiber interface had failed.

A ZnO nanowire coated fiber after pull-out is shown in Figure 4-19 C and D. Figure 4-19 A and B show the epoxy droplet after the fiber has been pulled out. It is clear that the nanowires embedded in the effectively infinite epoxy medium debond from the fiber and remain embedded in the polymer after failure. Some nanowires held together by a thin film of epoxy also remain on the surface of the fiber. These nanowires maintain orientation on the fiber and do not indicate that the interface of failure is nanowires polymer, but rather that the cohesive strength of the film is low when an insufficient volume of epoxy forms a composite. An examination of the polymer droplet shows the polycrystalline ZnO seed layer as an exact replica of the surface of the carbon fiber including the longitudinal striations created during fiber drawing. It is clear that the interface between the polycrystalline seed layer and the fiber is the interface of failure and that this interface needs to be the subject of development.

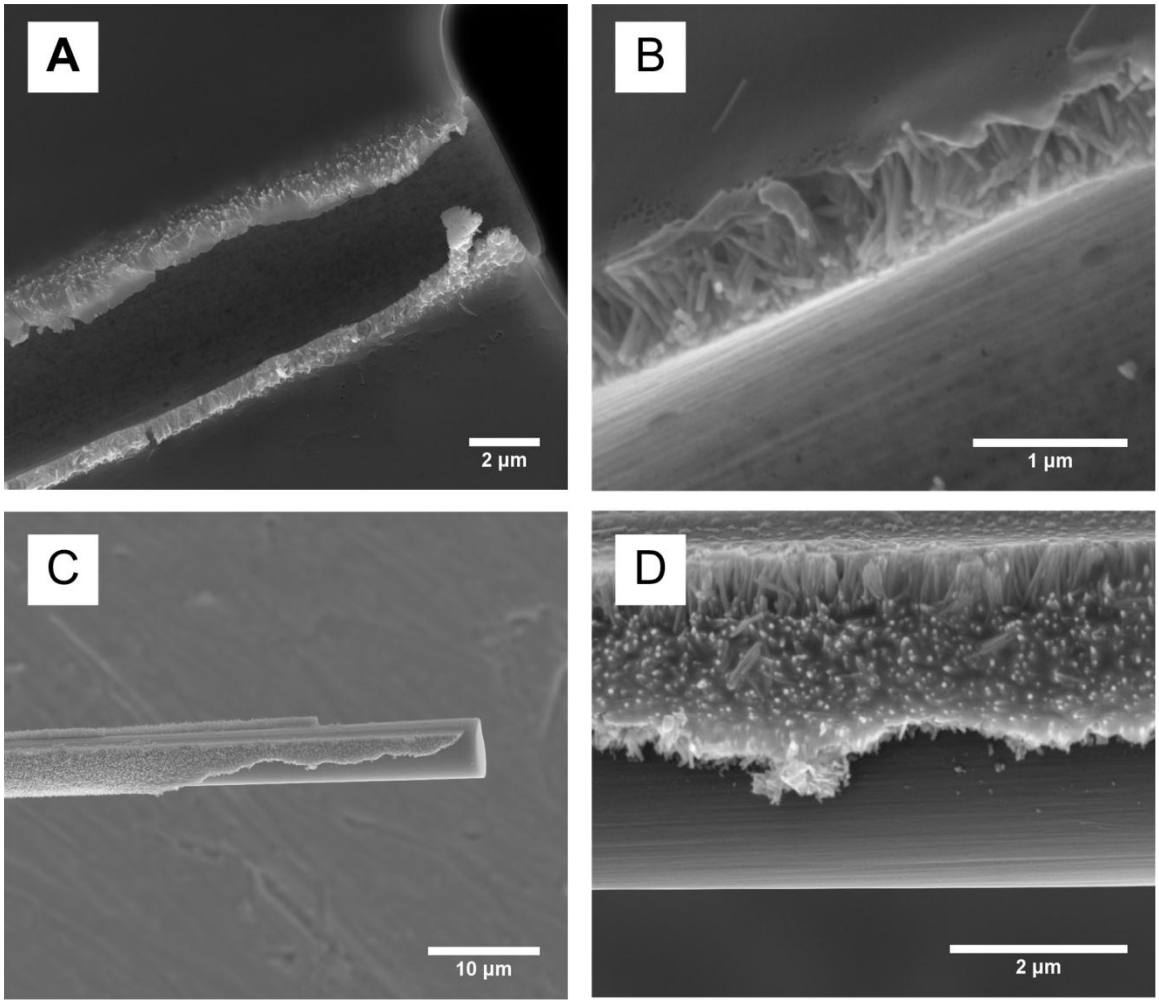

Figure 4-19. Failure surface of ZnO – carbon fiber during pull-out testing. The nanowires remain embedded in the polymer matrix in A. The nanowires are aligned and wetted by the epoxy to form a strong interface in B. Nanowires remain on the free fiber, C and D, after pull-out testing due to the strong interface of the ZnO and fiber and the thin section of the ZnO seed layer to support shear loads. Scale bars are 2 µm, 1 µm, 10 µm and 2 µm, respectively.

Occasionally, test results from the single fiber and bulk scale are not congruent which can mislead researchers. The failure surfaces of the larger scale specimen are examined for a consistent failure pattern. The nanowires were observed to debond from the fiber, remaining embedded in the polymer matrix after fracture. A consistent pattern of the remaining shell is visible, yielding a perfect replica of the fiber surface and the striations of the fiber along its axis. Failure of the large scale composite includes not

only the interface between the ZnO seeds and fiber, but also through the matrix. Cohesive failure of the matrix is substantial, with cracks spanning interfaces by traveling through the polymer region. In spite of the extensive failure of the polymer matrix, the dominant failure mechanism is the debonding of the ZnO nanowires from the structural fiber. The images of the failure surface in Figure 4-20 confirm what was observed in the single fiber pull-out testing, the interface of failure is in fact the fiber – ZnO nanowire interface and not the polymer – nanowire interface.

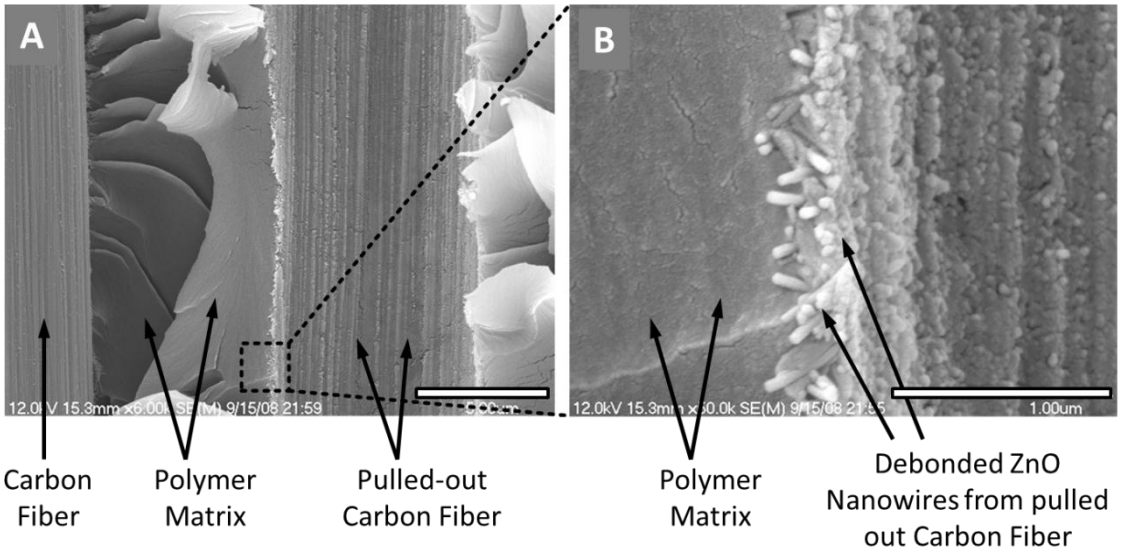

Figure 4-20. Fracture surface of failed v-notch shear specimen at A) low magnification and B) high magnification. Failure occurs at the fiber – ZnO interface, leaving the ZnO nanowires embedded in the polymer matrix. Scale bars are 5 µm and 1 µm, respectively.

4.3.2 Interface Enhancements due to a ZnO Nanowire Interphase

Small scale interface testing is preferred during development because it enables greater control over product quality and higher throughput of experiments. The preferred method of single fiber interface testing is the single fiber fragmentation test, for the reasons listed earlier in Chapter 4. Aramid fibers as well as carbon fibers are tested, each with varying surface functionalization to identify the role of surface

chemistry in the adhesion of nanowires. This section will detail the effectiveness of a ZnO nanowire interphase for improved composite properties by showing that a nanocomposite interphase is superior to the typical polymer interphase that naturally forms around the fibers. Single fiber interface testing, in the form of single fiber fragmentation, will demonstrate that ZnO nanowires can improve interface strength. Next, it will be shown that aramid fibers also benefit from the addition of ZnO nanowires. The effect of ZnO nanowires full scale carbon fiber composites will then be discussed.

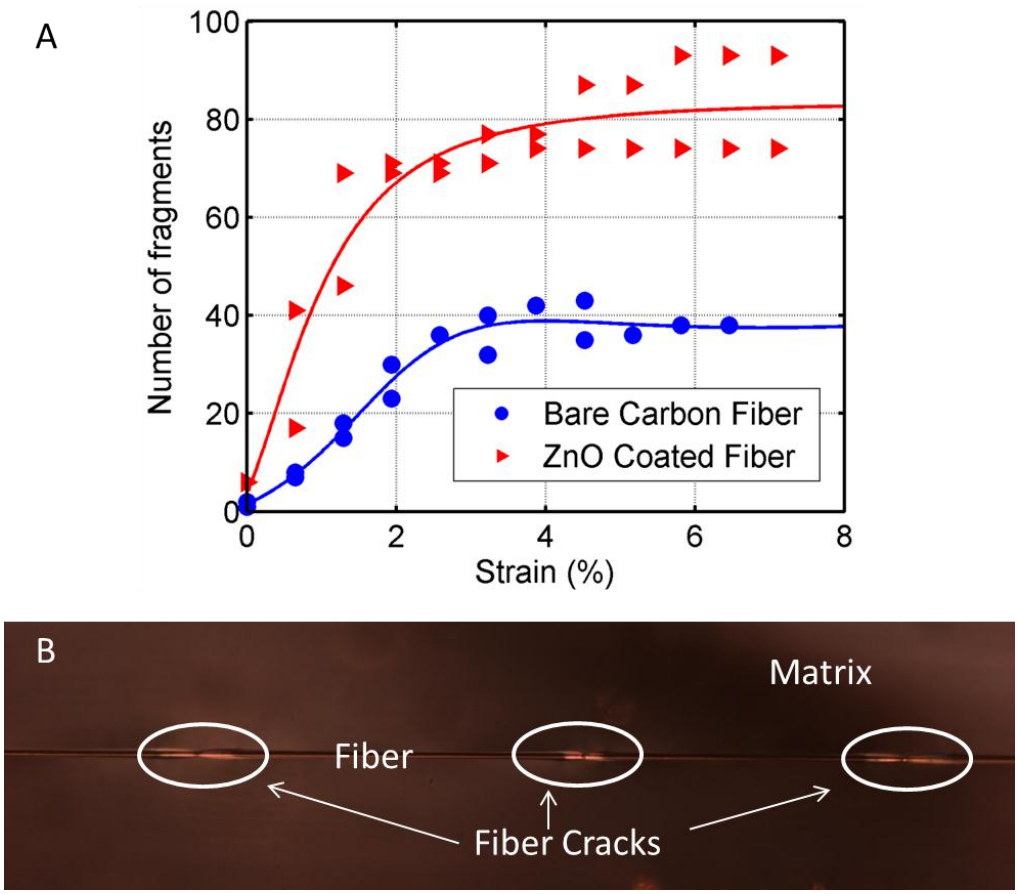

Figure 4-21. A) Single fiber fragmentation test results, showing the increase in the number of fragments in a 16 mm gauge section. The number of fragments saturates in both the bare carbon fiber and the ZnO nanowire coated fiber. The interfacial shear strength increases from 15.9 MPa to 33.9 MPa with the addition of a ZnO nanowire interphase. B) Micrograph of typical fragments viewed during the single fiber fragmentation test.

Figure 4-21 shows the measured number of fragments in a 16 mm gauge section of a single fiber composite with and without a ZnO nanowire interphase. The composite with the ZnO nanowire interphase has nearly double the number of fragments, which correlates to more than double the interface strength. Considering that the strength increases as the fragment length decreases, the interface strength increased by nearly 110%, from 15.9 MPa to 33.9 MPa. Both of these composites are produced with IM-7 fibers as received and thus do not have the functionalization that is expected to make a significant impact on the composite properties. The introduction of whiskers grades the interphase to reduce the stress concentration and improve the overall composite properties. This result demonstrates the potential impact that the addition of a ZnO nanowire interphase can have on composite interfacial shear strength.

Once the single fiber interface strength was shown to improve, large scale specimens were created. The preferred large scale specimen is the v-notch shear specimen as it directly measures the shear modulus and shear strength of a composite. Once the growth was scaled and the composites were fabricated, they were cut with a laser ablator to the geometry specified by ASTM D 3547 [222]. The specimens were tested with the appropriate fixture, including ±45° strain gauges mounted to the faces for strain and load to measure the stress. The response of the material, shown in Figure 4-22, is linear elastic followed by a plastic regime, consistent with classical behavior. The composite exhibits significant plasticity and hardening, leading to a high toughness. In spite of both constituents being somewhat brittle (the glass transition of the polymer is above room temperature), the plasticity afforded by the composite derives from the ability of a crack to grow within the material or between the phases and not break every

load bearing fiber. The plasticity inherent to the composite is one of the chief advantages that gives the composite material toughness beyond that of the constituents. The targeted reinforcement of the interface with the selective placement of the ZnO nanowires improves the strength and stiffness of the interface, enormously increasing the toughness of the composite. The resulting improvement in bulk properties, listed in Table 4-2, owes to the placement of the reinforcement directly at the location where it is needed most and demonstrates the ability of this technology to improve composites.

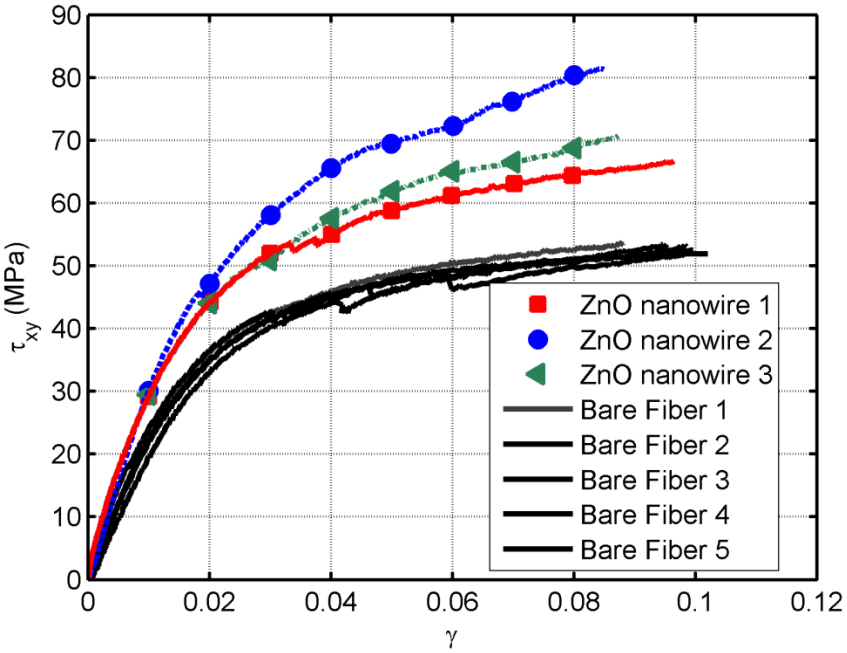

Figure 4-22. Iosipescu shear test of unidirectional composites, with and without a ZnO nanowire interphase. The average shear modulus and average shear strength of the composite increase from 2.54 GPa to 3.49 GPa and 52.9 MPa to 72.7 MPa, respectively.

This section demonstrated the improvements offered by ZnO nanowires to structural composites, both on a single fiber and on a lamina scale. The enhancement of properties is ascribed to the direct and selective reinforcement of the fiber – matrix interface; historically the weakest link of a composite. Significant improvements of over

100% on a single fiber scale and nearly 40% on a lamina scale make this technology very promising. This section demonstrates that this technology has great promise, it does not identify the chemical mechanism of adhesion. For this technology to become widely adopted, scientists and engineers must continue the development of an understanding of why the interface is strong and how to improve it further. This is what will ultimately limit how far this technology can pull composites forward.

Table 4-2. Average shear strength and shear modulus measured for unidirectional laminae in Figure 4-22. Both samples used unsized fibers without surface functionalization.

Sample Name	Ultimate Strength (MPa)	Shear Modulus (GPa)	Average Strength (MPa)	Average Modulus (GPa)
Bare 1	53.3	3.07		
Bare 2	53.3	2.53		
Bare 3	53.2	2.53	52.9	2.54
Bare 4	52.5	2.53		
Bare 5	52.0	2.08		
ZnO 1	66.5	3.64		
ZnO 2	81.4	3.25	72.7	3.49
ZnO 3	70.4	3.59		

4.3.3 Mechanism of Adhesion Assessed through Interface Strength

The major scientific contribution of this work is the identification of the mechanism of adhesion for ZnO nanowires, specifically by controlling interface chemistry to affect interface strength. This section will present single fiber fragmentation data from aramid and carbon fiber with various surface functionalization treatments. It will be demonstrated that oxygen containing functional groups are pivotal to creating strong interfaces with ZnO nanowires. There does not appear to be significant selectivity in the specific form of those groups.

Single fiber fragmentation results for aramid fibers are shown in Figure 4-23, with each bar corresponding to the combination of functionalization and ZnO interphase.

The fragmentation results show that simply adding a ZnO nanowire interphase to an aramid fiber affords no improvement in interfacial shear strength. This is because the oxygen present in the aramid fiber is highly constrained by interchain hydrogen bonding and the oxygen is unavailable to interact with the Zn^{2+} cations. The functionalization of aramid fibers disrupts the interchain bonding by hydrolyzing the amide link to create a carboxyl group and a primary amine. This combination interrupts the linear arrangement of the chains to permit the oxygen atoms more freedom of motion, enabling coordination and strong interaction with the Zn^{2+} cations.

The functionalization was originally conceived as a method to increase the presence of surface amine groups, the reactive group in the curing agent of epoxy polymers, in an attempt to directly cross link the polymer matrix to the aramid fiber. This was largely ineffective in a structural sense because the functionalization does not create an extraordinarily high number of functional groups. In addition, the steric hindrance presented by the polymer chain and surrounding functional groups will force the epoxide groups to give preference to the free amine groups within the polymer, limiting the yield of the crosslinking reaction with the fiber. This preference does not exist with ZnO growth for three reasons. First, the ZnO seed suspension is evaporated to deposit the ZnO seeds on the surface of the fiber, effectively constraining the ZnO to interact with the surface and preventing it from interacting with anything in bulk. In the absence of nothing in the bulk to interact with, the ZnO becomes anchored to the carboxylic acid groups on the aramid fiber. Secondly, the Zn^{2+} cations in the growth solution are significantly more mobile than a typical polymer precursor. Ions dissolved in solution will find the seeds or carboxyl groups to anchor to and begin to precipitate at

those locations from solution. Considering that a polymer chain must arrange and orient into a favorable configuration, dilute solution reactions provide a more probable scenario to enable deposition on the functional groups. Finally, significant cross linking between structural fibers and the polymer matrix will improve the interface strength, but there is some doubt as the global effects of an occasional crosslink. The polymer chains of a typical epoxy resin are quite flexible and at surface have substantially more liquid behavior than they do in bulk. It is well known that a low modulus interphase region generally exists around structural fibers in composites, which acts as a highly compliant interphase. The interphase may reduce the stress concentration caused by differences between the matrix and fiber, but this material might also serve more as shearable fluid than a keyed interphase to transfer load. Even in the event of full crosslinking with all available groups, this interphase will not show great sensitivity to the number of anchors as the cohesion of the softer interphase region will play a more substantial role in the observed strength. ZnO exhibits fully crystalline ceramic behavior, even in extremely small volumes, such as quantum dots. When the nanoparticles interact to form a crosslink, the particle is effectively rigid and becomes anchored to the surface of the fiber, undoubtedly stressing the crosslink. The high modulus particle will show great sensitivity to the number of cross links and likely the number of crosslinks will increase the interface strength exponentially. It follows that using functional groups to attach rigid ZnO nanoparticles will likely show a greater sensitivity and yield higher strengths than a typical polymer cross linking scheme.

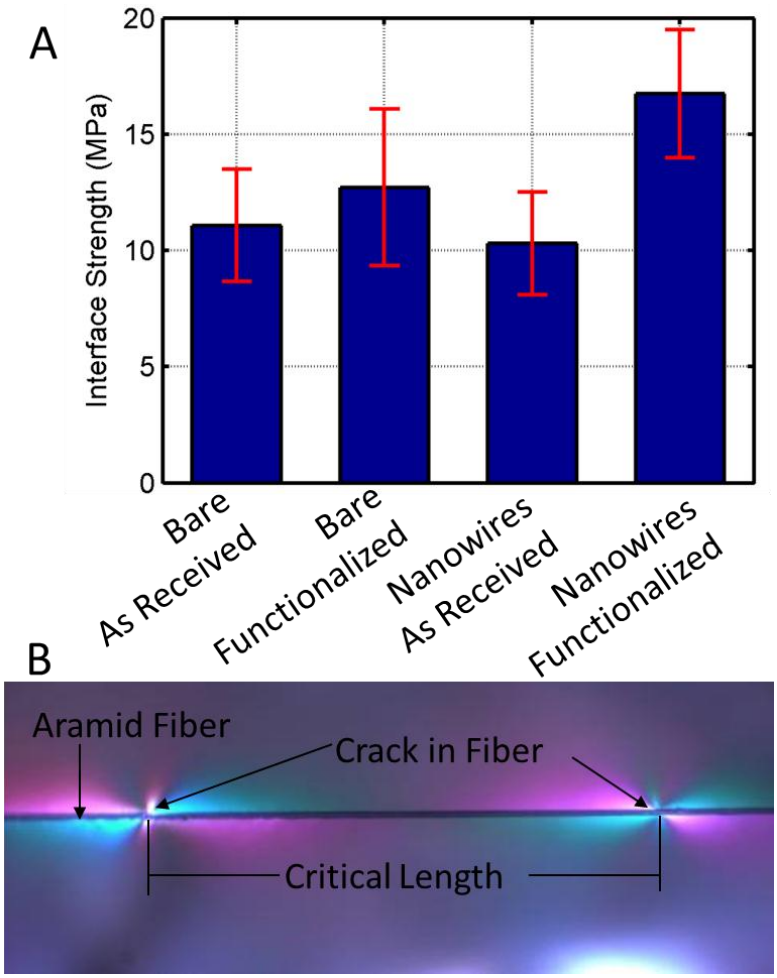

Figure 4-23. A) Interface strength of various aramid composites, as measured with single fiber fragmentation testing. Error bars represent the 95% confidence intervals on the average interface strength. B) Micrograph of composite fiber fractures as observed during single fiber fragmentation testing. The colored sections near each crack highlight the strain concentration through birefringence.

It is clear that the functionalization will provide great benefit to the adhesion of the ZnO interphase. This synergy of surface functionalization and rigid ceramic nanowire interphase enables ZnO to be a superior reinforcement for the interface between fiber and matrix. Directly growing ZnO nanowires on the surface of aramid fibers without surface functionalization does not provide any mechanism to attach the ZnO to the surface and predictably, the ZnO affords no real interface improvement. What is quite surprising is the readiness of the ZnO to completely break away from the aramid fiber in

the absence of functionalization. Routine handling of the fibers during preparation for analysis with the SEM was sufficient to cause large areas to cohesively separate from the fiber. Considering that the fiber at most is 20 μm in diameter and a radius of curvature of 500 μm, the strain applied during the bending of the fiber to this extreme is about 2% at the outermost surface. This level of strain is hardly sufficient for the widespread failure of the ceramic coating. The absence of viable functional groups to anchor the ZnO did cause large absences in the ZnO nanowire interphase as shown in Figure 4-24. Clearly, the attachment of the ZnO interphase is dictated by surface functionalization and the available carboxylic acid groups created with the functionalization are responsible for the improved interfacial shear strength.

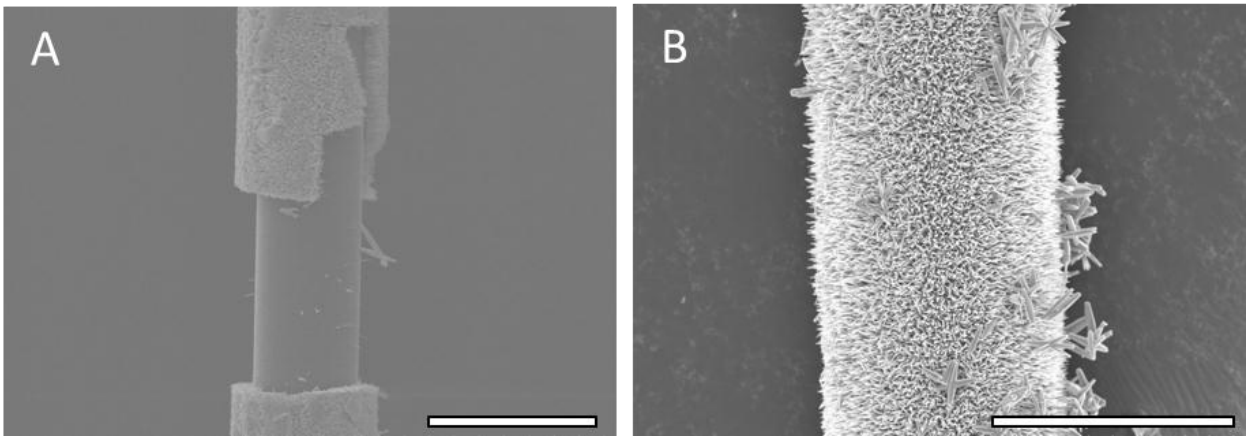

Figure 4-24. ZnO nanowires on an A) as received fiber and B) functionalized aramid fiber. Scale bars are 20 μm.

The observations from the aramid fiber composite motivated the development of novel carboxyl functionalization treatments for carbon fiber. These treatments would then be used to develop a similar relationship as what was observed for the aramid fiber composite. The functionalization treatments developed earlier were applied to several fibers, a ZnO nanowire interphase was grown and each specimen was evaluated using single fiber fragmentation. The results, presented in Figure 4-25, show that the

interface strength is largely the same for IM8, defect grafted and selectively oxidized fibers, and substantially lower for hydrazine reduced fibers. The functionalization procedures developed earlier in this work are conversion type processes, whereby existing defects and oxygen functional groups are converted directly to carboxylic acid or grafted to yield terminal carboxylic acid. The total amount of surface oxygen groups remains largely unchanged during the functionalization process with the exception of the hydrazine reduced fibers. The hydrazine reduction of IM8 fibers removes oxygen groups without preference, although no reduction procedure is 100% effective. These fibers show a relatively weaker interface with ZnO, which indicates that the removal oxygen has a deleterious effect on the composite. The ZnO interphase clearly does not show selectivity towards carboxylic acid, it does show sensitivity toward the presence of oxygen. Significant research exists to show that ZnO strongly interacts not only with carboxylic acid, but also with hydroxyls and other lower order oxygen functional groups. It is clear that the oxygen groups have an effect and control the interfacial shear strength, though it is not selective to carboxylic acid as might be indicated by the aramid fiber data.

The results of the carboxyl functionalization testing indicate that the presence of oxygen functional groups, without specificity to carboxylic acid, control the interfacial shear strength of the ZnO to the fiber. This motivated the use of oxidation to create additional oxygen functional groups, though not necessarily carboxylic acid groups. Oxidation produces a mixture of oxygen groups and is one of the most effective methods to increase the oxygen content; albeit at a cost to the tensile properties and typically roughness of the fiber. The mixture of functional groups produced by oxidation

is thought to enhance the anchoring of the ZnO seed layer to a carbon fiber. In addition to creating oxygen functional groups, oxidation also roughens the surface. Since the seed layer is deposited on the fiber, it will conform to the roughness of the fiber itself and thus form a perfect replica of the surface through the same process that created the replica in Figure 4-19 B. Not only will this seek out available functional groups, but this perfect keying process is expected to add to the interface strength as it does for ceramic matrix composites. The addition of roughness plus functional groups combine to improve the interface strength and the two features must be decoupled. To do this, the fibers are reduced with the same technique as before to remove as much of the oxygen as possible. Interface improvements between oxidized fibers over fibers as received may give some insight into the effect of roughness and shows that the roughness is a major contributor. The true assessment of the impact of surface chemistry comes from this comparison because the roughness, as indicated in Figure 4-16, is the same.

The interfacial shear strength of oxidized fibers shows the exact same sensitivity as before. This indicates that in fact the adhesion of the ZnO is dictated by the presence of nearly any oxygen functional group and not just carboxylic acid because oxidation produces a mixture of functional groups. The addition of roughness and interlocking between the two phases, a phenomenon well studied in ceramic matrix composites, also contributes to the interfacial shear strength. Figure 4-26 shows the interfacial shear strength as measured by single fiber fragmentation. The interfacial shear strength increases with oxidation and then decreases with the subsequent reduction. The reduced fiber has higher interface strength than the fiber as received because the reduction procedure does not remove all of the oxygen groups created

during the nitric acid oxidation step. The results from the fragmentation testing of the oxidized fibers prove that oxygen functional groups, arrived at through any mechanism, effectively control the adhesion of the ZnO nanowire interphase. The oxidation developed here as a test of the bonding mechanism is not intended to be a means for maximizing interface strength. It runs the risk of inducing unnecessary roughness and, although not specifically in this case, can reduce tensile strength of the fibers. Other articles within the scientific literature report that oxygen plasma functionalization can be tuned to reduce the impact on surface roughness and concurrently tensile strength while creating a substantial number of functional groups. This may be an attractive alternative now that the mechanism of adhesion of the ZnO nanowires is established.

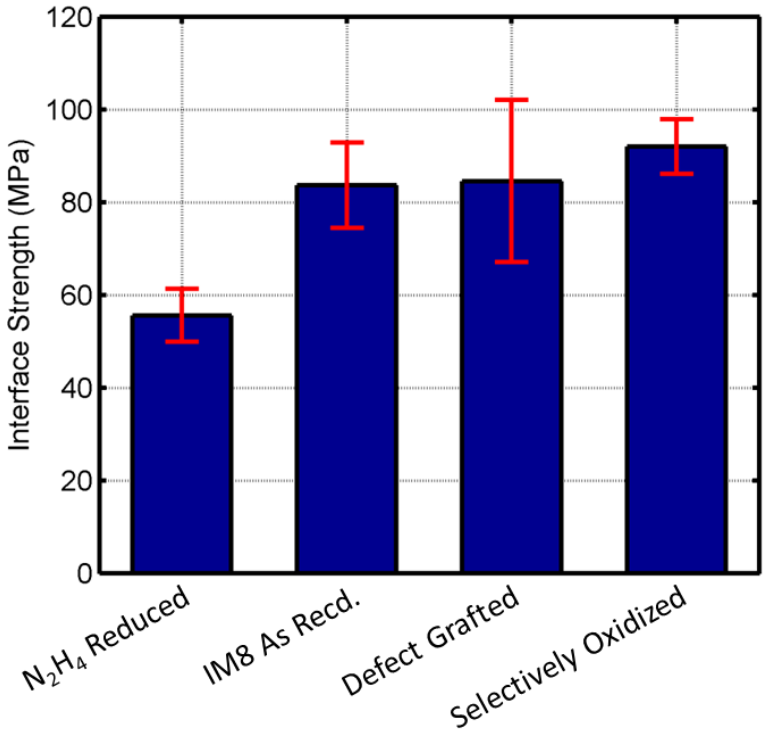

Figure 4-25. Interface strength of carboxyl functionalized carbon fiber composite samples, as measured by single fiber fragmentation testing.

The conclusions from this work are most clear when compiling the data from all of the carbon fibers created. The data certainly contains scatter, but there is a strong

correlation between interface strength and the content of oxygen groups, specifically ketone groups. Figure 4-27 shows the effect of oxygen content on the interfacial shear strength of carbon fiber composites with a ZnO nanowire interphase. The relative oxygen content is measured from XPS data for each set of fibers through the fitting procedures established in Chapter 2 and includes all oxygen functional groups (hydroxyl, carbonyl, carboxylic acid). The surface state of each fiber was presented in Chapter 2, specifically in Figure 2-18 and Table 2-5. Although only a limited number of functionalization cases exist, there remains a clear trend of increasing interfacial shear strength with increased oxygen functional group content. The blue line of best fit has an R^2 value of 0.89, which indicates a strong statistical correlation. Further increases to the oxygen functional group content will likely drive interfacial shear strength up until another interface limits the strength. Figure 4-27 B-D also shows the data broken out by specific functional group. As indicated on each figure, the correlation is only significant for ketone groups and not carboxylic acid groups. Ketone groups indicate a correlation of 0.87, while hydroxyl and carboxylic acid have a correlation of 0.47 and 0.13, respectively. Neither of these two correlations are significant enough to claim the correlation is strong and the carboxylic acid can only be considered random and not correlated. This is a significant finding because it demonstrates the selectivity of the ZnO and it clearly shows that only certain functional groups are ideal for the adhering a ZnO nanowire interphase. In principle, there are other materials (metal oxides, polymers, etc) could adhere to similar functional groups and this work could be extended to future interphase materials. The interaction of the ZnO particles with the

oxygen functional groups clearly improves interfacial shear strength and a physio-chemical mechanism must exist to enable this.

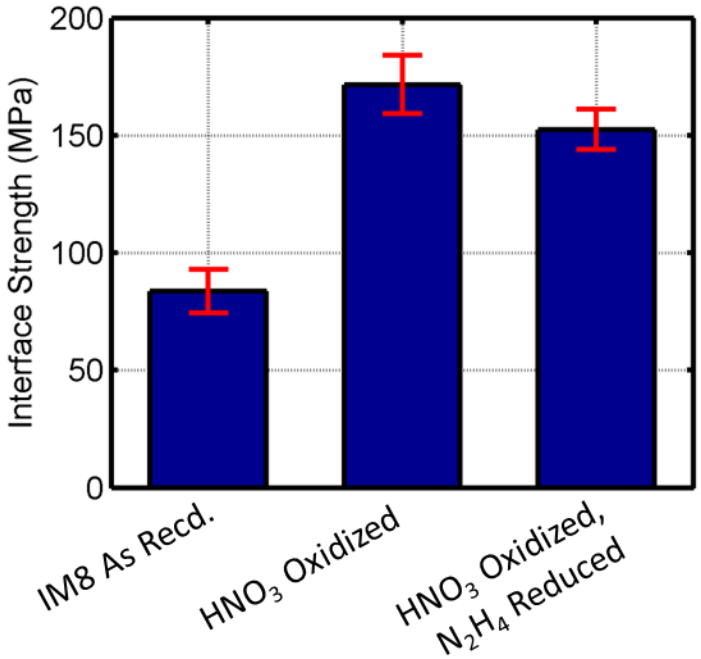

Figure 4-26. Interfacial shear strength of fibers with ZnO nanowire interphase with various surfaces. ZnO was grown on fibers as received, fibers after HNO_3 oxidation and fibers with HNO_3 oxidation then N_2H_2 reduction. Oxidation improved the interface strength. The application of both oxidation then reduction reduced the interface strength because some of the functional groups that enhanced adhesion were removed. Error bars represent the 95% confidence interval on the mean interfacial shear strength.

Analysis was performed using the interfacial shear strength data to examine the effect of each of the three regions of binding energy fit in the XPS data. The regions of the data that were fitted (hydroxyl, ~286.0; carbonyl, ~287.5; carboxyl, 289.0) were compared in a similar fashion to Figure 4-27. The ketone or carbonyl fit shows correlation almost as strong as that of oxygen and clearly the interface strength indicates that the ZnO shows preferential bonding with ketone groups. In Chapter 2, it was shown that the center carbon, carbon 3 in Figure 2-9, has a binding energy that gets combined with the ketone peak (R-CO-R) and thus adds to the signal without

necessarily adding the desired functional groups. Subtracting this contribution (~4%) from the fraction of ketone groups in Figure 4-27B, each data point demonstrates a clear trend that ketone functional groups have a strong correlation to the interfacial shear strength of the ZnO nanowire reinforced composite. The strong correlation as well as the clear trend in both the oxygen and ketone comparisons confirms that this is the best functional group for controlling the adhesion of the ZnO nanowire interphase for the composite.

Future designs of ceramic interphases could use the method developed here as a template toward developing ceramic nanowire interphases for enhanced and multi-functional composites. Specifically, the development of a nanowire interphase must first begin with an understanding of the surface reactivity of it. Typically, a fruitful place to begin the search is in the catalysis literature, specifically organic reactions. The original set of articles that helped to inspire this work, carbon dioxide reforming into methanol with a ZnO catalyst, discussed several surface reactions that included both carboxylic acid and hydroxyl groups. Both of these functional groups provided adequate adhesion for the ZnO nanowire interphase to significantly improve the interfacial shear strength of the composite. Other ceramics will likely also have previous work related to catalysis as processes to grow ceramic nanowire arrays remain limited to fewer than twenty different materials. These materials have been well studied and provide a sufficient understanding of surface chemistry and self-assembly. Catalytic properties provide some guidance – albeit in an unusual application. Once an appropriate functional group is selected, a functionalization technique can be developed. The interface strength,

bulk composite properties and any additional functional properties can be measured to implement the material system.

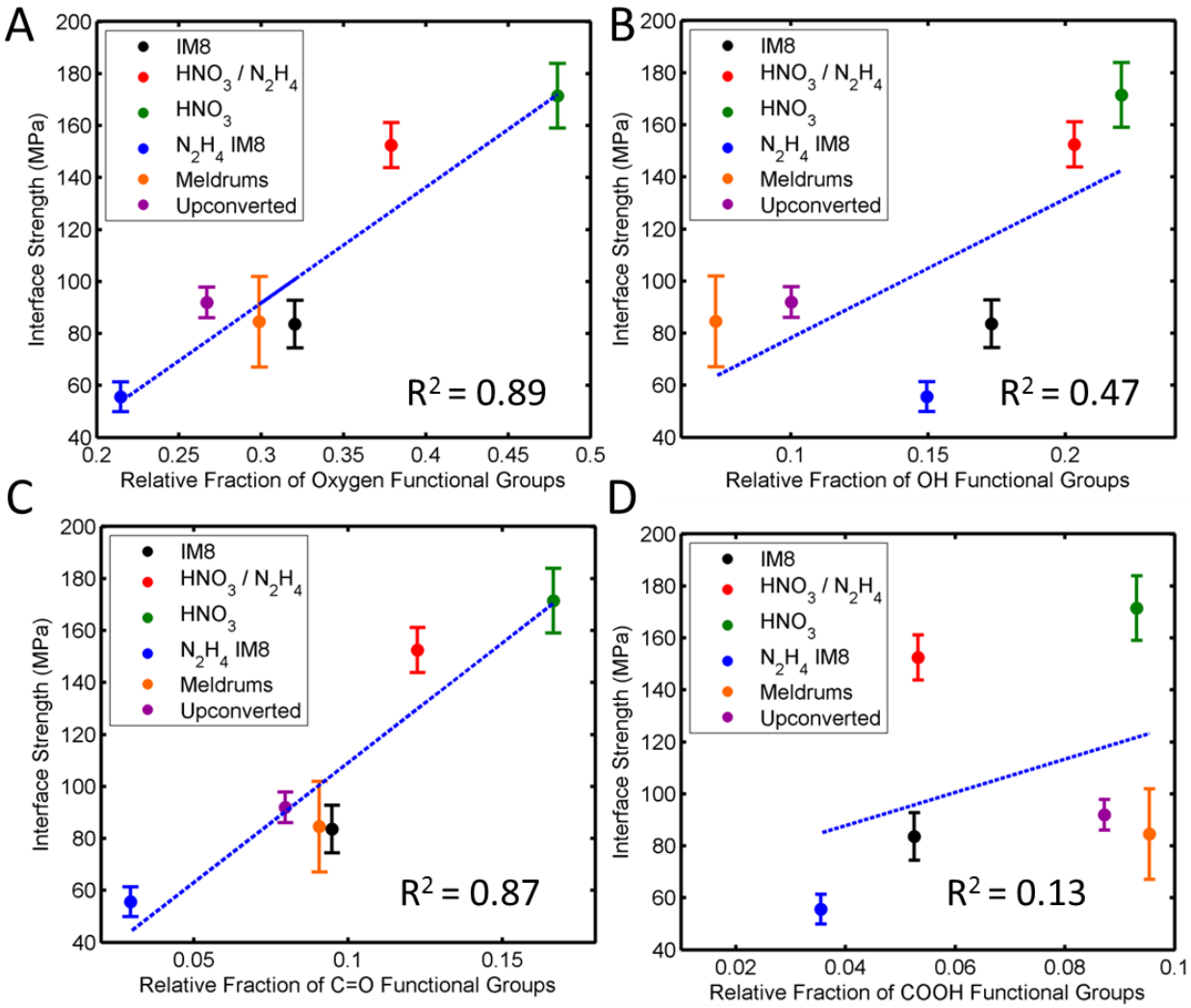

Figure 4-27. Effect of quantity of oxygen functional groups on the interfacial shear strength of carbon fiber composites with a ZnO nanowire interphase. The dashed lines indicate linear fits of the data, with the R^2 value indicated on each plot.

The mechanism of adhesion between ZnO and several different oxygen groups is well documented, which originates from the plethora of applications of ZnO in catalysis. One particular aspect of the catalysis literature particularly worth studying is the formation of methanol from syngas. Methanol, an alcohol, can be catalytically formed

from syngas, primarily a mixture of gaseous hydrogen and carbon monoxide. The conversion between these two molecules requires chemisorption of the various species in ionic forms to the ZnO surfaces during the catalytic processes. Two articles, Crook et al. and Thornton et al., demonstrated through spectroscopy that formate ions adsorb in both a monodentate and bidentate configuration on ZnO, with preference towards the bidentate configuration [241,242]. Petrie and Vohs suggested three different configurations and through their measurements identified hydroxyl groups that were attributed to the abstraction of hydrogen from the formic acid molecule [243]. The specific cause of the measured hydroxyl groups has been a matter of debate between the two groups. There remains little doubt that chemical interactions between formate ions and ZnO are strong, spontaneous and measureable with high resolution electron energy loss spectroscopy. Figure 4-28 shows the two major configurations of chemisorption along with another postulated by Petrie and Vohs, the bridging species. In the monodentate species, the oxygen groups form a new bond with the existing oxygen on the surface of the ZnO with the C – H bond oriented parallel to the plane of the ZnO surface. In the bidentate configuration, the two oxygen atoms share a resonant bond with the carbon and both form an interaction with a single Zn cation. The bridging configuration shows each oxygen coordinating with a Zn cation to anchor the formate ion to the ZnO surface. Other references reinforce the claims of these two, including review articles by Wöll [244] and Glemza [245], as well as a theoretical study by Persson et al. [246].

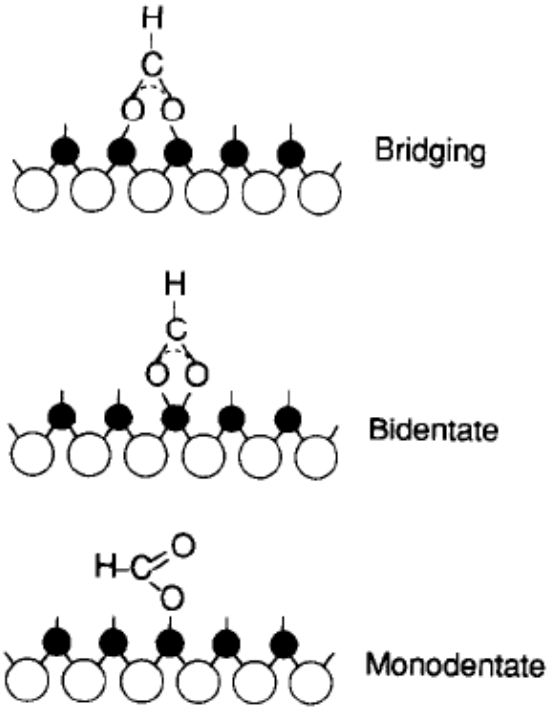

Figure 4-28. Three species of formate ion chemisorption on Zn terminated ZnO surfaces. Oxygen ions are white circles, zinc ions are black circles. [Reprinted with permission from Petrie WT, Vohs JM. An HREELS investigation of the adsorption and reaction of formic acid on the (0001)-Zn surface of ZnO. Surface Science 1991;245(3):315-323.]

The previous work in the study of formate chemisorption on ZnO reinforces the claims of this work by providing the theoretical framework for strong adhesion. The inspiration for the development of carboxylic acid functionalization techniques initially arose from the advantageous arrangement of the oxygen groups in carboxylic acid. Carboxylic acid not only stabilizes negative charges to create ionic interactions, but the 120° bond angle is intrinsically compatible with the 109.5° of the tetragonally coordinated Zn^{2+} ion. The theoretical and experimental evidence suggests that the bidentate orientation is most preferred; however the monodentate proves to be strong and spontaneous as well. The literature proves that the monodentate configuration occurs in both theoretical models and is experimentally observed through spectroscopy. The orientation of the ZnO seed layers is random and steric hindrances will often

prevent the specific ZnO surface from interacting in a bidentate manner with the surface oxygen groups on the fiber. The more forgiving orientations permitted by the monodentate configuration will often occur even in the presence of a higher fraction of carboxylic acid groups. The ZnO seeds are capable of forming anchors with any free oxygen group, in particular the hydroxyl and carboxylic acid groups. The evidence presented earlier indicates that ketone groups are the most important to the adhesion, which is consistent with the preceding theory because both configurations rely on bonding through the free lone pairs on the oxygen. Each oxygen in a ketone configuration has two such lone pairs and ketones are well known to be susceptible to bonding and protonation under the right circumstances. The theoretical and experimental evidence that both monodentate and bidentate configurations spontaneously form during chemisorption of formate ions to ZnO agrees with the finding of this work that oxygen and especially ketone functional groups in general are responsible for the adhesion of a ZnO interphase to carbon fiber composites.

The relation of whiskerization to other interphase treatments bears mentioning, especially in light of the adhesion results. The creation of a composite with fibers as produced yields a three phase composite; a fiber phase, a matrix phase and an interphase, shown schematically in Figure 4-29. The constraint imposed on the polymer matrix by the surface reduces the propensity for cross linking and inevitably leads to an interphase with different material properties than the surrounding bulk polymer matrix. Manufacturers have developed proprietary sizing layers that protect the fibers during weaving and stand to replace the polymer interphase. The bulk polymer is created to optimize many properties and the changes induced in the interphase by the surface

constraint often leads to a polymer that is not desirable. The sizing layer can have a different molecular structure than the bulk polymer and thus it can be optimized to cure effectively in the presence of the surface. The sizing is highly compatible with the chosen polymer matrix and enables mixing and entanglement of the polymer chains upon curing of the composite. The sizing layer, much like the naturally occurring interphase, wets the fiber and occasionally forms crosslinks with the fiber itself to adhere the sizing to fiber. Manufacturers typically employ a plasma functionalization step to improve this bonding somewhat and then apply the sizing layer to enhance the interface. Whiskerization takes much the same approach as the state of art processing technology used in carbon fiber manufacturer; however it holds great advantages. Instead of creating a polymer based interphase, the interphase is a graded nanocomposite with properties than can easily surpass neat polymers. Nevertheless, the salient issue then becomes how to adhere the interphase to the surface of the fiber. This work has shown that ketone functional groups effectively anchor the whisker interphase to the surface of the fiber for enhanced interface strength. It is particularly important to note that, barring changes in the roughness of the fiber, addressing chemical bonding between the fiber and the interphase is a persistent concern. This is easily identified in the schematic in Figure 4-29 because each interphase still maintains a discrete interface with the fiber. The mechanical properties and microstructure of the interphase are equally as important as the chemical bonding though, and this work has demonstrated that properly addressing both facets can substantially improve the interface and bulk properties of composite materials. The improvement of interface strength in composite materials requires a holistic approach that addresses all

deficiencies in the existing material, both chemical bonding and interphase elastic properties.

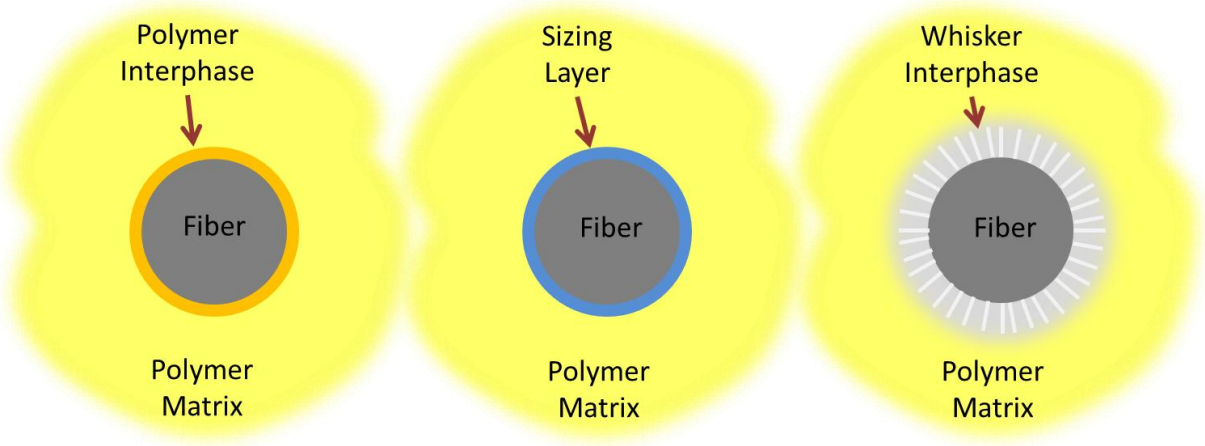

Figure 4-29. Schematic comparing the naturally occurring interphase, common manufacturer applied sizing and the ZnO nanowire interphase developed here.

This chapter has demonstrated that manipulating the surface chemistry of structural fibers causes substantial impacts on the interfacial shear strength. This begs the question, is there a limit at which increased functional group coverage does not increase interfacial shear strength? For this work, that limit was not achieved. Ostensibly, the linear fits in Figure 4-27 do not carry upward toward 100%, if for no other reason than steric hindrance would render many functional groups inactive. Linear fits, chosen on the basis of simplicity for the rather limited data set, do not accurately capture the behavior; rather sigmoidal or other asymptotic functions would much more accurately represent this; however that remains beyond the scope of this work. A qualitative estimation of the maximum interface strength is thus generated by analyzing maximum adhesion measurements through other methods. Atomic force microscopy offers just such a technique. By lifting a sharp cantilever from a surface with a very specific chemical environment, the energy required to separate the surfaces

can make accurate measurements of adhesion and enable prediction of the peak liftoff load. Noy et al. performed just such a set of experiments, varying surface interactions from CH_3 – CH_3 to COOH – COOH [247]. They observed that interactions of the CH_3 – CH_3 tip to surface were extremely low, estimated at as few as 15 molecular pairs, effectively zero interactions. The COOH – COOH interactions are among the strongest reversible interactions that could be expected in surface adsorption and consequently yielded much higher peak liftoff loads. Average peak load for the COOH – COOH case was about 2.1 nN while the CH_3 – CH_3 case had an average of about 0.5 nN. Certainly the relationship is not a perfect simulation of the interaction between ZnO nanoparticles and organic functional groups, but an order of magnitude assessment would indicate that the upper limit is approximately 4 times that of the lower limit. For these experiments, an upper limit of about 240 MPa is expected. The surface functionalization procedures developed here could be improved upon to yield even high interface strength; however increased ketone functional group coverage is likely entering a realm of diminishing returns.

4.4 Chapter 4 Summary

Chapter 4 examined the effects the ZnO nanowire interphase and functionalization treatments on the mechanical properties of composites. The chapter begins with an introduction to the methods of mechanical characterization of both single fiber and lamina scale composites. The tests selected for measuring the interfacial shear strength are the single fiber fragmentation test and the v-notch shear test. A detailed justification and review was provided, specifically focusing on the mechanics of the deformation and the effect of a ZnO interphase on the measured properties.

The impact of the functionalization and interphase treatments on the tensile properties of the fibers was also presented. Individual filament strength testing remains the preferred method for assessing the longitudinal strength of a composite so this testing was performed to assess any damage done by the creation of interphase or functional groups. Both the aramid and carbon fibers were tested and the procedures developed were found to have no discernible impact on the tensile strength. The only procedure that showed large reductions in the tensile strength was the electrochemical oxidation procedure which, even in mild conditions, exhibited significant reductions in the fiber strength. The majority of the testing results shown are not the standard average tensile strength results, but rather the confidence intervals on the estimate of the Weibull scale parameter which serves as a much better estimate of the fiber tensile strength. This section shows that the chosen mechanisms of selective oxidation, defect grafting and amide hydrolysis were consistent in minimizing the effect on the tensile strength.

The weakest interface was then identified as the fiber – ZnO interface, because it has the lowest surface area and least amount of interlocking. Single fiber and lamina scale failure surface analysis confirmed that the ZnO – fiber interface fails first. The effects of the ZnO nanowire interphase on both the interface strength and the bulk lamina scale properties were presented. The single fiber interface strength was observed to increase 228% for carbon fiber composites and 51% for aramid fiber composites . Upon scaling up the process to a full size lamina the shear modulus and shear strength of the composite increased by an average of 37% and 38%, respectively.

Finally, the mechanics of the adhesion of the ZnO nanowires to surface of the structural fibers was presented. The ZnO nanowires were only shown to enhance the interfacial shear strength of aramid fiber composites when the fiber was functionalized with carboxylic acid. The carbon fiber functionalization procedures developed in Chapter 2 merely converted existing oxygen functional groups to carboxylic acid through either defect grafting or selective oxidation. This was shown to have minimal effect on the interfacial shear strength and the functionalized fibers showed no benefit over the IM8 carbon fibers as received. It was also shown that hydrazine reduction removed oxygen functional groups and caused the interfacial shear strength to drop. This implies that oxygen groups of any form are critical to the adhesion of ZnO to carbon fibers. The oxidative procedure was found to improve the interfacial shear strength of a ZnO nanowire reinforced composite compared to an IM8 fiber as received. Reducing the same oxidized fibers produced a drop in the interfacial shear strength, demonstrating that the mechanism of adhesion stems from overall oxygen content on the surface. In addition to a general trend of oxygen groups, ketone groups specifically appear to contribute the most to the adhesion of the ZnO interphase. The random orientation of the functional groups as well as the problems associated with steric hindrance when attaching a nanoparticle creates some ambiguity in the specific mechanism of adhesion. These results were compared to in-depth spectroscopic studies that evaluated the configuration of formic acid adsorbed onto ZnO surfaces. It was found that both a bidentate and a monodentate form spontaneously occur. This implies that most oxygen functional groups can have some theoretical basis to serve as

anchors for the ZnO seed layer, while the experiments indicate that ketone groups have the largest direct impact.

CHAPTER 5
CONCLUSIONS

Composite materials currently offer high specific strength and high specific stiffness that promise increased structural efficiency in the next generation of engineered materials. Continuous fiber reinforced polymers have a great difference in elastic modulus between the reinforcing fibers and the polymer matrix which, regardless of the loading mechanism, creates a large stress concentration at the interface between the fiber and matrix. Failure of composites generally proceeds through cracks initiating or traveling along this interface because of this stress concentration. Reinforcing the interface has become an area of great research interest because improving the strength and toughness of the interface can directly lead to substantial improvements in the bulk composite properties. The interface between fiber and matrix of today's composites currently limits the ultimate performance of the material, improving the interface is of great scientific and commercial interest.

Several methods exist to reinforce the interface in composites that can be broadly classified into three basic categories. First, techniques exist that attempt to modify the chemical groups on the surface of the fiber in an attempt to both improve surface wetting of the polymer matrix and move toward creating chemical crosslinks between the fiber and the matrix. There exists a plethora of creative solutions for creating the desired functional groups, most relying primarily upon chemical functionalization or plasma functionalization. Generally, the most well studied matrix is the thermoset epoxy based polymer matrix as it is the most common high performance polymer matrix with widespread applications in aerospace structures. Many chemical functionalization procedures attempt to create primary amine groups on the fiber surface, which react

with epoxide groups in the matrix, because the creation of pendent epoxide groups tends to be difficult to achieve. A variety of chemical treatments or ammonia plasmas can create the desired functional groups; however these generally can cause tradeoffs by etching or weakening the fiber and have not been shown to completely eliminate the problem of interface reinforcement.

A second alternative is increasing the distance that the crack would have to travel by roughening the surface of the fiber. Small fibers exhibit high strength because of the very fact that they have few defects, roughening a fiber to increase the interlocking with the matrix directly reduces the tensile properties of the fiber. Most roughening processes are chemical or electrochemical and combine the effects of roughening with chemical functionalization. Chemical and electrochemical functionalization processes are generally able to intercalate and etch graphite and aramid fibers that open up pores and initiate defects in the fibers. While roughening is undoubtedly beneficial to the interfacial strength of a composite, it may require unacceptable tradeoffs. Roughening of fibers simply does not present a universal solution to the interface problem so alternatives must be pursued.

The third broad category of interface enhancement is whiskerization. Whiskerization reinforces the interphase region, the volume near the interface, with an array of aligned, acicular whiskers or wires. The localized reinforcement provides a high volume fraction of strong ceramic wires, typically on the nanoscale due to fiber diameter, in the region where it is most effective. The reinforcement, because of the cylindrical fibers, is inherently graded as progressed gradually from a high fraction of whiskers and low fraction of matrix to a high fraction of matrix and low fraction of

whiskers. This gradient of properties replicates natural systems and reduces stress concentrations to improve overall strength and toughness. Whiskerization offers the same advantages as roughening by increasing the distance that the crack needs to travel. Whiskerization can avoid the defects induced in roughening with the selection of the correct whisker material. If whiskers are well adhered to the surface of the fiber, whiskerization offers perhaps the most promising route to interface enhancement by reinforcing the interphase and fundamentally reducing the stress concentration.

This work has explored the development of a new material for the whiskerization of structural fibers, aligned ZnO nanowire arrays. ZnO nanowire arrays can be processed at low temperatures (less than 150 °C) from simple solution based chemistry and offer the advantage of whiskerization without causing additional defects to fiber that can reduce fiber strength. ZnO shows strong interactions with many organic molecules that can be leveraged to create a strong adhesion of the ZnO nanowires to the surface of the fiber. Finally, the well documented growth procedure can be easily manipulated and adjusted to create the desired reinforcement morphology. This will enable ZnO nanowires to act as a sizing layer on future structural fibers and enhance the overall properties of composite materials.

5.1 Brief Summary of Dissertation and Results

This work explores the development of a novel ZnO whiskerization process for structural composite reinforcement. The low processing temperatures and solution based chemistry of ZnO nanowire growth processes enables this method to enhance structural fiber interfaces without the typical tradeoffs in the axial properties of the fibers. The study begins with an analysis of two important structural fibers, aramid and carbon. A novel aramid fiber functionalization scheme is developed to provide a surface

chemistry that can interact with the ZnO nanowires to enhance adhesion of the ZnO to the surface of the aramid fibers. The reaction begins by hydrolyzing the amide link of some of the surface chains of the polymer to create a carboxylate salt and a primary amine. The reaction is followed by an ion exchange wash in hydrochloric acid, which strips the metal ions and replaces them with protons to create carboxylic acid groups on the surface of the fiber. The reaction is validated using both XPS and FTIR to show a surface coverage of carboxylic acid groups as a result of the functionalization procedure.

Carbon fiber is very different from the polymeric aramid fibers and thus requires different reactions to create the desired surface chemistry. Two novel functionalization treatments are developed. First, a new defect grafting procedure is investigated using isopropylidene malonate. Isopropylidene malonate, commonly Meldrum's acid, is susceptible to ring opening by hydroxyl groups to graft carboxyl terminated malonic esters to the surface of the fiber. Hydroxyl groups exist naturally on the surface of carbon fiber and are utilized to effectively purify the hydroxyl groups and create carboxylic acid on the surface. The reaction conditions are optimized for solvent, temperature and time with the optimal solvent toluene at full reflux for 30 minutes. XPS is used to validate the surface coverage of carboxylic acid groups and the reaction mechanism, noting that temperatures in excess of the boiling point of toluene are detrimental to the reaction and will likely lead to decomposition of the reactants. This process yields an effective surface coverage of carboxylic acid of 9.2%. A second process is also developed to produce the desired carboxylic acid groups. Selective oxidation, occasionally termed up-conversion, relies on the preference of permanganate

ions to oxidize C – O bonds instead of C – C bonds. This selectivity enables existing defects to be oxidized to carboxylic acid groups while the structural backbone of the fiber is maintained. Selective oxidation does not etch the fiber surface or create structural defects, which minimizes the impact on the fiber tensile strength. Surface chemistry is measured with XPS to yield maximum carboxylic acid coverage of 8.7%. Two other functionalization techniques for carbon fiber were developed for later use in assessing the interfacial adhesion mechanism. A reduction technique was developed to remove carboxylic acid by refluxing in hydrazine. Validated by XPS, this process reduced the carboxylic acid surface coverage to 2.9% without changing the topography of the sample or etching the fibers. Finally, a broader oxidation is also implemented as a part of this work. A nitric acid reflux is used to oxidize the surface of the fibers and create a variety of oxygen functional groups, not specifically carboxylic acid. The nitric acid oxidation, measured with XPS, shows an increase in the total oxygen content of the fibers of 48%, with no real preference for carboxylic acid over other oxygen functional groups.

With the surface chemistry providing suitable adhesion of the ZnO, this work progresses to describe the process and factors affecting the growth of ZnO nanowires on structural fibers. The chemical reactions as well as several areas in which the process is disrupted are detailed. The growth of ZnO nanowires on high surface area, highly curved structural fibers is partially described in the literature. There remain several processing techniques that improve yield and understanding of the nanowire growth. This work describes the growth in detail, both mechanism and failure modes to help disseminate knowledge and aid in development of future ZnO nanowire growth

systems. The growth of ZnO nanowires follows a two-step process, beginning first with the synthesis of ZnO nanoparticles that will be deposited as a seed layer. The size of the seeds as grown has a direct impact on the diameter of the nanowires realized on the fiber. This work indicates that the seeds coalesce into a solid, polycrystalline film with randomly oriented grains. ZnO nanowires gradually precipitate from the preferred crystal facets to form nanowires, growing radially outward from the fiber which forces alignment through competition. The growth for both high temperature graphite fibers and low temperature polymers, such as aramids, are demonstrated. There is potential to extended to other polymeric or even natural fibers.

Following the development and validation of the functionalization procedures, the fibers were evaluated for mechanical properties and interface strength. The motivation of this work is to avoid deleterious effects of whiskerization and functionalization processes on fiber strength. The tensile strength of the fibers used in this work was evaluated before and after functionalization, as well as after ZnO nanowire growth. Tensile tests of the fibers followed ASTM C1557 and the data was presented as the confidence interval estimates on the Weibull scale parameter. The functionalization process can damage the tensile properties of aramid fibers; however the process temperature was reduced to room temperature and the fibers strength was maintained after functionalization. A slight increase in the tensile strength of the fibers was observed with the addition of a ceramic seed layer on the fiber, which contributed an additional layer of protection to the fiber. Carbon fibers did not show reductions in tensile strength following defect grafting or selective oxidation. Both the shape and scale parameters of the Weibull fits were insignificantly different from the fits of the

original fibers. The reduction process was shown to have little effect on the tensile properties of the fibers as well, owed to the inability of hydrazine to etch or intercalate graphite. The effects of the oxidation process on tensile properties were also characterized.

This work also analyzes the resulting composites created with a ZnO nanowire interphase. First, single fiber composites are analyzed for the quality (presence of defects) of the ZnO – fiber interface. SEM and TEM studies illustrate the interface has no defects and the polycrystalline seed layer forms a nearly indistinguishable interface with the graphite fiber. There are no voids or defects present at the interface caused by incomplete deposition of the seed layer, as confirmed by multiple cross section studies. Nanowire wetting is observed next through similar cross section studies. In the polymer matrix wetting is observed down to the roots of the nanowires. The high surface area and favorable surface energy enables the nanowires to wick the liquid polymer matrix and form a defect free, three phase composite. With the single fiber composite verified, detailed processing information was presented on the selection and validation of processing techniques for the hierarchical fibers. The hierarchical fibers created were shown to be suitable for standard wet layup processing techniques and are expected to be suitable for reel to reel processing on existing resin preimpregnation systems. The volume fraction of the test composite was measured to be 50% and nearly identical to the 49% bare fiber composite volume fraction. The volume closely aligned with standard polymer matrix composites, demonstrating that the addition of the nanowires does not impinge on the processing or achievable fiber volume fractions.

Interface testing on aramid fibers was first performed qualitatively by examining the fibers during routine laboratory handling. While the nanowires readily debonded from the aramid fibers during routine handling without the functionalization the nanowire arrays were much more tolerant and did not show the same debonding behavior that was observed on the as received fibers. Single fiber interface testing was quantitatively performed using single fiber fragmentation. The aramid fibers showed an improvement of 51% with the combination of both proper functionalization and nanowire interphase. Either enhancement individually, the functionalization alone or the nanowire interphase alone, did not increase the interfacial shear strength. This demonstrates the efficacy of a ZnO nanowire interphase to enhance aramid fiber composites.

Interface testing on carbon fibers began with single fiber fragmentation testing. Fibers with ZnO nanowires as received showed a single fiber interface improvement of over 100%. Great interest exists for the extension of a nanowire interphase to full scale samples, both as a demonstration of technology as well as an opportunity for further understanding of the mechanics of the system. A ZnO nanowire interphase was grown on a sufficient number of fibers to lay up full scale, v-notch shear composite specimens. The composites with a ZnO nanowire interphase exhibited 37% higher shear modulus and 38% higher shear strength because the nanowire interphase improved load transfer and reduced the stress concentration at the interface.

Following this promising result, an investigation to determine the mechanism of adhesion was begun. The various functionalization procedures were all used to identify the active chemical group in the adhesion of the nanowires to the surface of the fiber. The aramid fibers with a ZnO nanowire interphase only showed improvement in the

interfacial properties when a carboxyl surface functionalization was applied. Carbon fibers did not show the same sensitivity. Four fibers were tested for interfacial shear strength: IM8 fibers as received, hydrazine reduced fibers with fewer carboxylic acid groups, defect grafted fibers with more carboxylic acid groups and selectively oxidized carbon fibers with more carboxylic acid groups. Both the defect grafting and selective oxidation procedures maintain largely the same amount of total oxygen as the IM8 fiber as received as both fibers simply convert existing functional groups to carboxylic acid. The hydrazine reduced fibers have oxygen universally removed or reduced the functional groups. The interfacial shear strength of the IM8, selectively oxidized and defect grafted fibers was measured to be the same; however the hydrazine reduced fibers have a weaker interface. This result implies that the carboxylic acid functionalization procedures, while important to aramid fibers, are not dictating the adhesion of the ZnO nanowire interphase. Oxygen functional groups were found to be important though as the removal of oxygen functional groups caused a reduction in the measured interfacial shear strength.

The hypothesized mechanism of adhesion of ZnO to structural fibers, carboxylic acid interaction, was proven incomplete in its description through the functionalization techniques created for carbon fibers. The removal of oxygen functional groups more generally, though, did have an impact. To assess this possibility, nitric acid oxidation was employed to create a mixture of various oxygen functional groups through the initiation of defects and oxidation of carbon – carbon bonds. Because there is a risk of roughness changes during the oxidation, the same hydrazine reduction was applied after reduction to remove the additional oxygen groups creating a control test to identify

the adhesive mechanism. The single fiber fragmentation results show that the interface of the nitric acid oxidized fibers is stronger than that of the hydrazine reduced fibers. This result, in conjunction with the carboxylic acid testing, confirms that the adhesive mechanism is extends to a wide variety of unspecified oxygen groups, not carboxylic acid specifically. Combining all of the interface test data enabled a clear picture to emerge about the mechanism of adhesion for the ZnO nanowire arrays. Ketone groups were shown to have the largest impact on the interface strength and thus control the adhesion of the ZnO nanowires. The is the first presentation of both the methodology for the systematic study of interfaces, as well as the result that ketone groups have the strongest effect on interfacial shear strength.

This result was also rationalized with the aramid fiber results. The creation of carboxylic acid groups on aramid fibers requires disrupting the strong hydrogen bonding that occurs between parallel polymer chains. Interrupting this bonding causes the carboxylic acid groups to become available for interaction with ZnO and enables the adhesion of the interphase. The adhesive mechanism of a ZnO nanowire interphase was determined to be the strong interaction between ZnO and ketone functional groups.

5.2 Contributions

The current generation of fiber reinforced polymers is limited by the strength of the interface between the fibers and the matrix. Several techniques to improve this interface exist, namely, chemical functionalization, fiber surface roughening and whiskerization. The development of whiskerization as a commercial technique for improving interface strength has been limited by processing issues. Existing whiskerization techniques rely upon high temperature processes that are difficult to set up, expensive to operate and can degrade the strength of the fibers. Whiskerization

does offer a superior benefit in reducing the stress concentration and affords the greatest opportunity for improvement if the processing challenges can be overcome. This work contributes a new nanowire interphase that is processed at low temperatures and offers a new avenue toward the implementation of whiskerization for advanced composite materials. The scientific contribution extends beyond the simple evaluation of this interphase. This work provides a deep and thorough probe of the mechanisms of adhesion to provide an understanding to the literature that will enable this and other interphases to be applied to dozens of different fibers.

The major contribution of this work is the development of the ZnO nanowire interphase processed at low temperatures in aqueous solutions. The low temperature processing enables this to be the first demonstration of structural whiskerization on aramid fibers as aramids cannot withstand the temperatures required for typical whisker deposition. This contribution extends beyond aramid fibers as other low temperature polymers could employ the exact same processes, possibly transforming high performance polymer fiber composites. The demonstration of the structural enhancement provided by a ZnO nanowire interphase in carbon fiber composites is significant because the whiskerization does not require tradeoffs in fiber properties that some high temperatures techniques tolerate. This demonstrates the low temperature, solution based growth method as suitable for high surface area structural fibers. Accommodations must be made to ensure that the fibers are suitably spread to enable growth. The demonstration of the ZnO nanowire interphase was accompanied by evaluation of the tensile properties as well, providing concrete proof that the tensile properties are unaffected by the presence of the ZnO interphase.

Another major contribution of this work is the demonstration of the efficacy of this technique with a full scale lamina. Most of the whiskerization techniques previously demonstrated focus on either single fiber testing or interlaminar short beam testing. This work shows that full scale specimens, hard to produce on a laboratory scale, are within reach and the property enhancements do extend to real composites. This reduces the risk of adopting the technology by showing scale up to be plausible, with a good chance of adding value to the final product. Producing full scale processes required also verifying that the nanowire enhanced composites were compatible with existing resins and processing technology, possibly a difficult hurdle to overcome. Nanoscale fillers can vastly increase the viscosity of a polymer resin which can make some processing methods inappropriate and necesitate vast reworking of industrial processes. This work has shown that a typical thermoset epoxy resin can easily wet the nanowire arrays to form a consolidated, high performance composite consistent in volume fraction with alternatives. Concerns that the nanowires collapse or are damaged during the routine fiber – fiber sliding, resin flow and compression during composite fabrication have also be addressed in this work. Analysis of the fracture surfaces of the composites after testing assuaged concerns that the nanowires did not maintain position and alignment after fabrication.

In addition to the interphase contributions, a part of this work analyzed fiber surface chemistry and developed new functionalization procedures. This work contributes a new functionalization procedure for aramid fibers that produces carboxylic acid without reducing the tensile strength. The functionalization began from existing hydrolysis, an acid ion exchange wash was added to eliminate deleterious Na^+ ions

from the fibers. Although carboxylic acid is employed for the adhesion of ZnO in this work, carboxylic acid is a versatile and useful functional group that can be further converted into a plethora of other chemical groups. This functionalization could easily serve as a starting point for other grafting procedures to use aramid fibers as a scaffold. This functionalization process desired to minimize the impact on the tensile strength and the measured strength was shown to be maintained throughout. The contribution of a mild, carboxylic acid functionalization to the aramid fiber literature represents a significant advance.

The functionalization of carbon fibers developed in this work is another area of substantial contribution. The use of Meldrum's acid in materials science is limited at best, with most of the literature related to macromolecular synthesis for biochemical applications. The demonstration of Meldrum's acid as an effective surface functionalization tool bridges traditional organic chemistry with the applications of materials engineering. One of the chief advantages of using Meldrum's acid for defect grafting is that the procedure was shown to have no measureable impact on material properties simply increasing the carboxylic acid content of the fiber without tradeoffs in surface area, tensile strength or surface modulus. The use of Meldrum's acid in materials science applications is a notable contribution in that it offers a rapid, selective and simple reaction by which solids can be functionalized without requiring the specialized insight of a formally trained organic chemist. Beyond defect grafting, the contribution of a selective oxidation process stands to benefit the carbon fiber community as well. The demonstration of an additional process for the creation of carboxylic acid without cost to the tensile properties through a new chemical reaction

enables chemists more options for creating a chosen surface chemistry. The selective oxidation reaction preferentially oxidizes existing functional groups instead of carbon – carbon bonds, preserving the integrity of the fiber and modifying the surface. These functionalization procedures could be used to graft nanoparticles, molecules or other materials to the surface of the carbon fibers to maintain the fiber properties and this work constitutes a significant contribution by laying the groundwork for these applications.

While the previous paragraphs addressed some practical engineering contributions of this work, a complete dissertation must include fundamental scientific contributions and provide new insight to observed phenomena. The scientific contribution of this work lies in the identification of the adhesive mechanism of the ZnO interphase to the structural fiber. This work identifies that a ZnO nanowire interphase can strongly interact with ketone functional groups to produce a strong mechanical interface. This was determined by applying the previously developed functionalization techniques and measuring the interfacial shear strength to determine which functional groups had the largest impact. This has much broader scientific contributions because the development of other materials as an interphase will be able to follow the same methodology. SiC whiskers and carbon nanotubes often grow using the fiber itself as a source of carbon, which not only strongly anchors the fiber, but also initiates a defect site that can compromise the fiber strength. ZnO nanowires are deposited from a solution growth process and do not burrow into the fiber to form a strong anchor. This difference is the source of one of the chief advantages of ZnO nanowires; however it introduces a significant question about the strength of the adhesion of the nanowires to

the fiber surface. This work has answered those questions and provided a framework for the development of nanowire interphases for structural enhancement. This work has demonstrated that the proper control over surface functional groups controls the interfacial shear strength and other ceramic nanowires could follow the same methods.

5.3 Recommendations for Future Work

While this work provides several key findings in the development of a ZnO nanowire interphase, it is by no means complete. This development focuses on proving the efficacy of the nanowire interphase for structural enhancement and identifying the adhesive mechanism. The first recommendation for future work is to create a continuous ZnO nanowire deposition system, proving that this growth is compatible with existing reel to reel processing. A new sizing layer or interphase is only commercially viable if it can be consistently and uniformly applied to structural fibers on a scale comparable to current fiber production. This work has shown that there is no fundamental reason why this is not possible, it must be proven if a ZnO nanowire interphase is to be widely adopted. It is also expected that reel to reel processing will result in growth on every fiber, avoiding the issues of the compacted tow that plagues small scale batch growth. This is expected to greatly enhance the resulting composites on the lamina scale, possibly exceeding the 38% improvement reported here.

The ZnO growth process is compatible with polymeric fibers that have previously been outside the realm of traditional whiskerization processes. Synthetic fibers, specifically ultra-high molecular weight polyethylene, can exhibit extraordinary mechanical properties with very poor interfaces. ZnO nanowires could enhance these materials and create new opportunities for composites with the enhanced shear and off axis properties for these incredible materials. As with the aramid fibers, appropriate

functionalization procedures must be developed concurrently to ensure that the fiber to ZnO interface is strong. Plasma functionalization offers a possible solution. It is also suggested that this work couple together with a modeling effort to enable both verification of the findings as well as provide guidance for future developments.

This work analyzed ZnO nanowires as a structural interphase but this is only the beginning of the uses of ZnO nanowires. As a wide band gap semiconductor, ZnO offers enormous potential in a variety of functional applications such as solar energy harvesting, mechanical energy harvesting or any number of different sensors. The development of future systems will not afford designers the luxury of structural and functional systems. To achieve the extraordinary performance goals of the next 100 years, engineering systems will need to adopt multifunctional materials. The addition of ZnO nanowires creates a plethora of opportunities to take advantage of the new functionality afforded by a semiconductive ceramic inside of a composite material. Future work should attempt to identify and demonstrate functional applications of the ZnO interphase to assist in overall system development.

LIST OF REFERENCES

[1] Chawla KK1. Composite materials : science and engineering / Krishan K. Chawla. New York: Springer-Verlag, 1987.

[2] Warren CD. Carbon Fiber Composites Technology Development. Workshop on Low Cost Carbon Fiber Composites for Energy Applications: Oak Ridge National Laboratories, 2009.

[3] U.S. Geological Survey. Aluminum. In: McNutt MK, editor. Mineral Commodity Summaries 2011. Reston, VA: U.S. Geological Survey, 2011.

[4] Hyer MW. Stress analysis of fiber-reinforced composite materials . Boston, Mass.: WCB McGraw-Hill, 1998.

[5] Gibson RF. Principles of composite material mechanics / Ronald F. Gibson. Boca Raton: CRC Press, 2007.

[6] Hashin Z. Analysis of Composite Materials---A Survey. J Appl Mech 1983;50(3):481-505.

[7] Hergenrother PM(, Stenzenberger HD(, Wilson D(. Polyimides / editors, D. Wilson, H.D. Stenzenberger, P.M.Hergenrother. Glasgow : New York: Blackie ; Chapman and Hall, 1990.

[8] Ghosh L, Kinoshita H, Ohmae N. Degradation on a mechanical property of high-modulus aramid fiber due to hyperthermal atomic oxygen beam exposures. Composites Sci Technol 2007;67(7-8):1611-1616.

[9] Milewski JV, Shyne JJ. Method of Treating the Surface of a Filament. 1967(US003580731).

[10] Rand B, Robinson R. Surface characteristics of carbon fibres from PAN. Carbon 1977;15(4):257-263.

[11] Waltersson K. ESCA studies of carbon fibres: part I—The chemical composition of a carbon fibre subsurface. Fibre Science and Technology 1982;17(4):289-302.

[12] Waltersson K. ESCA studies of carbon fibres: Part II—Surface reactions of carbon fibres with epoxides. Composites Sci Technol 1985;22(3):223-239.

[13] Waltersson K. ESCA studies of carbon fibres: Part III—Surface reactions of carbon fibres with amines. Composites Sci Technol 1985;23(4):303-321.

[14] Gardner SD, Singamsetty CSK, Wu Z, Pittman Jr. CU. XPS/ISS Investigation of Carbon Fibers Sequentially Exposed to Nitric Acid and Sodium Hydroxide. Surf Interface Anal 1996;24(5):311-320.

[15] Gardner SD, Singamsetty CSK, Wu Z, Pittman Jr. CU. XPS/ISS Investigation of Carbon Fibers Sequentially Exposed to Nitric Acid and Sodium Hydroxide. Surf Interface Anal 1996;24(5):311-320.

[16] Pittman CU, He G-, Wu B, Gardner SD. Chemical modification of carbon fiber surfaces by nitric acid oxidation followed by reaction with tetraethylenepentamine. Carbon 1997;35(3):317-331.

[17] Bruice PY. Organic chemistry . Upper Saddle River, N.J.: Pearson Education, 2004.

[18] Zhang G, Sun S, Yang D, Dodelet J, Sacher E. The surface analytical characterization of carbon fibers functionalized by H2SO4/HNO3 treatment. Carbon 2008;46(2):196-205.

[19] Donnet JB. Carbon fibers: Marcel Dekker, 1998.

[20] Proctor A, Sherwood PMA. X-ray photoelectron spectroscopic studies of carbon fibre surfaces—II: The effect of electrochemical treatment. Carbon 1983;21(1):53-59.

[21] Hossain MS, Tryk D, Yeager E. The electrochemistry of graphite and modified graphite surfaces: the reduction of O2. Electrochim Acta 1989;34(12):1733-1737.

[22] Proctor A, Sherwood PMA. X-ray photoelectron spectroscopic studies of carbon fibre surfaces—II: The effect of electrochemical treatment. Carbon 1983;21(1):53-59.

[23] Kozlowski C, Sherwood PMA. X-ray photoelectron spectroscopic studies of carbon-fibre surfaces. Part 4.-The effect of electrochemical treatment in nitric acid. J Chem Soc , Faraday Trans 1 1984;80(8):2099-2107.

[24] Kozlowski C, Sherwood PMA. X-ray photoelectron-spectroscopic studies of carbon-fibre surfaces. Part 5.-The effect of pH on surface oxidation. J Chem Soc , Faraday Trans 1 1985;81(11):2745-2756.

[25] Harvey J, Kozlowski C, SHERWOOD PMA. X-ray photoelectron spectroscopic studies of carbon fibre surfaces. J Mater Sci 1987;22(5):1585-1596.

[26] Wang Y, Zhang F, Sherwood PMA. X-ray Photoelectron Spectroscopic Study of Carbon Fiber Surfaces. 23. Interfacial Interactions between Polyvinyl Alcohol and Carbon Fibers Electrochemically Oxidized in Nitric Acid Solution. Chemistry of Materials 1999;11(9):2573-2583.

[27] Viswanathan H, Wang Y, Audi AA, Allen PJ, Sherwood PMA. X-ray Photoelectron Spectroscopic Studies of Carbon Fiber Surfaces. 24. Interfacial Interactions between Polyimide Resin and Electrochemically Oxidized PAN-Based Carbon Fibers. Chemistry of Materials 2001;13(5):1647-1655.

[28] Wang Y, Zhang F, Sherwood PMA. X-ray Photoelectron Spectroscopic Studies of Carbon Fiber Surfaces. 25. Interfacial Interactions between PEKK Polymer and Carbon Fibers Electrochemically Oxidized in Nitric Acid and Degradation in a Saline Solution. Chemistry of Materials 2001;13(3):832-841.

[29] C. J. The chemistry of carbon fibre surfaces and its effect on interfacial phenomena in fibre/epoxy composites. Composites Sci Technol 1991;42(1-3):275-298.

[30] Wang Y, Zhang F, Sherwood PMA. X-ray Photoelectron Spectroscopic Study of Carbon Fiber Surfaces. 23. Interfacial Interactions between Polyvinyl Alcohol and Carbon Fibers Electrochemically Oxidized in Nitric Acid Solution. Chemistry of Materials 1999;11(9):2573-2583.

[31] Lee WH, Lee JG, Reucroft PJ. XPS study of carbon fiber surfaces treated by thermal oxidation in a gas mixture of O2/(O2+N2). Appl Surf Sci 2001;171(1-2):136-142.

[32] Proctor A, Sherwood PMA. X-ray photoelectron spectroscopic studies of carbon fibre surfaces. III?Industrially treated fibres and the effect of heat and exposure to oxygen. Surf Interface Anal 1982;4(5):212-219.

[33] Zielke U, Hüttinger KJ, Hoffman WP. Surface-oxidized carbon fibers: I. Surface structure and chemistry. Carbon 1996;34(8):983-998.

[34] Zielke U, Hüttinger KJ, Hoffman WP. Surface-oxidized carbon fibers: IV. Interaction with high-temperature thermoplastics. Carbon 1996;34(8):1015-1026.

[35] Li J. Interfacial studies on the ozone and air-oxidation-modified carbon fiber reinforced PEEK composites. Surf Interface Anal 2009;41(4):310-315.

[36] Tsubokawa N. Preparation and Properties of Polymer-grafted Carbon Nanotubes and Nanofibers. Polym J 2005;37(9):637-655.

[37] Chen J, Wei G, Maekawa Y, Yoshida M, Tsubokawa N. Grafting of poly(ethylene-block-ethylene oxide) onto a vapor grown carbon fiber surface by γ-ray radiation grafting. Polymer 2003;44(11):3201-3207.

[38] Hayashi S, Handa S, Tsubokawa N. Introduction of peroxide groups onto carbon black surface by radical trapping and radical graft polymerization of vinyl monomers initiated by the surface peroxide groups. Journal of Polymer Science Part A: Polymer Chemistry 1996;34(8):1589-1595.

[39] Hayashi S, Naitoh A, Machida S, Okazaki M, Maruyama K, Tsubokawa N. Grafting of polymers onto a carbon black surface by the trapping of polymer radicals. Applied Organometallic Chemistry 1998;12(10-11):743-748.

[40] Hayashi S, Tsubokawa N. Grafting of Polymers Having Pendant Peroxycarbonate Groups Onto Carbon Black and Postpolymerization of Vinyl Monomers. Journal of Macromolecular Science, Part A 1998;35(11):1781-1796.

[41] Liu T, Jia S, Kowalewski T, Matyjaszewski K, Casado-Portilla R, Belmont J. Grafting Poly(n-butyl acrylate) from a Functionalized Carbon Black Surface by Atom Transfer Radical Polymerization†. Langmuir 2003;19(16):6342-6345.

[42] Delamar M, Désarmot G, Fagebaume O, Hitmi R, Pinsonc J, Savéant J-. Modification of carbon fiber surfaces by electrochemical reduction of aryl diazonium salts: Application to carbon epoxy composites. Carbon 1997;35(6):801-807.

[43] Kariuki JK, McDermott MT. Nucleation and Growth of Functionalized Aryl Films on Graphite Electrodes. Langmuir 1999;15(19):6534-6540.

[44] Chand S. Review Carbon fibers for composites. J Mater Sci 2000;35(6):1303-1313.

[45] Bahr JL, Yang J, Kosynkin DV, Bronikowski MJ, Smalley RE, Tour JM. Functionalization of Carbon Nanotubes by Electrochemical Reduction of Aryl Diazonium Salts: A Bucky Paper Electrode. J Am Chem Soc 2001;123(27):6536-6542.

[46] Brooksby PA, Downard AJ. Electrochemical and Atomic Force Microscopy Study of Carbon Surface Modification via Diazonium Reduction in Aqueous and Acetonitrile Solutions. Langmuir 2004;20(12):5038-5045.

[47] Pinson J, Podvorica F. Attachment of organic layers to conductive or semiconductive surfaces by reduction of diazonium salts. Chem Soc Rev 2005;34(5):429-439.

[48] Belanger D, Pinson J. Electrografting: a powerful method for surface modification. Chem Soc Rev 2011;40(7):3995-4048.

[49] Lin J. Effect of surface modification by bromination and metalation on Kevlar fibre-epoxy adhesion. European Polymer Journal 2002;38(1):79-86.

[50] Takayanagi M, Kajiyama T, Katayose T. Surface-modified kevlar fiber-reinforced polyethylene and ionomer. J Appl Polym Sci 1982;27(10):3903-3917.

[51] Liu T, Zheng Y, Hu J. Surface modification of Aramid fibers with new chemical method for improving interfacial bonding strength with epoxy resin. J Appl Polym Sci 2010;118(5):2541-2552.

[52] Park S, Seo M, Ma T, Lee D. Effect of Chemical Treatment of Kevlar Fibers on Mechanical Interfacial Properties of Composites. J Colloid Interface Sci 2002;252(1):249-255.

[53] Kim E, An S, Kim H. Graft copolymerization of ?-Caprolactam onto Kevlar-49 fiber surface and properties of grafted Kevlar fiber reinforced composite. J Appl Polym Sci 1997;65(1):99-107.

[54] Liu T, Zheng Y, Hu J. Surface modification of Aramid fibers with new chemical method for improving interfacial bonding strength with epoxy resin. J Appl Polym Sci 2010;118(5):2541-2552.

[55] Ho KKC, Lee AF, Lamoriniere S, Bismarck A. Continuous atmospheric plasma fluorination of carbon fibres. Composites Part A: Applied Science and Manufacturing 2008;39(2):364-373.

[56] Wolf H, Pajkic Z, Gerdes T, Willert-Porada M. Carbon–fiber–silicon-nanocomposites for lithium-ion battery anodes by microwave plasma chemical vapor deposition. J Power Sources 2009;190(1):157-161.

[57] Wen H, Yang K, Ou K, Wu W, Chou C, Luo R, Chang Y. Effects of ammonia plasma treatment on the surface characteristics of carbon fibers. Surface and Coatings Technology 2006;200(10):3166-3169.

[58] Zhang X, Huang Y, Wang T. Surface analysis of plasma grafted carbon fiber. Appl Surf Sci 2006;253(5):2885-2892.

[59] Montes-Morán MA, Gauthier W, Martínez-Alonso A, Tascón JMD. Mechanical properties of high-strength carbon fibres. Validation of an end-effect model for describing experimental data. Carbon 2004;42(7):1275-1278.

[60] Boudou JP, Paredes JI, Cuesta A, Martínez-Alonso A, Tascón JMD. Oxygen plasma modification of pitch-based isotropic carbon fibres. Carbon 2003;41(1):41-56.

[61] Montes-Morán MA, Young RJ. Raman spectroscopy study of HM carbon fibres: effect of plasma treatment on the interfacial properties of single fibre/epoxy composites: Part I: Fibre characterisation. Carbon 2002;40(6):845-855.

[62] Montes-Morán MA, Young RJ. Raman spectroscopy study of high-modulus carbon fibres: effect of plasma-treatment on the interfacial properties of single-fibre–epoxy composites: Part II: Characterisation of the fibre–matrix interface. Carbon 2002;40(6):857-875.

[63] Montes-Morán MA, Martínez-Alonso A, Tascón JMD, Paiva MC, Bernardo CA. Effects of plasma oxidation on the surface and interfacial properties of carbon fibres/polycarbonate composites. Carbon 2001;39(7):1057-1068.

[64] Montes-Morán MA, Martínez-Alonso A, Tascón JMD, Young RJ. Effects of plasma oxidation on the surface and interfacial properties of ultra-high modulus carbon fibres. Composites Part A: Applied Science and Manufacturing 2001;32(3-4):361-371.

[65] Jang J, Yang H. The effect of surface treatment on the performance improvement of carbon fiber/polybenzoxazine composites. J Mater Sci 2000;35(9):2297-2303.

[66] Pittman Jr CU, Jiang W, He G-, Gardner SD. Oxygen plasma and isobutylene plasma treatments of carbon fibers: Determination of surface functionality and effects on composite properties. Carbon 1998;36(1-2):25-37.

[67] Paiva MC, Bernardo CA, Nardin M. Mechanical, surface and interfacial characterisation of pitch and PAN-based carbon fibres. Carbon 2000;38(9):1323-1337.

[68] Smiley RJ, Delgass WN. AFM, SEM and XPS characterization of PAN-based carbon fibres etched in oxygen plasmas. J Mater Sci 1993;28(13):3601-3611.

[69] Yuan LY, Shyu SS, Lai JY. Plasma surface treatments of carbon fibers. Part 2: Interfacial adhesion with poly(phenylene sulfide). Composites Sci Technol 1992;45(1):9-16.

[70] Kowbel W, Shan CH. The mechanism of fiber—matrix interactions in carbon—carbon composites. Carbon 1990;28(2-3):287-299.

[71] Park S, Kim B. Roles of acidic functional groups of carbon fiber surfaces in enhancing interfacial adhesion behavior. Materials Science and Engineering: A 2005;408(1-2):269-273.

[72] Li J. Interfacial studies on the O3 modified carbon fiber-reinforced polyamide 6 composites. Appl Surf Sci 2008;255(5, Part 2):2822-2824.

[73] Li J. Interfacial studies on the ozone and air-oxidation-modified carbon fiber reinforced PEEK composites. Surf Interface Anal 2009;41(4):310-315.

[74] Tang L, Kardos JL. A review of methods for improving the interfacial adhesion between carbon fiber and polymer matrix. Polymer Composites 1997;18(1):100-113.

[75] Dilsiz N. Plasma surface modification of carbon fibers: a review. Journal of Adhesion Science & Technology 2000;14(7):975-987.

[76] Li R, Ye L, Mai Y. Application of plasma technologies in fibre-reinforced polymer composites: a review of recent developments. Composites Part A: Applied Science and Manufacturing 1997;28(1):73-86.

[77] Jones C, Sammann E. The effect of low power plasmas on carbon fibre surfaces. Carbon 1990;28(4):509-514.

[78] Jones C, Sammann E. The effect of low power plasmas on carbon fibre surfaces: A comparison between low and high modulus PAN based fibres with pitch based carbon fibres. Carbon 1990;28(4):515-519.

[79] Farrow GJ, Jones C. The Effect of Low Power Nitrogen Plasma Treatment of Carbon Fibres on the Interfacial Shear Strength of Carbon Fibre/Epoxy Composites. The Journal of Adhesion 1994;45(1-4):29-42.

[80] Bor Z. J. Control of interfacial adhesion in continuous carbon and kevlar fiber reinforced polymer composites. Composites Sci Technol 1992;44(4):333-349.

[81] Yuan LY, Shyu SS, Lai JY. Plasma surface treatments on carbon fibers. II. Mechanical property and interfacial shear strength. J Appl Polym Sci 1991;42(9):2525-2534.

[82] Küpper K, Schwartz P. Modification of the fiber-matrix interface of p-aramid fibers using gas plasmas J Adhes Sci Technol 1991;5(2):165 <last_page> 176.

[83] Brown J, Chappell P, Mathys Z. Plasma surface modification of advanced organic fibres. J Mater Sci 1991;26(15):4172-4178.

[84] Sheu GS, Shyu SS. Surface properties and interfacial adhesion studies of aramid fibres modified by gas plasmas. Composites Sci Technol 1994;52(4):489-497.

[85] Kalantar J, Drzal LT. The bonding mechanism of aramid fibres to epoxy matrices. J Mater Sci 1990;25(10):4194-4202.

[86] Sheu GS, Shyu SS. Surface modification of Kevlar 149 fibers by gas plasma treatment. J Adhes Sci Technol 1994;8(5):531-542.

[87] Sheu GS, Shyu SS. Surface modification of Kevlar 149 fibers by gas plasma treatment. Part II. Improved interfacial adhesion to epoxy resin. J Adhes Sci Technol 1994;8(9):1027-1042.

[88] Wu SR, Sheu GS, Shyu SS. Kevlar fiber?epoxy adhesion and its effect on composite mechanical and fracture properties by plasma and chemical treatment. J Appl Polym Sci 1996;62(9):1347-1360.

[89] Brown J, Chappell P, Mathys Z. Plasma surface modification of advanced organic fibres. J Mater Sci 1991;26(15):4172-4178.

[90] El Asloun M, Donnet J, Guilpain G, Nardin M, Schultz J. On the estimation of the tensile strength of carbon fibres at short lengths. J Mater Sci 1989;24(10):3504-3510.

[91] Zhdan PA, Bors M, Castle JE. In situ scanning force microscopy (SFM) study of the electrochemical activation of carbon fibres. Composites Sci Technol 1998;58(3-4):559-570.

[92] Fitzer E, Geigl K-, Hüttner W, Weiss R. Chemical interactions between the carbon fibre surface and epoxy resins. Carbon 1980;18(6):389-393.

[93] Hammer GE, Drzal LT. Graphite fiber surface analysis by X-ray photoelectron spectroscopy and polar/dispersive free energy analysis. Applications of Surface Science 1980;4(3-4):340-355.

[94] J.D.H. H. The carbon fibre/epoxy interface—A review. Composites Sci Technol 1991;41(1):13-45.

[95] Krekel G, Zielke UJ, Hüttinger KJ, Hoffman WP. The relevance of the surface structure and surface chemistry of carbon fibres in their adhesion to high temperature thermoplastics. J Mater Sci 1994;29(15):3984-3992.

[96] Fitzer E, Weiss R. Effect of surface treatment and sizing of c-fibres on the mechanical properties of cfr thermosetting and thermoplastic polymers. Carbon 1987;25(4):455-467.

[97] Farrow GJ, Atkinson KE, Fluck N, Jones C. Effect of low-power air plasma treatment on the mechanical properties of carbon fibres and the interfacial shear strength of carbon fibre?epoxy composites. Surf Interface Anal 1995;23(5):313-318.

[98] Gao S, Mäder E, Zhandarov SF. Carbon fibers and composites with epoxy resins: Topography, fractography and interphases. Carbon 2004;42(3):515-529.

[99] Milewski JV, Shyne JJ, Shaver RC. Whiskers and Their Composites. In: Lubin G, editor. Handbook of Fiberglass and Advanced Plastic Composites, vol. 1. Huntington, NY: Krieger Publishing Co, 1969.

[100] Downs WB, Baker RTK. Novel carbon fiber-carbon filament structures. Carbon 1991;29(8):1173-1179.

[101] DuPont Corporation. Kevlar Technical Guide. 2011.

[102] Zhang Q, Liu J, Sager R, Dai L, Baur J. Hierarchical composites of carbon nanotubes on carbon fiber: Influence of growth condition on fiber tensile properties. Composites Sci Technol 2009;69(5):594-601.

[103] Shah TK, Gardner SH, Alberding MR, Malecki HC. CNT-Infused Aramid Fiber Materials and Process Therefore. 2011(2011/0171469).

[104] Handbook of fiberglass and advanced plastics composites. Huntington, N.Y: R. E. Krieger Pub. Co, 1975.

[105] Kowbel W, Bruce C, Withers JC, Ransone PO. Effect of carbon fabric whiskerization on mechanical properties of C□C composites. Composites Part A: Applied Science and Manufacturing 1997;28(12):993-1000.

[106] Qiangang F, Hejun L, Xiaohong S, Kezhi L, Zhibiao H, Jian W. Microstructure and growth mechanism of SiC whiskers on carbon/carbon composites prepared by CVD. Mater Lett 2005;59(19-20):2593-2597.

[107] Gunyaev GM, Zhigun IG, Sorina TG, Yakushin VA. Shear strength of composites based on whiskerized fibers. Mechanics of Composite Materials 1973;9(3):437-444.

[108] Gunyaev GM. Improving transverse tensile, interlaminar shear, and compressive strengths of karbovoloknits. Mechanics of Composite Materials 1977;13(6):819-823.

[109] Coleman JN, Khan U, Blau WJ, Gun'ko YK. Small but strong: A review of the mechanical properties of carbon nanotube–polymer composites. Carbon 2006;44(9):1624-1652.

[110] Baker RTK, Rodriguez NM. 1995(5413866).

[111] Thostenson ET, Li WZ, Wang DZ, Ren ZF, Chou TW. Carbon nanotube/carbon fiber hybrid multiscale composites J Appl Phys 2002;91(9):6034.

[112] Sager RJ, Klein PJ, Lagoudas DC, Zhang Q, Liu J, Dai L, Baur JW. Effect of carbon nanotubes on the interfacial shear strength of T650 carbon fiber in an epoxy matrix. Composites Sci Technol 2009;69(7-8):898-904.

[113] Qian H, Bismarck A, Greenhalgh ES, Shaffer MSP. Synthesis and characterisation of carbon nanotubes grown on silica fibres by injection CVD. Carbon 2010;48(1):277-286.

[114] Qian H, Bismarck A, Greenhalgh ES, Shaffer MSP. Carbon nanotube grafted carbon fibres: A study of wetting and fibre fragmentation. Composites Part A: Applied Science and Manufacturing 2010;41(9):1107-1114.

[115] Qian H, Greenhalgh ES, Shaffer MSP, Bismarck A. Carbon nanotube-based hierarchical composites: a review. J Mater Chem 2010;20(23):4751-4762.

[116] Qian H, Bismarck A, Greenhalgh ES, Kalinka G, Shaffer MSP. Hierarchical Composites Reinforced with Carbon Nanotube Grafted Fibers: The Potential Assessed at the Single Fiber Level Chemistry of Materials 2008;20(5):1862 <last_page> 1869.

[117] Garcia EJ, Wardle BL, John Hart A, Yamamoto N. Fabrication and multifunctional properties of a hybrid laminate with aligned carbon nanotubes grown In Situ. Composites Sci Technol 2008;68(9):2034-2041.

[118] Yamamoto N, John Hart A, Garcia EJ, Wicks SS, Duong HM, Slocum AH, Wardle BL. High-yield growth and morphology control of aligned carbon nanotubes on ceramic fibers for multifunctional enhancement of structural composites. Carbon 2009;47(3):551-560.

[119] Juntaro J, Pommet M, Kalinka G, Mantalaris A, Shaffer MSP, Bismarck A. Creating Hierarchical Structures in Renewable Composites by Attaching Bacterial Cellulose onto Sisal Fibers. Adv Mater 2008;20(16):3122-3126.

[120] Pommet M, Juntaro J, Heng JYY, Mantalaris A, Lee AF, Wilson K, Kalinka G, Shaffer MSP, Bismarck A. Surface Modification of Natural Fibers Using Bacteria: Depositing Bacterial Cellulose onto Natural Fibers To Create Hierarchical Fiber Reinforced Nanocomposites. Biomacromolecules 2008;9(6):1643-1651.

[121] Drzal LT, Rich MJ, Lloyd PF. Adhesion of Graphite Fibers to Epoxy Matrices: I. The Role of Fiber Surface Treatment. The Journal of Adhesion 1983;16(1):1-30.

[122] Drzal LT, Rich MJ, Koenig MF, Lloyd PF. Adhesion of Graphite Fibers to Epoxy Matrices: II. The Effect of Fiber Finish. The Journal of Adhesion 1983;16(2):133-152.

[123] Chatzi EG, Tidrick SL, Koenig JL. Characterization of the surface hydrolysis of kevlar-49 fibers by diffuse reflectance FTIR spectroscopy. Journal of Polymer Science Part B: Polymer Physics 1988;26(8):1585-1593.

[124] Ehlert GJ, Sodano HA. Zinc Oxide Nanowire Interphase for Enhanced Interfacial Strength in Lightweight Polymer Fiber Composites. ACS Applied Materials & Interfaces 2009;1(8):1827-1833.

[125] Keller T, Hoffman A, Ratner B, McElroy B. In: Mittal KL, editor. Physicochemical aspects of polymer surfaces, vol. 2. New York: Plenum Press, 1983.

[126] International Symposium on Physicochemical Aspects of Polymer Surfaces (1981,: New York. Physicochemical aspects of polymer surfaces. New York: Plenum Press, 1983.

[127] Chatzi EG, Tidrick SL, Koenig JL. Characterization of the surface hydrolysis of kevlar-49 fibers by diffuse reflectance FTIR spectroscopy. Journal of Polymer Science Part B: Polymer Physics 1988;26(8):1585-1593.

[128] Panar M, Avakian P, Blume RC, Gardner KH, Gierke TD, Yang HH. Morphology of poly(p-phenylene terephthalamide) fibers. Journal of Polymer Science: Polymer Physics Edition 1983;21(10):1955-1969.

[129] Kalantar J, Drzal LT. The bonding mechanism of aramid fibres to epoxy matrices. J Mater Sci 1990;25(10):4186-4193.

[130] Fratzl P, Weinkamer R. Nature's hierarchical materials. Progress in Materials Science 2007;52(8):1263-1334.

[131] Benrashid R, Tesoro GC. Effect of Surface-Limited Reactions on the Properties of Kevlar® Fibers. Textile Research Journal 1990;60(6):334-344.

[132] Young RJ, Lu D, Day RJ, Knoff WF, Davis HA. Relationship between structure and mechanical properties for aramid fibres. J Mater Sci 1992;27(20):5431-5440.

[133] Joo J, Chow BY, Prakash M, Boyden ES, Jacobson JM. Face-selective electrostatic control of hydrothermal zinc oxide nanowire synthesis. Nat Mater 2011;10(8):596-601.

[134] Schmidt-Mende L, MacManus-Driscoll JL. ZnO – nanostructures, defects, and devices. Materials Today 2007;10(5):40-48.

[135] Günzler H, Gremlich H. IR Spectroscopy: An Introduction: Wiley-VCH, July 2002.

[136] Carey FA. Organic chemistry: McGraw-Hill, 2000.

[137] Culler SR, McKenzie MT, Fina LJ, Ishida H, Koenig JL. Fourier Transform Diffuse Reflectance Infrared Study of Polymer Films and Coatings: A Method for Studying Polymer Surfaces. Appl Spectrosc November/December 1984;38:791-795(5).

[138] Beamson G, Briggs D. High resolution XPS of organic polymers: the Scienta ESCA300 database: Wiley, 1992.

[139] Madhukar MS, Drzal LT. Fiber-Matrix Adhesion and Its Effect on Composite Mechanical Properties: I. Inplane and Interlaminar Shear Behavior of Graphite/Epoxy Composites. Journal of Composite Materials 1991;25(8):932-957.

[140] Montes-Morán MA, Martínez-Alonso A, Tascón JMD, Young RJ. Effects of plasma oxidation on the surface and interfacial properties of ultra-high modulus carbon fibres. Composites Part A: Applied Science and Manufacturing 2001;32(3-4):361-371.

[141] Montes-Morán MA, Martínez-Alonso A, Tascón JMD, Paiva MC, Bernardo CA. Effects of plasma oxidation on the surface and interfacial properties of carbon fibres/polycarbonate composites. Carbon 2001;39(7):1057-1068.

[142] Boudou JP, Paredes JI, Cuesta A, Martínez-Alonso A, Tascón JMD. Oxygen plasma modification of pitch-based isotropic carbon fibres. Carbon 2003;41(1):41-56.

[143] Smiley RJ, Delgass WN. AFM, SEM and XPS characterization of PAN-based carbon fibres etched in oxygen plasmas. J Mater Sci 1993;28(13):3601-3611.

[144] Ho KKC, Lamoriniere S, Kalinka G, Schulz E, Bismarck A. Interfacial behavior between atmospheric-plasma-fluorinated carbon fibers and poly(vinylidene fluoride). J Colloid Interface Sci 2007;313(2):476-484.

[145] Ho KKC, Lee AF, Lamoriniere S, Bismarck A. Continuous atmospheric plasma fluorination of carbon fibres. Composites Part A: Applied Science and Manufacturing 2008;39(2):364-373.

[146] Gardner SD, Singamsetty CSK, Wu Z, Pittman Jr. CU. XPS/ISS Investigation of Carbon Fibers Sequentially Exposed to Nitric Acid and Sodium Hydroxide. Surf Interface Anal 1996;24(5):311-320.

[147] Pittman Jr CU, He G-, Wu B, Gardner SD. Chemical modification of carbon fiber surfaces by nitric acid oxidation followed by reaction with tetraethylenepentamine. Carbon 1997;35(3):317-331.

[148] Zhang G, Sun S, Yang D, Dodelet J, Sacher E. The surface analytical characterization of carbon fibers functionalized by H2SO4/HNO3 treatment. Carbon 2008;46(2):196-205.

[149] Lindsay B, Abel M, Watts JF. A study of electrochemically treated PAN based carbon fibres by IGC and XPS. Carbon 2007;45(12):2433-2444.

[150] Wang Y, Zhang F, Sherwood PMA. X-ray Photoelectron Spectroscopic Study of Carbon Fiber Surfaces. 23. Interfacial Interactions between Polyvinyl Alcohol and Carbon Fibers Electrochemically Oxidized in Nitric Acid Solution. Chem Mater 1999;11(9):2573-2583.

[151] Proctor A, Sherwood PMA. X-ray photoelectron spectroscopic studies of carbon fibre surfaces—II: The effect of electrochemical treatment. Carbon 1983;21(1):53-59.

[152] Yue ZR, Jiang W, Wang L, Gardner SD, Pittman Jr. CU. Surface characterization of electrochemically oxidized carbon fibers. Carbon 1999;37(11):1785-1796.

[153] Park S, Kim M. Effect of acidic anode treatment on carbon fibers for increasing fiber-matrix adhesion and its relationship to interlaminar shear strength of composites. J Mater Sci 2000;35(8):1901-1905.

[154] Kowbel W, Shan CH. The mechanism of fiber—matrix interactions in carbon—carbon composites. Carbon 1990;28(2-3):287-299.

[155] Fu X, Lu W, Chung DDL. Ozone treatment of carbon fiber for reinforcing cement. Carbon 1998;36(9):1337-1345.

[156] Zielke U, Hüttinger KJ, Hoffman WP. Surface-oxidized carbon fibers: I. Surface structure and chemistry. Carbon 1996;34(8):983-998.

[157] Delamar M, Désarmot G, Fagebaume O, Hitmi R, Pinsonc J, Savéant J-. Modification of carbon fiber surfaces by electrochemical reduction of aryl diazonium salts: Application to carbon epoxy composites. Carbon 1997;35(6):801-807.

[158] Chen J, Wei G, Maekawa Y, Yoshida M, Tsubokawa N. Grafting of poly(ethylene-block-ethylene oxide) onto a vapor grown carbon fiber surface by γ-ray radiation grafting. Polymer 2003;44(11):3201-3207.

[159] Peng H, Alemany LB, Margrave JL, Khabashesku VN. Sidewall Carboxylic Acid Functionalization of Single-Walled Carbon Nanotubes. J Am Chem Soc 2003;125(49):15174-15182.

[160] Chen J, Tsubokawa N. Novel gas sensor from polymer-grafted carbon black: Vapor response of electric resistance of conducting composites prepared from poly(ethylene-block-ethylene oxide)-grafted carbon black. J Appl Polym Sci 2000;77(11):2437-2447.

[161] Liu H, Wang X, Fang P, Wang S, Qi X, Pan C, Xie G, Liew KM. Functionalization of multi-walled carbon nanotubes grafted with self-generated functional groups and their polyamide 6 composites. Carbon 2010;48(3):721-729.

[162] Banerjee S, Hemraj-Benny T, Wong S?. Covalent Surface Chemistry of Single-Walled Carbon Nanotubes. Adv Mater 2005;17(1):17-29.

[163] Chen J, Hamon MA, Hu H, Chen Y, Rao AM, Eklund PC, Haddon RC. Solution Properties of Single-Walled Carbon Nanotubes. Science 1998;282(5386):95-98.

[164] Lindsay B, Abel M, Watts JF. A study of electrochemically treated PAN based carbon fibres by IGC and XPS. Carbon 2007;45(12):2433-2444.

[165] Chen J, Tsubokawa N. Novel gas sensor from polymer-grafted carbon black: Vapor response of electric resistance of conducting composites prepared from poly(ethylene-block-ethylene oxide)-grafted carbon black. J Appl Polym Sci 2000;77(11):2437-2447.

[166] Peng H, Alemany LB, Margrave JL, Khabashesku VN. Sidewall Carboxylic Acid Functionalization of Single-Walled Carbon Nanotubes. J Am Chem Soc 2003;125(49):15174-15182.

[167] Banerjee S, Hemraj-Benny T, Wong S?. Covalent Surface Chemistry of Single-Walled Carbon Nanotubes. Adv Mater 2005;17(1):17-29.

[168] Ryu Y, Scott AI. Self-condensation of activated malonic acid half esters: a model for the decarboxylative Claisen condensation in polyketide biosynthesis. Tetrahedron Lett 2003;44(40):7499-7502.

[169] Schreiber SL, Sammakia T, Hulin B, Schulte G. The epoxidation of unsaturated macrolides. Stereocontrolled routes to ionophore subunits. J Am Chem Soc 1986;108(8):2106-2108.

[170] McNab H. Meldrum's acid. Chem Soc Rev 1978;7(3):345-358.

[171] Chen B. Meldrum's acid in organic synthesis. 1991;32(3):529-597.

[172] Ivanov AS. Meldrum's acid and related compounds in the synthesis of natural products and analogs. Chem Soc Rev 2008;37(4):789-811.

[173] Blaquiere N, Shore DG, Rousseaux S, Fagnou K. Decarboxylative Ketone Aldol Reactions: Development and Mechanistic Evaluation under Metal-Free Conditions. J Org Chem 2009;74(16):6190-6198.

[174] Panteleon V, Kostakis IK, Marakos P, Pouli N, Andreadou I. Synthesis and free radical scavenging activity of some new spiropyranocoumarins. Bioorg Med Chem Lett 2008;18(21):5781-5784.

[175] Evans DA, Mito S, Seidel D. Scope and Mechanism of Enantioselective Michael Additions of 1,3-Dicarbonyl Compounds to Nitroalkenes Catalyzed by Nickel(II)−Diamine Complexes. J Am Chem Soc 2007;129(37):11583-11592.

[176] Burghard M, Krstic V, Duesberg GS, Philipp G, Muster J, Roth S, Journet C, Bernier P. Carbon SWNTs as wires and structural templates between nanoelectrodes. Synth Met 1999;103(1-3):2540-2542.

[177] Sainsbury T, Fitzmaurice D. Carbon-Nanotube-Templated and Pseudorotaxane-Formation-Driven Gold Nanowire Self-Assembly. Chem Mater 2004;16(11):2174-2179.

[178] Kordás K, Mustonen T, Tóth G, Jantunen H, Lajunen M, Soldano C, Talapatra S, Kar S, Vajtai R, Ajayan P. Inkjet Printing of Electrically Conductive Patterns of Carbon Nanotubes. Small 2006;2(8-9):1021-1025.

[179] Jeong W, Kessler MR. Toughness Enhancement in ROMP Functionalized Carbon Nanotube/Polydicyclopentadiene Composites. Chem Mater 2008;20(22):7060-7068.

[180] Zhou J, Sui Z, Zhu J, Li P, Chen D, Dai Y, Yuan W. Characterization of surface oxygen complexes on carbon nanofibers by TPD, XPS and FT-IR. Carbon 2007;45(4):785-796.

[181] Lee WH, Lee JG, Reucroft PJ. XPS study of carbon fiber surfaces treated by thermal oxidation in a gas mixture of O2/(O2+N2). Appl Surf Sci 2001;171(1-2):136-142.

[182] Briggs D, Briggs D(. Handbook of x-ray and ultraviolet photoelectron spectroscopy. London ; Philadelphia: Heyden, 1977.

[183] Fitzpatrick NJ, Sayal P, Al-Obadie MS, Katrib A. XPS and molecular orbital study of malonic acid and its derivatives. J Mol Struct 1982;78(1-2):129-130.

[184] Tojo G, Fernández M, Tojo G, Fernández M. Permanganate. In: Anonymous Oxidation of Primary Alcohols to Carboxylic Acids: Springer New York, 2006.

[185] Lee DG, Brownridge JR. Oxidation of hydrocarbons. IV. Kinetics and mechanism of the oxidative cleavage of cinnamic acid by acidic permanganate. J Am Chem Soc 1974;96(17):5517-5523.

[186] Ermolenko IN(. Chemically modified carbon fibers and their applications / I.N. Ermolenko, I.P. Lyubliner, N.V. Gulko ; translated by E.P. Titovets. Weinheim, Germany ; New York, NY, USA: VCH, 1990.

[187] Marcano DC, Kosynkin DV, Berlin JM, Sinitskii A, Sun Z, Slesarev A, Alemany LB, Lu W, Tour JM. Improved Synthesis of Graphene Oxide. ACS Nano 2010;4(8):4806-4814.

[188] Erickson K, Erni R, Lee Z, Alem N, Gannett W, Zettl A. Determination of the Local Chemical Structure of Graphene Oxide and Reduced Graphene Oxide. Adv Mater 2010;22(40):4467-4472.

[189] Galan U. Zinc oxide nanowire interphase for carbon reinforced composites. , 2010.

[190] Zhong Lin W. ZnO nanowire and nanobelt platform for nanotechnology. Materials Science and Engineering: R: Reports 2009;64(3-4):33-71.

[191] Song, WangWang, Riedo E, Wang ZL. Systematic Study on Experimental Conditions for Large-Scale Growth of Aligned ZnO Nanwires on Nitrides. J Phys Chem B 2005;109(20):9869-9872.

[192] WangWang, Song J, Summers CJ, Ryou JH, Li P, Dupuis RD, Wang ZL. Density-Controlled Growth of Aligned ZnO Nanowires Sharing a Common Contact: A Simple, Low-Cost, and Mask-Free Technique for Large-Scale Applications. J Phys Chem B 2006;110(15):7720-7724.

[193] WangWang, Song, Li P, Ryou JH, Dupuis RD, Summers CJ, Wang ZL. Growth of Uniformly Aligned ZnO Nanowire Heterojunction Arrays on GaN, AlN, and Al0.5Ga0.5N Substrates. J Am Chem Soc 2005;127(21):7920-7923.

[194] Banerjee D, Jo S?, Ren Z?. Enhanced Field Emission of ZnO Nanowires. Adv Mater 2004;16(22):2028-2032.

[195] Jo S. Field emission of zinc oxide nanowires grown on carbon cloth. Appl Phys Lett 2004;85(8):1407-3.

[196] Greene LE, Law M, Tan DH, Montano M, Goldberger J, Somorjai G, Yang P. General Route to Vertical ZnO Nanowire Arrays Using Textured ZnO Seeds. Nano Lett 2005;5(7):1231-1236.

[197] Joo J, Chow BY, Prakash M, Boyden ES, Jacobson JM. Face-selective electrostatic control of hydrothermal zinc oxide nanowire synthesis. Nat Mater 2011;10(8):596-601.

[198] Zhang H, Yang D, Li D, Ma X, Li S, Que D. Controllable Growth of ZnO Microcrystals by a Capping-Molecule-Assisted Hydrothermal Process. Crystal Growth & Design 2005;5(2):547-550.

[199] Zhang H, Yang D, Li S, Ma X, Ji Y, Xu J, Que D. Controllable growth of ZnO nanostructures by citric acid assisted hydrothermal process. Mater Lett 2005;59(13):1696-1700.

[200] Vayssieres L, Keis K, Lindquist S, Hagfeldt A. Purpose-Built Anisotropic Metal Oxide Material: 3D Highly Oriented Microrod Array of ZnO. J Phys Chem B 2001;105(17):3350-3352.

[201] Vayssieres L. Growth of Arrayed Nanorods and Nanowires of ZnO from Aqueous Solutions. Adv Mater 2003;15(5):464-466.

[202] Tian ZR, Voigt JA, Liu J, Mckenzie B, Mcdermott MJ, Rodriguez MA, Konishi H, Xu H. Complex and oriented ZnO nanostructures. Nat Mater 2003;2(12):821-826.

[203] Xu F, Yuan Z-, Du G-, Ren T-, Volcke C, Thiry P, Su B-. A low-temperature aqueous solution route to large-scale growth of ZnO nanowire arrays. J Non Cryst Solids 2006;352(23-25):2569-2574.

[204] Lu C, Qi L, Yang J, Tang L, Zhang D, Ma J. Hydrothermal growth of large-scale micropatterned arrays of ultralong ZnO nanowires and nanobelts on zinc substrate. Chem Commun 2006(33):3551-3553.

[205] Kenanakis G, Vernardou D, Koudoumas E, Katsarakis N. Growth of c-axis oriented ZnO nanowires from aqueous solution: The decisive role of a seed layer for controlling the wires' diameter. J Cryst Growth 2009;311(23-24):4799-4804.

[206] Chen Z, Gao L. A facile route to ZnO nanorod arrays using wet chemical method. J Cryst Growth 2006;293(2):522-527.

[207] Richardson JJ, Lange FF. Controlling Low Temperature Aqueous Synthesis of ZnO. 1. Thermodynamic Analysis. Crystal Growth & Design 2009;9(6):2570-2575.

[208] McPeak KM, Le TP, Britton NG, Nickolov ZS, Elabd YA, Baxter JB. Chemical Bath Deposition of ZnO Nanowires at Near-Neutral pH Conditions without Hexamethylenetetramine (HMTA): Understanding the Role of HMTA in ZnO Nanowire Growth. Langmuir 2011;27(7):3672-3677.

[209] Govender K, Boyle DS, Kenway PB, O'Brien P. Understanding the factors that govern the deposition and morphology of thin films of ZnO from aqueous solution. J Mater Chem 2004;14(16):2575-2591.

[210] McPeak KM, Becker MA, Britton NG, Majidi H, Bunker BA, Baxter JB. In Situ X-ray Absorption Near-Edge Structure Spectroscopy of ZnO Nanowire Growth During Chemical Bath Deposition. Chem Mater 2010;22(22):6162-6170.

[211] McPeak KM, Baxter JB. ZnO Nanowires Grown by Chemical Bath Deposition in a Continuous Flow Microreactor. Crystal Growth & Design 2009;9(10):4538-4545.

[212] Richardson JJ, Lange FF. Controlling Low Temperature Aqueous Synthesis of ZnO. 2. A Novel Continuous Circulation Reactor. Crystal Growth & Design 2009;9(6):2576-2581.

[213] Galan U, Lin y, Ehlert GJ, Sodano HA.
Effect of ZnO Nanowire Morphology on the Interfacial Strength of Nanowire Coated Carbon Fibers. Composites Science and Technology 2011;In Review.

[214] Greene LE, Yuhas BD, Law M, Zitoun D, Yang P. Solution-Grown Zinc Oxide Nanowires. Inorg Chem 2006;45(19):7535-7543.

[215] Law M, Greene LE, Johnson JC, Saykally R, Yang P. Nanowire dye-sensitized solar cells. Nat Mater 2005;4(6):455-459.

[216] Wang ZL, Song J. Piezoelectric Nanogenerators Based on Zinc Oxide Nanowire Arrays. Science 2006;312(5771):242-246.

[217] Xu C, Shin P, Cao L, Gao D. Preferential Growth of Long ZnO Nanowire Array and Its Application in Dye-Sensitized Solar Cells. J Phys Chem C 2010;114(1):125-129.

[218] Hu Z, Oskam G, Searson PC. Influence of solvent on the growth of ZnO nanoparticles. J Colloid Interface Sci 2003;263(2):454-460.

[219] Galan U, Lin Y, Ehlert GJ, Sodano HA. Effect of ZnO nanowire morphology on the interfacial strength of nanowire coated carbon fibers. Composites Sci Technol 2011;71(7):946-954.

[220] Cui J, Gibson UJ. Enhanced Nucleation, Growth Rate, and Dopant Incorporation in ZnO Nanowires. J Phys Chem B 2005;109(46):22074-22077.

[221] Feih S, Wonsyld K, Minzari D, Westermann P, Lilholt H. Testing procedure for the single fiber fragmentation test. 2004;Risø-R-1483.

[222] Committee D30.04 on Lamina and Laminate Test Methods. ASTM D3171-11. In: Anonymous Annual Book of ASTM Standards, vol. 15.03. West Conshohocken, PA: ASTM International, 2008.

[223] Schaefer DW, Justice RS. How Nano Are Nanocomposites? Macromolecules 2007;40(24):8501-8517.

[224] Drzal LT, Herrera-Franco PJ, Ho H. 5.05 - Fiber–Matrix Interface Tests. In: Editors-in-Chief: Anthony Kelly, Carl Zweben, editors. Comprehensive Composite Materials. Oxford: Pergamon, 2000.

[225] Pitkethly MJ, Favre JP, Gaur U, Jakubowski J, Mudrich SF, Caldwell DL, Drzal LT, Nardin M, Wagner HD, Di Landro L, Hampe A, Armistead JP, Desaeger M, Verpoest I. A round-robin programme on interfacial test methods. Composites Sci Technol 1993;48(1–4):205-214.

[226] H LC. The elasticity and strength of paper and other fibrous materials. British Journal of Applied Physics 1952;3(3):72.

[227] Zhou L, Kim J, Mai Y. Micromechanical characterisation of fibre/matrix interfaces. Composites Sci Technol 1993;48(1–4):227-236.

[228] Broutman LJ. ASTM STP44698S. In: Committee D30.04 on Lamina and Laminate Test Methods, editor. Annual Book of ASTM Standards. West Conshohocken, PA: ASTM International, 1969.

[229] Zhao F, Huang Y. Grafting of polyhedral oligomeric silsesquioxanes on a carbon fiber surface: novel coupling agents for fiber/polymer matrix composites. J Mater Chem 2011;21(11):3695-3703.

[230] Chou CT, Gaur U, Miller B. Fracture mechanisms during fiber pull-out for carbon-fiber-reinforced thermosetting composites. Composites Sci Technol 1993;48(1–4):307-316.

[231] Zinck P, Wagner HD, Salmon L, Gerard JF. Are microcomposites realistic models of the fibre/matrix interface? II. Physico-chemical approach. Polymer 2001;42(15):6641-6650.

[232] Zhou X-, Wagner HD, Nutt SR. Interfacial properties of polymer composites measured by push-out and fragmentation tests. Composites Part A: Applied Science and Manufacturing 2001;32(11):1543-1551.

[233] Walrath D, Adams D. The Iosipescu shear test as applied to composite materials. Exp Mech 1983;23(1):105-110.

[234] Adams DF, Walrath DE. Current Status of the Iosipescu Shear Test Method. Journal of Composite Materials 1987;21(6):494-507.

[235] Creighton CJ, Clyne TW. The compressive strength of highly-aligned carbon-fibre/epoxy composites produced by pultrusion. Composites Sci Technol 2000;60(4):525-533.

[236] Wicks SS, de Villoria RG, Wardle BL. Interlaminar and intralaminar reinforcement of composite laminates with aligned carbon nanotubes. Composites Sci Technol 2010;70(1):20-28.

[237] Garcia EJ, Wardle BL, John Hart A. Joining prepreg composite interfaces with aligned carbon nanotubes. Composites Part A: Applied Science and Manufacturing 2008;39(6):1065-1070.

[238] Committee C28.07 on Ceramic Matrix Composites. ASTM C1557 - 03. In: Anonymous Annual Book of ASTM Standards, vol. 15.01. West Conshohocken, PA: ASTM International, 2008.

[239] Klein CA. Characteristic strength, Weibull modulus, and failure probability of fused silica glass. Opt Eng 2009;48(11):113401-10.

[240] El Asloun M, Donnet J, Guilpain G, Nardin M, Schultz J. On the estimation of the tensile strength of carbon fibres at short lengths. J Mater Sci 1989;24(10):3504-3510.

[241] Crook S, Dhariwal H, Thornton G. HREELS study of the interaction of formic acid with ZnO(10$\bar{1}$0) and ZnO(000$\bar{1}$)-O. Surf Sci 1997;382(1–3):19-25.

[242] Thornton G, Crook S, Chang Z. A HREELS study of the effect of Cu on the interaction of HCOOH with ZnO(000$\bar{1}$)-O. Surf Sci 1998;415(1–2):122-130.

[243] Petrie WT, Vohs JM. An HREELS investigation of the adsorption and reaction of formic acid on the (0001)-Zn surface of ZnO. Surf Sci 1991;245(3):315-323.

[244] Christof W. The chemistry and physics of zinc oxide surfaces. Prog Surf Sci 2007;82(2–3):55-120.

[245] Glemza R, Kokes RJ. Chemisorption of Oxygen on Zinc Oxide. J Phys Chem 1965;69(10):3254-3262.

[246] Persson P, Ojamäe L. Periodic Hartree–Fock study of the adsorption of formic acid on ZnO(1010). Chemical Physics Letters 2000;321(3–4):302-308.

[247] Noy A, Frisbie CD, Rozsnyai LF, Wrighton MS, Lieber CM. Chemical Force Microscopy: Exploiting Chemically-Modified Tips To Quantify Adhesion, Friction, and Functional Group Distributions in Molecular Assemblies. J Am Chem Soc 1995;117(30):7943-7951.

BIOGRAPHICAL SKETCH

Gregory John Ehlert was born in 1986 in Michigan, the second child of George and Georganne Ehlert. He attended South Lyon Public Schools throughout his primary and secondary education. He earned his Bachelors of Science in Mechanical Engineering in December of 2007 from Michigan Technological University. While at Michigan Tech, Greg began working with Prof. Henry Sodano as a dedicated tutor for his course in vibrations. He moved to Arizona State University to work toward his PhD studying advanced composites. He earned his Masters of Science of Engineering in Mechanical Engineering from Arizona State University in December of 2009. During the summer of 2010, Greg was a research intern at the US Air Force Research Laboratory (Materials and Manufacturing Directorate), working with Dr. Jeffery Baur and Dr. Matthew Maschmann in the development of novel hierarchical fiber flow sensors. In December of 2010, Greg moved with Prof. Sodano to the University of Florida to finish his research and degree. During the summer of 2011, Greg returned to the US Air Force Research Laboratory to continue his own research in hierarchical fibers for structural applications as a part of the student career experience program. Upon returning to University of Florida, Greg defended his dissertation in the spring of 2012 and looks forward to a career pursuing new technology.